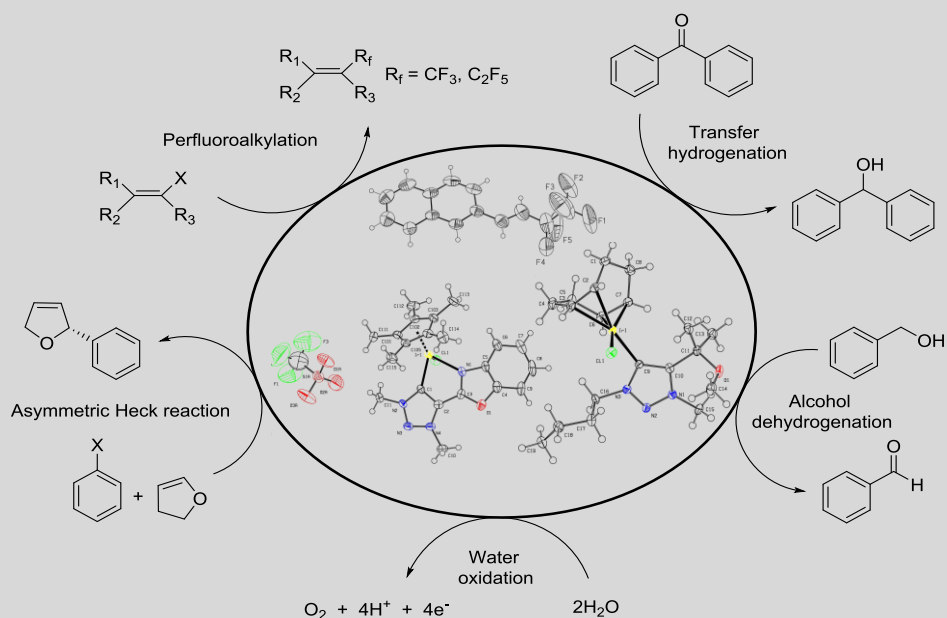




UNIVERSITAT
ROVIRA I VIRGILI

New approaches to perfluoroalkylation of aromatic compounds, and tailor-made catalysts for C-X forming and water oxidation reactions. Mechanistic insights

Zahra Mazloomi



DOCTORAL THESIS

2017

Zahra Mazloomi

**New approaches to perfluoroalkylation of aromatic
compounds, and tailor-made catalysts for C-X
forming and water oxidation reactions.**

Mechanistic insights

DOCTORAL THESIS

Supervised by

Prof. Dr. Montserrat Diéguez and Dr. Oscar Pàmies

Departament de Química Física i Inorgànica

and

Institut Català d'Investigació Química



UNIVERSITAT
ROVIRA i VIRGILI



INSTITUTE of CHEMICA
RESEARCH of
CATALONIA

Tarragona, 2017



UNIVERSITAT
ROVIRA I VIRGILI

We STATE that the present study, entitled “**New approaches to perfluoroalkylation of aromatic compounds, and tailor-made catalysts for C-X forming and water oxidation reactions. Mechanistic insights**”, presented by Zahra Mazloomi for the award of the degree of Doctor, has been carried out under our supervision at the Department of Physical and Inorganic Chemistry of this university. The first part of the thesis has been done in the Institut Català d’Investigació Química (Tarragona) in the group of Prof. V. V. Grushin

Tarragona, 31st May 2017.

Prof. Dr. Montserrat Diéguez

Dr. Oscar Pàmies

*Dedicated to the soul of my dear father
and my lovely mother and brother*

تقدیم به روح پدر عزیزم و به مادر و برادر دوست داشتنی ام

Acknowledgement

First and foremost, I would like to express my sincere appreciation to my supervisors Professors Montserrat Diéguez and Oscar Pàmies that believe in me and giving me the great opportunity to perform my Ph.D. study in their research group. Without their guidance, patience and resolute supports, this dissertation would not have been conceivable. I could never thank them enough for what they have done for me, and I'm always indebted to them.

I'm very thankful to Professor Vladimir Grushin for all his valuable guidance during the time that a part of my Ph.D. has been done in his research group.

Special and earnest thanks go to Professor Martin Albrecht as my visiting advisor for his important suggestions and remarks during my stage and also collaboration meetings and serving as my external referee. I also like to offer a very genuine appreciation to Professor Piet van Leeuwen for helpful discussions about the kinetic for the Heck reaction project and for fruitful collaboration as well as serving as my external referee.

I want to gratitude my former teachers and supervisors, especially Professor Sirous Jamali for his endless help throughout my M.Sc. study.

I am grateful to the thesis committee and external referees for their time and consideration.

It is a pleasure to thanks the URV and ICIQ research and administrative staff for all their help and cooperation during my research work. Chiefly the NMR units, X-ray and mass spectroscopy units.

I owe many thanks to all my lab mates in ICIQ and URV university; Noel Nebra, Hamidreza Samouei, Fedor Miloserdov, Bianca K. Muñoz, Jhenia Gorbacheva, Andrew Romine, Marc Magre, Jessica Margalef, Maria Biosca, Carlota Borrás, Efreem Del Valle and Joan Saltó. Also my lab mates in Bern university, specially Rene Petrorius, Marta, Angela, Candela and Racheal.

In addition, I would like to extend my thanks to our technician Raquel Rivas for all her kind helps and to all OMICH (TECAT) people (Marc, Nuria, Jordi, Albert, Toni, Fran, Eli, Lia, Nanette, Myriam, Alberto, Enrico) who made me very enjoyable times.

The ICIQ Foundation and the Spanish Government are gratefully acknowledged for their financial supports as well as COST Action CM1205 –CARISMA for the STSM scholarship, even for the chance attending to the CARISMA conferences and giving oral presentations and for the financial help attending to the 40th international summer school.

Last but not least, this Ph.D. journey would not have been possible without the support of my family, countless gratitude to my Mom and Dad, for cheering me in all of my pursuits and inspiring me to follow my dreams. I always knew that you believed in me and desired the best for me. Special thanks to my lovely brother Farshid, your love, support and encouragement was worth more than I can state on paper.

List of abbreviations

AAD	acceptorless alcohol dehydrogenation
ATH	asymmetric transfer hydrogenation
BINAP	2,2'-bis(diphenylphosphino)-1,1'-binaphthyl
bpy	2,2'-bipyridine
CAN	cerium ammonium nitrate
CCDC	Cambridge crystallographic data center
Cp*	pentamethylcyclopentadiene
CV	cyclic voltametry
dba	dibenzylideneacetone
DCM	dichloromethane
DLS	dynamic light scattering
DMAC	<i>N,N</i> -dimethylacetamide
DMAP	4-dimethylaminopyridine
DMF	<i>N,N</i> -dimethylformamide
DMPU	<i>N,N'</i> -dimethylpropyleneurea
DMSO	dimethyl sulfoxide
DPV	differential pulse voltammetry
EC	electrochemistry
EDA	electron-donor-acceptor
<i>ee</i>	enantiomeric excess
GC	gas chromatography
GC-MS	gas chromatography-mass spectroscopy
HPLC	high performance liquid chromatography
IPr	1,3-bis(2,6-diisopropylphenyl)imidazol-2-ylidene
IPr*	1,3-bis(2,6-bis(diphenylmethyl)-4-methylphenyl)imidazol-2-ylidene)
KIE	kinetic isotope effect
MFC	mass flow controller
MIC	mesoionic carbene
MPV reduction	Meerwein-Ponndorf-Verlay reduction
NHC	<i>N</i> -heterocyclic carbene
NMP	<i>N</i> -methyl-2-pyrrolidone
OA	oxidative addition

<i>p</i> -cymene	1-isopropyl-4-methylbenzene
Phen	1,10-phenanthroline
PPh ₃	triphenylphosphine
PPy	2-phenyl pyridine
PTFE	polytetrafluoroethylene; teflon
Py	pyridine
RE	reductive elimination
R _f	perfluoroalkyl group
RT	residence time
SCE	standard calomel electrode
TBAP	tetrabutylammonium perchlorate
TEM	transmission electron microscopy
TH	transfer hydrogenation
THF	tetrahydrofuran
TMEDA	<i>N,N,N',N'</i> -tetramethylethylenediamine
TMS	trimethylsilyl group
TOF	turnover frequency
TON	turnover number
TREAT HF	triethylamine trihydrofluoride
trz	triazolylidene
UV-VIS	ultraviolet-visible
WOCs	water oxidation catalysts
ZS	zwitterion nano

Table of contents

Preface	iii
Chapter 1. Objectives	1
Chapter 2. General introduction I: Progress in perfluoroalkylation of aromatic compounds	5
2.1. Aromatic trifluoromethylation with metal complexes	8
2.2. Aromatic pentafluoroethylation with metal complexes	16
2.3 References	19
Chapter 3. Perfluoroalkylation of aromatic compounds	25
3.1 Continuous process for production of CuCF_3 via direct cupration of fluoroform	27
3.2. Trifluoromethylation and pentafluoroethylation of vinylic halides with low-cost R_fH -derived CuR_f ($\text{R}_f = \text{CF}_3, \text{C}_2\text{F}_5$)	49
Chapter 4. General introduction II: Catalyst design for C-X forming and water oxidation reactions	81
4.1. Metal-catalyzed transfer hydrogenation reactions	84
4.2. Ir-catalyzed dehydrogenation of alcohols	95
4.3. Ir molecular catalysts for water oxidation	99
4.4. Pd-catalyzed asymmetric Heck reaction	104
4.5 References	114
Chapter 5. Ru- and Ir-catalyzed transfer hydrogenation and dehydrogenation reactions	129
5.1. Synthesis, hemilability, and catalytic transfer hydrogenation activity of iridium(III) and ruthenium(II) complexes containing oxygen-functionalised triazolylidene ligands	131
5.2. Ir-complexes containing mesoionic carbenes for the highly efficient and versatile transfer hydrogenation of $\text{C}=\text{O}$, $\text{C}=\text{N}$ and $\text{C}=\text{C}$ functionalities and for dehydrogenation of alcohols	155

Chapter 6. Iridium molecular catalysts for catalytic water oxidation	207
6.1. Benzoxazole/thiazole-triazolidene iridium complexes as new efficient molecular catalysts for water oxidation	209
Chapter 7. Pd-catalyzed asymmetric intermolecular Heck reaction	229
7.1. Air stable and simple phosphite-oxazoline ligands for Pd-intermolecular asymmetric Heck reaction	231
Chapter 8. Conclusions	263
Chapter 9. Summary	269
Chapter 10. Appendix	275
10.1. List of papers	277
10.2. Meeting contributions	277
10.3. Stays in other research groups	278

Structure of the thesis

The thesis is divided into two different parts. The first part contains two chapters on perfluoroalkylation of aromatic compounds. This part of the thesis have been done in the Institut Català d'Investigació Química (ICIQ, Tarragona) in the group of Prof. V.V. Grushin. The second part contains four chapters on catalysts design for C-X forming and water oxidation reactions. This part has been done in the Department of Química Física i Inorgànica under the supervision of Prof. M. Diéguez and Dr. O. Pàmies.

-Chapter 1. *Objectives*. This chapters contains de objectives of the thesis.

-Chapter 2. *General introduction I: progress in perfluoroalkylation of aromatic compounds* contains a general introduction about the progress made in perfluoroalkylation of aromatic compounds with the discussion of antecedents, performance and main achievements.

-Chapter 3. *Perfluoroalkylation of aromatic compounds*. This chapter contains two section. The first section *Continuous process for production of CuCF₃ via direct cupration of fluorofrom*, includes the first continuous flow process for the synthesis of a superior trifluoromethylating reagent, "ligandless" CuCF₃, from fluorofrom, by far the best CF₃ source in terms of availability, cost and atom economy. The second section *Trifluoromethylation and pentafluoroethylation of vinylic halides with low-cost R_fH-derived CuR_f (R_f = CF₃, C₂F₅)*, presents the trifluoromethylation and pentafluoroethylation of a variety of vinylic bromides and iodides with R_fH-derived CuR_f (R_f = CF₃, C₂F₅) to give the corresponding fluoroalkylated olefins. These reactions proceed with high yields and excellent chemo- and stereoselectivity under mild reaction conditions.

-Chapter 4. *General introduction II: Catalyst design for C-X forming and water oxidation reactions*. This chapter first presents the importance of metal catalysis in the synthesis of compounds. An important step in this synthesis is the design and preparation of ligands. Among them, new oxygen/oxazole/thiazole-mesoionic carbene ligands and phosphite-oxazoline ligands are presented. These ligands are applied to four catalytic reactions, which are reviewed in detail in this chapter. For each reaction, the antecedents, performance and main achievements are discussed. The state-of-the-art and current needs in this field justify the objectives of this part of the thesis.

-Chapter 5. *Ru and Ir-transfer hydrogenation and dehydrogenation reactions*. This chapter contains two sections on the development of new Ru and Ir complexes with

mesionic carbene-based ligands. The first section, *synthesis, hemilability, and catalytic transfer hydrogenation activity of iridium(III) and ruthenium(II) complexes containing oxygen-functionalised triazolylidene ligands*, includes the synthesis and characterisation of iridium(III) and ruthenium(II) complexes bearing pendant hydroxy- and ester-wingtip substituents. Both monodentate and C,O-bidentate binding modes were observed for these O-functionalised triazolylidene complexes. The two bonding modes are interconvertible, which demonstrates the hemilability of this coordinating group. The catalytic activity of the complexes was compared in transfer hydrogenation, revealing that pendant hydroxyfunctionalities are beneficial for enhancing the performance of triazolylidene iridium(III) catalysts, while they have no effect in ruthenium-catalyzed transfer hydrogenation. The second section, *Ir-complexes containing mesoionic carbenes for the highly efficient and versatile transfer hydrogenation of C=O, C=N and C=C functionalities and for dehydrogenation of alcohols*, reports the first examples of mixed benzoxazole/thiazole-MIC ligands. We used these ligands to generate the corresponding Ir(I) and Ir(III) benzoxazole/thiazole/ether-appended MIC complexes. The coordination was achieved by a transmetallation protocol and the corresponding complexes were fully characterized by ^1H and ^{13}C spectroscopies, high resolution mass spectrometry, elementary analysis and X-ray diffraction. Apart from synthetic and structural aspects, we also present the successful application of these complexes in transfer hydrogenation of a broad range of substrates (ketones, aldehydes, imines, etc.) and also the more challenging mono-, di- and trisubstituted olefins and in the base-free dehydrogenation reactions of alcohols. We also discuss some mechanistic insights for both transformations.

-Chapter 6. *Iridium molecular catalysts for catalytic water oxidation*. This chapter contains one section, *benzoxazole/thiazole-triazolylidene iridium complexes as new efficient molecular catalysts for water oxidation*, that includes the application of the new iridium complexes previously synthesized in chapter 4 in the water oxidation reactions using CAN and NaIO_4 as oxidants. Using CAN as oxidant at low pH, the catalyst precursors provided similar activities (TOF's ca 0.06s^{-1}) and lower than those achieved using parent pyridine complex. However, excellent activities (much better than related pyridine analogues; TOF's up to 0.58s^{-1}) were achieved when using more appealing almost neutral conditions (pH = 5.6) and NaIO_4 as oxidant. In this chapter we have also disclosed the electrochemical properties of the complexes in a non-protic

solvent as well as in aqueous solution at different pHs. We have also studied the Cl⁻/H₂O ligand exchange propensity of the complexes in water solution.

-Chapter 7. *Pd-catalyzed asymmetric intermolecular Heck reaction*. This chapter contains one section, *air stable and simple phosphite-oxazoline ligands for Pd-intermolecular asymmetric Heck reaction. Mechanistic insights* that includes the synthesis of a reduced but structurally valuable library of phosphite-oxazoline ligands for the enantioselective Pd-catalyzed Heck reaction of several cyclic substrates and triflates. These ligands, which are prepared in a few steps from commercially available materials include the benefits of the high robustness of the phosphite moiety and the additional control provided by the flexibility of the chiral pocket through a modular ligand scaffold. Other advantages of these ligands are that they are solid, stable to air and other oxidizing agents and are, therefore, easy to handle and can be manipulated and stored in air. In a simple two or four step-procedure, several ligand parameters have been easily tuned to maximize the catalyst performance. In this paper we have also carried out mechanistic investigations by combining in situ NMR studies of key intermediates and kinetics studies.

-Chapter 8. *Conclusions*. This chapter presents the conclusions of the work presented in this thesis.

-Chapter 9. *Summary*. This chapter contains a summary of the thesis.

-Chapter 10. The *Appendix* contains the list of papers, including the papers from the master period, meeting presentations (also those during the master period) given by the author, and the stages in other research groups during the period of development of this thesis.

Chapter 1.

Objectives

Objectives

This thesis focusses on the development of new protocols for the perfluoroalkylation of aromatic compounds and the development of new robust and highly efficient catalytic systems for relevant C-X forming and water oxidation reactions.

The more specific aims are:

1. The development of a reliable continuous process for the production of CuCF_3 from CHF_3 as well as their use as an efficient trifluoromethylating agent of aromatic compounds.

2. The development of new protocols for the highly chemo- and stereoselective perfluoroalkylation of of vinylic halides using cheap and environmentally friendly CuR_f ($\text{R}_f = \text{CF}_3, \text{C}_2\text{F}_5$) reagents.

3. The synthesis and application of heterodonor oxygen/benzoxazole/thiazole-triazolylidene ligands (Figure 1.1) in the following metal-catalyzed reactions: a) Ru- and Ir-catalyzed transfer-hydrogenation of ketones, aldehydes, imines and olefins; b) Ir-catalyzed base-free dehydrogenation of alcohols; and c) Ir-catalyzed water oxidation. In all the catalytic reactions mechanistic and kinetic studies have been carried out to better understand their catalytic behavior.

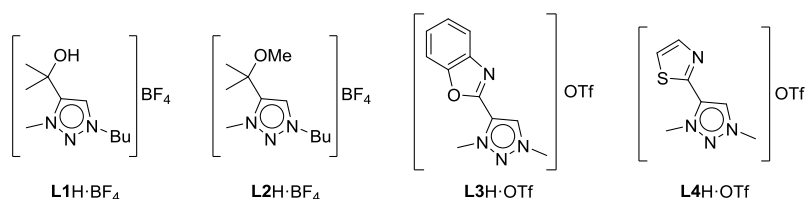


Figure 1.1. Heterodonor oxygen/benzoxazole/thiazole-triazolylidene salts.

4. The synthesis and application of novel robust phosphite-oxazoline ligands (Figure 1.2) for the asymmetric Pd-catalyzed Heck reaction using aryl- and vinyl triflates and halides. Valuable catalytic intermediates have been synthesized and kinetic studies have been performed to elucidate the rate determining step.

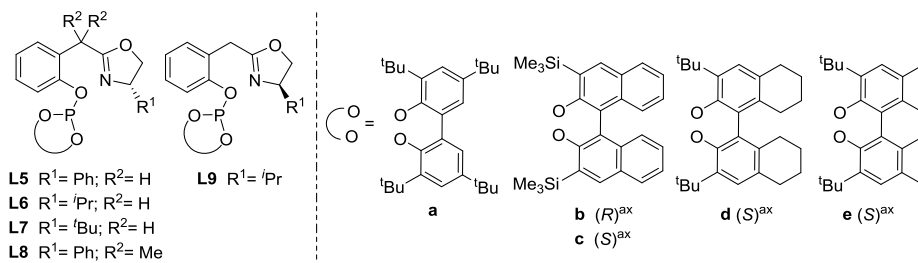


Figure 1.2. Phosphite-oxazoline ligand library **L5-L9a-e**.

Chapter 2.

*General introduction: progress in perfluoroalkylation
of aromatic compounds*

Organic compounds bearing fluoroalkyl groups play a dominant role in the development of pharmaceuticals, agrochemicals, polymers and specialty materials. Incorporation of fluorinated fragments into organic compounds might affect their physical, chemical and biological properties.^{1,2} For instance from a biological point of view, by introducing the perfluoroalkyl moiety into the molecule the lipophilicity increased which make a better in-vivo absorption and transport rate and even this group makes the molecules metabolically more resistance. In addition these fluoroalkyl groups are chemically more stable rather than their hydrocarbon counterparts while they are sterically similar to them.³

The first report of the pharmacological evaluation of compounds containing the trifluoromethyl group was that of Lehmann in 1928 and it is important from a historical point of view.⁴

Up to 20% of all modern drugs and more than 30% of agrochemicals commercially used are based on fluorine-containing active ingredients.⁵ Although trifluoromethylated molecules have an important place in chemistry, pentafluoroethylated compounds also have special place as they are more lipophilic and often have better activity than their CF_3 analogs. Therefore some biologically active compounds are including C_2F_5 group. Some examples of active ingredients of agrochemicals and pharmaceuticals containing CF_3 and C_2F_5 groups are shown in Figure 2.1.

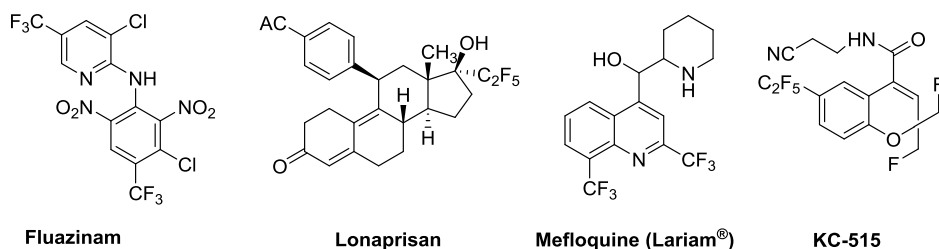
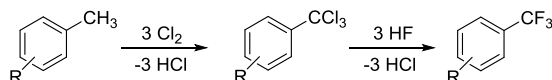


Figure 2.1. Selected commercially available pharmaceuticals and agrochemicals containing CF_3 and C_2F_5 groups.

In this chapter the progress in trifluoromethylation and pentafluoroethylation of aromatic substrates will be mentioned separately.

2.1. Aromatic trifluoromethylation with metal complexes

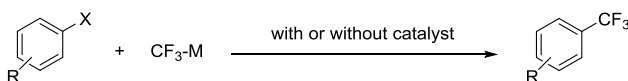
Nowadays trifluoromethylated aromatic compounds are manufactured by a Swarts-type process which is neither atom-economical nor environmentally benign as it involves hazardous chemicals and generate big amount of chlorine waste in order to convert CH_3 group on the ring to CCl_3 (that produce 3 equiv of HCl as a byproduct) and then subsequent Cl/F exchange by HF (3 more equiv of HCl) to make CF_3 group (Scheme 2.1).



Scheme 2.1. Trifluoromethylated aromatic compounds manufactured in industry.

In general 3 equiv of Cl_2 are consumed and 6 equiv of HCl are produced to generate 1 equiv of the trifluoromethylated aromatic product.⁶ In addition, this transformation is solely limited to the number of functional groups and even harsh reaction conditions is another obstacle.

Despite all these drawbacks the Swarts reaction still remains the method used for the large scale manufacturing of trifluoromethylated aromatic compounds as there is no industrially possible alternative. A possible desired alternative to the Swarts reaction is shown in Scheme 2.2.⁹ It consists in a selective trifluoromethylation of prefunctionalized aromatic substrates.

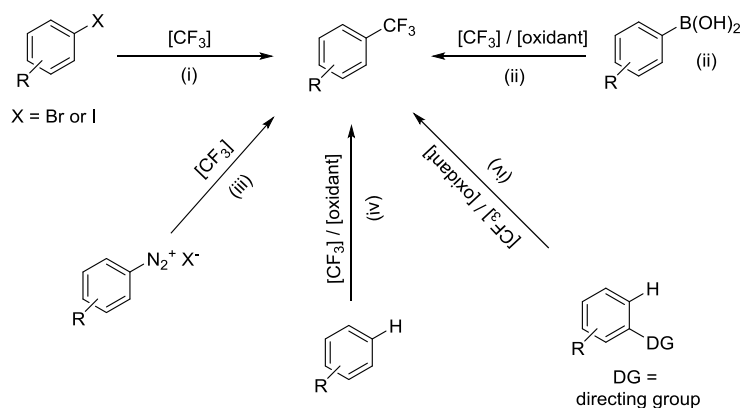


Scheme 2.2. Selective trifluoromethylation of aromatic compounds.

Since the first discovery of metal-mediated perfluoroalkylation of iodoarenes by McLoughlin and Thrower in the late 1960s⁷ and further advancement by Kumadaki et al.,⁸ enormous progress has been done by different groups in this area. The most metals that particularly capable of activating Ar-X bonds ($\text{X} = \text{I}, \text{Br}, \text{Cl}, \text{OTf}, \text{etc.}$) are palladium, copper and nickel and among them copper used mostly as a catalyst with various CF_3 sources such as polyfluorinated methanes ($\text{CF}_3\text{I}, \text{CF}_3\text{Br}, \text{CF}_3\text{H}$), trifluoromethyl silicon compounds which is often referred to Ruppert's reagent

(CF_3SiMe_3 , CF_3SiEt_3), trifluoroacetic acid salts and derivatives ($\text{CF}_3\text{CO}_2\text{X}$, where $\text{X} = \text{Na}, \text{K}, \text{Me}$, etc.) and preisolated well-defined or generated in situ CuCF_3 compounds.⁹

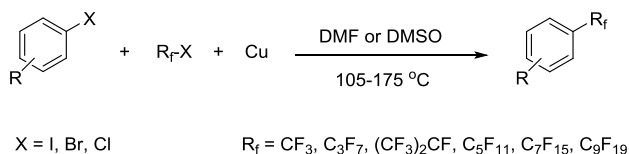
The aromatic trifluoromethylation methods can be classified into four different types depending on the source of aromatic substrates (Scheme 2.3).^{9,10} They are: (i) nucleophilic trifluoromethylation of haloarenes, (ii) oxidative trifluoromethylation of aryl boronic acids or borates, (iii) trifluoromethylation of arenediazonium salts based on Sandmeyer reactions of these substrates and (iv) direct C–H aryl trifluoromethylation with or without directing group assistance.



Scheme 2.3. General protocols for trifluoromethylation of aromatic compounds with copper.

2.1.1. Trifluoromethylation of aryl halides

As mentioned before, McLoughlin and Trower reported the first perfluoroalkylation of aromatic halides using stoichiometric or super-stoichiometric amounts of Cu metal powder in 1969 (Scheme 2.4).^{7b} This reaction can be successfully applied in many examples. In addition, different functional groups can be presented like OAc, OH, CO_2H , NH_2 and NO_2 and the order of ease of replacement of aryl halides is $\text{I} > \text{Br} \gg \text{Cl}$ that is supported by reaction mechanism.

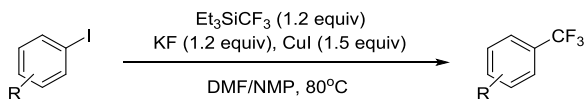


Scheme 2.4. The McLoughlin and Trower protocol.

In the same year, further work was done by Kobayashi and Kumadaki on optimization of the reaction of $\text{R}_f = \text{CF}_3$ with a series of haloarenes and heteroarenes.⁸ In both cases the cross-coupling of aromatic halides with stoichiometric amount of CuCF_3 that generated in situ controlled the trifluoromethylation process. Kondratenko, Vechirko, and Yagupolskii reported the formation of CuCF_3 from $(\text{CF}_3)_2\text{Hg}$ or CF_3HgI and copper powder in NMP (N-methylpyrrolidone) or DMAC (dimethylacetamide) in 1980.¹¹ In 1985 Wiemers and Burton¹² reported the transformation of CF_3 from Zn or Cd to Cu for trifluoromethylation of iodobenzene. Even later trifluoromethyl copper species were also prepared via combination of $[\text{Zn}(\text{CF}_3)\text{Br} \cdot 2\text{DMF}]$ with CuBr^{13} or Bu_3SnCF_3 with CuCl^{14} .

The methodologies between 1970-1980 were based on pre-formed or generated in situ $\text{CuCF}_3^{11,12,15}$ and the first spectroscopic study of this species was performed by Wiemers and Burton in 1986.^{12, 16} By treatment of CuBr with CF_3CdX ($\text{X} = \text{Br}$ or Cl) in DMF at -50°C a CuCF_3 species was observed at -28.8 ppm in the ^{19}F NMR.

By using silylated reagent and CuX under mild conditions, CuCF_3 was generated in order to trifluoromethylate the aryl iodides (Scheme 2.5).¹⁷ Copper was used in stoichiometric amount because the copper-mediated trifluoromethylation on the iodoarenes proceeded more slowly than the generation of CuCF_3 species.



Scheme 2.5. Trifluoromethylation with trifluoroethylsilyl reagent.

For these trifluoromethylation reactions until 2008 that Vivic and co-workers reported the first structurally characterized $\text{CF}_3\text{Cu(I)}$ complexes,¹⁸ there was no structural information about CuCF_3 and a clear mechanism was missing. After that

more $\text{CF}_3\text{Cu(I)}$ compounds have been synthesized and characterized by X-ray analysis specially by Grushin et al.¹⁹ Some of these structures are represented in Figure 2.2.

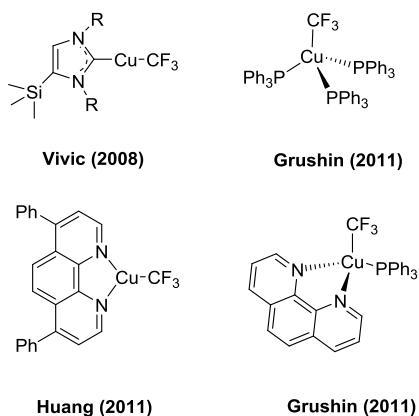
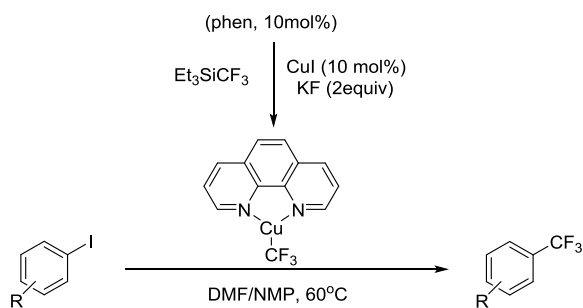


Figure 2.2. X-ray structures of some $\text{CF}_3\text{Cu(I)}$ complexes as examples.

Ancillary ligands on Cu(I) species can affect the trifluoromethylation of haloarenes by increasing or decreasing the rate of the reaction. One of the examples is 1,10-phenanthroline.²⁰ It seems available vacant coordination site on Cu has a dominant effect in the formation of final trifluoromethyl aromatic compound.

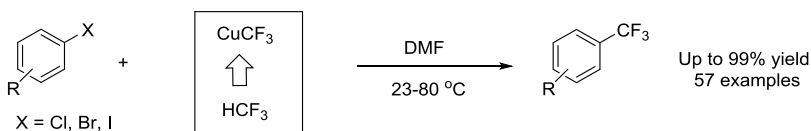
The first Cu-catalyzed trifluoromethylation of aryl iodides was originally developed by Amii et al in 2009.²¹ In this case they added chelating ligands like (Phen) in order to improve the trifluoromethylation reactions. It was suggested that the reaction went through a phenanthroline-ligated Cu(I) complex (Scheme 2.6).



Scheme 2.6. Cu-catalyzed trifluoromethylation of haloarenes.

In general considerable progress has been done in the area of trifluoromethylation of aryl halides with copper complexes containing different ligands.^{9,10a,19b,22,23,24,25}

One of the best and efficient methods for trifluoromethylation of aryl halides with fluoroform-derived CuCF_3 has been recently developed by Grushin et al (Scheme 2.7).^{19a} It is the first direct cupration of fluoroform that is low-cost and highly chemoselective as there is no observation of side products. Moreover, addition of an auxiliary ligand to this CuCF_3 reagent is not beneficial.

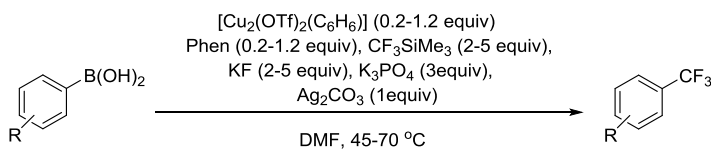


Scheme 2.7. Direct cupration of fluoroform.

Due to the importance of the fluoroform-driven CuCF_3 reagent in the first part of this thesis, it will be discussed in details in chapter 2.1.

2.1.2. Trifluoromethylation of arylboronic acids and borates

The first example of oxidative trifluoromethylation of aryl boronic acids was reported by Chu and Qing in 2010.²⁶ The reaction was applied in a range of substrates by in situ formation of CuCF_3 in smoothly high yield with different additives and Ag_2CO_3 as an oxidant. The reaction is presented in Scheme 2.8.

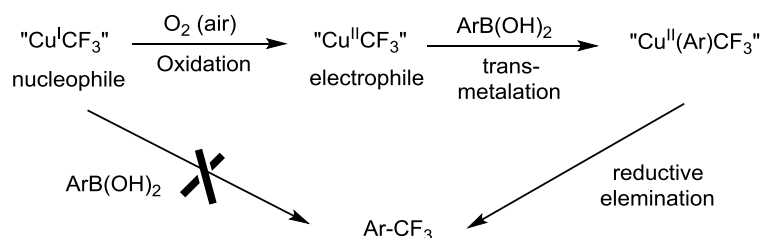


Scheme 2.8. Trifluoromethylation of arylboronic acids by Chu and Qing reaction.

Senecal, Parsons, and Buchwald developed a more economical methodology using dry O_2 as an oxidant and twofold excess of CF_3SiMe_3 (2 equiv).²⁷ Moreover, a similar methodologies were used with other arylboronic derivatives such as fluoroborates²⁸ and pinacol esters.^{28a, b,29}

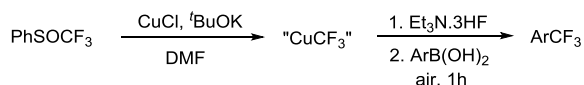
The best method for selective trifluoromethylation of arylboronic acid in nondried air was reported by Grushin et al in 2012. This protocol is much simple, low-cost, safe

and highly efficient.³⁰ As both Cu(I)CF_3 and ArB(OH)_2 are nucleophiles they do not react together, then the O_2 [air] oxidizes the Cu(I)CF_3 to Cu(II)CF_3 which is electrophile and then it can smoothly react with aryl boronic acids. The mechanism is proposed in Scheme 2.9.



Scheme 2.9. Suggested simple mechanism for trifluoromethylation of aryl boronic acids.

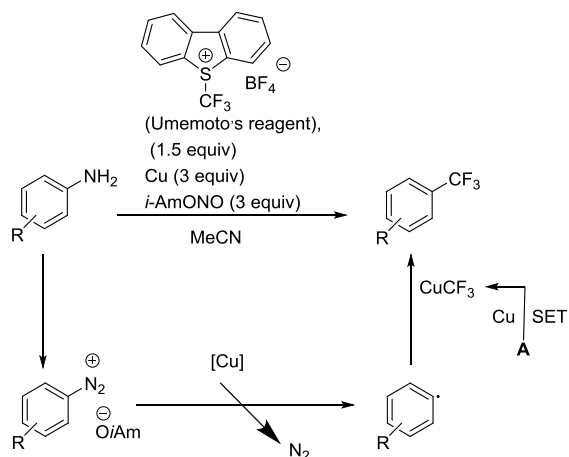
Later on, a similar methodology for trifluoromethylation of arylboronic acid was published under air atmosphere at room temperature. The source of trifluoromethyl group was phenyltrifluoromethyl sulfoxide instead of fluoromorm.²⁴ The general reaction is represented in Scheme 2.10.



Scheme 2.10. Trifluoromethylation of arylboronic acids with “ CuCF_3 ” generated from PhSOCF_3 .

2.1.3. Trifluoromethylation of arenediazonium salts

The amino group of the aromatic amines can be transformed into the trifluoromethyl group by converting to the diazonium salt like Sandmeyer reaction.³¹ Very recently, Fue et al. mentioned the first report on this transformation with copper mediated Sandmeyer protocol.³² The simplified mechanism is shown in Scheme 2.11 and it is a radical type reaction.



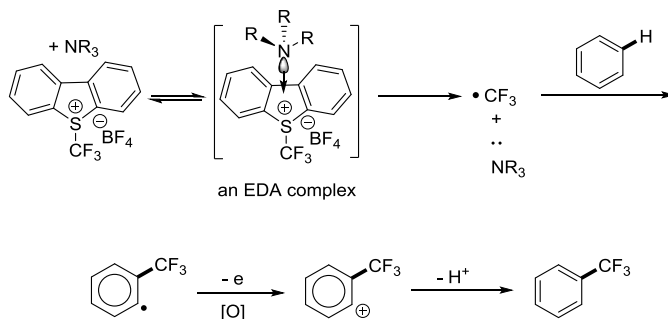
Scheme 2.11. Copper mediated Sandmeyer protocol for trifluoromethylation of aromatic amines in Fue reaction.

Goossen and coworkers developed one pot procedure for the trifluoromethylation of a variety of aromatic amines.³³ Afterward, Wang et al. reported trifluoromethylation of aromatic diazonium salts by using AgCF₃ instead of CuCF₃.³⁴ Later the group of Grushin used fluorocarbon derived CuCF₃ to do this transformation in aqueous conditions with several arylamines and with a variety of electron-donating and electron-withdrawing functional groups via a radical mechanism.³⁵ It was found that acetonitrile as a solvent or co-solvent was critical to improve the reaction yield and selectivity.

2.1.4. Direct C-H aromatic trifluoromethylation

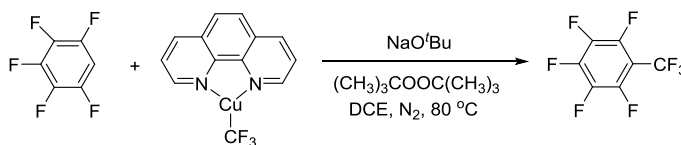
The most effective way to prepare CF₃-substituted arenes would be direct trifluoromethylation of C-H bonds in aromatic substrates. In general transition metal-free C-H aromatic trifluoromethylation reagents has been used since 1960s^{36,37} such as CF₃I,³⁸ (CF₃)₂Te³⁹ and CF₃Br/Na₂S₂O₄.⁴⁰ However, the use of these reagents in the direct radical trifluoromethylation of aromatic C-H moieties in substituted arenes provides low regioselectivity. Studer has a comprehensive overview on the recent developments in radical trifluoromethylation reactions.⁴¹

A new protocol, EDA (electron-donor-acceptor) complex-mediated process can also be successfully used to render trifluoromethylation of arenes without a directing group.⁴² An example is shown in Scheme 2.12 where Umemoto's reagent is envisaged as an electron acceptor and tertiary amine as an electron donor to form the EDA complex.



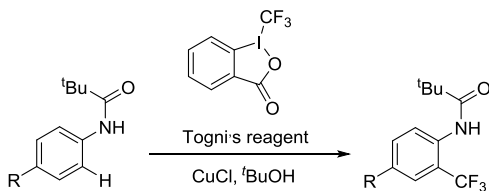
Scheme 2.12. C-H trifluoromethylation of arenes via an EDA complex.

In the literature there are few examples about Cu-mediated trifluoromethylation of aromatic C-H bonds. The first transformation of this type was reported by Chu and Qing in 2012.⁴³ The oxidative trifluoromethylation of electron deficient arenes such as pentafluorobenzene were performed in the presence of Cu(I) complex, base or cobases (cobases ^tBuONa/NaOAc) and oxidant. The reaction is shown in Scheme 1.13.



Scheme 2.13. Cu-mediated oxidative trifluoromethylation of an electron-deficient arene.

As mentioned above, lack of regioselectivity in the products is the main difficulty in the trifluoromethylation of aromatic C-H bonds without a directing group. To avoid the mixture of regioisomers, arenes bearing different directing groups like amide (they have a good *ortho*-selectivity) has been used.^{10a} For instance, Cu-catalyzed radical trifluoromethylation of pivalamido arenes with high selectivity at the *ortho*-position. This transformation is presented in Scheme 2.14.⁴⁴ The proposed mechanism is the oxidative addition between CuCl and Togni's reagent to generate the CF₃ radical.

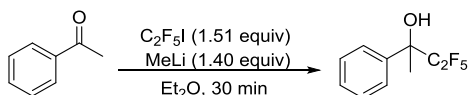


Scheme 2.14. Radical trifluoromethylation of pivalamido arenes.

2.2. Aromatic pentafluoroethylation with metal complexes

Pentafluoroethylation reactions are less developed than trifluoromethylation^{9,45} although in certain cases compounds with C_2F_5 group exhibit premier properties in comparison with their CF_3 counterparts. There are several reported examples about biologically active pentafluoroethylated compounds that are superior than trifluoromethylated congeners.⁴⁶ For example, some valylprolylvalylpentafluoroethyl ketones act as active inhibitors of human neutrophil elastase while the valylprolylvalyltrifluoromethyl ketones present no activity.^{46a}

C_2F_5Li has been successfully applied for pentafluoroethylation of carbonyl compounds and other electrophiles since 1985 that Gassman and O'Reilly reported the original work in this area.^{3,47} They found that pentafluoroethylolithium could be easily generated in situ by the exchange reaction between C_2F_5I and MeLi at $-78^\circ C$ (Scheme 2.15). This reaction was selective in many reported cases.



Scheme 2.15. Pentafluoroethylation reactions developed by Gassman and O'Reilly.

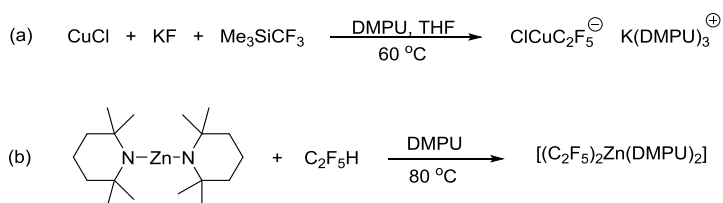
Then more developments have been done by other research groups.⁴⁸ For instance, Rösenthaler and coworkers performed C_2F_5Li by using the easily available and inexpensive pentafluoroethane (C_2F_5H).

Several efficient methods for the production of $C_2F_5^-$ carbanion have been reported⁴⁹⁻⁵² but neither they are nor the previous ones^{47,48} are not applicable to pentafluoroethylation of some organic halides like haloarenes. In addition by the Swarts reaction⁶ which industrially prepares trifluoromethylated aromatic compounds it is not possible to produce pentafluoroethylated aromatic counterparts.

The available synthetic methods for aromatic pentafluoroethylation found in the literature are two dozen or so. Moreover, the majority of them are limited in substrate scope and the number of functional groups. For instance, decarboxylative pentafluoroethylation of iodoarenes with $\text{CuI}/\text{C}_2\text{F}_5\text{CO}_2\text{M}$ ($\text{M} = \text{Na}, \text{K}, \text{Me}$) required high reaction temperature ($150\text{-}180\text{ }^\circ\text{C}$)⁵³ which assists the decarboxylation but it causes functional group incompatibility. Another source for pentafluoroethylation of aromatic iodides is C_2F_5 silane source ($\text{CuI}/\text{C}_2\text{F}_5\text{SiMe}_3/\text{KF}$ system)⁵⁴ that is costly for large scale operation, moreover low availability and limited functional group tolerance are other drawbacks.

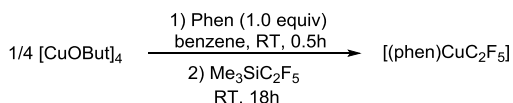
The mentioned protocols are all copper-mediated pentafluoroethylation of aromatic iodides. Although there are some reports of $\text{C}_2\text{F}_5\text{Cu(I)}$ complexes as fluoroalkylating agents and in this case the number of these complexes are less than in the case of $\text{CF}_3\text{Cu(I)}$ complexes but like in the case of $\text{CF}_3\text{Cu(I)}$ complexes ancillary ligands might affect the perfluoroalkylation.

Daugulis and coworkers detected the crystal structure of $[\text{K}(\text{DMPU})_3]^+[\text{Cu}(\text{C}_2\text{F}_5)\text{Cl}]^-$ that was extremely unstable and formed by thermal decomposition of a CuCF_3 derivative in just 14% yield (Scheme 2.16 (a)).^{55,13} Another X-ray structure reported in the same article was $[(\text{C}_2\text{F}_5)_2\text{Zn}(\text{DMPU})_2]$ in 59% yield as a first zincation of pentafluoroethane (Scheme 1.16 (b)).⁵⁵



Scheme 2.16. (a) Anionic copper complex characterized by X-ray crystallography. (b) Activation of pentafluoroethane by zinc characterized by X-ray crystallography.

Hartwig group reported stable $(\text{Phen})\text{CuC}_2\text{F}_5$ prepared from $[\text{CuOBU}^t]_4$ and $\text{C}_2\text{F}_5\text{SiMe}_3$ (Scheme 2.17) to be successfully used in the pentafluoroethylation of arylboronate esters and heteroaryl bromides.⁵⁶



Scheme 2.17. Synthesis of phenanthroline-ligated (pentafluoroethyl) copper (I) complex.

Grushin et al reported several $[\text{L}_n\text{CuC}_2\text{F}_5]$ complexes with X-ray structures (L = PPh_3 , bpy, Phen and IPr^*) that they were applied in pentafluoroethylation of acid chlorides.⁵⁷ Some of their crystal structures are shown in Figure 2.4.

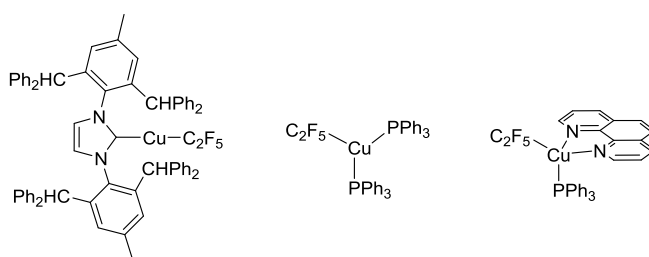
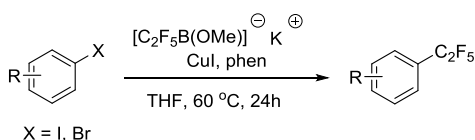


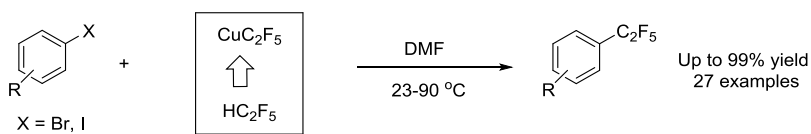
Figure 2.4. X-ray structures of $\text{C}_2\text{F}_5\text{Cu}(\text{I})$ complexes.

Recently, Amii and coworkers reported Cu-catalyzed aromatic pentafluoroethylation of haloarenes using potassium (pentafluoroethyl)trimethoxyborate.⁵⁸ The general process is exhibited in Scheme 2.18.



Scheme 2.18. Catalytic perfluoroalkylation of aryl halides.

As mentioned above the first cupration reaction of fluorocarbon was discovered by Grushin and coworkers.^{19a} For more developments they also examined this method for higher H-perfluoroalkanes. They found that $\text{C}_2\text{F}_5\text{H}$ underwent direct cupration process to give $\text{C}_2\text{F}_5\text{Cu}$ in almost quantitative yield (Scheme 2.19).⁵⁹ This reagent was successfully applied in the pentafluoroethylation of a number of substrates in high yields.⁵⁹ More details about $\text{C}_2\text{F}_5\text{H}$ -driven CuC_2F_5 reagent will be mentioned in chapter 2.2.



Scheme 2.19. Direct cupration of pentafluoroethane.

In the next two chapters the results of the research works using trifluoromethylated and pentafluoromethylated reagents will be fully discussed.

2.3. References

- (a) Hudlicky, M. *Chemistry of Organic Fluorine Compounds*; Ellis Horwood: New York, 1976. (b) Banks, R. E. *Organofluorine Chemicals and Their Industrial Applications*; Ellis Horwood: West Sussex, U.K., 1979. (c) Filler, R.; Kobayashi, Y. *Biomedical Aspects of Fluorine Chemistry*; Kodansha-Elsevier: New York, 1982. (d) Clark, J. H.; Wails, D.; Bastock, T. W. *Aromatic Fluorination*; CRC Press: Boca Raton, FL, 1996. (e) Hiyama, T.; Yamamoto, T., Eds. *Organofluorine Compounds Chemistry and Applications*; Springer, 2000. Kirsch, P. *Modern Fluoroorganic Chemistry*; Wiley-VCH: Weinheim, 2004. (f) Uneyama, K. *Organofluorine Chemistry*; Blackwell: Oxford, U. K., 2006. (g) Ojima, I. *Fluorine in Medicinal Chemistry and Chemical Biology*; Wiley-Blackwell: Chichester, U. K., 2009. (h) Petrov, V. A. *Fluorinated Heterocyclic Compounds. Synthesis, Chemistry and Applications*; Wiley: Hoboken, NJ, 2009.
- (a) Mykhailiuk, P. K. *Bielstein J. Org. Chem.* **2015**, 11, 16. (b) Xu, J.; Liu, X.; Fu, Y. *Tetrahedron Lett.* **2014**, 585.
- Gassman, P. G.; O'Reilly, N. J. *Tetrahedron Lett.* **1985**, 26, 5243.
- Lehmann, F. *Arch. Exptl. Path. Pharmacol.* **1928**, 130, 250.
- (a) Andrzejewska, M.; Yépez-Mulia, L.; Cedillo-Rivera, R.; Tapia, A.; Vilpo, L.; Vilpo, J.; Kazimierzczuk, Z. *Eur. J. Med. Chem.* **2002**, 37, 973. (b) Johansson, A.; Poliakov, A.; Åkerblom, E.; Wiklund, K.; Lindeberg, G.; Winiwarter, S.; Danielson, U. H.; Samuelsson, B.; Hallberg, A. *Bioorg. Med. Chem.* **2003**, 11, 2551.
- Filler, R. *Adv. Fluorine Chem.* **1970**, 6, 1.
- (a) McLoughlin, V. C. R.; Thrower, J. U.S. Patent 3408411, 1968. (b) McLoughlin, V. C. R.; Thrower, J. *Tetrahedron* **1969**, 25, 5921.

8. (a) Kobayashi, Y.; Kumadaki, I. *Tetrahedron Lett.* **1969**, 4095. (b) Sato, K.; Tarui, A.; Omote, M.; Ando, A.; Kumadaki, I. *Synthesis* **2010**, 1865.
9. Tomashenko, O. A.; Grushin, V. V. *Chem. Rev.* **2011**, 111, 4475.
10. For selected reviews, see: (a) Alonso, C.; Marigorta, E. M.; Rubiales, G.; Palacios F. *Chem. Rev.* **2015**, 115, 1847. (b) McClinton, M. A.; McClinton, D. A. *Tetrahedron* **1992**, 32, 6555. (c) Burton, D. J.; Yang, Z. Y. *Tetrahedron* **1992**, 48, 189.
11. Kondratenko, N. V.; Vechirko, E. P.; Yagupolskii, L. M. *Synthesis* **1980**, 932.
12. Burton, D. J.; Wiemers, D. M. *J. Am. Chem. Soc.* **1985**, 107, 5014.
13. Kremlev, M. M.; Tyrira, W.; Mushta, A. I.; Naumann, D.; Yagupolskii, Y. L. *J. Fluorine Chem.* **2010**, 131, 212.
14. Sanhueza, I. A.; Nielsen, M. C.; Ottiger, M.; Schoenebeck, F. *Helv. Chim. Acta* **2012**, 95, 2232.
15. (a) Kobayashi, Y.; Kumadaki, I.; Sato, S.; Hara, N.; Chikami, E. *Chem. Pharm. Bull.* **1970**, 18, 2334. (b) Kobayashi, Y.; Yamamoto, K.; Asai, T.; Nakano, M.; Kumadaki, I. *J. Chem. Soc., Perkin Trans. 1* **1980**, 2755. (c) Matsui, K.; Tobita, E.; Ando, M.; Kondo, K. *Chem. Lett.* **1981**, 1719. (d) Suzuki, H.; Yoshida, Y.; Osuka, A. *Chem. Lett.* **1982**, 135. (e) LeRoy, J.; Rubinstein, M.; Wakselman, C. *J. Fluorine Chem.* **1985**, 27, 291. (f) Burton, D. J.; Wiemers, D. M. *J. Am. Chem. Soc.* **1985**, 107, 5014.
16. MacNeil, J. G.; Burton, D. J. *J. Fluorine Chem.* **1991**, 55, 225.
17. Urata, H.; Fuchikami, T. *Tetrahedron Lett.* **1991**, 32, 91.
18. (a) Dubinina, G. G.; Furutachi, H.; Vicic, D. A. *J. Am. Chem. Soc.* **2008**, 130, 8600. (b) Dubinina, G. G.; Ogikubo, J.; Vicic, D. A. *Organometallics* **2008**, 27, 6233.
19. (a) Zanardi, A.; Novikov, M. A.; Martin, E.; Benet-Buchholz, J.; Grushin, V. V. *J. Am. Chem. Soc.* **2011**, 133, 20901. (b) Tomashenko, O. A.; Escudero-Adán E. C.; Martínez Belmonte, M.; Grushin, V. V. *Angew. Chem., Int. Ed.* **2011**, 50, 7655. (c) Weng, Z.; Lee, R.; Jia, W.; Yuan, Y.; Wang, W.; Feng, X.; Huang, K.-W. *Organometallics* **2011**, 30, 3229. (d) Konovalov, A. I.; Benet-Buchholz, J.; Martin, E.; Grushin, V. V. *Angew. Chem., Int. Ed.* **2013**, 52, 11637. (e) Jover, J.; Miloserdov, F. M.; Benet-Buchholz, J.; Grushin, V. V.; Maseras, F. *Organometallics* **2014**, 33, 6531.
20. Nakamura, Y.; Fujiu, M.; Murase, T.; Itoh, Y.; Serizawa, H.; Aikawa, K.; Mikami, K. *Beilstein J. Org. Chem.* **2013**, 9, 2404.
21. Oishi, M.; Kondo, H.; Amii, H. *Chem. Commun.* **2009**, 1909
22. For selected monographs, see: (a) Zhang, C. P.; Wang, Z. L.; Chen, Q. Y.; Zhang, C. T.; Gu, Y. C.; Xiao, J. C. *Angew. Chem., Int. Ed.* **2011**, 50, 1896. (b) Popov.,;

- Lindeman, S.; Daugulis, O. *J. Am. Chem. Soc.* **2011**, 133, 9286. (c) Morimoto, H.; Tsubogo, T.; Litvinas, N. D.; Hartwig, J. F. *Angew. Chem., Int. Ed.* **2011**, 50, 3793. (d) Weng, Z.; Lee, R.; Jia, W.; Yuan, Y.; Wang, W.; Feng, X.; Huang, K.-W. *Organometallics* **2011**, 30, 3229. (e) Li, Y.; Chen, T.; Wang, H.; Zhang, R.; Jin, K.; Wang, X.; Duan, C. *Synlett* **2011**, 1713. (f) Kondo, H.; Oishi, M.; Fujikawa, K.; Amii, H. *Adv. Synth. Catal.* **2011**, 353, 1247. (g) Kremlev, M. M.; Mushta, A. I.; Tyrra, W.; Yagupolskii, Y. L.; Naumann, D.; Müller, A. *J. Fluorine Chem.* **2012**, 133, 67. (h) Sanhueza, I. A.; Nielsen, M. C.; Ottiger, M.; Schoenebeck, F. *Helvetica Chim. Acta* **2012**, 95, 2231. (i) Chen, M.; Buchwald, S. L. *Angew. Chem., Int. Ed.* **2013**, 52, 11628. (j) Serizawa, H.; Aikawa, K.; Mikami, K. *Chem. Eur. J.* **2013**, 19, 17692. (k) Mulder, J. A.; Frutos, R. P.; Patel, N. D.; Qu, B.; Sun, X.; Tampone, T. G.; Gao, J.; Sarvestani, M.; Eriksson, M. C.; Haddad, N.; Shen, S.; Song, J. J.; Senanayake, C. H. *Org. Process Res. Dev.* **2013**, 17, 940. (l) Nakamura, Y.; Fujii, M.; Murase, T.; Itoh, Y.; Serizawa, H.; Aikawa, K.; Mikami, K. *Beilstein J. Org. Chem.* **2013**, 9, 2404. (m) Mormino, M. G.; Fier, P. S.; Hartwig, J. F. *Org. Lett.* **2014**, 16, 1744. (n) Serizawa, H.; Aikawa, K.; Mikami, K. *Org. Lett.* **2014**, 16, 3456. (o) Gonda, Z.; Kovács, S.; Wéber, C.; Gáti, T.; Mészáros, A.; Kotschy, A.; Novák, Z. *Org. Lett.* **2014**, 16, 4268.
23. Lishchynskyi, A.; Novák, P.; Grushin, V. V. In *Science of Synthesis: C-1 Building Blocks in Organic Synthesis 2*; van Leeuwen, P. W. N. M., Ed.; Thieme: Stuttgart, 2013; p. 367.
24. Li, X.; Zhao, J.; Zhang, L.; Hu, M.; Wang, L.; Hu, J. *Org. Lett.* **2015**, 17, 298.
25. Lin, X.; Hou, Ch.; Li, H.; Weng, Zh. *Chem. Eur. J.* **2016**, 22, 2075.
- 26.(a) Chu, L.; Qing, F.-L. *Org. Lett.* **2010**, 12, 5060. (b) Jiang, X.; Chu, L.; Qing, F.-L. *J. Org. Chem.* **2012**, 77, 1251 (c) Chu, L.; Qing, F.-L. *Acc. Chem. Res.* **2014**, 47, 1513.
27. Senecal, T. D.; Parsons, A.; Buchwald, S. L. *J. Org. Chem.* **2011**, 76, 1174.
28. (a) Liu, T.; Shao, X.; Wu, Y.; Shen, Q. *Angew. Chem., Int. Ed.* **2012**, 51, 540. (b) Huang, Y.; Fang, X.; Lin, X.; Li, H.; He, W.; Huang, K.-W.; Yuan, Y.; Weng, Z. *Tetrahedron* **2012**, 68, 9949. (c) Passet, M.; Oehlrich, D.; Rombouts, F.; Molander, G. A. *J. Org. Chem.* **2013**, 78, 12837.
29. (a) Litvinas, N. D.; Fier, P. S.; Hartwig, J. F. *Angew. Chem., Int. Ed.* **2012**, 51, 536. (b) Khan, B. A.; Buba, A. E.; Goßen, L. J. *Chem. Eur. J.* **2012**, 18, 1577.
30. Novák, P.; Lishchynskyi, A.; Grushin, V. V. *Angew. Chem., Int. Ed.* **2012**, 51, 7767.

31. For reviews of the Sandmeyer reaction, see: (a) Hodgson, H. H. *Chem. Rev.* **1947**, 40, 251. (b) Galli, C. *Chem. Rev.* **1988**, 88, 765. (c) Merkushev, E. B. *Synthesis* **1988**, 923.
32. Dai, J.-J.; Fang, C.; Xiao, B.; Yi, J.; Xu, J.; Liu, Z.-J.; Lu, X.; Liu, L.; Fu, Y. *J. Am. Chem. Soc.* **2013**, 135, 8436.
33. Bayarmagnai, B.; Matheis, C.; Risto, E.; Gooßen, L. *J. Adv. Synth. Catal.* **2014**, 356, 2343.
34. Wang, X.; Xu, Y.; Mo, F.; Ji, G.; Qiu, D.; Feng, J.; Ye, Y.; Zhang, S.; Zhang, Y.; Wang, J. *J. Am. Chem. Soc.* **2013**, 135, 10330.
35. Lishchynskiy, A.; Berthonb, G.; Grushin, V. V. *Chem. Commun.* **2014**, 50, 10237.
36. (a) Tiers, G. V. D. *J. Am. Chem. Soc.* **1960**, 82, 5513. (b) Drysdale, J. J.; Coffman, D. D. *J. Am. Chem. Soc.* **1960**, 82, 5111.
37. Dolbier, W. R., Jr. *Chem. Rev.* **1996**, 96, 1557.
38. Cowell, A. B.; Tamborski, C. *J. Fluorine Chem.* **1981**, 17, 345.
39. (a) Naumann, D.; Kischkewitz, J. *J. Fluorine Chem.* **1990**, 47, 283. (b) Naumann, D.; Wilkes, B.; Kischkewitz, J. *J. Fluorine Chem.* **1985**, 30, 73.
40. Tordeux, M.; Langlois, B.; Wakselman, C. *J. Chem. Soc., PerkinTrans. 1* **1990**, 2293.
41. Studer, A. *Angew. Chem., Int. Ed.* **2012**, 51, 8950.
42. Cheng, Y.; Yuan, X.; Ma, J.; Yu, sh. *Chem. Eur. J.* **2015**, 21, 8355 – 8359
43. Chu, L.; Qing, F.-L. *J. Am. Chem. Soc.* **2012**, 134, 1298.
44. Cai, S.; Chen, C.; Sun, Z.; Xi, C. *Chem. Commun.* **2013**, 49, 4552.
45. (a) Liang, T.; Neumann, C. N.; Ritter, T. *Angew. Chem., Int. Ed.* **2013**, 52, 8214. (b) Landelle, G.; Panossian, A.; Pazenok, S.; Vors, J.-P.; Leroux, F. R. Beilstein *J. Org. Chem.* **2013**, 9, 2476. (c) Prakash, G. K. S.; Wang, Y.; Mogi, R.; Hu, J.-B.; Mathew, T.; Olah, G. A. *Org. Lett.* **2010**, 12, 2932.
46. (a) Angelastro, M. R.; Baugh, L. E.; Bey, P.; Burkhart, J. P.; Chen, T.-M.; Durham, C S. L.; Hare, M.; Huber, E. W.; Janusz, M. J.; Koehl, J. R.; Marquart, A. L.; Mehdi, S.; Peet, N. P. *J. Med. Chem.* **1994**, 37, 4538. (b) Andrzejewska, M.; Yepez-Mulia, L.; Cedillo-Rivera, R.; Tapia, A.; Vilpo, L.; Vilpo, J.; Kazimierzczuk, Z. *Eur. J. Med. Chem.* **2002**, 37, 973. (c) Johansson, A.; Poliakov, A.; Åkerblom, E.; Wiklund, K.; Lindeberg, G.; Winiwarer, S.; Danielson, U. H.; Samuelsson, B.; Hallberg, A. *Bioorg. Med. Chem.* **2003**, 11, 2551. (d) Kokotos, G.; Hsu, Y.-H.; Burke, J. E.; Baskakis, C.; Kokotos, C. G.; Magrioti, V.; Dennis, E. A. *J. Med. Chem.* **2010**, 53, 3602. (e) Philippe, C.; Kaffy, J.;

- Milcent, T.; Bonnet-Delpon, D. *J. Fluorine Chem.* **2012**, 134, 136. (f) Nickisch, K.; Elger, W.; Cessac, J.; Kesavaram, N.; Das, B.; Garfield, R.; Shi, S.-Q.; Amelkina, O.; Meister, R. *Steroids* **2013**, 78, 255.
47. Gassman, P. G.; O'Reilly, N. J. *J. Org. Chem.* **1987**, 52, 2481.
48. (a) Schneider, M.; Marhold, A.; Kolomeitsev, A.; Kadyrov, A.; Rösenthaller, G.-V.; Barten, J. U.S. Patent 6,872,861, 2005. (b) Kolomeitsev, A. A.; Kadyrov, A. A.; Szczepkowska-Sztolcman, J.; Milewska, M.; Koroniak, H.; Bissky, G.; Barten, J. A.; Rösenthaller, G.-V. *Tetrahedron Lett.* **2003**, 44, 8273. (c) Shevchenko, N. E.; Nenajdenko, V. G.; Rösenthaller, G.-V. *J. Fluorine Chem.* **2008**, 129, 390. (d) Kazakova, O.; Rösenthaller, G.-V. In *Efficient Preparations of Fluorine Compounds*; Roesky, H. W., Ed.; Wiley: Hoboken, NJ, 2013; p 205 and references cited therein. (e) Nagaki, A.; Tokuoka, S.; Yamada, S.; Tomida, Y.; Oshiro, K.; Amii, H.; Yoshida, J.-i. *Org. Biomol. Chem.* **2011**, 9, 7559.
49. Uneyama, K.; Katagiri, T.; Amii, H. *Acc. Chem. Res.* **2008**, 41, 817.
50. (a) Krishnamurti, R.; Bellew, D. R.; Prakash, G. K. S. *J. Org. Chem.* **1991**, 56, 984. (b) Dilman, A. D.; Arkhipov, D. E.; Levin, V. V.; Belyakov, P. A.; Korlyukov, A. A.; Struchkova, M. I.; Tartakovsky, V. A. *J. Org. Chem.* **2008**, 73, 5643. (c) Prakash, G. K. S.; Wang, Y.; Mogi, R.; Hu, J.; Mathew, T.; Olah, G. A. *Org. Lett.* **2010**, 12, 2932.
51. (a) Petrov, V. A. *Tetrahedron Lett.* **2001**, 42, 3267. (b) Pooput, C.; Dolbier, W. R., Jr.; Médebielle, M. *J. Org. Chem.* **2006**, 71, 3564.
52. (a) Barhdadi, R.; Troupel, M.; Perichon, J. *Chem. Commun.* **1998**, 1251. (b) Russell, J.; Roques, N. *Tetrahedron* **1998**, 54, 13771.
53. (a) Carr, G. E.; Chambers, R. D.; Holmes, T. F.; Parker, D. G. *J. Chem. Soc., Perkin Trans. 1* **1988**, 921. (b) Freskos, J. N. *Synth. Commun.* **1988**, 18, 965. (c) Langlois, B. R.; Roques, N. *J. Fluorine Chem.* **2007**, 128, 1318. (d) Schareina, T.; Wu, X.-F.; Zapf, A.; Cotté, A.; Gotta, M.; Beller, M. *Top. Catal.* **2012**, 55, 426.
54. Urata, H.; Fuchikami, T. *Tetrahedron Lett.* **1991**, 32, 91.
55. I. Popov, S. Lindeman, O. Daugulis, *J. Am. Chem. Soc.* **2011**, 133, 9286.
56. (a) Morimoto, H.; Tsubogo, T.; Litvinas, N. D.; Hartwig, J. F. *Angew. Chem., Int. Ed.* **2011**, 50, 3793. (b) Litvinas, N. D.; Fier, P. S.; Hartwig, J. F. *Angew. Chem., Int. Ed.* **2012**, 51, 536. (c) Mormino, M. G.; Fier, P. S.; Hartwig, J. F. *Org. Lett.* **2014**, 16, 1744.
57. Panferova, L. I.; Miloserdov, F. M.; Lishchynskiy, A.; Belmonte, M. M.; Benet-Buchholz, J.; Grushin, V. V. *Angew. Chem., Int. Ed.* **2015**, 54, 5218.

58. Sugiishi, T.; Kawauchi, D.; Sato, M.; Sakai, T.; Amii, H. *Synthesis* **2017**, 49, 1874.
59. Lishchynskiy, A.; Grushin, V. V. *J. Am. Chem. Soc.* **2013**, 135, 12584.

Chapter 3.

Perfluoroalkylation of aromatic compounds

3.1 Continuous process for production of CuCF_3 via direct cupration of fluoroform

Mazloomi, Z.; Bansode, A.; Benavente, P.; Lishchynskiy, A.; Urakawa, A.; Grushin, V. *V. Org. Process Res. Dev.* **2014**, 18, 1020.

3.1.1. Introduction

Trifluoromethylated organic compounds play an important role in the synthesis of modern pharmaceuticals, agrochemicals, and specialty materials.^{1,2} Over the last 25 years, considerable progress has been made toward the development of efficient and selective methods for the introduction of the CF_3 group into a variety of organic substrates.² The vast majority of these methods, however, employ cost-prohibitive trifluoromethylating reagents and therefore cannot be used on an industrial scale.³

Fluoroform (CHF_3 , trifluoromethane, HFC-23, R-23) is a colorless gas (bp = -82.1 °C and mp = -155.2 °C) that is soluble in organic solvents and it is weakly acidic (pKa = 27 in H_2O).⁴ It is by far the best source of CF_3 group for the synthesis of trifluoromethylated building blocks^{2a-h,2r} by the following reasons:⁵

(1) Fluoroform is readily available and cheap. The fluorochemical and fluoropolymer industries sidegenerate large quantities of HFC-23 in chlorodifluoromethane (HCFC-22, R-22) manufacture. Approximately 20,000 t of HFC-23 that are produced annually⁷ lack applications on a commensurate scale.

(2) Fluoroform is nontoxic and ozone-friendly. Unlike many polyfluorinated small molecules, CHF_3 is not on the Montreal Protocol list of substances that deplete the ozone layer.

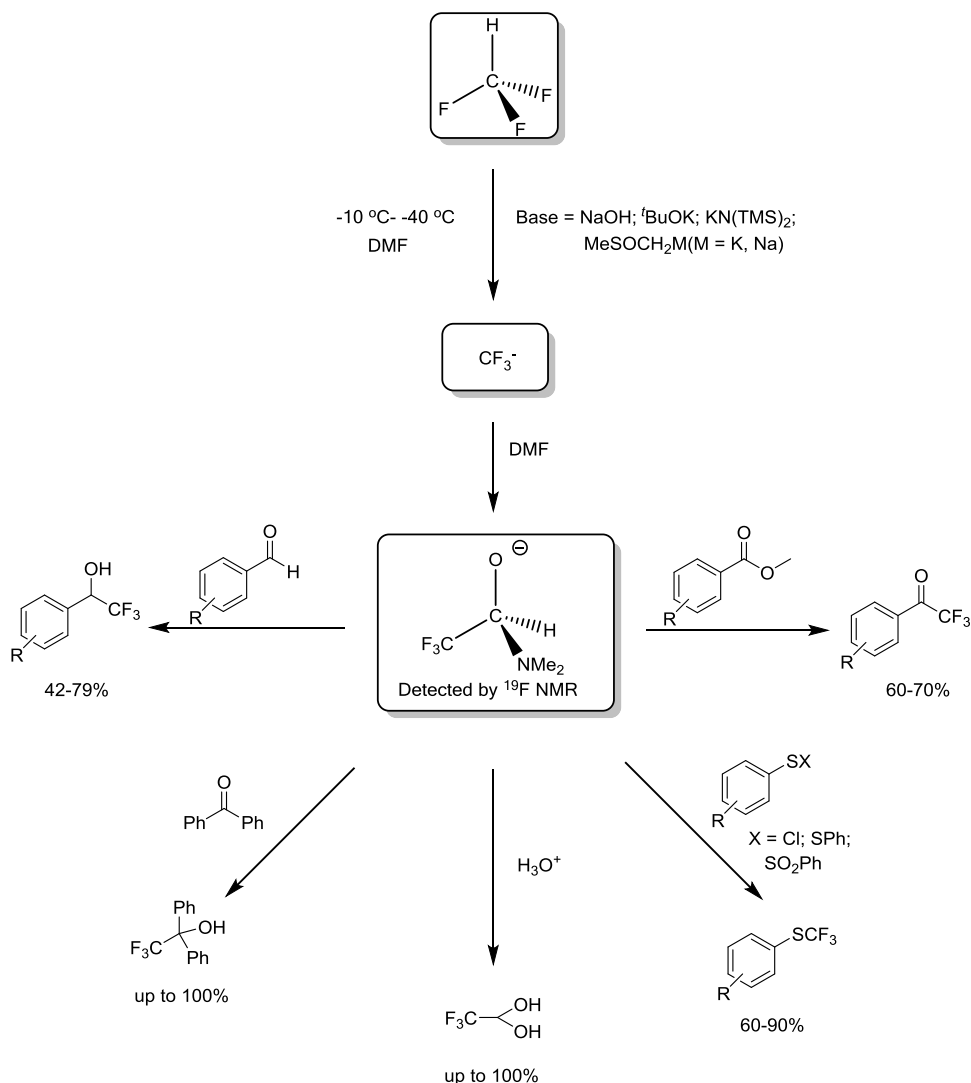
(3) As a CF_3 source for trifluoromethylation reactions, fluoroform is second to none in terms of atom economy.

(4) The extremely high warming potential of HFC-23 (11,700 times that of CO_2) and its long atmospheric lifetime (>250 years) have raised serious environmental concerns.⁶⁻⁸ To eliminate the risk of the so-called “climate bomb”,⁸ HFC-23 waste streams cannot be released into the atmosphere and therefore should be treated. The obviously preferred alternative to the costly destruction of HFC-23 is its use as a chemical feedstock for valuable fluorinated compounds.

Fluoroform is highly thermodynamically stable, the reported C-F and C-H bond activation energies are 106 and 127 kcal/mol respectively⁹ thus it is inert enough in a

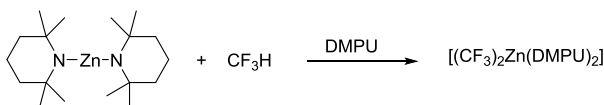
chemoselective reactions and activation of CHF_3 with low-cost materials for industrial applications is a significant challenge.^{5a}

The usual methodology for synthetic application of fluoroform was deprotonation of the weakly acidic CHF_3 (Scheme 3.1.1).¹⁰ This protocol is limited in large scale reactions for several reasons such as need of low temperatures to avoid the formation of difluorocarbene CF_2 by decomposition of the CF_3^- carbanion.



Scheme 3.1.1. Deprotonation of CHF_3 and its application in trifluoromethylation of carbonyl and sulfur electrophiles.

Another different approach to activate CHF_3 is metal-mediated C-H bond activation of fluoroform to form a stable M-CF_3 . Daugulis et al. communicated the first direct zincation of fluoroform in 2011 (Scheme 3.1.2).¹¹



Scheme 3.1.2. Fluoroform activation by zinc.

Later Grushin and coworkers reported the first direct cupration of fluoroform in 2011 (Scheme 3.1.3).¹²



Scheme 3.1.3. C-H activation of CHF_3 by copper.

Goldman and co-workers in 2011 showed oxidative addition of CHF_3 on an Ir-pincer complex¹³ and Takemoto and Grushin in 2013 reported the highly selective activation of CHF_3 by a palladium diphosphine complex.¹⁴ These complexes are represented in Figure 3.1.1.

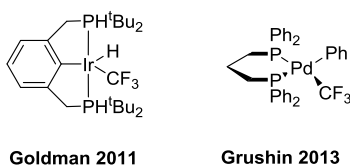
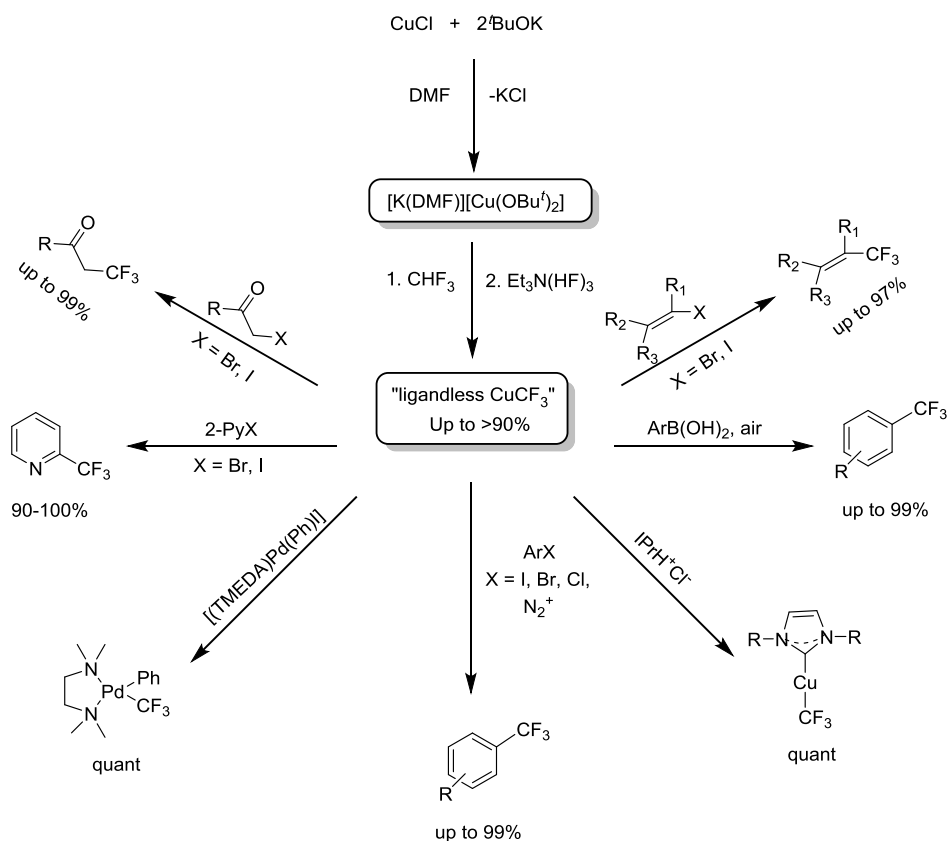


Figure 3.1.1. C-H bond activation of CHF_3 by Ir and Pd complexes.

Among the mentioned methods for utilization of fluoroform direct cupration reaction is more beneficial as it employs the best conditions such as room temperature, atmospheric pressure and low-cost substrates (the most expensive chemical used being potassium *tert*-butoxide) without using any ligand. In addition the group of Grushin has demonstrated the efficiency of “ligandless CuCF_3 ” for trifluoromethylation of different substrates in high yield with excellent selectivity (Scheme 3.1.4).^{12,15} Apart from CuCF_3 reagent there are several different methods for trifluoromethylation of

various organic substrates catalyzed by copper.¹⁶ There are some mechanism studies that show copper-mediated C-H bond activation of fluoroform.¹⁷



Scheme 3.1.4. Direct cupration of fluoroform and various trifluoromethylation reactions with CuCF_3 .

3.1.2. Objectives

Based on the evidences that mentioned above about the high efficiency of fluoroform-driven CuCF_3 reagent in a variety of high-yielding trifluoromethylation reactions,^{12,15} there is a demand for scale up the production of CuCF_3 reagent. In a nonindustrial batch setting, it was possible to perform the synthesis of CuCF_3 via direct cupration of fluoroform up to a 0.1 mol scale.^{15c}

Continuous flow systems have numerous advantages rather than batch operations¹⁸ for instance they serve as a safe and effective method for precise control of chemical

reactions and accurate temperature, pressure and residence time control can be achieved by applying continuous flow methodology.¹⁹

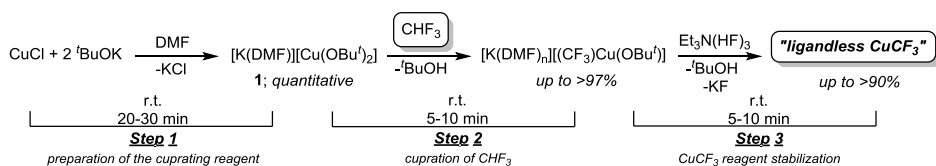
Considering the potential of fluoroform-driven CuCF_3 , we explored the possibility of making the direct cupration of fluoroform in a continuous flow manner to be able to handle it easily and scale up the production industrially.

The objective of the work describe in this chapter was to investigate the reliable continuous process for the production of CuCF_3 from CHF_3 and also demonstrate the efficiency of the CuCF_3 prepared in our flow setup which was as efficient a trifluoromethylating agent as the one performed in the batch system.

3.1.3. Results and discussion

3.1.3.1. Background and general considerations

The preparation of CuCF_3 from fluoroform consists of three steps that are shown in Scheme 3.1.5. In **Step 1**, a solution of the cuprating reagent is prepared by agitating CuCl and $t\text{BuOK}$ in a 1:2 molar ratio in DMF. The reaction is usually complete within 20-30 min in a batch reactor to give quantitatively the dialkoxycuprate $[\text{K}(\text{DMF})][\text{Cu}(\text{OBu}^t)_2]$ (**1**), whose solid state structure has been previously established by single-crystal diffraction.¹² As **1** goes into the DMF solution during the reaction, the KCl byproduct precipitates out. Although we conventionally separate the KCl precipitate by filtration, this is not critical for the next step and the overall CuCF_3 synthesis. What is critical, however, is to maintain rigorously anhydrous, air-free conditions throughout the preparation and use of **1** since this reagent is highly moisture- and O_2 -sensitive.

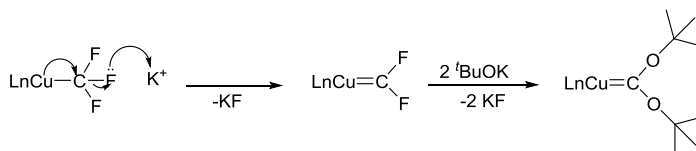


Scheme 3.1.5. Reaction sequence for the cupration of fluoroform.

A DMF solution of **1** prepared in **Step 1** is then used to cuprate fluoroform in **Step 2**. The reaction of CHF_3 with **1** occurs smoothly and quickly at room temperature and atmospheric pressure to give the CuCF_3 product within minutes. If carried out properly, the yield of the cupration reaction is reproducibly close to quantitative. Although the

product of **Step 2** is too unstable for isolation and structural characterization, sufficient evidence has been obtained^{20,21} for this compound being a mixed cuprate bearing one CF₃ and one ^tBuO ligand on the Cu(I) center, [K(DMF)_n][(CF₃)Cu(OBu^t)]. In particular, the treatment of the reaction solution obtained in **Step 2** with 18-crown-6 has been shown²⁰ to give [K(18-crown-6)][(CF₃)Cu(OBu^t)] (X-ray structure).

Once formed in **Step 2**, begins to decay¹² in some hours and it is not stable in order to be isolated and should be promptly stabilized with Et₃N·3HF (TREAT HF) or another HF source (for example Py(HF)_n) in **Step 3**. This stabilization serves the dual purpose of (i) sequestering, in the form of KF, the potassium ions that decompose the CF₃ group on Cu via to give Cu(I) carbene (Scheme 3.1.6)^{2r,12} and (ii) acidolyzing the ^tBuO-Cu bond to suppress the unwanted competition of t-butoxylation with the desired trifluoromethylation, as previously observed for some substrates.^{12,15c} The “ligandless” CuCF₃ reagent thus prepared can be stored in an inert atmosphere at room temperature for a few days without signs of significant decomposition.¹²



Scheme 3.1.6. α-F-elimination of CuCF₃ enforced by K⁺.

3.1.3.2. Flow process design and optimization

The above analysis provided guidelines for the development of a continuous process to produce CuCF₃ from fluoroform. In the current work, the cupration and stabilization steps (**Steps 2** and **3** in Scheme 3.1.5) were selected for continuous process development.²³ The cuprating reagent **1** was prepared separately and fed into the flow reactor using a syringe pump, as shown in Figure 3.1.2. Fluoroform gas was fed into the reactor through a separate line (Figure 3.1.2) by means of a mass flow controller (MFC). All experiments were carried out at room temperature (ca. 23 °C) and atmospheric pressure under argon. The results of a series of runs toward optimization of process efficiency and the yield of CuCF₃ are compiled in Table 2.1.1. In all experiments, the concentration of **1** in DMF was close to the solubility limit (0.48 M). The yield of the CuCF₃ was monitored by ¹⁹F NMR analysis with an internal standard every 5-10 min during each run. In the first 2-3 min, the yield of CuCF₃ was lower because of the presence of residual traces of air in the system and the time required for

the addition and efficient mixing of the reagents in the reactor to synchronize and level off. During this short initial period prior to system stabilization, the yield invariably increased to plateau for the rest of the run. It is these yields of fluoroform-derived CuCF_3 that are presented in Table 3.1.1 and discussed throughout this report.

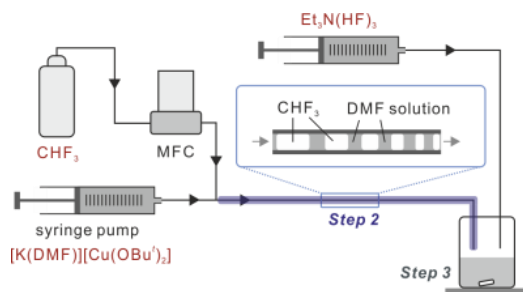


Figure 3.1.2. Flow process setup for the production of CuCF_3 from fluoroform.

Table 3.1.1. Cupration of CHF_3 in a flow reactor.

Entry ^a	Tube length, m	CHF_3 , equiv	CHF_3 addition rate, mL min^{-1}	Residence time, min	CuCF_3 yield, % ^b
1	0.61	2	6	1.25	85
2	1.04	2	6	2.00	87
3	1.40	2	6	2.50	94
4	1.52	2	6	2.75	94
5	1.53	1.5	4.5	6.00	90
6	1.95	1.5	4.5	8.83	92
7	2.32	1.5	4.5	9.33	94
8	2.73	1.5	4.5	11.33	88
9	1.10	1.2	3.6	5.58	75
10	1.32	1.2	3.6	8.83	86
11	1.53	1.2	3.6	11.83	79

^(a) In all experiments, the rates of addition of **1** in DMF (0.48 M) and TREAT HF in DMF (2.00 M) were 18 mL h^{-1} and 1.5 mL h^{-1} , respectively. ^(b) ^{19}F NMR yield determined with an internal standard.

Initially, the flow rates of **1** in DMF and fluoroform were set to 18 mL h^{-1} and 6 mL min^{-1} , respectively, in order to maintain the CHF_3 to Cu ratio at 2:1 (Table 3.1.1, entries 1-4). The residence time (RT), i.e. the reaction time before the addition of TREAT HF, was controlled by the length of the reaction zone, a 1.55 mm inner diameter PTFE (polytetrafluoroethylene; Teflon) tube. As pictorially shown in Figure 3.1.2, the volume of the fluoroform gas decreased as it moved inside the cupration reaction zone due to

dissolution and reaction with **1**. Changing RT from 1.25 to 2.00 and then to 2.50 min led to an increase in the yield of CuCF₃ from 85% to 87%, and to 94%, respectively (entries 1-3); a further increase in RT to 2.75 min, however, did not affect the yield (entry 4). Although the best yield of 94% obtained in this series of experiments (entries 3 and 4) was as high as that from the batch process,¹¹ further optimization was performed in order to minimize the amount of CHF₃ used. Toward this goal, the fluoroform feed rate was lowered to 4.5 mL min⁻¹ to change the CHF₃ to Cu ratio to 1.5. By subsequently varying RT in a 6.00-11.33 min range (entries 5-8) we found the optimal value of 9.33 min for the formation of CuCF₃ in the highest possible yield of 94% (entry 7). Still high yet slightly lower yields (88-92%) resulted from both shorter (entries 5 and 6) and longer (entry 8) reaction times. Finally, a series of runs were performed with a CHF₃ to Cu ratio of 1.2 that was achieved by slowing the fluoroform feed rate to 3.6 mL min⁻¹. In these experiments, the yield of CuCF₃ passed through a maximum (86%; entry 10) at RT = 8.83 min, an intermediate value between the other two points (entries 9 and 11). The lower CHF₃ concentration in these three runs resulted in slower cupration rates and hence the CuCF₃ product began to decompose (see above)¹¹ to a noticeable extent even before full conversion could be reached. While at the shorter RT of 5.58 min (entry 9) the yield of CuCF₃ was only 75% because of incomplete conversion, the longer RT of 11.83 min (entry 11) resulted in partial decomposition of the product, resulting in 79% yield. It is believed, however, that an engineering solution could be found for the cupration of CHF₃ in a continuous manner in over 90% yield while using CHF₃ in only 20% excess and even less. One option is to run the process at an increased pressure in the reaction zone. Another possibility is to recycle and reuse the easily separable fluoroform gas from the head space of the receiver during the process employing CHF₃ in the 1.5-fold excess that is sufficient to obtain CuCF₃ in 94% yield under normal pressure (entry 7). Performing such experiments, however, was beyond the scope of our work.

In all of the experiments described above, the stabilization of CuCF₃ was performed by adding TREAT HF to the receiving vessel, as shown in Figure 2.1.2. An alternative setup with a T-connector at the end of the cupration reaction zone for TREAT HF addition was also tested but found less efficient (~70% yield). The inferior results were caused by the KF precipitate produced in the stabilization step, thereby preventing the free passage of the reaction mixture through the small diameter tube and eventually

clogging the system. Although increasing the reactor tube diameter could eliminate this problem, such further developments are the subject of a separate project.

3.1.3.3. Trifluoromethylation reactions with CuCF_3 produced in the flow process

Having developed and optimized the continuous flow synthesis of CuCF_3 from fluoroform, we examined the usefulness of the thus prepared reagent for a series of known trifluoromethylation reactions. In these studies we used the temperature and reactant ratios previously found and optimized for the analogous transformations^{15a-c} performed with the CuCF_3 reagent from the batch process.¹² The different setups used in the current studies are shown in Figure 3.1.3 and a summary of the results is presented in Table 3.1.2. All yields were determined by ^{19}F NMR because isolation procedures for the products forming in these reactions have been developed and reported previously.^{15a-c}

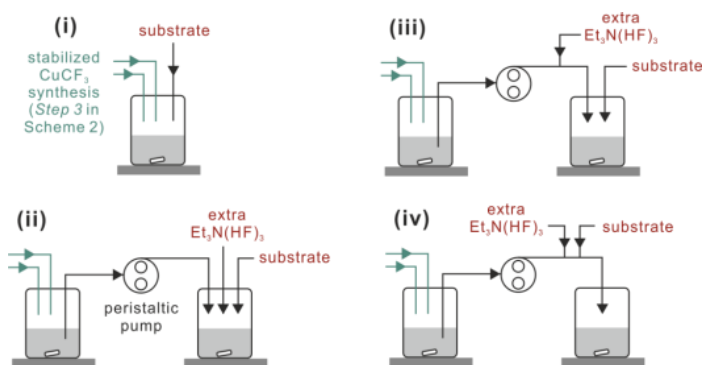


Figure 3.1.3. Four different configurations for the trifluoromethylation reactions with the CuCF_3 reagent from the continuous flow process.

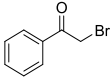
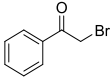
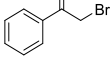
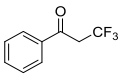
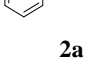
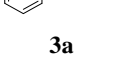
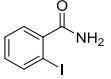
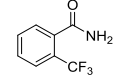
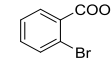
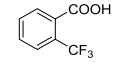
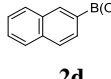
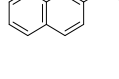
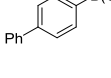
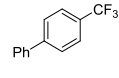
First, the trifluoromethylation reaction of 2-bromoacetophenone (**2a**)^{15a} was examined using configuration (i). In that experiment (Table 2.1.2, entry 1), TREAT HF was employed in superstoichiometric quantities (0.63 mol per mol Cu; see the Experimental Section for specifics). Of the total of 0.63 mol of TREAT HF used, 0.33 mol (1 equiv) was required for the conventional stabilization of the copper reagent (Scheme 3.1.5), whereas the extra 0.30 mol was needed to avoid the HF elimination from the desired trifluoromethylated product.^{15b} As the CuCF_3 was produced and

stabilized with TREAT HF in excess, a solution of **2a** was fed simultaneously to the glass receiver/reactor at such a rate so as to maintain the CuCF₃ to substrate ratio at 1.2. Under such conditions, **2a** was trifluoromethylated in 72–73% yield (Table 3.1.2, entry 1). This yield was noticeably lower than that (93–96%) previously reported^{15b} for the same reaction with the CuCF₃ reagent from the batch process. In the latter, however, the CuCF₃ was first prepared and stabilized with only 1 equiv of HF from TREAT HF and then used for the reaction in the presence of an additional amount of TREAT HF.^{15b} The lower yields obtained under the current flow conditions were caused by the enhanced side formation of the hydrodebromination product, acetophenone (~12% by GC–MS). This undesired hydrodebromination was likely prompted by the reasonably DMF-soluble KHF₂, generated from extra HF and KF formed upon addition of superstoichiometric amounts of TREAT HF to the just produced unstabilized CuCF₃ solution. In contrast, the stabilization with *stoichiometric* quantities of TREAT HF produces only KF that is poorly soluble in DMF and efficiently precipitates out on standing. In this way, virtually potassium-free CuCF₃ solutions are produced,¹² to which extra TREAT HF can be added^{15b} without the risk of KHF₂ formation. The trifluoromethylation of α -haloketones with such fluoroform-derived CuCF₃ solutions containing extra TREAT HF, but not KHF₂, is significantly higher yielding and chemoselective, producing only very small quantities, if any, of the hydrodehalogenation side-products.^{15b} However, a substantially more complex flow setup would be required to perform the trifluoromethylation of α -haloketones with such KHF₂-free, TREAT HF-enriched CuCF₃ reagent in a fully continuous manner.

Considering the above, we tested the three other configurations (ii), (iii), and (iv) shown in Figure 3.1.3 for the trifluoromethylation of **2a**. In all these experiments, the CuCF₃ stabilized with 0.33 mol of TREAT HF per 1 mol of Cu was prepared using the flow reactor (Figure 3.1.2), as described above. The resultant reagent solution was then transferred with a peristaltic pump to a glass reactor for the trifluoromethylation to be performed. Using configuration (ii), the required extra amount of TREAT HF, **2a**, and the already stabilized CuCF₃ were fed into the reactor simultaneously. In this way, **3a** was produced in 85–87% yield (Table 3.1.2, entry 2), nearly as high as the best yields reported previously for the batch method.^{15b} With configuration (iii), extra TREAT HF (0.2 equiv) was first added to the already stabilized CuCF₃, which was then used for the reaction with **2a**. This technique afforded **3a** in a yield (81–83%) that was indistinguishable, within the determination error, from the one achieved in the setup (ii)

experiment (entries 2 and 3). It is worth noting that the error of yield determination by ^{19}F NMR is at least $\pm 5\%$. Performing the trifluoromethylation of **2a** in a continuous manner with setup (iv) using a T-connection (Figure 3.1.3) resulted in a lower yield of **3a** (75%, entry 4) because of precipitation of inorganic copper byproducts and eventual clogging of the tube. As expected, the side formation of acetophenone in the trifluoromethylations of **2a** performed with the two-step addition of TREAT HF in configurations (ii)–(iv) did not exceed 4–6%, whereas the all at-once TREAT HF addition method gave $\sim 12\%$ of the hydrodebrominated side-product.

Table 3.1.2. Trifluoromethylation of different substrates with fluoroform-derived CuCF_3 produced in the flow process.

Entry ^a	Substrate	CuCF_3 , equiv	Extra $\text{Et}_3\text{N}\cdot 3\text{HF}$, equiv	t, (h) ^b	product	Yield, % ^c	setup ^d
1		1.2	0.3	0.25		72-73	(i)
2		1.3	0.2	0.25		85-87	(ii)
3		1.3	0.2	0.25		80-83	(iii)
4	2a	1.3	0.2	0.25	3a	71-75	(iv)
5		1.1	0.2	0.25		79-85	(ii)
	2b				3b		
6		1.1	0	0.25		80-89	(ii) (iii) ^e
	2c				3c		
7 ^f		2	0	1.0		92-99	(ii) (iii) ^e
	2d				3d		
8 ^f		2	0	0.5		99	(ii) (iii) ^e
	2e				3e		

^(a) All reactions were performed at 23 °C, using CuCF_3 prepared in the optimized flow process (Table 2.1.1, entry 7). ^(b) Reaction time after mixing the substrate with CuCF_3 . ^(c) Yields determined by ^{19}F NMR. ^(d) See Figure 2.1.2 for setup configurations. ^(e) No extra TREAT HF used. ^(f) Reactions performed in air.

The results described above indicated that configurations (ii) and/or (iii) should be used for further runs, in which we intended to trifluoromethylate aromatic substrates. Thus, 2-iodobenzamide (**2b**) and 2-bromobenzoic acid (**2c**) were trifluoromethylated

using configuration (ii) to give **3b** and **3c** in 79–85% and 80–89% yield, respectively (Table 3.1.2, entries 5 and 6). These yields are nearly identical with those (82–87%) previously reported for the same transformations employing the CuCF₃ reagent from the batch preparation.^{15c} It is noteworthy that no extra TREAT HF was needed for the reaction of **2c** that bears an acidic functionality (COOH). Finally, we performed oxidative trifluoromethylation of 2-naphthylboronic acid (**2d**) and 4-biphenylboronic acid (**2e**) with CuCF₃ produced in the continuous process. As in the reported^{15a} batch method, both reactions were performed in open air, without extra TREAT HF to give **3d** and **3e** quantitatively (entries 7 and 8).

3.1.4. Conclusions

We have successfully demonstrated the first continuous flow process for the synthesis of the valuable trifluoromethylating reagent CuCF₃ via the direct cupration of fluoroform. The reaction smoothly occurs at room temperature and atmospheric pressure. Under optimized conditions, the yield of CuCF₃ in the flow reactor (up to 94%) is as high as in the previously developed batch process. The continuously produced CuCF₃ has been found to trifluoromethylate a number of organic substrates with excellent efficiencies and yields comparable to those previously observed for the same reagent prepared by the batch methodology. It is hoped that the demonstrated feasibility of the flow synthesis of the low-cost fluoroform-derived CuCF₃ adds to its attractiveness as a trifluoromethylating reagent for larger-scale operations.

3.1.5. Experimental section

3.1.5.1. General information

Fluoroform (98%) in a cylinder was purchased from Apollo Scientific. All other chemicals and solvents were purchased from Aldrich, Alfa Aesar, TCI, and Acros chemical companies. Anhydrous DMF (Alfa Aesar or from an MBraun SPS) was stored over freshly calcined 4 Å molecular sieves in a glovebox. All manipulations were performed under argon, unless noted otherwise. NMR spectra were obtained with a Bruker Avance 400 Ultrashield NMR spectrometer. Quantitative ¹⁹F NMR analyses were carried out with D1 = 5 s. An Agilent Technologies 7890A chromatograph equipped with a 5975C MSD unit was used for GC–MS analysis.

3.1.5.2. Continuous reaction system

Gaseous fluoroform was fed into the system (Figure 3.1.2) by a thermal mass flow controller (MFC, Alicat Scientific) calibrated for CHF_3 . A PTFE tube of 3.25 mm outer diameter and 1.55 mm inner diameter was used as both the reactor and connector between the syringes and valves with standard SS-316 compression fittings (Hy-Lok). The MFC outlet was connected to an SS-316 T-piece where the solution of **1** and gaseous CHF_3 met and were mixed together. An in-house fabricated PTFE adapter facilitated the coupling of the syringe to the reaction system. To keep solutions of **1** and TREAT HF in syringes isolated from oxygen and moisture during the transfer from the glovebox to the reaction system, a standard 1/8 in. ball valve was fitted on the PTFE adapter. The liquid reagents were transferred to a syringe of appropriate volume and fed to the reaction system using high-accuracy syringe pumps (Fisher Scientific). The outlet streams were connected via PTFE-to-glass fittings (Bola, Germany) to a glass receiver/reactor for the stabilization with TREAT HF (Step 3). The receiver/reactor was equipped with a stopcock for evacuation/backfilling with argon, an airlock to maintain a slow argon flow throughout the experiment, and a PTFE-coated magnetic stir bar for continuous agitation. A TREAT HF solution was added to the receiver/reactor using a separate syringe pump. In the trifluoromethylation experiments, the CuCF_3 solution product was pumped out continuously from the glass receiver/reactor using a peristaltic pump and fed to the second glass reactor or premixed with the substrate, depending on the configuration employed (see above, Figure 3.1.3 and Table 3.1.2). Vigorous agitation of the trifluoromethylation reaction mixtures was used in all experiments.

3.1.5.3. Preparation of $[\text{K}(\text{DMF})][\text{Cu}(\text{O}i\text{Bu})_2]$ (**1**)¹² and the continuous cupration of fluoroform

In a glovebox, a mixture of CuCl (purity 99%; 1.50 g; 15.1 mmol), KO^iBu (purity 97%; 3.54 g; 30.6 mmol), and DMF (25 mL) was vigorously stirred for 30 min at room temperature. The precipitated KCl was filtered off and washed on the filter with DMF (5 mL). To the combined filtrate and the washing, was added PhF (purity 99%; 0.42 mL; 4.5 mmol) as an internal standard for CuCF_3 yield determination. The thus prepared solution was placed in a 20 mL syringe. A 2 M solution of TREAT HF in DMF prepared inside the glovebox from 3.3 mL (20 mmol) of TREAT HF in a 10 mL graduated flask was placed in a 10 mL syringe. Both syringes equipped with PTFE

adapters fitted with 1/8 in. ball valves were brought out and connected to the continuous flow reactor. After the system was evacuated to ~1–2 mbar and backfilled with argon three times, the flow synthesis was commenced. As described above, the yield of CuCF₃ in the first 2–3 min of the run was always lower, and the product solution was dark because of partial decomposition with trace residual air in the system. After this initial period, the solution produced was pale yellow, and the CuCF₃ yield was consistently high (see Table 3.1.1 for specifics), as established by frequent ¹⁹F NMR monitoring (every 5–10 min).

3.1.5.4. Preparation of trifluoromethylated compounds under flow conditions

3,3,3-Trifluoro-1-phenylpropan-1-one (3a; Table 3.1.2, entries 1–4).

Procedure A (entry 1). Configuration (i) shown in Figure 2.1.3 was used. All reaction solutions for the synthesis were prepared inside a glovebox and placed in syringes equipped with PTFE adapters fitted with 1/8 in. ball valves. A 5 mL syringe was charged with 2.9 mL of a DMF solution of 2-bromoacetophenone (**2a**; 995 mg; 5.00 mmol; [**2a**] = 1.72 M) and 1,3-bis(trifluoromethyl)benzene (194 μL; 1.25 mmol; internal standard). A 20 mL syringe was filled up with a 0.48 M solution of **1** in DMF prepared as described above. A 10 mL syringe was charged with 5 mL of a 2 M TREAT HF solution prepared as described above. The three syringes were brought out and connected to the reaction system of configuration (i) shown in Figure 3.1.3, and the continuous cupration process was commenced using the parameters specified in entry 7 of Table 1, except that the rate of addition of the TREAT HF solution was 2.9 mL h⁻¹. The first ~2 mL portion of the dark, partially oxidized CuCF₃ solution product was completely removed from the receiver/ reactor and discarded. ¹⁹F NMR analysis of the fully withdrawn next, light-yellow 1 mL fraction of the product indicated 90% yield of CuCF₃. At that point, the addition of the solution of **2a** was started at a rate of 3.87 mL h⁻¹ as the CuCF₃ was continuously produced. After ~3 mL of the reaction mixture accumulated in the reactor, the entire amount was withdrawn via syringe, kept under argon for an additional 15 min, and treated with ~10 mL of water and ~4 mL of ether in air. After agitation, the organic layer was separated and filtered through a short silica gel plug. Quantitative ¹⁹F NMR analysis of the filtrate indicated that **3a** was produced in 73% yield. ¹⁹F NMR, δ: = -61.2 (t, J = 10.3 Hz). ¹³b Acetophenone (~11%) was detected

in the filtrate by GC–MS. The continuously produced reaction mixture was withdrawn from the reactor two more times. Analysis of these two fractions as described above indicated 73% and 72% yield of **3a** (^{19}F NMR) and ~12% and ~12% of acetophenone (GC–MS).

Procedure B (entry 2). Configuration (ii) shown in Figure 3.1.3 was used. CuCF_3 in DMF was prepared as described in Table 3.1.1 (entry 7) in 92% yield. After the KF byproduct had settled at the bottom of the receiver, the solid-free supernatant was pumped into the glass reactor with the peristaltic pump through a PTFE tube equipped with a microfiber filter at the inlet. Simultaneously, solutions of **2a** and TREAT HF in DMF were fed to the same reactor via two independently operating syringe pumps. A 5 mL syringe was used for the addition of the substrate solution (2.8 mL) in DMF containing **2a** (995 mg; 5.00 mmol; $[\mathbf{2a}] = 1.79 \text{ M}$) and 1,3-bis(trifluoromethyl)-benzene (194 μL ; 1.25 mmol; internal standard). The TREAT HF solution (2 M; 4 mL) was added via a 10 mL syringe. The rates of addition of the CuCF_3 , **2a**, and TREAT HF solutions were 19 mL h^{-1} , 3.34 mL h^{-1} , and 0.9 mL h^{-1} , respectively. After the first ~3 mL portion was discarded, three sequential fractions of ~3 mL each were withdrawn and analyzed by ^{19}F NMR and GC–MS as described above. The yields of **3a** (acetophenone) were 85 (5)%, 87 (5)%, and 85 (4)%.

Procedure C (entry 3). CuCF_3 in DMF was prepared as described in Table 3.1.1 (entry 7) in 91% yield. After the KF byproduct had settled at the bottom of the receiver, the solidfree supernatant was pumped into the glass reactor with the peristaltic pump through a PTFE tube equipped with a microfiber filter at the inlet. Simultaneously, solutions of **2a** and TREAT HF in DMF were fed to the system via two independently operating syringe pumps, as shown in Figure 3, setup (iii). A 5 mL syringe was used for the addition to the reactor of the substrate solution (2.8 mL) in DMF containing **2a** (995 mg; 5.00 mmol; $[\mathbf{2a}] = 1.79 \text{ M}$) and 1,3-bis(trifluoromethyl)benzene (194 μL ; 1.25 mmol; internal standard). The TREAT HF solution (2 M; 4 mL) was added via a 10 mL syringe into the CuCF_3 solution flow. The rates of addition of the CuCF_3 , **2a**, and TREAT HF solutions were 19 mL h^{-1} , 3.30 mL h^{-1} , and 0.9 mL h^{-1} , respectively. After the first ~3 mL portion was discarded, three sequential fractions of ~3 mL each were withdrawn and analyzed by ^{19}F NMR and GC–MS as described above. The yields of **3a** (acetophenone) were 81 (4)%, 80 (5)%, and 83 (5)%.

Procedure D (entry 4). CuCF_3 in DMF was prepared as described in Table 3.1.1 (entry 7) in 94% yield. After the KF byproduct had settled at the bottom of the receiver, the

solidfree supernatant was pumped into the glass reactor with the peristaltic pump through a PTFE tube equipped with a microfiber filter at the inlet. Simultaneously, solutions of **2a** and TREAT HF in DMF were fed to the flow of the CuCF₃ reagent solution via two independently operating syringe pumps, as shown in Figure 3.1.3, setup (iv). A 5 mL syringe was used for the addition of the substrate solution (2.8 mL) in DMF containing **2a** (995 mg; 5.00 mmol; [**2a**] = 1.79 M) and 1,3-bis(trifluoromethyl)benzene (194 μ L; 1.25 mmol; internal standard). The TREAT HF solution (2 M; 4 mL) was added via a 10 mL syringe into the CuCF₃ solution flow. The rates of addition of the CuCF₃, **2a**, and TREAT HF solutions were 19 mL h⁻¹, 3.49 mL h⁻¹, and 0.9 mL h⁻¹, respectively. As the reaction occurred in the tube, a solid was produced. Three sequential fractions of \sim 3 mL each were withdrawn from the reactor and analyzed by ¹⁹F NMR and GC–MS as described above. The yields of **3a** (acetophenone) were 71 (6)%, 75 (5)%, and 74 (4)%. Also, unreacted **2a** (\sim 5%) was detected in the first fraction by GC–MS. A few min after the third fraction was withdrawn, signs of clogging of the system with the solid byproduct were observed and the experiment was stopped.

2-(Trifluoromethyl)benzamide (3b; Table 3.1.2, entry 5). Configuration (ii) shown in Figure 3.1.3 was used. CuCF₃ in DMF was prepared as described in Table 3.1.1 (entry 7) in 88% yield. After the KF byproduct had settled at the bottom of the receiver, the solid-free supernatant was pumped into the glass reactor with the peristaltic pump through a PTFE tube equipped with a microfiber filter at the inlet. Simultaneously, solutions of **2b** and TREAT HF in DMF were fed to the same reactor via two independently operating syringe pumps. A 5 mL syringe was used for the addition of the substrate solution (2.8 mL) in DMF containing **2b** (617 mg; 2.50 mmol; [**2b**] = 0.89 M) and 1,3-bis(trifluoromethyl)benzene (194 μ L; 1.25 mmol; internal standard). The TREAT HF solution (2 M; 4 mL) was added via a 10 mL syringe. The rates of addition of the CuCF₃, **2b**, and TREAT HF solutions were 19 mL h⁻¹, 7.77 mL h⁻¹, and 0.9 mL h⁻¹, respectively. Three sequential fractions of \sim 3 mL each were withdrawn and analyzed by ¹⁹F NMR “as is”. The yields of **3b** were 85%, 83%, and 79%. ¹⁹F NMR, δ : -58.3 (s).^{13c} After treatment of the samples with H₂O/ether, the organic layers were analyzed by GC–MS. No side products were detected. A small quantity of the starting material (**2b**) was detected in the third fraction but not in the first two.

2-(Trifluoromethyl)benzoic acid (3c; Table 2.1.2, entry 6). Configuration (ii) or (iii) shown in Figure 3.1.3 was used (no extra TREAT HF). CuCF_3 in DMF was prepared as described in Table 2.1.1 (entry 7) in 88% yield. After the KF byproduct had settled at the bottom of the receiver, the solid-free supernatant was pumped into the glass reactor with the peristaltic pump through a PTFE tube equipped with a microfiber filter at the inlet. Simultaneously, a solution of **2c** was fed to the same reactor via a syringe pump. A 5 mL syringe was used for the addition of the substrate solution (2.4 mL) in DMF containing **2c** (503 mg; 2.50 mmol; $[\mathbf{2c}] = 1.04 \text{ M}$) and 1,3-bis(trifluoromethyl)benzene (194 μL ; 1.25 mmol; internal standard). The rates of addition of the CuCF_3 and **2c** solutions were 19 mL h^{-1} , and 6.49 mL h^{-1} , respectively. Four sequential fractions of $\sim 3 \text{ mL}$ each were withdrawn and analyzed by ^{19}F NMR “as is”. The yields of **3c** were 80%, 88%, 88%, and 89%. ^{19}F NMR, δ : -58.4 (s) .^{13c}

2-(Trifluoromethyl)naphthalene (3d; Table 3.1.2, entry 7). Configuration (ii) or (iii) shown in Figure 3.1.3 was used (no extra TREAT HF). CuCF_3 in DMF was prepared as described in Table 3.1.1 (entry 7) in 89% yield. After the KF byproduct had settled at the bottom of the receiver, the solid-free supernatant was pumped into the glass reactor with the peristaltic pump through a PTFE tube equipped with a microfiber filter at the inlet. Simultaneously, a solution of **2d** (430 mg; 2.50 mmol) and 4,4'-difluorobiphenyl (178 mg; 0.94 mmol; internal standard) in a mixture of DMF (1.2 mL) and toluene (2.0 mL) of 3.8 mL total volume ($[\mathbf{2d}] = 0.66 \text{ M}$) was fed to the reactor in air via a syringe pump. The rates of addition of the CuCF_3 and **2d** solutions were 19 mL h^{-1} and 5.68 mL h^{-1} , respectively. Three sequential fractions of $\sim 3 \text{ mL}$ each were withdrawn. Each fraction was vigorously agitated in air for 1 h and then treated with H_2O /ether, and the organic layers were analyzed by ^{19}F NMR. The yields of **3d** were 92%, 99%, and 99%. ^{19}F NMR, δ : -62.7 (s) .^{13a} The yield of naphthalene in these fractions was 4%, 2%, and 1%, respectively (GC-MS).

4-(Trifluoromethyl)biphenyl (3e; Table 2.1.2, entry 8). Configuration (ii) or (iii) shown in Figure 3.1.3 was used (no extra TREAT HF). CuCF_3 in DMF was prepared as described in Table 3.1.1 (entry 7) in 91% yield. After the KF byproduct had settled at the bottom of the receiver, the solid-free supernatant was pumped into the glass reactor with the peristaltic pump through a PTFE tube equipped with a microfiber filter at the inlet. Simultaneously, a solution of **2e** (495 mg; 2.50 mmol) and 4,4'-difluorobiphenyl (178 mg; 0.94 mmol; internal standard) in a mixture of DMF (1.0 mL) and toluene (3.4 mL) of 4.9 mL total volume ($[\mathbf{2e}] = 0.51 \text{ M}$) was fed to the reactor in air via a

syringe pump. The rates of addition of the CuCF₃ and **2e** solutions were 19 mL h⁻¹ and 7.54 mL h⁻¹, respectively. Four sequential fractions of ~3 mL each were withdrawn. Each fraction was vigorously agitated in air for 0.5 h and then treated with H₂O/ether, and the organic layers were analyzed by ¹⁹F NMR. The yields of **3e** were 99%, 98%, 99%, and 98%. ¹⁹F NMR, δ: -62.8 (s).^{13a} The yield of biphenyl could not be estimated in this experiment because of the close retention times of Ph₂ and 4,4'-difluorobiphenyl (internal standard) under the GC-MS conditions used. Therefore, the trifluoromethylation was repeated in the absence of 4,4'-difluorobiphenyl. The yield of biphenyl was estimated at ≤1%.

3.1.6. References

1. For selected monographs, see: (a) Hudlicky, M. *Chemistry of Organic Fluorine Compounds*; Ellis Horwood: New York, 1976. (b) Banks, R. E. *Organofluorine Chemicals and Their Industrial Applications*; Ellis Horwood: West Sussex, U.K., 1979. (c) Filler, R.; Kobayashi, Y. *Biomedical Aspects of Fluorine Chemistry*; Kodansha-Elsevier: New York, 1982. (d) Clark, J. H.; Wails, D.; Bastock, T. W. *Aromatic Fluorination*; CRC Press: Boca Raton, FL, 1996. (e) Kirsch, P. *Modern Fluoroorganic Chemistry*; Wiley-VCH: Weinheim, 2004. (f) Uneyama, K. *Organofluorine Chemistry*; Blackwell: Oxford, U. K., 2006. (g) Ojima, I. *Fluorine in Medicinal Chemistry and Chemical Biology*; Wiley-Blackwell: Chichester, U. K., 2009. (h) Petrov, V. A. *Fluorinated Heterocyclic Compounds. Synthesis, Chemistry and Applications*; Wiley: Hoboken, NJ, 2009.
2. For selected reviews, see: (a) Burton, D. J.; Yang, Z. Y. *Tetrahedron* **1992**, 48, 189. (b) McClinton, M. A.; McClinton, D. A. *Tetrahedron* **1992**, 48, 6555. (c) Umemoto, T. *Chem. Rev.* **1996**, 96, 1757. (d) Burton, D. J.; Lu, L. *Top. Curr. Chem.* **1997**, 193, 45. (e) Prakash, G. K. S.; Yudin, A. K. *Chem. Rev.* **1997**, 97, 757. (f) Guittard, F.; Taffin de Givenchy, E.; Geribaldi, S.; Cambon, A. *J. Fluorine Chem.* **1999**, 100, 85. (g) Singh, R. P.; Shreeve, J. M. *Tetrahedron* **2000**, 56, 7613. (h) Jeschke, P. *ChemBioChem.* **2004**, 5, 570. (i) Ma, J.-A.; Cahard, D. *Chem. Rev.* **2004**, 104, 6119. (j) Schlosser, M. *Angew. Chem., Int. Ed.* **2006**, 45, 5432. (k) Ma, J.-A.; Cahard, D. *J. Fluorine Chem.* **2007**, 128, 975. (l) Uneyama, K.; Katagiri, T.; Amii, H. *Acc. Chem. Res.* **2008**, 41, 817. (m) Ma, J.-A.; Cahard, D. *Chem. Rev.* **2008**, 108, PR1. (n) Shibata, N.; Matsnev, A.; Cahard, D. *Beilstein J. Org. Chem.* **2010**, 6, DOI: 10.3762/bjoc.6.65. (o) Sato, K.; Tarui, A.;

- Omote, M.; Ando, A.; Kumadaki, I. *Synthesis* **2010**, 1865. (p) Dhara, M. G.; Banerjee, S. *Prog. Polym. Sci.* **2010**, 35, 1022. (q) Roy, S.; Gregg, B. T.; Gribble, G. W.; Le, V.-D.; Roy, S. *Tetrahedron* **2011**, 67, 2161. (r) Tomashenko, O. A.; Grushin, V. V. *Chem. Rev.* **2011**, 111, 4475. (s) Qing, F.-L.; Zheng, F. *Synlett* **2011**, 1052. (t) Dilman, A. D.; Levin, V. V. *Eur. J. Org. Chem.* **2011**, 831. (u) Nie, J.; Guo, H.-C.; Cahard, D.; Ma, J.-A. *Chem. Rev.* **2011**, 111, 455. (v) Grygorenko, O. O.; Artamonov, O. S.; Komarov, I. V.; Mykhailiuk, P. K. *Tetrahedron* **2011**, 67, 803. (w) Aceña, J. L.; Sorochinsky, A. E.; Soloshonok, V. A. *Synthesis* **2012**, 44, 1591. (x) Macé, Y.; Magnier, E. *Eur. J. Org. Chem.* **2012**, 2479. (y) Chen, P.; Liu, G. *Synthesis* **2013**, 45, 2919. (z) Lishchynskiy, A.; Novák, P.; Grushin, V. V. In *Science of Synthesis: C-1 Building Blocks in Organic Synthesis 2*; van Leeuwen, P. W. N. M., Ed.; Thieme: Stuttgart, 2013; pp 367–408.
3. For a very rare example of trifluoromethylation on a kilogram scale, see: Mulder, J. A.; Frutos, R. P.; Patel, N. D.; Qu, B.; Sun, X.; Tampone, T. G.; Gao, J.; Sarvestani, M.; Eriksson, M. C.; Haddad, N.; Shen, S.; Song, J. J.; Senanayake, C. H. *Org. Process Res. Dev.* **2013**, 17, 940.
4. Symons, E. A.; Clermont, M. J. *J. Am. Chem. Soc.* **1981**, 103, 3127.
5. (a) Grushin, V. V. *Chim. Oggi* **2014**, 32, 81. (b) Han, W.; Li, Y.; Tang, H.; Liu, H. *J. Fluorine Chem.* **2012**, 140, 7.
6. McCulloch, A.; Lindley, A. A. *Atmos. Environ.* **2007**, 41, 1560.
7. Han, W.; Li, Y.; Tang, H.; Liu, H. *J. Fluorine Chem.* **2012**, 140, 7.
8. Bomgardner, M. M. *Chem. Eng. News* **2013**, 91 (26), 6.
9. (a) Amphlett J. C.; Coomber J. W.; Whittle E. *J. Phys. Chem.* **1966**, 70, 593. (b) Shia J.; Hea J.; Wang H.-J. *J. Phys. Org. Chem.* **2011**, 24, 65.
10. (a) Shono, T.; Ishifune, M.; Okada, T.; Kashimura, S. *J. Org. Chem.* **1991**, 56, 2. (b) Roques, N.; Russell, J. PCT Int. Appl. WO 97/19038, 1997. (c) Roques, N.; Russell, J. U. S. Patent 6355849, 2002. (d) Russell, J.; Roques, N. *Tetrahedron* **1998**, 54, 13771. (e) Barhdadi, R.; Troupel, M.; Perichon, M. *Chem. Commun.* **1998**, 1251. (f) Folleas, B.; Marek, I.; Normant, J.-F.; Saint-Jalmes, L. *Tetrahedron Lett.* **1998**, 39, 2973. (g) Folleas, B.; Marek, I.; Normant, J.-F.; Saint-Jalmes, L. *Tetrahedron* **2000**, 56, 275. (h) Billard, T.; Bruns, S.; Langlois, B. R. *Org. Lett.* **2000**, 2, 2101. (i) Large, S.; Roques, N.; Langlois, B. R. *J. Org. Chem.* **2000**, 65, 8848. (j) Langlois, B. R.; Billard, T. *ACS Symp. Ser.* **2005**, 911, 57. (k) Prakash, G. K. S.; Jog, P. V.; Batamack, P. T. D.; Olah, G. A. *Science* **2012**, 338, 1324. (l) Kawai, H.; Yuan, Z.; Tokunaga, E.; Shibata, N. *Org.*

- Biomol. Chem.* **2013**, 11, 1446. (m) Zhang Y.; Fujii M.; Serizawa H.; Mikami K. *J. Fluorine Chem.* **2013**, 156, 367.
11. Popov, I.; Lindeman, S.; Daugulis, O. *J. Am. Chem. Soc.* **2011**, 133, 9286.
12. Zanardi, A.; Novikov, M. A.; Martin E.; Benet-Buchholz, J.; Grushin, V. V. *J. Am. Chem. Soc.* **2011**, 133, 20901.
13. Choi, J.; Wang, D. Y.; Kundu, S.; Choliy, Y.; Emge, T. J.; Krogh-Jespersen, K.; Goldman, A. S. *Science* **2011**, 332, 1545.
14. Takemoto, S.; Grushin, V. V. *J. Am. Chem. Soc.* **2013**, 135, 16837.
15. (a) Novák, P.; Lishchynskiy, A.; Grushin, V. V. *Angew. Chem., Int. Ed.* **2012**, 51, 7767. (b) Novák, P.; Lishchynskiy, A.; Grushin, V. V. *J. Am. Chem. Soc.* **2012**, 134, 16167. (c) Lishchynskiy, A.; Novikov, M. A.; Martin, E.; Escudero-Adán, E. C.; Novák, P.; Grushin, V. V. *J. Org. Chem.* **2013**, 78, 11126. (d) Lishchynskiy, A.; Berthon, G.; Grushin, V. V. *Chem. Commun.* **2014**, 50, 10237. (e) Lishchynskiy, A.; Mazloomi, Z.; Grushin, V. V. *Synlett* **2015**, 26, 45.
16. (a) Sugiishi, T.; Amii, H.; Aikawa, K.; Mikami, K. *Beilstein J. Org. Chem.* **2015**, 11, 2661. (b) Aikawa, K.; Nakamura, Y.; Yokota, Y.; Toya, W.; Mikami, K. *Chem. Eur. J.* **2015**, 21, 96. (c) He, L.; Tsui, G. C. *Org. Lett.* **2016**, 18, 2800.
17. (a) Nebra, N.; Grushin, V. V. *J. Am. Chem. Soc.* **2014**, 136, 16998. (b) Rijs, N. J.; Gonzalez-Navarrete, P.; Schlangen, M.; Schwarz, H. *J. Am. Chem. Soc.* **2016**, 138, 3125.
18. (a) See, for example: *Chemical Reactions and Processes under Flow Conditions*; Luis, S. V., Garcia-Verdugo, E., Eds.; RSC: Cambridge, U.K., 2010. (b) For a recent, excellent review of flow microreactor synthesis in organofluorine chemistry, see: Amii, H.; Nagaki, A.; Yoshida, J.-i. *Beilstein J. Org. Chem.* **2013**, 9, 2793. (c) S. V. Ley, *Chem. Rec.* **2012**, 12, 378. (b) Wegner, J.; Ceylan, S.; Kirschning, A. *Chem. Commun.* **2011**, 47, 4583. (d) Mason, B. P.; Price, K. E.; Steinbacher, J. L.; Bogdan, A. R.; McQuade, D. T. *Chem. Rev.* **2007**, 107, 2300. (e) Yoshida, J.-i.; Nagaki, A.; Yamada, T. *Chem. Eur. J.* **2008**, 14, 7450. (f) Wiles, C.; Watts, P. *Chem. Commun.* **2011**, 47, 6512. (g) Cukalovic, A.; Monbaliu, J. C. M. R.; Stevens, C. V. *Top. Heterocycl. Chem.* **2010**, 23, 161. (h) Fukuyama, T.; Rahman, M. T.; Sata, M.; Ryu, I. *Synlett* **2008**, 151.
19. (a) Chen, M.; Buchwald, S. L. *Angew. Chem., Int. Ed.* **2013**, 52, 11628. (b) Natan J. W. Straathof, N. J. W.; Gemoets, H. P. L.; Wang, X.; Schouten, J. C.; Hessel, V.; Noel, T. *ChemSusChem* **2014**, 7, 1612. (c) Bottecchia, C.; Wei, X.-J.; Kuijpers, K. P. L.; Hessel, V.; Noel, T. *J. Org. Chem.* **2016**, 81, 7301.

-
20. Konovalov, A. I.; Benet-Buchholz, J.; Martin, E.; Grushin, V. V. *Angew. Chem., Int. Ed.* **2013**, *52*, 11637.
21. Lishchynskiy, A.; Grushin, V. V. *J. Am. Chem. Soc.* **2013**, *135*, 12584.
22. (a) Hughes, R. P. *Adv. Organomet. Chem.* **1990**, *31*, 183. (b) Morrison, J. A. *Adv. Organomet. Chem.* **1993**, *35*, 211. (c) Hughes, R. P. *Eur. J. Inorg. Chem.* **2009**, 4591. (d) García-Monforte, M. A.; Martínez-Salvador, S.; Menjón, B. *Eur. J. Inorg. Chem.* **2012**, 4945.
23. Although inclusion of Step 1 in the overall flow setup was beyond the scope of the current work, our preliminary experiments indicated that this is possible.

3.2. Trifluoromethylation and pentafluoroethylation of vinylic halides with low-cost R_fH -derived CuR_f ($R_f = CF_3, C_2F_5$)

Lishchynskiy, A.; Mazloomi, Z.; Grushin, V. V. *Synlett* **2015**, 26, 45.

3.2.1. Introduction

Perfluoroalkylation of aromatic compounds have been the subject of interesting research topics recently as it plays the important role for the synthesis of biologically active ingredients and specialty materials.^{1,2}

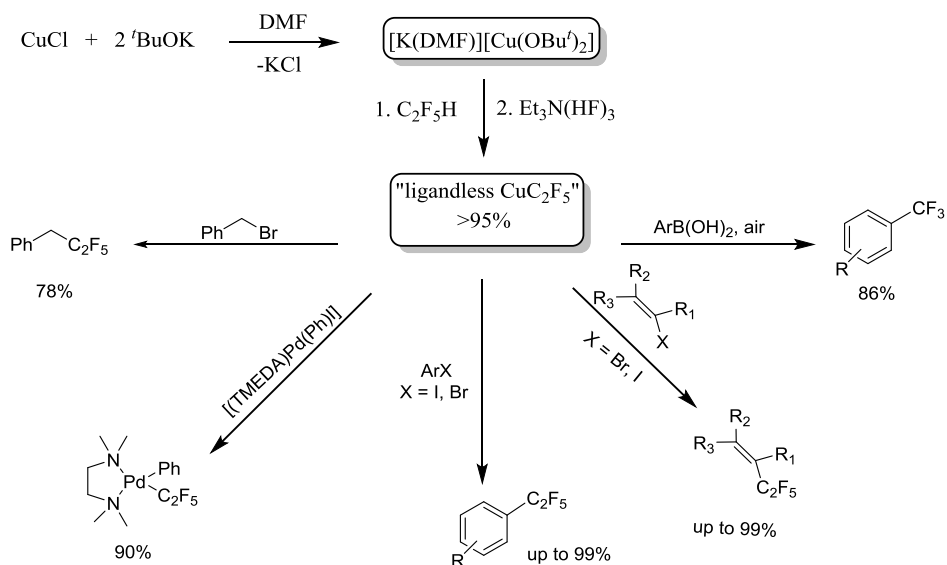
Different methodologies for trifluoromethylation and pentafluoroethylation of aromatic compounds were discussed in chapter 2 and 3.1 in details. Cupration of fluoroform and pentafluoroethane were among the best known processes for perfluoroalkylation. Direct cupration of trifluoromethane was mentioned in chapter 3.1 and cupration of pentafluoroethane as a higher H-perfluoroalkane will be considered in this chapter.

Pentafluoroethane (C_2F_5H , HFC-125, R-125) is a colorless gas (bp = -48.5 °C and mp = -103 °C) that is soluble in organic solvents. It is nontoxic and ozone-friendly. It has high warming potential (3450 times that of CO_2) therefore cannot be released into the atmosphere. It can be applied as a chemical feedstock for fluorinated compounds instead of releasing in air.

Adding C_2F_5H to $[K(DMF)][(tBuO)_2Cu]$,³ which is generated in situ from $CuCl$ and $tBuOK$ (1:2) in DMF at room temperature resulted CuC_2F_5 solution in ca. 95% yield (Scheme 3.2.1). This product is more robust than the $CuCF_3$ counterpart prepared from fluoroform in the very similar way and the reason is the less favored α -F-elimination of CuC_2F_5 than of $CuCF_3$ analog. Due to the higher stability of pentafluoroethane cupration product, it was possible to isolate the compound and make a crystal. The structure of the $[K(DMF)_2][(tBuO)Cu(C_2F_5)]$ was shown by single-crystal X-ray diffraction.³

The “ligandless CuC_2F_5 ” has been efficiently applied for pentafluoroethylation of different substrates (Scheme 3.2.1).^{3,4} Perfluoroalkylation of vinylic halides have methodologically less developed. There are some primary reports about copper-mediated coupling of perfluoroalkyl iodides (R_fI) with haloalkenes⁵ which has been

modified by using different CF_3 and C_2F_5 sources such as $\text{FO}_2\text{SCF}_2\text{I}$,⁶ $\text{FO}_2\text{SCF}_2\text{CO}_2\text{Me}$,⁷ $\text{FSO}_2(\text{CF}_2)_2\text{OCF}_2\text{CO}_2\text{Me}$,⁸ $\text{Hg}(\text{CF}_3)_2$,⁹ $\text{ClCF}_2\text{CO}_2\text{Me}$,¹⁰ $\text{CF}_3\text{SiR}_3/\text{KF}$,¹¹ and $\text{C}_2\text{F}_5\text{COX}$ ($\text{X} = \text{ONa}$,¹² Ph^{13}),¹⁴ In the most of these reports, styryl chloride⁸ or bromide^{6,7a,8,12,13} being the only vinylic halides investigated. Some examples of trifluoromethylation of $\text{RCH}=\text{CHX}$ ($\text{R} = \text{H}$, $\text{X} = \text{Br}^{10}$, $\text{R} = \text{C}_8\text{H}_{17}$, $\text{X} = \text{I}^{11a}$) and pentafluoroethylation of $\text{RCH}=\text{CHX}$ ($\text{R} = \text{C}_6\text{H}_{13}$, $\text{X} = \text{Br}$, I)¹⁵ have been noted briefly. One paper^{7b} mentions the trifluoromethylation of structurally alike 4-bromo-3-oxo- Δ^4 -steroids and two more describe some of rather specific 1,2-diiodo-^{7c} and 1,1-dibromoolefin^{7d} substrates. There are two reports that perform this type of transformations for several vinylic halides other than bromo- and iodostyrene. Nowak and Robins⁹ have shown trifluoromethylation of 18 vinylic bromides and iodides in 75–95% yield. Unfortunately, they applied toxic $\text{Hg}(\text{CF}_3)_2$ as a CF_3 source in their method. Hafner and Bräse^{11b} have improved the Urata–Fuchikami protocol.^{11a} They applied CF_3TMS to make the trifluoromethylation reaction on five vinylic bromides and six iodides in 23–99% yield. The reaction was performed in costly DMPU^{11b} to avoid the formation of C_2F_5 -substituted side products due to α -F elimination.¹¹ Contamination of a desired trifluoromethylated product with its C_2F_5 counterpart is a serious problem because separation of the two is difficult, if not impossible.



Scheme 3.2.1. Direct cupration of pentafluoroethane and various pentafluoroethylation reactions with CuC_2F_5 .

3.2.2. Objectives

The CuCF_3 and CuC_2F_5 reagents synthesized by direct cupration of fluoroform^{3,16} and pentafluoroethane¹⁷ have been applied for fluoroalkylation of a broad variety of substrates in high yield and excellent selectivities.¹⁵⁻¹⁹ These R_fCu reagents are not neither toxic nor expensive. Even there is no formation of side products whenever they are handled for perfluoroalkylation reactions. Considering the great potential of R_fCu reagents we explored the possibility of fluoroalkylation of vinylic halides with the R_fH -driven CuCF_3 and CuC_2F_5 reagents as it was the objective of the work which describe in this chapter.

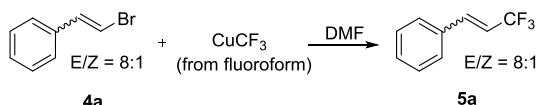
3.2.3. Results and discussion

We initially found that fluoroform-derived CuCF_3 readily trifluoromethylates β -bromostyrene (**4a**, *E/Z* = 8:1), the substrate of choice for our initial studies, with full retention of stereochemistry. A summary of the optimization work is presented in Table 3.2.1 showing that the trifluoromethylation of **4a** occurs at as low as ambient temperature. Our goal was to drive the reaction to nearly full conversion in order to eliminate the need to separate the product PhCH=CHCF_3 from the unreacted starting material. To achieve >90% yield at $\geq 99\%$ conversion, the reaction was performed at 40–50 °C with 2.5 equivalents of CuCF_3 in the presence of $\text{Et}_3\text{N}\cdot 3\text{HF}$ as a promoter.^{19c}

After the optimization work, we proceeded to explore the substrate scope, using various vinylic bromides. The trifluoromethylation and pentafluoroethylation were performed in parallel (Table 3.2.2). The enhanced thermal stability of the CuC_2F_5 reagent¹⁷ allowed us to use it in only 10% excess to achieve full conversion for most of the substrates, while running the reactions at 70–80 °C. The data collected in Table 2.2.2 show that styryl bromides bearing such substituents as Me (**4b–d**), MeO (**4e**), F (**4f**), Cl (**4g,h**), and Br (**4i,j**) in various positions of the aromatic ring undergo clean perfluoroalkylation to give the desired products in $\geq 90\%$ yield (Table 3.2.2, entries 1–20). The stereochemistry of the starting material is retained in the product. While F and Cl on the ring remain intact during the reaction, the aromatic C–Br bond in **4i** and **4j** (Table 3.2.2, entries 17–20) undergoes fluoroalkylation, albeit only to a minor extent (5–8%). Therefore, unactivated bromoarenes are estimated to be approximately an order of magnitude less reactive toward CuR_f than β -bromostyrene. This difference in reactivity provides an opportunity for further functionalization of the R_f -substituted

styrene products bearing a halogen atom on the ring, for example, via a variety of coupling reactions.

Table 3.2.1. Optimization of the reaction conditions for trifluoromethylation of β -bromostyrene with fluoroform-derived CuCF_3 .



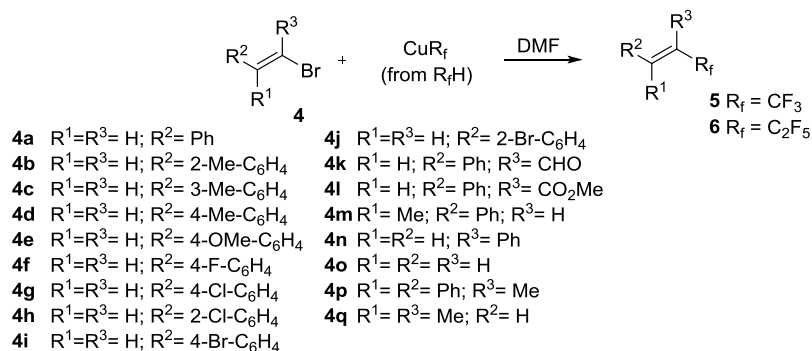
Entry ^a	CuCF_3 (equiv)	$\text{Et}_3\text{N}\cdot 3\text{HF}$ (equiv) ^b	Temp. (°C)	Time (h)	Conv. (%) ^c	Yield (%) ^d
1	1.5	0.33	50	23	84	76
2	2	0.33	23	120	95	86
3	2	0.33	50	25	97	84
4	2	0.43	50	24	96	92
5	2	0.53	50	20	94	87
6	2	0.63	50	20	92	85
7	2.5	0.43	50	24	99	93
8	2.5	0.53	50	26	98	91
9	2.5	0.63	50	26	96	90
10	2.5	0.43	40	62	99	90
11	2.5	0.53	40	62	98	90
12	2	0.53	80	4+1 ^e	89	86

^(a) Reaction conditions: **1a** (0.125–0.25 mmol), CuCF_3 in DMF (0.35–0.38 M) in the presence of 1,3-bis(trifluoromethyl)benzene or 4,4'-difluoro-1,1'-biphenyl as internal standards (see experimental section for details). ^(b) Equiv per 1 equiv of CuCF_3 . ^(c) Determined by GC–MS. ^(d) Determined by ^{19}F NMR spectroscopy (accuracy $\pm 5\%$). ^(e) CuCF_3 in DMF was added during 4 h via a syringe pump, followed by heating for one additional hour.

The fluoroalkylation of β -bromostyrenes with geminal CHO (**4k**) or CO_2Me (**4l**) also proceeded smoothly to furnish the corresponding products in 68–80% yield (Table 3.2.2, entries 21–24). Although the stereochemistry is not fully preserved in the reactions of these substrates, the *E/Z* ratio ranges from good (85:15, Table 3.2.2, entries 21 and 23) to excellent (99:1, Table 3.2.2, entry 24). In accord with the literature data,^{11b} α -bromostyrene (**4n**) was less reactive, likely for steric reasons, furnishing the desired product in only 26% and 64% yield at 50% and 100% conversion in the reactions with CuCF_3 and CuC_2F_5 , respectively (Table 3.2.2, entries 27 and 28). In contrast, α -methyl- β -bromostyrene (**4m**) underwent perfluoroalkylation in >90% yield with full retention of stereochemistry (Table 2.2.2, entries 25 and 26). Bromoethylene

(**4o**), isopropenyl bromide (**4p**), and 2-bromo-2-butene (**4q**) were perfluoroalkylated in 35–78% yield (Table 3.2.2, entries 29–33).

Table 3.2.2. Trifluoromethylation and pentafluoroethylation of bromoalkenes with CuR_f in DMF.



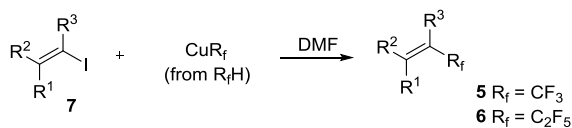
Entry ^a	Product	Temp. (°C)	Time (h)	Conv. (%) ^b	Yield (%) ^c	E/Z ratio	
						Prod. ^d	Subs. ^d
1	5a	50	24	99	93	89:11	89:11
2	6a	70	14	100	97		
3	5b	50	23	100	93	99:1	99:1
4	6b	70	20	100	92		
5	5c	50	23	100	92	99:1	99:1
6	6c	70	20	100	99		
7	5d	50	23	99	96	100:0	100:0
8	6d	70	14	100	99		
9	5e	50	24	100	90	99:1	99:1
10	6e	70	18	100	91		
11	5f	50	23	100	97	98:2	98:2
12	6f	70	20	100	98		
13	5g	50	23	100	94	100:0	100:0
14	6g	70	14	100	97		
15	5h	50	24	100	90	99:1	99:1
16	6h	70	18	100	94		
17 ^e	5i	50	21	99	87+5 ^f	100:0	100:0
18 ^e	6i	70	16	100	89+5 ^f		

19 ^e	5j	50	21	100	89+7 ^f	99:1	99:1
20 ^e	6j	70	16	100	89+8 ^f		
21	5k	50	24	100	71	0:100	15:85
22	6k	50	16	100	80		6:94
23	5l	50	25	86	74	28:72	16:84
24	6l	70	16	98	68		1:99
25	5m	50	25	96	94	97:3	97:3
26	6m	80	14	100	92		
27	5n	50	28	50	26	-	-
28	6n	70	30	100	64		
29	5o	50	30	60	35	-	-
30	6o	50	28	55	58	-	-
31	5p	80	21	92	70		
32	6p	50	28	65	60	50:50	63:37
33	5q	80	21	91	78		56:44

^(a)Reaction conditions: bromoalkene **1** (0.125–0.25 mmol), CuCF₃ in DMF (0.35–0.38 M, 2.5 equiv) or CuC₂F₅ in DMF (0.67–0.70 M, 1.1 equiv), 1,3-bis(trifluoromethyl)benzene or 4,4'-difluoro-1,1'-biphenyl (internal standards). See experimental section for details. ^(b) Determined by GC–MS. ^(c) Determined by ¹⁹F NMR spectroscopy (accuracy ±5%). ^(d) Determined by ¹H NMR spectroscopy. ^(e) 2.2 equiv of CuCF₃ or 1 equiv of CuC₂F₅. ^(f) Bis-perfluoroalkylated side product was also formed.

Although more costly and often less accessible than their bromo counterparts, vinylic iodides are considerably more reactive coupling partners. We therefore explored fluoroalkylation of a series of iodoalkenes with CuCF₃ and CuC₂F₅ (Table 3.2.3).

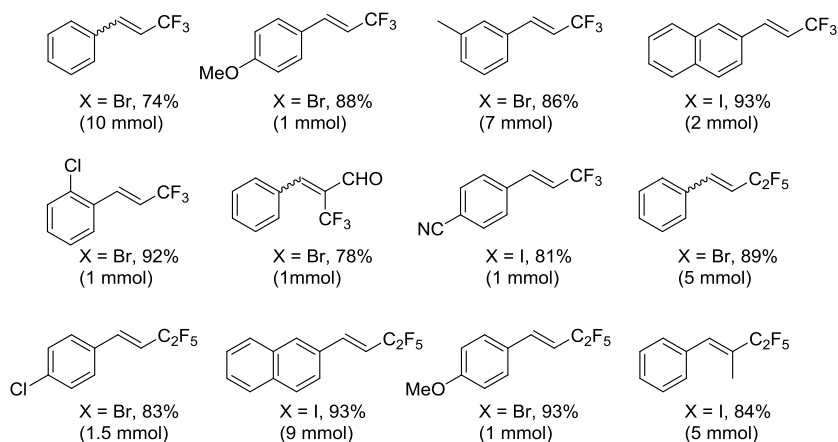
The mono β-substituted iodoethylenes appeared reactive enough to undergo the fluoroalkylation at room temperature (Table 3.2.3, entries 1–8). Importantly, full conversion of these substrates was reached with only 1.1 equivalents of the CuR_f reagent not only for R_f = C₂F₅, but also for R_f = CF₃. The fluoroalkylations of more sterically hindered and therefore less reactive iodoalkenes were performed at 50–70 °C (Table 3.2.3, entries 9–12). The formation of the desired products in excellent yields of up to 97% was observed in all cases.

Table 3.2.3. Trifluoromethylation and pentafluoroethylation of iodoalkenes.

Entry ^a	R ¹	R ²	R ³	Product	Temp (°C)	Time (h)	Yield (%) ^b
1	H	2-ClC ₆ H ₄	H	5h	23	1.5	92
2				6h	23	10	90
3	H	4-NCC ₆ H ₄	H	5r	23	1.5	92
4				6r	23	10	92
5	H	2-naphthyl	H	5s	23	2	91
6				6s	23	10	90
7	1-naphthyl	H	H	5t	23	6	89
8				6t	23	16	87
9	Ph	H	Me	5u	50	8	97
10				6u	50	24	95
11	H	(CH ₂) ₄	-	5v	50	13	93
12				6v	70	7	91

^(a) Reaction conditions: iodoalkene **4** (0.125-0.25 mmol), CuCF₃ in DMF (0.36-0.38 M; 1.1 equiv) or CuC₂F₅ in DMF (0.68-0.7 M; 1.1 equiv), 1,3-bis(trifluoromethyl)benzene or 4,4'-difluoro-1,1'-biphenyl (internal standards). See experimental section for details. ^(b) Determined by ¹⁹F NMR.

After the substrate scope studies (Tables 3.2.2 and 3.2.3), a number of vinylic halides were selected for the synthesis and isolation of the corresponding CF₃ and C₂F₅ derivatives on a 1–10 mmol scale (Scheme 3.2.2). As can be seen from Scheme 3.2.2, the new protocol is suitable for the preparation and isolation in pure form of trifluoromethylated and pentafluoroethylated olefins in up to 93% yield. Note that the diminished yields of 74–86% are mainly due to losses during the isolation of these rather volatile compounds and hence likely can be improved in the synthesis on a larger scale.



Scheme 3.2.2. Isolated trifluoromethylated and pentafluoroethylated products (1-10 mmol).

Single-crystal X-ray diffraction studies of two of the isolated products, (E)-1-(trifluoromethyl)-2-(4-methoxyphenyl) ethylene (**5e**, Figure 3.2.1) and (E)-1-(pentafluoroethyl)-2-(2-naphthyl)ethylene (**6s**, Figure 3.2.2) confirmed the structures and stereochemistry in the solid state.²⁰

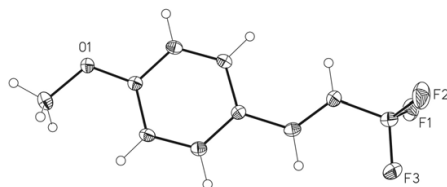


Figure 3.2.1. ORTEP drawing of **2e** with thermal ellipsoids drawn at the 50% probability level.²⁰

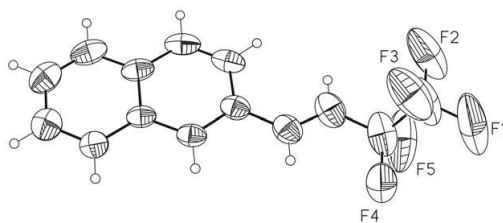


Figure 3.2.2. ORTEP drawing of **3s** with thermal ellipsoids drawn at the 50% probability level.²⁰

The high chemo- and stereoselectivity of the fluoroalkylation reactions described above suggests that radical processes are unlikely involved in the olefinic C–R_f bond

formation. The fluoroalkylation reactions of vinylic halides are in many respects similar to those of aryl halides.^{3,16,17,19c} As has been recently established,²¹ the trifluoromethylation of haloarenes with fluoroform-derived CuCF_3 is a nonradical process that involves ArX oxidative addition (OA) to Cu(I) , followed by ArR_f reductive elimination (RE) from the copper(III) intermediate. The fluoroalkylation reactions developed in the current work are likely governed by a similar OA–RE mechanism. The new method compares favorably with the previously reported ones^{6–14} for perfluoroalkylation of haloalkenes. Apart from the vastly lower cost of the R_f sources used, our procedures obviate the need for toxic mercury compounds⁹ or expensive DMPU^{11b} employed in the only two reported methods with a defined substrate scope.

3.2.4. Conclusions

In summary, a general new protocol has been developed for the trifluoromethylation and pentafluoroethylation of vinylic bromides and iodides with R_fH -derived CuCF_3 and CuC_2F_5 . The reactions occur at 23–80 °C with high chemo and stereoselectivity to furnish the desired fluoroalkylated olefin products in high, often >90% yield. Various functional groups are well tolerated. The method employs the most economical CuR_f reagents known to date and neither costly nor toxic materials. Scalability and isolation of pure products have been demonstrated on selected examples. The new protocol may find use in both academic and industrial research.

3.2.5. Experimental section

3.2.5.1. General information

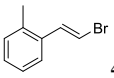
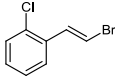
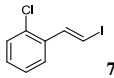
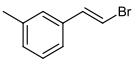
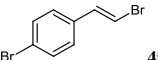
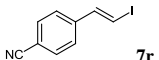
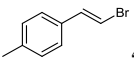
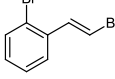
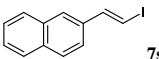
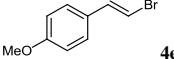
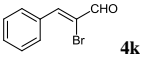
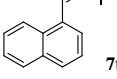
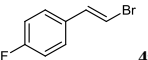
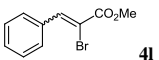
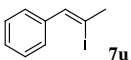
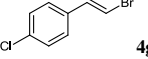
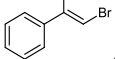
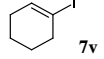
All chemicals, solvents, and deuterated solvents were purchased from Aldrich, Alfa Aesar, Apollo Scientific, TCI, Acros, and Deutero companies. Anhydrous DMF (Alfa Aesar or from an MBraun SPS) was used without additional purification. Ether and THF were distilled from Na/benzophenone. All anhydrous solvents were stored over freshly calcined 4 Å molecular sieves in a glove-box. Glass pressure reaction vessels (Fischer-Porter tubes) were purchased from Andrews Glass Co., Inc. Fluoroform-derived CuCF_3 was prepared on a 15–120 mmol scale, stabilized with $\text{Et}_3\text{N}\cdot 3\text{HF}$ (0.33 equiv per equiv of CuCF_3), and extra amount of $\text{Et}_3\text{N}\cdot 3\text{HF}$ (0.1–0.3 equiv per equiv of CuCF_3) was added to the reagent after stabilization, as previously reported.^{3,19c} The CuC_2F_5 reagent was prepared from $\text{C}_2\text{F}_5\text{H}$ on a 20–50 mmol scale, neutralized with

Et₃N·3HF (0.33 equiv per equiv of CuC₂F₅) and extra amount of Et₃N·3HF (0.2 equiv per equiv of CuC₂F₅) was added, as previously reported.¹⁷ Literature procedures were used to synthesize sodium bis(trimethylsilyl)amide,²² (iodomethyl)-triphenylphosphonium iodide,²³ and ethyltriphenylphosphonium iodide.²⁴ NMR spectra were recorded on Bruker Avance 400 Ultrashield and Bruker Avance 500 Ultrashield NMR spectrometers. Quantitative ¹⁹F NMR analyses were carried out with D1 = 5 s. An Agilent Technologies 7890A chromatograph equipped with a 5975C MSD unit was used for GC-MS analysis. Single-crystal X-ray diffraction studies were performed using a Bruker-Nonius diffractometer equipped with an APEX II 4K CCD area detector.

3.2.5.2. Preparation of vinyl halides

All vinyl halides, except for commercial β-bromostyrene **4a**, α-bromostyrene **4n**, vinyl bromide **4o** (1M solution in THF), 2-bromopropene **4p**, and 2-bromobutene **4q**, were synthesized following the literature procedures (Table 3.2.4).

Table 3.2.4. Vinyl halides prepared following literature procedures.

Vinyl halide	Ref.	Vinyl halide	Ref.	Vinyl halide	Ref.
 4b	25	 4h	25	 7h	25
 4c	25	 4i	25	 7r	25
 4d	25	 4j	25	 7s	25 ^a
 4e	25	 4k	26	 7t	9
 4f	25	 4l	9	 7u	28
 4g	25	 4m	27	 7v	25

^(a)Purified by recrystallization from hexanes rather than by flash chromatography, as reported in ref. 7.

3.2.5.3. Trifluoromethylation of β -bromostyrene. Optimization experiments

Procedure A. In a glovebox, to 4,4'-difluoro-1,1'-biphenyl (18 mg; internal standard) in an NMR tube was added CuCF_3 in DMF (0.35 M; 1.5-2 equiv), the tube was sealed with a rubber septum and brought out. β -Bromostyrene (**4a**; 16 μL ; 0.125 mmol) was added at room temperature via a microsyringe, and the NMR tube was kept at 50 $^\circ\text{C}$ (oil bath) for 23-25 h (entries 1 and 3, Table 3.2.5). Ether (0.5 mL) and water (1 mL) were added in air. After agitation, the organic layer was filtered through a short silica gel plug and analyzed by GC-MS to determine the conversion of **4a**. The yield of **5a** was determined by quantitative ^{19}F NMR analysis of the filtrate.

Procedure B. In a glovebox, an NMR tube was charged with CuCF_3 in DMF (0.37-0.38 M; 2-2.5 equiv), sealed with a rubber septum, and brought out. β -Bromostyrene (**4a**; 16 μL ; 0.125 mmol) and 1,3-bis(trifluoromethyl)benzene (10 μL ; internal standard) were added at room temperature via microsyringe, and the NMR tube was kept at 23-50 $^\circ\text{C}$ for an indicated period of time (entries 2 and 4-11, Table 3.2.5). Ether (0.5 mL) and water (1 mL) were added in air. After agitation, the organic layer was filtered through a short silica gel plug and analyzed by GC-MS to determine the conversion of **4a**. The yield of **5a** was determined by quantitative ^{19}F NMR analysis of the filtrate.

Procedure C. To a solution of β -bromostyrene (**4a**; 32 μL ; 0.25 mmol) in DMF (0.25 mL) placed in an oil bath at 80 $^\circ\text{C}$ under argon, was added, via a syringe pump over a period of 4 h, a solution of CuCF_3 in DMF (0.38 M; 1.3 mL; 2 equiv) containing 0.2 extra equiv of $\text{Et}_3\text{N}\cdot 3\text{HF}$. The mixture was then stirred for an additional 1 h at the same temperature (entry 12, Table 3.2.5). After the reaction mixture was allowed to cool to room temperature, ether (5 mL), 1,3-bis(trifluoromethyl)benzene (internal standard; 19 μL), and water (8 mL) were added in air. After agitation, the organic layer was filtered through a short silica gel plug and analyzed by GC-MS to determine the conversion of **4a** (89%). Quantitative ^{19}F NMR analysis of the filtrate indicated that **5a** was produced in 86% yield.

Table 3.2.5. Trifluoromethylation of β -bromostyrene with fluoroform-derived CuCF_3 . Optimization of the reaction conditions.

Entry	CuCF_3 , equiv	$\text{Et}_3\text{N}\cdot 3\text{HF}$, equiv ^a	Temp., (°C)	Time, (h)	Conc. of CuCF_3 , M	Proc.	Conv., (%) ^c	Yield, (%) ^d
1	1.5	0.33	50	23	0.35	A	84	76
2	2	0.33	23	120	0.38	B	95	86
3	2	0.33	50	25	0.35	A	97	84
4	2	0.43	50	24	0.37	B	96	92
5	2	0.53	50	20	0.37	B	94	87
6	2	0.63	50	20	0.37	B	92	85
7	2.5	0.43	50	24	0.37	B	99	93
8	2.5	0.53	50	26	0.37	B	98	91
9	2.5	0.63	50	26	0.37	B	96	90
10	2.5	0.43	40	62	0.38	B	99	90
11	2.5	0.53	40	62	0.38	B	98	90
12	2	0.53	80	4+1 ^d	0.38	C	89	86

^(a) Equiv per 1 equiv of CuCF_3 . ^(b) The reaction scale is 0.125 mmol except entry 12 that is 0.250 mmol. ^(c) Determined by GC-MS. ^(d) Determined by ^{19}F NMR. ^(e) CuCF_3 in DMF was added during 4 h via a syringe pump, followed by heating for one additional h.

3.2.5.4. Trifluoromethylation of bromoalkenes

Procedure A. In a glovebox, to bromoalkene **4** (0.125 mmol) and 4,4'-difluoro-1,1'-biphenyl (18 mg; internal standard) in an NMR tube was added, at room temperature, CuCF_3 in DMF (0.36-0.38 M; 2.5 equiv) containing 0.1 extra equiv of $\text{Et}_3\text{N}\cdot 3\text{HF}$. The tube was sealed with a rubber septum, brought out, and kept at 50 °C (oil bath) for 21-28 h (entries 1-12 and 16, Table 3.2.6). Ether (0.5 mL) and water (1 mL) were added in air. After agitation, the organic layer was filtered through a short silica gel plug and analyzed by GC-MS to determine the conversion of **4**. The yield of **5** was determined by quantitative ^{19}F NMR analysis of the filtrate.

Procedure B. In a glove-box, to CuCF_3 in DMF (0.35-0.38 M; 2.5 equiv) containing 0.1 extra equiv of $\text{Et}_3\text{N}\cdot 3\text{HF}$ (0.2 equiv in the case of **5o**; entry 14) in an NMR tube was added, at room temperature, bromoalkene **4** (0.125 mmol) and 1,3-bis(trifluoromethyl)benzene (10 μL ; internal standard) via microsyringe. The tube was

sealed with a rubber septum, brought out, and kept at 50 °C (oil bath) for 28-30 h (entries 13-15, Table 3.2.6). Ether (0.5 mL) and water (1 mL) were added in air. After agitation, the organic layer was filtered through a short silica gel plug and analyzed by GC-MS to determine the conversion of **4**. The yield of **5** was determined by quantitative ^{19}F NMR analysis of the filtrate (for **5p**, the yield was determined before workup; entry 15).

3.2.5.5. Pentafluoroethylation of bromoalkenes

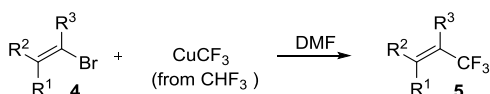
Procedure A. In a glovebox, to 4,4'-difluoro-1,1'-biphenyl (18 mg; internal standard) in an NMR tube was added CuC_2F_5 reagent (0.69 M; 0.2 mL; 1.1 equiv) containing extra 0.2 equiv of $\text{Et}_3\text{N}\cdot 3\text{HF}$, the tube was sealed with a rubber septum and brought out. β -Bromostyrene (**4a**; 16 μL ; 0.125 mmol) was added, at room temperature, via microsyringe and the NMR tube was kept at 70 °C (oil bath) for 14 h (entry 1, Table 3.2.7). Ether (1 mL) and water (2 mL) were added in air. After agitation, the organic layer was filtered through a short silica gel plug and analyzed by GC-MS to determine the full conversion of **4a**. Quantitative ^{19}F NMR analysis of the filtrate indicated that **6a** was produced in 97% yield.

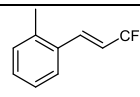
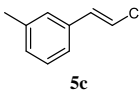
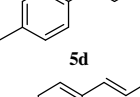
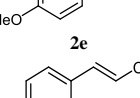
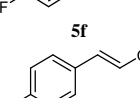
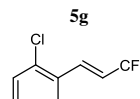
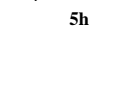
Procedure B. In a glovebox, to bromoalkene **4** (0.125 or 0.25 mmol) in an NMR tube was added, at room temperature, CuC_2F_5 in DMF (0.67-0.7 M; 1.1 equiv) containing 0.2 extra equiv of $\text{Et}_3\text{N}\cdot 3\text{HF}$. The tube was sealed with a rubber septum, brought out, and 1,3-bis(trifluoromethyl)benzene (10 or 19 μL ; internal standard) was added via microsyringe. The NMR tube was kept at 50-80 °C (oil bath) for an indicated period of time (entries 2, 3, 5, 6 and 8-14, Table 3.2.7). Ether (1 mL) and water (2 mL) were added in air. After agitation, the organic layer was filtered through a short silica gel plug and analyzed by GC-MS to determine the conversion of **4**. The yield of **3** was determined by quantitative ^{19}F NMR analysis of the filtrate.

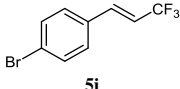
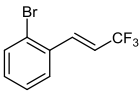
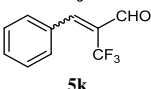
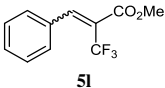
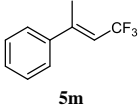
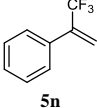
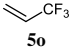
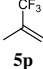
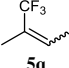
Procedure C. In a glove-box, to bromoalkene **4** (0.125 mmol) and 4,4'-difluoro-1,1'-biphenyl (18 mg; internal standard) in an NMR tube was added, at room temperature, CuC_2F_5 in DMF (0.67 M; 0.21 mL; 1.1 equiv) containing 0.2 extra equiv of $\text{Et}_3\text{N}\cdot 3\text{HF}$. The tube was sealed with a rubber septum, brought out, and kept at 70 °C (oil bath) for 14 h (entries 4 and 7, Table 3.2.7). Ether (1 mL) and water (2 mL) were added in air. After agitation, the organic layer was filtered through a short silica gel plug and analyzed by GC-MS to determine the full conversion of **4**. The yield of **6** was determined by quantitative ^{19}F NMR analysis of the filtrate.

Procedure D. In a glovebox, to CuC_2F_5 in DMF (0.7 M; 0.39 mL; 1.1 equiv) containing 0.2 extra equiv of $\text{Et}_3\text{N}\cdot 3\text{HF}$ in an NMR tube equipped with a J. Young valve was added, at room temperature, bromoalkene **4** (0.25 mmol) and 1,3-bis(trifluoromethyl)benzene (19 μL ; internal standard) via microsyringe. The NMR tube was sealed, brought out, and kept at 80 °C (oil bath) for 21 h (entries 15 and 16, Table 3.2.7). The NMR tube was brought back to the glovebox, the reaction mixture was diluted with ether (1 mL), and filtered through a Teflon syringe filter. The filtrate was placed in a clean NMR tube, which was then sealed with a rubber septum and brought out. The yield of **3** was determined by quantitative ^{19}F NMR analysis. Then the tube was unsealed in air, the solution was washed with water (3 mL), filtered through a short silica gel plug, and analyzed by GC-MS to determine the conversion of **4**.

Table 3.2.6. Trifluoromethylation of bromoalkenes with CuCF_3 in DMF.

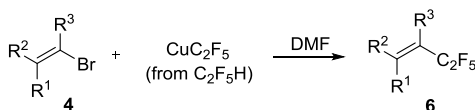


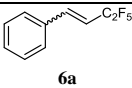
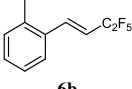
Entry ^a	Product	Time, (h)	Conc. of CuCF_3 , M ^b	Proc.	Conv., (%) ^c	Yield, (%) ^d	E/Z ratio	
							Subs. ^e	Prod. ^d
1	 5b	23	0.38	A	100	93	99:1	99:1
2	 5c	23	0.36	A	100	92	99:1	99:1
3	 5d	23	0.38	A	99	96	100:0	100:0
4	 2e	24	0.38	A	100	90	99:1	99:1
5	 5f	23	0.38	A	100	97	98:2	98:2
6	 5g	23	0.38	A	100	94	100:0	100:0
7	 5h	24	0.38	A	100	90	99:1	99:1

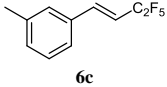
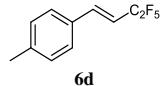
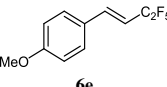
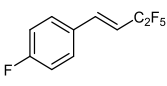
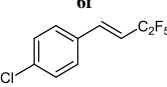
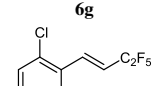
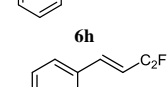
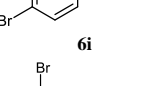
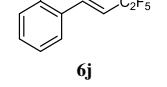
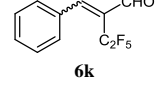
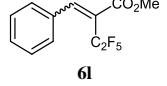
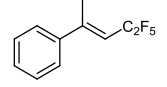
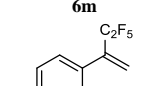
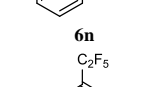
8 ^f		21	0.38	A	99	87+5 ^g	100:0	100:0
9 ^f		21	0.38	A	100	89+7 ^g	99:1	99:1
10		24	0.38	A	100	71	0:100	15:85
11		25	0.38	A	86	74	28:72	16:84
12		25	0.38	A	96	94	97:3	97:3
13		28	0.38	B	50	26	-	-
14		30	0.35 ^h	B	60	35	-	-
15		28	0.38	B	55	58 ⁱ	-	-
16		28	0.38	A	75	73 ⁱ	50:50	63:37

(^a) Reactions were performed on 0.125 mmol scale, at 50 °C. (^b) CuCF₃ reagent (2.5 equiv) containing 0.1 equiv of extra Et₃N·3HF (0.43 equiv overall) was used. (^c) Determined by GC-MS. (^d) Determined by ¹⁹F NMR. (^e) Determined by ¹H NMR. (^f) 2.2 equiv of CuCF₃ was used. (^g) Bis-trifluoromethylated side-product was also formed. (^h) CuCF₃ reagent containing 0.2 equiv of extra Et₃N·3HF was used. (ⁱ) The yield of the reaction was determined before workup.

Table 3.2.7. Pentafluoroethylation of bromoalkenes with CuC₂F₅ in DMF.



Entry	Product	Temp, (°C)	Time, (h)	Conc. of CuC ₂ F ₅ , M ^a	Proc.	Conv., % ^c	Yield, % ^d	E/Z ratio	
								Subs. ^e	Prod. ^f
1		70	14	0.69	A	100	97	89:11	89:11
2		70	20	0.67	B	100	92	99:1	99:1

3		70	20	0.67	B	100	99	99:1	99:1
4		70	14	0.67	C	100	99	100:0	100:0
5		70	18	0.7	B	100	91	99:1	99:1
6		70	20	0.67	B	100	98	98:2	98:2
7		70	14	0.67	C	100	97	100:0	100:0
8		70	18	0.68	B	100	94	99:1	99:1
9 ^c		70	16	0.68	B	100	89+5 ^f	100:0	100:0
10 ^e		70	16	0.68	B	100	89+8 ^f	99:1	99:1
11		50	16	0.68	B	100	80	0:100	6:94
12		70	16	0.7	B	98	68	28:72	1:99
13		80	14	0.7	B	100	92	97:3	97:3
14		70	30	0.7	B	100	64	-	-
15		80	21	0.7	D	92	70 ^g	-	-
16		80	21	0.7	D	91	78 ^g	50:50	56:44

^(a) CuC₂F₅ reagent (1.1 equiv) containing 0.2 equiv of extra Et₃N·3HF (0.53 equiv overall) was used. ^(b) The reaction scale is 0.125 mmol for entry 1-8 except entry 5 and for entry 5 and 9-18 it is 0.250 mmol. ^(c) Determined by GC-MS. ^(d) Determined by ¹⁹F NMR. ^(e) Determined by ¹H NMR. ^(f) 1 equiv of CuC₂F₅ was used. ^(g) Bis-pentafluoroethylated side-product was also formed. ^(h) The yield was determined before workup.

3.2.5.6. Trifluoromethylation of iodoalkenes

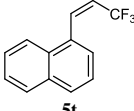
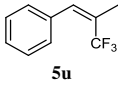
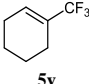
In a glovebox, to iodoalkene **7** (0.125 mmol) and 4,4'-difluoro-1,1'-biphenyl (18 mg; internal standard) in an NMR tube was added, at room temperature, CuCF_3 in DMF (0.36-0.38 M; 1.1 equiv) containing 0.1 extra equiv of $\text{Et}_3\text{N}\cdot 3\text{HF}$. The tube was sealed with a rubber septum, brought out, and kept at 23-50 °C for an indicated period of time (Table 3.2.8). Ether (0.5 mL) and water (1 mL) were added in air. After agitation, the organic layer was filtered through a short silica gel plug and analyzed by GC-MS to determine the conversion of **7**. The yield of **5** was determined by quantitative ^{19}F NMR analysis of the filtrate.

3.2.5.7. Pentafluoroethylation of iodoalkenes

In a glovebox, to iodoalkene **7** (0.125 or 0.25 mmol) in an NMR tube was added, at room temperature, CuC_2F_5 in DMF (0.68-0.7 M; 1.1 equiv) containing 0.2 extra equiv of $\text{Et}_3\text{N}\cdot 3\text{HF}$. The tube was sealed with a rubber septum, brought out, and 1,3-bis(trifluoromethyl)benzene (10 or 19 μL ; internal standard) was added via microsyringe. The NMR tube was kept at 23-70 °C for an indicated period of time (Table 3.2.9). Ether (1 mL) and water (2 mL) were added in air. After agitation, the organic layer was filtered through a short silica gel plug and analyzed by GC-MS to determine the conversion of **7**. The yield of **6** was determined by quantitative ^{19}F NMR analysis of the filtrate.

Table 3.2.8. Trifluoromethylation of iodoalkenes with CuCF_3 in DMF

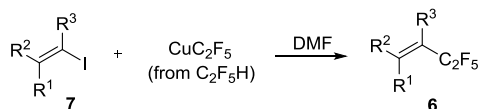
Entry ^a	Product	Temp., (°C)	Time, (h)	Conc. of CuCF_3 , M^b	Conv., (%) ^c	Yield, (%) ^d	E/Z ratio	
							Subs. ^e	Prod. ^d
1		23	1.5	0.36	100	92	95:5	95:5
2		23	1.5	0.38	100	92	98:2	98:2
3		23	2	0.38	100	91	99:1	99:1

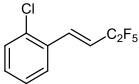
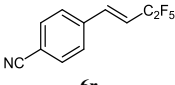
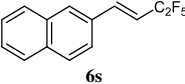
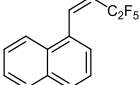
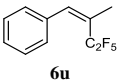
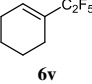
4		23	6	0.38	>99	89	99:1 ^f	99:1
5		50	8	0.38	100	97	100:0	100:0
6		50	13	0.38	100	93	100:0	100:0

^(a) Reactions were performed on 0.125 mmol scale using 4,4'-difluoro-1,1'-biphenyl (18 mg) as internal standard.

^(b) CuCF_3 reagent (1.1 equiv) containing 0.1 equiv of extra $\text{Et}_3\text{N}\cdot 3\text{HF}$ (0.43 equiv overall) was used. ^(c) Determined by GC-MS. ^(d) Determined by ^{19}F NMR. ^(e) Determined by ^1H NMR. ^(f) Substrate also contained 6 mol % of 1-(2,2-diiodovinyl)naphthalene (^1H NMR, GC-MS).

Table 3.2.9. Pentafluoroethylation of iodoalkenes with CuC_2F_5 in DMF.



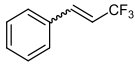
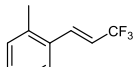
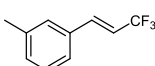
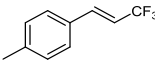
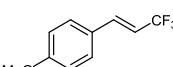
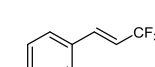
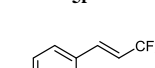
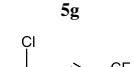
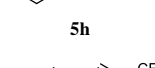
Entry ^a	Product	Temp., (°C)	Time, (h)	Conc. of CuC_2F_5 , M^b	Conv., (%) ^d	Yield, (%) ^e	E/Z ratio	
							Subs. ^f	Prod. ^g
1		23	10	0.68	>99	90	95:5	95:5
2		23	10	0.7	100	92	98:2	98:2
3		23	10	0.68	100	90	99:1	99:1
4		23	16	0.7	100	87	99:1 ^f	99:1
5		50	24	0.7	100	95	100:0	100:0
6		70	7	0.7	100	91	100:0	100:0

^(a) Reactions were performed in the presence of 1,3-bis(trifluoromethyl)benzene (10 μl per 0.125 mmol of iodoalkene) as internal standard. ^(b) The reaction scale is 0.250 mmol except for entry 2, 5 and 6 it is 0.125 mmol. ^(c) CuC_2F_5 reagent (1.1 equiv) containing 0.2 equiv of extra $\text{Et}_3\text{N}\cdot 3\text{HF}$ (0.53 equiv overall) was used. ^(d) Determined by GC-MS. ^(e) Determined by ^{19}F NMR. ^(f) Determined by ^1H NMR. ^(g) Substrate also contained 6 mol % of 1-(2,2-diiodovinyl)naphthalene (^1H NMR, GC-MS).

3.2.5.8. ^{19}F NMR data

Tables 3.2.10 and 3.2.11 list ^{19}F NMR chemical shifts of the trifluoromethylated and pentafluoroethylated products as measured directly for the organic solvent extracts used for the quantitative ^{19}F NMR yield determination with 1,3-bis(trifluoromethyl)benzene ($\delta = -62.1$ ppm) or 4,4'-difluoro-1,1'-biphenyl ($\delta = -116.3$ ppm) as internal standards (see above).

Table 3.2.10. ^{19}F NMR shifts of trifluoromethylated products (unlocked).

Product	^{19}F NMR, ppm	Ref.
 5a	<i>E</i> : -62.5 (dd, $^3J_{\text{F-H}} = 6.5$ Hz; $^4J_{\text{F-H}} = 2.1$ Hz); <i>Z</i> : -56.6 (d, $^3J_{\text{F-H}} = 9.0$ Hz)	11b
 5b	<i>E</i> : -63.5 (dd, $^3J_{\text{F-H}} = 6.2$ Hz, $^4J_{\text{F-H}} = 1.9$ Hz); <i>Z</i> : -58.0 (d, $^3J_{\text{F-H}} = 8.7$ Hz)	29
 5c	<i>E</i> : -63.4 (dd, $^3J_{\text{F-H}} = 6.6$ Hz, $^4J_{\text{F-H}} = 2.0$ Hz); <i>Z</i> : -57.5 (d, $^3J_{\text{F-H}} = 9.2$ Hz)	29
 5d	-63.5 (dd, $^3J_{\text{F-H}} = 6.3$ Hz, $^4J_{\text{F-H}} = 1.7$ Hz)	30
 5e	<i>E</i> : -63.3 (dd, $^3J_{\text{F-H}} = 6.5$ Hz, $^4J_{\text{F-H}} = 1.5$ Hz); <i>Z</i> : -58.0 (d, $^3J_{\text{F-H}} = 9.4$ Hz)	31
 5f	<i>E</i> : -63.6 (dd, $^3J_{\text{F-H}} = 6.5$ Hz, $^4J_{\text{F-H}} = 1.9$ Hz, 3F), -111.0 (m, 1F); <i>Z</i> : -57.8 (d, $^3J_{\text{F-H}} = 9.1$ Hz, 3F), -112.2 (m, 1F).	32
 5g	-63.9 (dd, $^3J_{\text{F-H}} = 6.5$ Hz, $^4J_{\text{F-H}} = 2.0$ Hz)	30
 5h	<i>E</i> : -64.2 (dd, $^3J_{\text{F-H}} = 6.4$, $^4J_{\text{F-H}} = 2.0$ Hz); <i>Z</i> : -58.3 (d, $^3J_{\text{F-H}} = 8.5$ Hz)	30
 5i	mono: -63.8 (d, $^3J_{\text{F-H}} = 6.5$ Hz, $^4J_{\text{F-H}} = 1.6$ Hz); bis: -63.2 (s), -64.1 (dd, $^3J_{\text{F-H}} = 6.4$ Hz, $^4J_{\text{F-H}} = 1.4$ Hz)	30

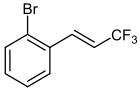
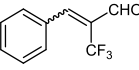
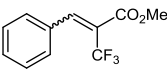
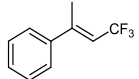
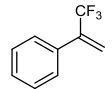
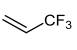
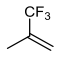
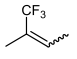
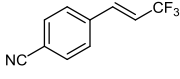
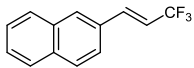
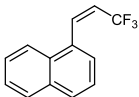
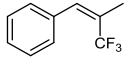
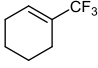
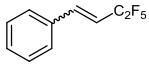
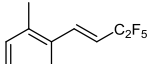
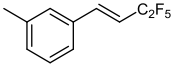
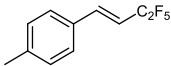
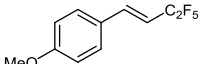
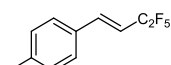
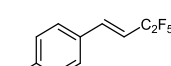
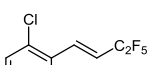
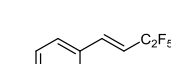

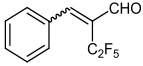
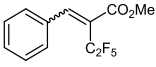
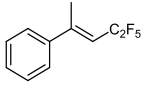
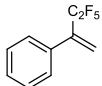
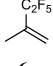
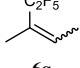
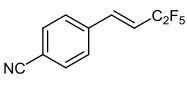
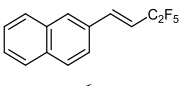
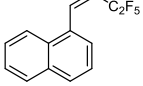
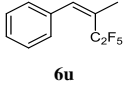
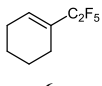
	mono, <i>E</i> : -64.1 (dd, $^3J_{F-H} = 6.4$ Hz, $^4J_{F-H} = 2.0$ Hz); bis, <i>E</i> : -59.3 (s), -64.5 (dd, $^3J_{F-H} = 6.3$ Hz, $^4J_{F-H} = 2.0$ Hz); mono, <i>Z</i> : -58.2 (d, $^3J_{F-H} = 8.5$ Hz)	11b
5j		
	<i>Z</i> : -64.2 (dd; $^4J_{F-H} = 2.3, 1.4$ Hz); <i>E</i> : -58.9 (s)	9
5k		
	<i>Z</i> : -64.2 (s); <i>E</i> : -58.1 (s)	9
5l		
	<i>E</i> : -57.3 (m); <i>Z</i> : -56.6 (m)	11b
5m		
	-63.9 (s)	11b
5n		
	-65.6 (d, $^3J_{F-H} = 5.8$ Hz)	33
5o		
	-69.7 (s)	34
5p		
	<i>E</i> : -68.8 (m); <i>Z</i> : -60.9 (m)	35
5q		
	<i>E</i> : -64.2 (dd, $^3J_{F-H} = 6.3, ^4J_{F-H} = 2.0$ Hz); <i>Z</i> : -58.0 (d, $^3J_{F-H} = 8.7$ Hz)	36
5r		
	<i>E</i> : -62.4 (dd, $^3J_{F-H} = 6.5, ^4J_{F-H} = 2.0$ Hz); <i>Z</i> : -56.6 (d, $^3J_{F-H} = 9.1$ Hz)	37
5s		
	<i>Z</i> : -58.1 (d, $^3J_{F-H} = 8.3$ Hz); <i>E</i> : -63.8 (dd, $^3J_{F-H} = 6.5$ Hz, $^4J_{F-H} = 2.2$ Hz)	37
5t		
	-61.2 (s)	-
5u		
	-70.2 (s)	38
5v		

Table 3.2.11. ^{19}F NMR shifts of pentafluoroethylated products (unlocked).

Product	^{19}F NMR, ppm	Ref.
 6a	<i>E</i> : -85.5 (t, $^3J_{\text{F-F}} = 2.2$ Hz, 3F), -115.0 (ddq, $^3J_{\text{F-H}} = 12.0$ Hz, $^4J_{\text{F-H}} = ^3J_{\text{F-F}} = 2.2$ Hz, 2F); <i>Z</i> : -86.0 (t, $^3J_{\text{F-F}} = 2.6$ Hz, 3F), -109.1 (ddq, $^3J_{\text{F-H}} = 15.6$ Hz, $^4J_{\text{F-H}} = ^3J_{\text{F-F}} = 2.6$ Hz, 2F)	13
 6b	<i>E</i> : -84.3 (m, 3F), -113.7 (ddq, $^3J_{\text{F-H}} = 11.8$ Hz, $^4J_{\text{F-H}} = ^3J_{\text{F-F}} = 2.1$ Hz, 2F); <i>Z</i> : -84.8 (m, 3F), -108.9 (m, 2F)	-
 6c	<i>E</i> : -84.3 (m, 3F), -113.7 (ddq, $^3J_{\text{F-H}} = 12.0$ Hz, $^4J_{\text{F-H}} = ^3J_{\text{F-F}} = 2.0$ Hz, 2F); <i>Z</i> : -84.8 (m, 3F), -107.8 (d, $^3J_{\text{F-H}} = 15.2$, 2F)	-
 6d	-85.6 (s, 3F), -114.8 (d, $^3J_{\text{F-H}} = 12.7$ Hz, 2F)	-
 6e	<i>E</i> : -84.4 (t, $^3J_{\text{F-F}} = 2.4$ Hz, 3F), -113.6 (ddq, $^3J_{\text{F-H}} = 12.1$ Hz, $^4J_{\text{F-H}} = ^3J_{\text{F-F}} = 2.4$ Hz, 2F); <i>Z</i> : -84.9 (m, 3F), -108.3 (d, $^3J_{\text{F-H}} = 15.0$ Hz, 2F)	-
 6f	<i>E</i> : -84.3 (s, 3F), -109.4 (m, 1F), -113.7 (d, $^3J_{\text{F-H}} = 11.5$ Hz, 2F); <i>Z</i> : -84.8 (s, 3F), -107.9 (d, $^3J_{\text{F-H}} = 15.5$ Hz, 2F), -111.1 (m, 1F)	-
 6g	85.5 (t, $^3J_{\text{F-F}} = 2.4$ Hz, 3F), -115.1 (ddq, $^3J_{\text{F-H}} = 11.6$ Hz, $^4J_{\text{F-H}} = ^3J_{\text{F-F}} = 2.4$ Hz, 2F)	-
 6h	<i>E</i> : -84.2 (s, 3F), -114.0 (d, $^3J_{\text{F-H}} = 11.9$ Hz, 2F); <i>Z</i> : -84.6 (s, 3F), -108.9 (d, $^3J_{\text{F-H}} = 15.0$ Hz, 2F)	-
 6i	mono: -84.3 (m, 3F), -113.9 (d, $^3J_{\text{F-H}} = 12.1$ Hz, 2F); bis: -83.9 (s, 3F), -84.2 (s, 3F), -114.0 (s, 2F), -114.2 (d, $^3J_{\text{F-H}} = 12.3$ Hz, 2F)	-
 6j	mono, <i>E</i> : -84.2 (m, 3F), -114.1 (ddq, $^3J_{\text{F-H}} = 11.7$ Hz, $^4J_{\text{F-H}} = ^3J_{\text{F-F}} = 2.0$ Hz, 2F); bis, <i>E</i> : -83.2 (s, 3F), -84.2 (s, 3F), -108.1 (s, 2F), -114.5 (d, $^3J_{\text{F-H}} = 12.1$ Hz, 2F); mono, <i>Z</i> : -84.5 (s, 3F), -109.2 (d, $^3J_{\text{F-H}} = 15.0$ Hz, 2F)	-

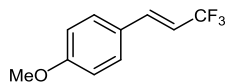
 <p>6k</p>	Z: -82.7 (s, 3F), -113.2 (s, 2F); E: -82.3 (m, 3F), -109.5 (m, 2F)	-
 <p>6l</p>	Z: -82.8 (s, 3F), -111.8 (s, 2F); E: -80.6 (s, 3F), -104.9 (s, 2F)	-
 <p>6m</p>	E: -84.6 (s, 3F), -108.0 (m, 2F); Z: -84.7 (s, 3F), -107.1 (d, $^3J_{F-H} = 15.1$ Hz, 2F)	-
 <p>6n</p>	-81.9 (m, 3F), -112.1 (m, 2F)	39
 <p>6p</p>	-82.9 (s, 3F), -116.3 (s, 2F)	-
 <p>6q</p>	E: -83.0 (s, 3F), -115.7 (s, 2F); Z: -83.7 (s, 3F), -111.2 (s, 2F)	-
 <p>6r</p>	E: -84.1 (t, $^3J_{F-F} = 2.3$ Hz, 3F), -114.7 (ddq, $^3J_{F-H} = 11.5$ Hz, $^4J_{F-H} = ^3J_{F-F} = 2.3$ Hz, 2F); Z: -84.6 (t, $^3J_{F-F} = 2.3$ Hz, 3F), -108.9 (ddq, $^3J_{F-H} = 15.3$ Hz, $^4J_{F-H} = ^3J_{F-F} = 2.4$ Hz, 2F)	-
 <p>6s</p>	E: -84.2 (t, $^3J_{F-F} = 2.3$ Hz, 3F), -113.6 (ddq, $^3J_{F-H} = 12.1$ Hz, $^4J_{F-H} = ^3J_{F-F} = 2.3$ Hz, 2F); Z: -84.7 (s, 3F), -107.6 (d, $^3J_{F-H} = 15.9$ Hz, 2F)	-
 <p>6t</p>	Z: -84.5 (s, 3F), -108.7 (d, $^3J_{F-H} = 14.8$ Hz, 2F); E: -84.2 (s, 3F), -113.7 (d, $^3J_{F-H} = 12.0$ Hz, 2F)	-
 <p>6u</p>	E: -82.0 (s, 3F), -108.9 (s, 2F)	-
 <p>6v</p>	-83.0 (s, 3F), -116.4 (s, 2F)	-

3.2.5.9. Products isolation

(3,3,3-Trifluoroprop-1-enyl)benzene (5a). To β -bromostyrene (**4a**; *trans/cis* = 8:1; purity 96%, 1.91 g, 10 mmol) was added under argon at room temperature CuCF_3 in DMF (0.36 M; 69.0 mL; 2.5 equiv) containing an extra 0.1 equiv of TREAT HF, and the mixture was stirred for 24 h at 50 °C. Pentane (50 mL), water (500 mL), and aqueous NH_3 (33%; 5 mL) were added. The organic layer was separated and the aqueous layer was washed with pentane (2×25 mL). The combined pentane solutions were washed with brine (2×100 mL), dried over MgSO_4 , and filtered through a short silica gel plug. Evaporation (23 °C, 10 mbar) of the filtrate gave **5a** as a slightly yellowish oil (1.27 g; 74%; *E/Z* = 8:1). *E* isomer: ^1H NMR (CDCl_3 , 400 MHz): δ = 7.50 – 7.43 (m, 2H), 7.43 – 7.34 (m, 3H), 7.16 (dq, $^3J_{\text{H-H}} = 16.1$ Hz, $^4J_{\text{F-H}} = 2.2$ Hz, 1H), 6.21 (dq, $^3J_{\text{H-H}} = 16.1$ Hz, $^3J_{\text{F-H}} = 6.5$ Hz, 1H). ^{13}C NMR (CDCl_3 , 101 MHz): δ = 137.8 (q, $^3J_{\text{C-F}} = 6.8$ Hz), 133.6, 130.2, 129.1, 127.7, 123.8 (q, $^1J_{\text{C-F}} = 268.8$ Hz), 116.0 (q, $^2J_{\text{C-F}} = 33.8$ Hz). ^{19}F NMR (376 MHz, CDCl_3): δ = -63.4 (dd, $^3J_{\text{H-F}} = 6.5$ Hz, $^4J_{\text{H-F}} = 2.1$ Hz, 3F).¹²

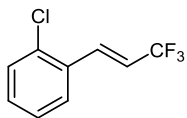
(*E*)-1-Methyl-3-(3,3,3-trifluoroprop-1-enyl)benzene (5c). To (*E*)-1-(2-bromovinyl)-3-methylbenzene (**4c**; 1.38 g, 7 mmol) was added under argon at room temperature CuCF_3 in DMF (0.38 M; 46.1 mL; 2.5 equiv) containing an extra 0.1 equiv of TREAT HF, and the mixture was stirred for 23 h at 50 °C. Pentane (100 mL), water (200 mL), and aqueous NH_3 (33%; 5 mL) were added. The organic layer was separated and the aqueous layer was washed with pentane (2×50 mL). The combined pentane solutions were washed with brine (2×50 mL), dried over MgSO_4 , filtered, and evaporated (23 °C, <100 mbar). Column chromatography of the residue in pentane produced **5c** as a colorless oil (1.125 g; 86%). The product contained 2% of 1-methyl-3-vinylbenzene (GC-MS; ^1H NMR). ^1H NMR (CDCl_3 , 500 MHz): δ = 7.31 – 7.24 (m, 3H), 7.22 – 7.18 (m, 1H), 7.12 (dq, $^2J_{\text{H-H}} = 16.1$ Hz, $^4J_{\text{F-H}} = 2.1$ Hz, 1H), 6.19 (dq, $^3J_{\text{H-H}} = 16.1$ Hz, $^3J_{\text{F-H}} = 6.6$ Hz, 1H), 2.38 (s, 3H). ^{13}C NMR (CDCl_3 , 101 MHz): δ = 138.8, 138.0 (q, $^3J_{\text{C-F}} = 6.8$ Hz), 133.5, 131.0, 128.9, 128.3, 124.9, 123.9 (q, $^1J_{\text{C-F}} = 268.7$ Hz), 115.7 (q, $^2J_{\text{C-F}} = 33.7$ Hz), 21.4. ^{19}F NMR (376 MHz, CDCl_3): δ = -63.4 (dd, $^3J_{\text{H-F}} = 6.6$ Hz, $^4J_{\text{H-F}} = 2.0$ Hz, 3F).¹³

(E)-1-Methoxy-4-(3,3,3-trifluoroprop-1-enyl)benzene (5e). To (E)-1-(2-



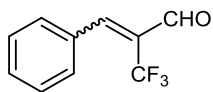
bromovinyl)-4-methoxybenzene (**4e**; 213 mg, 1mmol) was added under argon at room temperature CuCF_3 in DMF (0.38 M; 6.6 mL; 2.5 equiv) containing an extra 0.1 equiv of TREAT HF, and the mixture was stirred for 24 h at 50 °C. Pentane (50 mL), water (50 mL), and aqueous NH_3 (33%; 1 mL) were added. The organic layer was separated and the aqueous layer was washed with pentane (2×20 mL). The combined pentane solutions were washed with brine (2×25 mL), dried over MgSO_4 , filtered, and evaporated (23 °C, 10 mbar). Column chromatography of the residue in pentane produced **5e** as a white solid (178 mg; 88%). The product contained 1% of the corresponding *Z*-isomer, and 1% of 1-methoxy-4-vinylbenzene (GC-MS; ^1H and ^{19}F NMR). ^1H NMR (CDCl_3 , 400 MHz): δ = 7.43 – 7.37 (m, 2H), 7.09 (dq, $^3J_{\text{H-H}}=16.1$ Hz, $^4J_{\text{F-H}}=2.1$ Hz, 1H), 6.94 – 6.88 (m, 2H), 6.06 (dq, $^3J_{\text{H-H}}=16.1$ Hz, $^3J_{\text{F-H}}=6.6$ Hz, 1H), 3.84 (s, 3H). ^{13}C NMR (CDCl_3 , 101 MHz): δ = 161.2, 137.3 (q, $^3J_{\text{C-F}}=6.8$ Hz), 129.2, 126.2, 124.1 (q, $^1J_{\text{C-F}}=268.5$ Hz), 114.4, 113.5 (q, $^2J_{\text{C-F}}=33.6$ Hz), 55.4. ^{19}F NMR (376 MHz, CDCl_3): δ = -62.9 (dd, $^3J_{\text{H-F}}=6.6$ Hz, $^4J_{\text{H-F}}=1.5$ Hz, 3F).¹⁵

(E)-1-Chloro-2-(3,3,3-trifluoroprop-1-enyl)benzene (5h). To 1-chloro-2-(2-



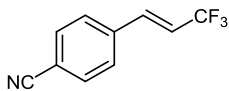
bromovinyl)benzene (**4h**; 218 mg, 1mmol) was added under argon at room temperature CuCF_3 in DMF (0.38 M; 6.6 mL; 2.5 equiv) containing an extra 0.1 equiv of TREAT HF, and the mixture was stirred for 24 h at 50 °C. Pentane (50 mL), water (50 mL), and aqueous NH_3 (33%; 1 mL) were added. The organic layer was separated and the aqueous layer was washed with pentane (2×20 mL). The combined pentane solutions were washed with brine (2×25 mL), dried over MgSO_4 , filtered, and evaporated (23 °C, 10 mbar). After column chromatography of the residue in pentane and subsequent trap-to-trap distillation **5h** was obtained as a colorless oil (192 mg; 92%). The product contained 1% of the corresponding *Z*-isomer (GC-MS; ^{19}F NMR). ^1H NMR (CDCl_3 , 400 MHz): δ = 7.60 (dq, $^3J_{\text{H-H}}=16.2$ Hz, $^4J_{\text{F-H}}=2.1$ Hz, 1H), 7.56 – 7.51 (m, 1H), 7.45 – 7.40 (m, 1H), 7.36 – 7.27 (m, 2H), 6.22 (dq, $^3J_{\text{H-H}}=16.1$ Hz, $^3J_{\text{F-H}}=6.4$ Hz, 1H). ^{13}C NMR (CDCl_3 , 101 MHz): δ = 134.6, 134.2 (q, $^3J_{\text{C-F}}=6.9$ Hz), 131.9, 131.1, 130.3, 127.5, 127.3, 123.4 (q, $^1J_{\text{C-F}}=269.2$ Hz), 118.5 (q, $^2J_{\text{C-F}}=34.1$ Hz). ^{19}F NMR (376 MHz, CDCl_3): δ = -63.7 (dd, $^3J_{\text{H-F}}=6.4$ Hz, $^4J_{\text{H-F}}=2.1$ Hz, 3F).¹⁴

3-Phenyl-2-(trifluoromethyl)acrylaldehyde (5k). To (*Z*)-2-bromo-3-



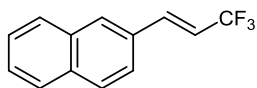
phenylacrylaldehyde (**4k**; 215 mg, 1mmol) was added under argon at room temperature CuCF_3 in DMF (0.38 M; 6.6 mL; 2.5 equiv) containing an extra 0.2 equiv of TREAT HF, and the mixture was stirred for 24 h at 50 °C. Ether (40 mL), water (80 mL), and aqueous NH_3 (33%; 1 mL) were added. The organic layer was separated and the aqueous layer was washed with ether (2×20 mL). The combined ether solutions were washed with brine (2×40 mL), dried over MgSO_4 , filtered, and evaporated. Purification of the residue on a short silica gel plug with pentane gave **5k** as a yellow oil (155 mg; 78%). The product contained 17% of the corresponding *E*-isomer, and 1% of cinnamaldehyde (GC-MS; ^1H and ^{19}F NMR). *Z*-isomer: ^1H NMR (CDCl_3 , 400 MHz): $\delta = 9.86$ (q, $^4J_{\text{F-H}} = 2.8$ Hz, 1H), 8.17 (s, 1H), 7.59-7.41 (m, 5H). ^{13}C NMR (CDCl_3 , 101 MHz): $\delta = 186.7$, 149.7 (q, $^3J_{\text{C-F}} = 5.5$ Hz), 131.6, 130.8 (q, $^4J_{\text{C-F}} = 2.6$ Hz), 130.7, 129.9 (q, $^2J_{\text{C-F}} = 28.1$ Hz), 129.1, 122.2 (q, $^1J_{\text{C-F}} = 274.8$ Hz). ^{19}F NMR (376 MHz, CDCl_3): $\delta = -64.9$ (q, $^4J_{\text{F-H}} = 1.6$ Hz, 3F).⁹

(E)-4-(3,3,3-Trifluoroprop-1-enyl)benzonitrile (5r). To (*E*)-4-(2-



iodovinyl)benzonitrile (**4r**; 255 mg, 1mmol) was added under argon at room temperature CuCF_3 in DMF (0.38 M; 2.9 mL; 1.1equiv) containing an extra 0.1 equiv of TREAT HF, and the mixture was stirred for 1.5 h at 23 °C. Ether (30 mL), water (60 mL), and aqueous NH_3 (33%; 5 mL) were added. The organic layer was separated and the aqueous layer was washed with ether (2×20 mL). The combined ether solutions were washed with brine (2×15 mL), dried over MgSO_4 , filtered, and evaporated (23 °C, 5 mbar). Column chromatography of the residue in pentane produced **5r** as a yellow solid (160 mg; 81%). The product contained 1% of the corresponding *Z*-isomer (GC-MS; ^{19}F NMR). ^1H NMR (CDCl_3 , 500 MHz): $\delta = 7.72 - 7.67$ (m, 2H), 7.58 - 7.53 (m, 2H), 7.17 (dq, $^3J_{\text{H-H}} = 16.1$ Hz, $^4J_{\text{F-H}} = 2.0$ Hz, 1H), 6.31 (dq, $^3J_{\text{H-H}} = 16.2$ Hz, $^3J_{\text{F-H}} = 6.3$ Hz, 1H). ^{13}C NMR (CDCl_3 , 100 MHz): $\delta = 137.8$, 136.0 (q, $^3J_{\text{C-F}} = 6.8$ Hz), 132.8, 128.2, 123.1 (q, $^1J_{\text{C-F}} = 269.4$ Hz), 119.5 (q, $^2J_{\text{C-F}} = 34.3$ Hz), 118.3, 113.6. ^{19}F NMR (376 MHz, CDCl_3): $\delta = -64.0$ (dd, $^3J_{\text{H-F}} = 6.3$ Hz, $^4J_{\text{H-F}} = 2.0$ Hz, 3F).²⁰

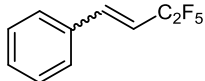
(E)-2-(3,3,3-Trifluoroprop-1-enyl)naphthalene (5s). To *(E)*-2-(2-



iodovinyl)naphthalene (**4s**; 560 mg, 2mmol) was added under argon at room temperature CuCF_3 in DMF (0.38 M; 5.8 mL; 1.1 equiv) containing an extra 0.1 equiv of TREAT

HF, and the mixture was stirred for 2 h at 23 °C. Ether (50 mL), water (80 mL), and aqueous NH_3 (33%; 5 mL) were added. The organic layer was separated and the aqueous layer was washed with ether (2 × 20 mL). The combined ether solutions were washed with brine (2 × 25 mL), dried over MgSO_4 , filtered, and evaporated (23 °C, 5 mbar). Column chromatography of the residue in pentane produced **5s** as a white solid (413 mg; 93%). The product contained 1% of the corresponding *Z*-isomer (GC-MS; ^{19}F NMR). ^1H NMR (CDCl_3 , 400 MHz): δ = 7.89 – 7.82 (m, 4H), 7.60 (dd, $^3J_{\text{H-H}} = 8.6$ Hz, $^4J_{\text{H-H}} = 1.7$ Hz, 1H), 7.55 – 7.49 (m, 2H), 7.32 (dq, $^3J_{\text{H-H}} = 16.2$ Hz, $^4J_{\text{F-H}} = 2.0$ Hz, 1H), 6.32 (dq, $^3J_{\text{H-H}} = 16.1$ Hz, $^3J_{\text{F-H}} = 6.5$ Hz, 1H). ^{13}C NMR (CDCl_3 , 101 MHz): δ = 137.9 (q, $^3J_{\text{C-F}} = 6.8$ Hz), 134.2, 133.4, 131.0, 129.2 (q, $^4J_{\text{C-F}} = 0.7$ Hz), 128.9, 128.6, 127.9, 127.3, 126.9, 123.9 (q, $^1J_{\text{C-F}} = 268.8$ Hz), 123.3, 116.1 (q, $^2J_{\text{C-F}} = 33.8$ Hz). ^{19}F NMR (376 MHz, CDCl_3): δ = -63.2 (dd, $^2J_{\text{H-F}} = 6.5$ Hz, $^4J_{\text{H-F}} = 2.0$ Hz, 3F).²¹

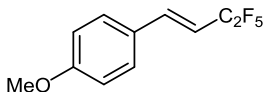
(3,3,4,4,4-Pentafluorobut-1-enyl)benzene (6a). To β -bromostyrene (**4a**; *trans/cis* =



8:1; purity 96%, 953 mg, 5 mmol) was added under argon at room temperature CuC_2F_5 in DMF (0.7 M; 7.9 mL; 1.1 equiv) containing an extra 0.2 equiv of TREAT HF, and the mixture

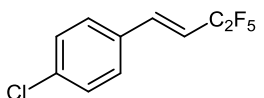
was stirred for 14 h at 70 °C. Pentane (50 mL), water (80 mL), and aqueous NH_3 (33%; 3 mL) were added. The organic layer was separated and the aqueous layer was washed with pentane (2 × 20 mL). The combined pentane solutions were washed with brine (2 × 40 mL), dried over MgSO_4 , filtered, and evaporated (23 °C, 10 mbar). Column chromatography of the residue in pentane produced **6a** as a colorless oil (990 mg; 89%; *E/Z* = 8:1). *E* isomer: ^1H NMR (CDCl_3 , 400 MHz): δ = 7.52 – 7.45 (m, 2H), 7.44 – 7.34 (m, 3H), 7.19 (dt, $^3J_{\text{H-H}} = 16.2$ Hz, $^4J_{\text{F-H}} = 2.3$ Hz, 1H), 6.18 (dtq, $^3J_{\text{H-H}} = 16.2$ Hz, $^3J_{\text{F-H}} = 11.9$ Hz, $^4J_{\text{F-H}} = 0.8$ Hz, 1H). ^{13}C NMR (CDCl_3 , 101 MHz): δ = 139.9 (t, $^3J_{\text{C-F}} = 9.2$ Hz), 133.7, 130.3, 129.1, 127.8 (t, $^4J_{\text{C-F}} = 1.0$ Hz), 119.3 (qt, $^1J_{\text{C-F}} = 285.5$, $^2J_{\text{C-F}} = 38.5$ Hz), 114.2 (t, $^2J_{\text{C-F}} = 23.1$ Hz), 113.0 (tq, $^1J_{\text{C-F}} = 250.4$ Hz, $^2J_{\text{C-F}} = 38.6$ Hz). ^{19}F NMR (376 MHz, CDCl_3): δ = -85.5 (t, $^3J_{\text{F-F}} = 2.2$ Hz, 3F), -115.0 (ddq, $^3J_{\text{F-H}} = 12.0$ Hz, $^4J_{\text{F-H}} = ^3J_{\text{F-F}} = 2.2$ Hz, 2F).^{3,23}

(E)-1-Methoxy-4-(3,3,4,4,4-pentafluorobut-1-enyl)benzene (6e). To (E)-1-(2-



bromovinyl)-4-methoxybenzene (213 mg, 1 mmol) was added under argon at room temperature CuC_2F_5 in DMF (0.68 M; 1.6 mL; 1.1 equiv) containing an extra 0.2 equiv of TREAT HF, and the mixture was stirred for 18 h at 70 °C. Ether (30 mL), water (30 mL), and aqueous NH_3 (33%; 1 mL) were added. The organic layer was separated and the aqueous layer was washed with ether (2×15 mL). The combined ether solutions were washed with brine (2×25 mL), dried over MgSO_4 , filtered, and evaporated (23 °C, 10 mbar). Column chromatography of the residue in pentane produced **6e** as a colorless oil (235 mg; 93%). ^1H NMR (CDCl_3 , 500 MHz): $\delta = 7.44 - 7.40$ (m, 2H), 7.12 (dt, $^3J_{\text{H-H}} = 16.2$ Hz, $^4J_{\text{F-H}} = 2.3$ Hz, 1H), 6.94 – 6.89 (m, 2H), 6.03 (dtq, $^3J_{\text{H-H}} = 16.1$ Hz, $^3J_{\text{F-H}} = 12.0$ Hz, $^4J_{\text{F-H}} = 0.7$ Hz, 1H). ^{13}C NMR (CDCl_3 , 101 MHz): $\delta = 161.4$, 139.2 (t, $^3J_{\text{C-F}} = 9.2$ Hz), 129.3, 126.4, 119.3 (qt, $^1J_{\text{C-F}} = 285.4$ Hz, $^2J_{\text{C-F}} = 38.9$ Hz), 114.5, 113.2 (tq, $^1J_{\text{C-F}} = 250.1$ Hz, $^2J_{\text{C-F}} = 38.4$ Hz), 111.6 (t, $^2J_{\text{C-F}} = 23.1$ Hz), 55.4. ^{19}F NMR (376 MHz, CDCl_3): $\delta = -84.4$ (t, $^3J_{\text{F-F}} = 2.4$ Hz, 3F), -113.6 (ddq, $^3J_{\text{F-H}} = 12.1$ Hz, $^4J_{\text{F-H}} = ^3J_{\text{F-F}} = 2.4$ Hz, 2F). Anal. Calcd. for $\text{C}_{11}\text{H}_9\text{F}_5\text{O}$: C, 52.4; H, 3.6. Found: C, 53.0; H, 3.8.

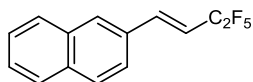
(E)-1-Chloro-4-(3,3,4,4,4-pentafluorobut-1-enyl)benzene (6g). To (E)-1-(2-



bromovinyl)-4-chlorobenzene (327 mg, 1.5 mmol) was added under argon at room temperature CuC_2F_5 in DMF (0.68 M; 2.4 mL; 1.1 equiv) containing an extra 0.2 equiv of TREAT HF, and the mixture was stirred for 14 h at 70 °C. Ether (50 mL) and water (100 mL) were added. The organic layer was separated and the aqueous layer was washed with ether (2×25 mL). The combined ether solutions were washed with brine (2×30 mL), dried over MgSO_4 , filtered, and evaporated (23 °C, 10 mbar). After column chromatography of the residue in pentane and subsequent trap-to-trap distillation **6g** was obtained as a colorless oil (320 mg; 83%). ^1H NMR (CDCl_3 , 400 MHz): $\delta = 7.44 - 7.34$ (m, 4H), 7.14 (dt, $^3J_{\text{H-H}} = 16.2$ Hz, $^4J_{\text{F-H}} = 2.3$ Hz, 1H), 6.17 (dtq, $^3J_{\text{H-H}} = 16.1$ Hz, $^3J_{\text{F-H}} = 11.7$ Hz, $^4J_{\text{F-H}} = 0.7$ Hz, 1H). ^{13}C NMR (CDCl_3 , 126 MHz): $\delta = 138.5$ (t, $^3J_{\text{C-F}} = 9.2$ Hz), 136.2, 132.0, 129.3, 129.0, 119.1 (qt, $^1J_{\text{C-F}} = 285.5$ Hz, $^2J_{\text{C-F}} = 38.4$ Hz), 114.7 (t, $^2J_{\text{C-F}} = 23.1$ Hz), 112.7 (tq, $^1J_{\text{C-F}} = 251.5$ Hz, $^2J_{\text{C-F}} = 38.7$ Hz). ^{19}F NMR (376 MHz, CDCl_3): $\delta = 85.5$ (t, $^3J_{\text{F-F}} = 2.4$ Hz, 3F), -115.1 (ddq, $^3J_{\text{F-H}} =$

11.6 Hz, $^4J_{F-H} = ^3J_{F-F} = 2.4$ Hz, 2F). Anal. Calcd. for $C_{10}H_6ClF_5$: C, 46.8; H, 2.4. Found: C, 46.9; H, 2.6.

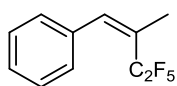
(E)-2-(3,3,4,4,4-Pentafluorobut-1-enyl)naphthalene (6s). To (E)-2-(2-



iodovinyl)naphthalene (2.52 g, 9 mmol) was added under argon at room temperature $CuCl_2 \cdot 2H_2O$ in DMF (0.7 M; 14.1 mL; 1.1 equiv) containing an extra 0.2 equiv of TREAT HF,

and the mixture was stirred for 10 h at 23 °C. Pentane (50 mL), water (100 mL), and aqueous NH_3 (33%; 10 mL) were added. The organic layer was separated and the aqueous layer was washed with pentane (2 × 25 mL). The combined pentane solutions were washed with brine (2 × 25 mL), dried over $MgSO_4$, filtered, and evaporated. Column chromatography of the residue in pentane produced **6s** as a white solid (2.27 g; 93%). 1H NMR ($CDCl_3$, 400 MHz): $\delta = 7.91 - 7.82$ (m, 4H), 7.62 (dd, $^3J_{H-H} = 8.6$ Hz, $^4J_{H-H} = 1.7$ Hz, 1H), 7.56 – 7.50 (m, 2H), 7.35 (dq, $^3J_{H-H} = 16.2$ Hz, $^4J_{H-F} = 2.3$ Hz, 1H), 6.29 (dtq, $^3J_{H-H} = 16.1$ Hz, $^3J_{F-H} = 11.7$ Hz, $^4J_{F-H} = 0.7$ Hz, 1H). ^{13}C NMR ($CDCl_3$, 101 MHz): $\delta = 139.9$ (t, $^3J_{C-F} = 9.2$ Hz), 134.2, 133.4, 131.1 (t, $^4J_{C-F} = 1.2$ Hz), 129.4 (t, $^4J_{C-F} = 1.2$ Hz), 128.9, 128.6, 127.9, 127.4, 127.0, 123.2, 119.3 (qt, $^1J_{C-F} = 285.6$ Hz, $^2J_{C-F} = 38.6$ Hz), 114.3 (t, $^2J_{C-F} = 23.1$ Hz), 113.1 (tq, $^1J_{C-F} = 250.3$ Hz, $^2J_{C-F} = 38.5$ Hz). ^{19}F NMR (376 MHz, $CDCl_3$): $\delta = -84.2$ (t, $^3J_{F-F} = 2.3$ Hz, 3F), -113.6 (ddq, $^3J_{F-H} = 12.1$ Hz, $^4J_{F-H} = ^3J_{F-F} = 2.3$ Hz, 2F). Anal. Calcd. for $C_{14}H_9F_5$: C, 61.8; H, 3.3. Found: C, 61.7; H, 3.3.

(Z)-2-(3,3,4,4,4-Pentafluoro-2-methylbut-1-enyl)benzene (6u). To (Z)-2-



iodopropenylbenzene (1.22 g, 5 mmol) was added under argon at room temperature $CuCl_2 \cdot 2H_2O$ in DMF (0.7 M; 7.9 mL; 1.1 equiv) containing an extra 0.2 equiv of TREAT HF, and the mixture was

stirred for 24 h at 50 °C. Pentane (50 mL), water (80 mL), and aqueous NH_3 (33%; 5 mL) were added. The organic layer was separated and the aqueous layer was washed with pentane (2 × 20 mL). The combined pentane solutions were washed with brine (2 × 40 mL), dried over $MgSO_4$, filtered, and evaporated (23 °C, 10 mbar). Column chromatography of the residue in pentane produced **6u** as a colorless oil (0.99 g; 84%). The product contained 3% of phenylmethylacetylene (GC-MS; ^{13}C NMR). 1H NMR ($CDCl_3$, 400 MHz): $\delta = 7.34 - 7.24$ (m, 3H), 7.24 – 7.16 (m, 2H), 7.01 (s, 1H), 2.06 (s, 3H). ^{13}C NMR ($CDCl_3$, 101 MHz): $\delta = 138.4$ (t, $^3J_{C-F} = 4.3$ Hz), 135.7, 128.1 (t, $^4J_{C-F} =$

2.8 Hz), 127.9, 127.6, 125.3 (t, $^2J_{C-F}$ = 20.9 Hz), 119.5 (qt, $^1J_{C-F}$ = 287.6 Hz, $^2J_{C-F}$ = 38.3 Hz), 114.0 (tq, $^1J_{C-F}$ = 255.4 Hz, $^2J_{C-F}$ = 38.5 Hz), 19.7 (tq, $^3J_{C-F}$ = 4.3 Hz, $^4J_{C-F}$ = 1.9 Hz). ^{19}F NMR (376 MHz, CDCl_3): δ = -82.0 (s, 3F), -108.9 (s, 2F). Anal. Calcd. for $\text{C}_{11}\text{H}_9\text{F}_5$: C, 55.9; H, 3.8. Found: C, 56.6; H, 3.9.

3.2.5. References

1. For selected recent reviews, see: (a) Tomashenko, O. A.; Grushin, V. V. *Chem. Rev.* **2011**, 111, 4475. (b) Roy, S.; Gregg, B. T.; Gribble, G. W.; Le, V.-D.; Roy, S. *Tetrahedron* **2011**, 67, 2161. (c) Liu, T.; Shen, Q. *Eur. J. Org. Chem.* **2012**, 6679. (d) Chu, L.; Qing, F.-L. *Acc. Chem. Res.* **2014**, 47, 1513.
2. For selected more recent reports not covered in the comprehensive review,^{1a} see: (a) Zhang, C.-P.; Wang, Z.-L.; Chen, Q.-Y.; Zhang, C.-T.; Gu, Y.-C.; Xiao, J.-C. *Angew. Chem., Int. Ed.* **2011**, 50, 1896. (b) Popov, I.; Lindeman, S.; Daugulis, O. *J. Am. Chem. Soc.* **2011**, 133, 9286. (c) Morimoto, H.; Tsubogo, T.; Litvinas, N. D.; Hartwig, J. F. *Angew. Chem., Int. Ed.* **2011**, 50, 3793. (d) Tomashenko, O. A.; Escudero-Adán, E. C.; Martínez Belmonte, M.; Grushin, V. V. *Angew. Chem., Int. Ed.* **2011**, 50, 7655. (e) Kondo, H.; Oishi, M.; Fujikawa, K.; Amii, H. *Adv. Synth. Catal.* **2011**, 353, 1247. (f) Chen, M.; Buchwald, S. L. *Angew. Chem., Int. Ed.* **2013**, 52, 11628. (g) Mormino, M. G.; Fier, P. S.; Hartwig, J. F. *Org. Lett.* 2014, 16, 1744. (h) Gonda, Z.; Kovács, S.; Wéber, C.; Gáti, T.; Mészáros, A.; Kotschy, A.; Novák, Z. *Org. Lett.* **2014**, 16, 4268.
3. Zanardi, A.; Novikov, M. A.; Martin, E.; Benet-Buchholz, J.; Grushin, V. V. *J. Am. Chem. Soc.* **2011**, 133, 20901.
4. Lishchynskiy, A.; Mazloomi, Z.; Grushin, V. V. *Synlett* **2015**, 26, 45.
5. (a) Burdon, J.; Coe, P. L.; Marsh, C. R.; Tatlow, J. C. *Chem. Commun.* **1967**, 1259. (b) McLoughlin, V. C. R.; Thrower, J. *Tetrahedron* **1969**, 25, 5921. (c) Burdon, J.; Coe, P. L.; Marsh, C. R.; Tatlow, J. C. *J. Chem. Soc., Perkin Trans. I* **1972**, 639. (d) De Pasquale, R. J.; Padgett, C. D.; Rosser, R. W. *J. Org. Chem.* **1975**, 40, 810. (e) Kobayashi, Y.; Yamamoto, K.; Kumadaki, I. *Tetrahedron Lett.* **1979**, 20, 4071.
6. Chen, Q.-Y.; Wu, S.-W. *J. Chem. Soc., Perkin Trans. I* **1989**, 2385.
7. (a) Chen, Q.-Y.; Wu, S.-W. *J. Chem. Soc., Chem. Commun.* **1989**, 705. (b) Fei, X.-S.; Tian, W.-S.; Chen, Q.-Y. *J. Chem. Soc., Perkin Trans. I* **1998**, 1139. (c) Duan, J.; Dolbier, W. R. Jr.; Chen, Q.-Y. *J. Org. Chem.* **1998**, 63, 9486. (d) Zhang, X.; Qing, F.-L.; Yu, Y. *J. Org. Chem.* **2000**, 65, 7075. (e) Qing, F.-L.; Zhang, X.; Peng, Y. *J. Fluorine Chem.* **2001**, 111, 185.

8. Chen, Q.-Y.; Duan, J.-X. *J. Chem. Soc., Chem. Commun.* **1993**, 1389.
9. Nowak, I.; Robins, M. J. *J. Org. Chem.* **2007**, *72*, 2678.
10. Duan, J.-X.; Su, D.-B.; Chen, Q.-Y. *J. Fluorine Chem.* **1993**, *61*, 279.
11. (a) Urata, H.; Fuchikami, T. *Tetrahedron Lett.* **1991**, *32*, 91. (b) Hafner, A.; Bräse, S. *Adv. Synth. Catal.* **2011**, *353*, 3044.
12. Carr, G. E.; Chambers, R. D.; Holmes, T. F.; Parker, D. G. *J. Chem. Soc., Perkin Trans. I* **1988**, 921.
13. Serizawa, H.; Aikawa, K.; Mikami, K. *Org. Lett.* **2014**, *16*, 3456.
14. For Pd-catalyzed trifluoromethylation of vinylic electrophiles, see: (a) Kitazume, T.; Ishikawa, N. *Chem. Lett.* **1982**, 137. (b) Kitazume, T.; Ishikawa, N. *J. Am. Chem. Soc.* **1985**, *107*, 5186. (c) Cho, E. J.; Buchwald, S. L. *Org. Lett.* **2011**, *13*, 6552.
15. Aikawa, K.; Nakamura, Y.; Yokota, Y.; Toya, W.; Mikami, K. *Chem. Eur. J.* **2015**, *21*, 96.
16. Mazloomi, Z.; Bansode, A.; Benavente, P.; Lishchynskiy, A.; Urakawa, A.; Grushin, V. V. *Org. Process Res. Dev.* **2014**, *18*, 1020.
17. Lishchynskiy, A.; Grushin, V. V. *J. Am. Chem. Soc.* **2013**, *135*, 12584.
18. Konovalov, A. I.; Benet-Buchholz, J.; Martin, E.; Grushin, V. V. *Angew. Chem. Int. Ed.* **2013**, *52*, 11637.
19. (a) Novák, P.; Lishchynskiy, A.; Grushin, V. V. *Angew. Chem. Int. Ed.* **2012**, *51*, 7767. (b) Novák, P.; Lishchynskiy, A.; Grushin, V. V. *J. Am. Chem. Soc.* **2012**, *134*, 16167. (c) Lishchynskiy, A.; Novikov, M. A.; Martin, E.; Escudero-Adán, E. C.; Novák, P.; Grushin, V. V. *J. Org. Chem.* **2013**, *78*, 11126. (d) Lishchynskiy, A.; Berthon, G.; Grushin, V. V. *Chem. Commun.* **2014**, *50*, 10237. (e) Lishchynskiy, A.; Mazloomi, Z.; Grushin, V. V. *Synlett* **2015**, 26, 45.
20. CCDC-1026478 (**2e**) and CCDC-1026964 (**3s**) contain the supplementary crystallographic data for this paper. These data can be obtained free of charge from the Cambridge Crystallographic Data Centre via www.ccdc.cam.ac.uk/data_request/cif.
21. Konovalov, A. I.; Lishchynskiy, A.; Grushin, V. V. *J. Am. Chem. Soc.* **2014**, *136*, 13410.
22. Xiangmin, H. China Patent CN101492466 A, 2009.
23. Conway, J. C.; Quayle, P.; Regan, A. C.; Urch, C. J. *Tetrahedron* **2005**, *61*, 11910.
24. Buss, A. D.; Warren, S. *J. Chem. Soc. Perkin Trans I* **1985**, 2307.
25. Mousseau, J. J.; Bull, J. A.; Ladd, C. L.; Fortier, A.; Roman, D. S.; Charette, A. B. *J. Org. Chem.* **2011**, *76*, 8243.

26. Kowalski, C. J.; Weber, A. E.; Fields, K.W. *J. Org. Chem.* **1982**, *47*, 5088.
27. Alem, K. V.; Belder, G.; Lodder, G.; Zuilhof, H. *J. Org. Chem.* **2005**, *70*, 179.
28. Chen, J.; Wang, T.; Zhao, K. *Tetrahedron Lett.* **1994**, *35*, 2827.
29. Yasu, Y.; Koike, T.; Akita, M. *Chem. Commun.* **2013**, *49*, 2037.
30. Parsons, A. T.; Senecal, T. D.; Buchwald, S. L. *Angew. Chem., Int. Ed.* **2012**, *51*, 2947.
31. Prakash, G. K. S.; Krishnan, H. S.; Jog, P. V.; Iyer, A. P.; Olah, G. A. *Org. Lett.* **2012**, *14*, 1146.
32. Li, Y.; Wu, L.; Neumann, H.; Beller, M. *Chem. Commun.* **2013**, *49*, 2628.
33. Hanack, M.; Ullmann, J. *J. Org. Chem.* **1989**, *54*, 1432.
34. Haszeldine, R. N., Keen, D. W.; Tipping, A. E. *J. Chem. Soc. C*, **1970**, 414.
35. Davies, T.; Haszeldine, R. N.; Tipping, A. E. *J. Chem. Soc., Perkin Trans. 1*, **1980**, 927.
36. Kobayashi, T.; Eda, T.; Tamura, O.; Ishibashi, H. *J. Org. Chem.* **2002**, *67* 3156.
37. Fuchikami, T.; Yatabe, M.; Ojima, I. *Synthesis* **1981**, 365.
38. Haas, A.; Pluemer, R.; Schiller, A. *Chem. Ber.* **1985**, *118*, 3004.
39. Nader, B. S.; Cordova, J. A.; Reese, K. E.; Powell, C. L. *J. Org. Chem.* **1994**, *59*, 2898.

Chapter 4.

***General introduction II: Catalyst design for C-X
forming and water oxidation reactions***

It is widely accepted that sustainable industrial production and the generation of clean energy must be two of the pillars of our society. Huge amounts of resources for research and technological development in this direction have been dedicated and are expected to be dedicated. The European Union's H2020 program, for example, has identified one of its seven priority lines as “safe, clean and efficient energy”, which has allocated almost 6 billion € for the period 2014-2020. Catalysis is one of the driving force of these advances. Catalyzed chemical processes allow increase production, reduce the number of reaction steps, work under more favorable energy conditions and generate less byproducts than the uncatalyzed processes.¹ The improvement of the catalyst stability and selectivity for existing processes and the development of catalysts for processes that are not yet available is a fundamental and strategic research for achieving sustainable industrial production and clean energy generation.

To attain the highest levels of reactivity and selectivity in catalytic reactions, several parameters must be optimized. Of these, the selection and design of the ligands, in which an electronically and sterically well defined scaffold is the most crucial step.¹ In this context, thousands of homo- and hetero-donor ligands, mainly P- and N-containing ligands with either C_2 - or C_1 -symmetry, have been developed although only a few of them have a general scope and are easy to handle and prepared in few step from cheap starting materials.¹ Among them, heterodonor ligands (P-N, P-S, P-P', etc.) equipped with strong and weak donor heteroatom pairs have made some of the most fundamental contributions to the development of catalysis.¹ The most widely used ligands in catalysis are phosphines and, to a lesser extent phosphinites. Phosphite-based ligands has also emerged as very suitable ligands for catalysis.^{1,2} Phosphite-containing ligands are very attractive from a synthetic point of view, since they are easy to prepare from readily accessible alcohols. The availability of many alcohols makes simple ligand tuning possible, which allows the synthesis of series of chiral ligands than can be screened in the search for high activities and selectivities for each type of substrate. Another advantage of phosphite compounds is that they are less sensitive to air than phosphines and phosphinites. Although they are prone to decomposition reactions, such as alcoholysis, hydrolysis, and the Arbuzov reaction, these side reactions can be suppressed when bulky aryl phosphites are used. Our groups have contributed with improved generations of modular homodonor and heterodonor biaryl phosphite-containing ligand libraries, obtained from readily available starting materials and easy to handle.^{2,3}

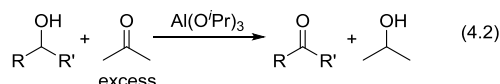
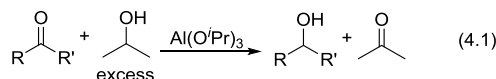
In the last two decades N-heterocyclic carbenes (NHCs) have emerged as powerful ligands in catalysis. Owing to their strong σ -donation ability, air stability and low toxicity they have become practical alternatives to the most commonly used phosphines.⁴ A large number of transformations are known to proceed only with NHC-based catalysts. For that reason, exploring new classes of NHCs is a very important goal in recent organometallic chemistry. 1,2,3-Triazol-5-ylidenes are a relevant subclass of NHCs possessing a mesoionic carbene (MIC) structure.⁵ Several reactions have been explored where triazolylidene-based metal complexes are equally or more efficient compared to their NHC analogues, such as cross-coupling reactions, olefin metathesis, oxidative transformations, transfer hydrogenation catalysis, and the click reaction.⁶ The triazole framework adds the advantages of increased σ -donation compared to classical NHCs and the ability to potentially stabilize different metal oxidation states. In addition, they are accessible via synthetically highly efficient and modular nature of "click reaction". The click reaction tolerates a wide variety of functional groups in the azide and in the alkyne reactant which facilitate preparing series of modular MIC-containing ligands, with different steric and electronic properties. Despite this, the development of heterodonor 1,2,3-triazol-5-ylidene-containing ligands have been scarcely explored. To our knowledge the 1,2,3-triazol-5-ylidene carbene moiety has mainly been combined with pyridine/pyrimidine and hydroxyl groups.^{6e,i,7} More research is therefore still needed to explore new classes of chelating 1,2,3-triazolylidene based ligands.

In this context, this second part of the thesis focused on the development of new mesoionic carbene-based ligands and phosphite-oxazoline ligands, and their application to several catalytic transformations. In this respect, we have designed new mixed oxazole/thiazole-MIC ligands and evaluated them in the transfer hydrogenation, dehydrogenation and water oxidation reactions. Finally, we also successfully developed and evaluated new biaryl phosphite-oxazoline ligands in the asymmetric intermolecular Heck reaction. In the following sections we describe the background of each catalytic reaction studied in this thesis.

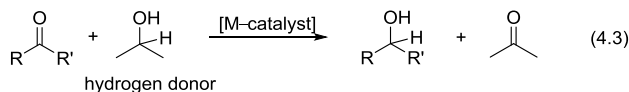
4.1. Metal-catalyzed transfer hydrogenation reactions

Hydrogen transfer (HT) reactions as a reduction of ketones to alcohols have been known since 1925.⁸ In the original version, which was discovered by Meerwein, Ponnendorf and Verlay, aluminium isopropoxide was applied to promote transfer of hydrogen from isopropanol to a ketone (Eq. (4.1)). Latter in the middle of 1930s,

Oppenauer discovered that aluminium isopropoxide was also able to catalyze the opposite reaction (Eq. (4.2)).⁹



In hydrogen transfer reactions the equilibrium can push the reaction to the desired direction by using an excess of either alcohol or ketone in the starting material. Therefore, for the Meerwein-Ponndorf-Verlay (MPV) reduction of ketones, i.e. transfer hydrogenation, isopropanol is utilized in excess and for the opposite reaction, the Oppenauer oxidation, acetone as a ketone is employed in excess. A main drawback with classical aluminum oxide promoted hydrogen transfer reactions is that the stoichiometric amount of aluminum salts is often needed and this is a big obstacle for scaling up in industrial application. Catalytic hydrogen transfer reactions have been applied as an alternative with an increased interest for more than a decade (Eq. (4.3)).¹⁰ In this regard lanthanides and transition metals (i.e. Ru, Rh, Ir, Fe) have been found to work in catalytic way.



Various “sacrificial” hydrogen sources were employed for transition-metal catalyst-promoted TH such as cyclohexene, cyclohexadiene, alcohols (including ⁱPrOH, MeOH, EtOH, glycerol), formic acid, Hantzsch esters,¹¹ hydrazine, benzothiazoles, dimethylamine-borane, ... Isopropanol and formate (HCOOH/NEt₃) are the main used sources of reducing reagent because of their low price.

A series of organic and inorganic bases have been used in TH such as Et₃N, KOH, NaOH, Na₂CO₃, NaO₂CH, KOⁱPr, NaOⁱPr, LiOⁱPr, KOⁱBu, NaOⁱBu, KHMDS (potassium hexamethylsilazane), K₃PO₄, Cs₂CO₃, CsOH, NaOAc and NaOMe. The pK_a value and the nature of the cation of the base may have an influence the catalytic efficiencies of transition-metal catalysts.¹²

Several unsaturated compounds including ketones, aldehydes, imines, nitro compounds, nitriles, oximes, α,β -unsaturated esters, α,β -unsaturated acids, α,β -

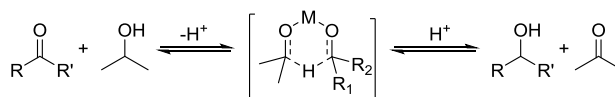
unsaturated carbonyl compounds, heterocycles, alkenes, and alkynes have been reduced through TH processes in the presence of transition-metal catalysts.

4.1.1. Mechanism

From a mechanistic point of view, two main catalytic pathways have been proposed for hydrogen transfer reactions. The first one is the direct hydrogen transfer that is involved for main group metals. The second one is the so called hydridic route which is suggested for transition metals.

4.1.1.1. Direct hydrogen transfer

This pathway which has been proposed for the MPV reduction, is a concerted process that proceeds through a six-membered transition state without involvement of metal hydride intermediates (Scheme 4.1).



Scheme 4.1. Direct hydrogen transfer mechanism.

4.1.1.2. The hydridic route

This pathway, which is claimed to occur for transition metal catalysts proceeds via involvement of metal hydride species.^{13,14} In some cases, the hydrides were isolated from transition metal-catalyzed hydrogenation reactions and some examples are represented in Figure 4.1.^{15,16b}

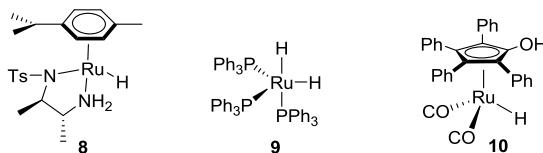
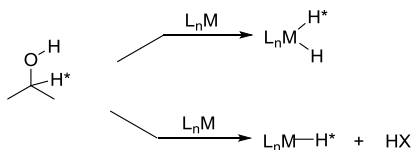


Figure 4.1. Examples of isolated metal hydride intermediates.

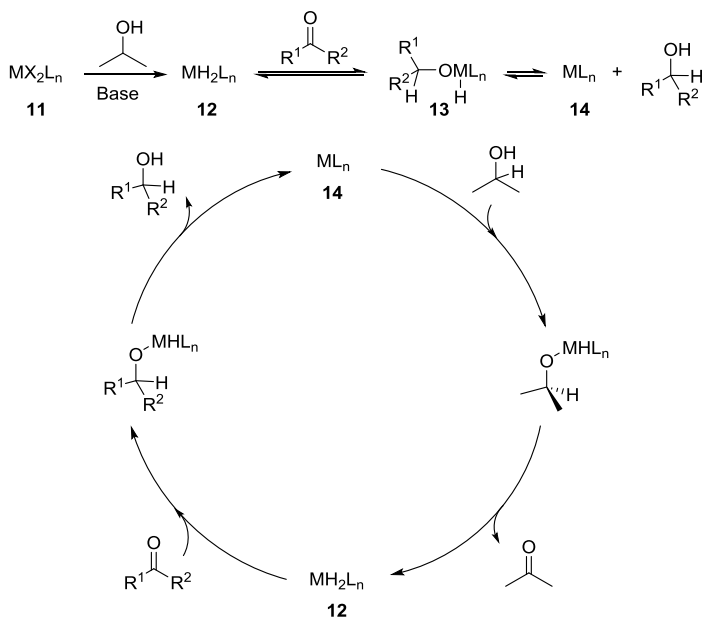
For the hydridic route, two general mechanisms have been disclosed depending on the origin of the hydride on the metal (Scheme 4.2). In the first one, a metal dihydride is formed (called dihydride mechanism), while in the second pathway a metal monohydride is formed (called monohydride mechanism).



Scheme 4.2. General mechanisms for the hydric route.

4.1.1.2.1. The dihydride mechanism

A common feature for catalysts function via the dihydride mechanism is that both C-H and O-H from the alcohol are transferred to metal center. In that way both hydrogen atoms lose their identity when transferred to the ketone.¹⁷ The proposed catalytic cycle for the transfer hydrogenation of ketones via dihydride pathway is shown in Scheme 4.3. The catalyst precursor **11** reacts with isopropanol in the presence of base to produce the dihydride complex **12**. Reaction of **12** with the substrate produce metal (0) species **14** via complex **13** after reductive elimination. Both the dihydride **12** and metal (0) **14** species are key intermediates in the catalytic cycle of the hydrogen transfer reaction.

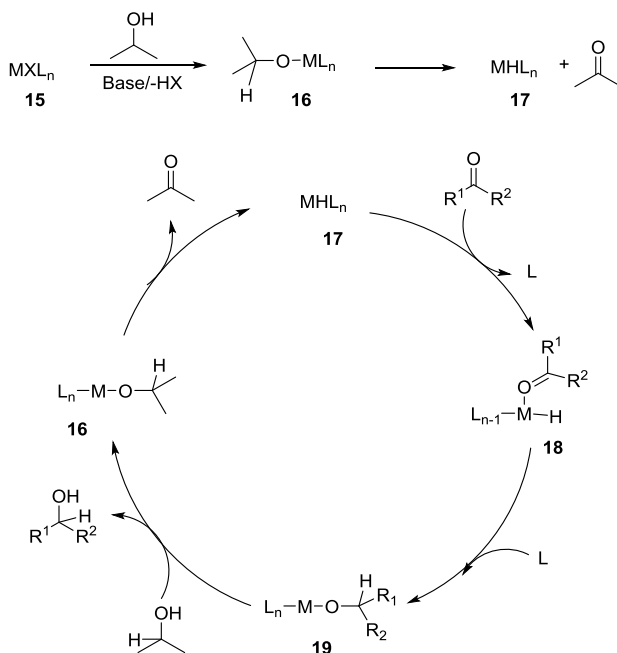


Scheme 4.3. Proposed catalytic cycle for transfer hydrogenation of ketones using isopropanol as hydrogen donor via dihydride mechanism.

In the catalytic cycle, species **14** undergoes oxidative addition of the hydrogen donor (isopropanol) followed by β -hydride elimination to produce acetone and the metal dihydride species **12**. Ketone then adds to species **12** to give the corresponding alkoxide complex that after reductive elimination provides the desired alcohol and regenerates metal (0) species **14**.

4.1.1.2.2. The monohydride mechanism

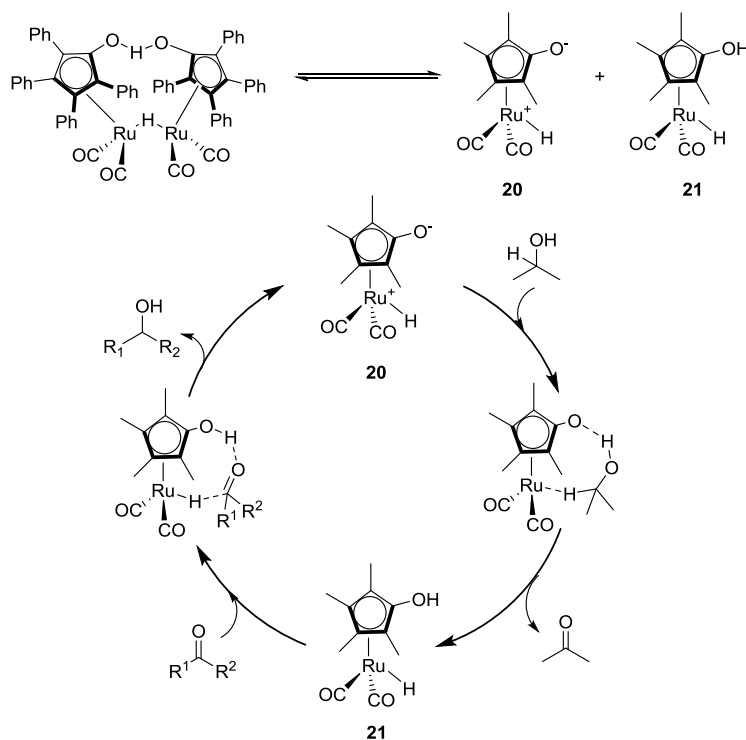
A general feature for catalyst function through the monohydride mechanism is that both C-H and O-H hydrogens keep their identity (i.e. the C-H from the hydrogen donor ends up as a C-H in the product). This is due to the fact that the hydride on the metal is just formed from the C-H hydrogen of the donor (that transfers to the carbonyl carbon) while the OH of the donor remains as a proton during the process (and adds to the carbonyl oxygen). The metal monohydride can be, however, formed via different mechanisms. In one of them the metal monohydride is formed via formation of the corresponding alkoxide followed by β -elimination (Scheme 4.4).



Scheme 4.4. Proposed catalytic cycle for the TH of ketones using isopropanol as hydrogen donor via monohydride mechanism involving the formation of metal-alkoxide intermediates.

In this pathway, the catalyst precursor MXL_n is transformed to the metal-alkoxyde species **16** by reaction with the hydrogen donor in the presence of base. The key metal monohydride intermediate **17** is formed after β -hydride elimination of intermediate **16**. In the catalytic cycle, coordination of the corresponding ketone to **17** followed by 1,2-insertion of the ketone into the metal hydride bond results in the formation of the corresponding alkoxyde **19**. Alkoxyde ligand exchange with the hydrogen donor provides the desired alcohol. The catalytic cycle is completed by means of the β -elimination of the isopropoxide ligand.

The second pathway involves the simultaneous transfer of the C-H to the metal and O-H to one of the ligands. The latter does not therefore involve the formation of any metal alkoxyde intermediate. This pathway requires that the presence of metal ligand bifunctional catalyst (i.e. Ru-Noyori catalyst, Shvo's catalyst, ...), in which one of the sites of the ligand plays the role of base.¹⁸ The mechanism using Shvo's system is shown as example in Scheme 4.5.^{16d}



Scheme 4.5. Proposed concerted proton and hydride transfer mechanism using the Shvo's catalyst. Phenyl rings of the cyclopentadiene ring are omitted for clarity.

Coordination of the hydrogen donor to the 16-electron species **20** provides the corresponding monohydride intermediate **21**. The monohydride catalyst then reacts with the ketone and the hydride and proton are simultaneously transferred to form the desired alcohol and regenerate species **20**.

4.1.2. Transition-metal catalysts

The utilization of late transition-metal catalysts involving first-, second-, and third-row transition metals of groups 8, 9, 10, and 11 was the outstanding discovery in transfer hydrogenation. The pioneering work reported by Henbest, Mitchell, and co-workers in the 1960s¹⁹⁻²¹ showed that the iridium hydride complex [IrH(dmsO)₃] catalyzed the hydrogenation of ketones to alcohols with isopropanol. In the 1970s, Sasson and Blum²² mentioned the first example of Ru complex applicable in TH. They showed that [RuCl₂(PPh₃)₃] was active in the TH of acetophenone with isopropanol at high temperature.²⁴ Two decades later, Chowdhury and Bäckvall²⁵ demonstrated that adding a catalytic amount of NaOH to the [RuCl₂(PPh₃)₃]-catalyst precursor accelerated the reaction by 10³–10⁴ times. It was shown that the rate enhancement is because of the formation of highly active RuH₂(PPh₃)₃.^{16b} The first report of the Ru catalyzed asymmetric transfer hydrogenation (ATH) was appeared in the early 1980s.²⁶⁻²⁸ One of the most important breakthroughs in ATH came with the discovery of Noyori and co-workers that ruthenium η⁶-arene complexes in combination with vicinal amino alcohol or diamine ligands (complexes **22**; Figure 4.2) served as efficient catalysts for the reduction of ketones and ketimines, respectively, under ATH conditions.²⁹ Since then ATH has been received attention as they are important process in the fragrance and pharmaceutical industries.^{30,31}

To date, great advancement has been done about late transition metal-catalyzed TH and ATH. A diversity of transition metals, ligands, hydrogen sources, bases, reaction media, and unsaturated compounds have been involved in the transformations that are critical subjects of TH. Apart from numerous Ru-complexes³² that have been developed in this field, Ir- and Rh-complexes³³ are well-documented for this transformation.

Recently there has been an increased attention to the earth-abundant metal catalysts in a broad range of synthetic transformations, such as iron³⁴⁻³⁶ and cobalt.³⁷⁻³⁹ Iron-catalyzed TH has been developed during the last decade.³⁴ In 2010 Morris group^{35,36} demonstrated that iron(II) complexes containing PNNP pincer ligands (complexes **23**; Figure 4.2) are effective catalytic precursors for the transfer hydrogenation of ketones

with t PrOH and KO t Bu under mild conditions. More recently, cobalt catalyst precursors have also shown their usefulness in this transformation. Thus for instance, the use of Co-PNP catalyst precursors (complex **24**, Figure 4.2) showed high activities in the TH of several substrates such as ketones, aldehydes and imines.³⁹

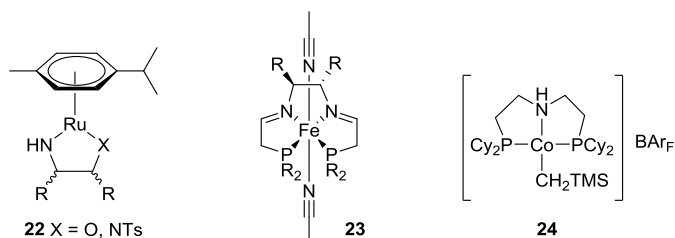


Figure 4.2. Representative examples of Ru-, Fe- and Co- catalysts precursors for TH.

Other transition metal catalyst precursor based on Pd,⁴⁰ Re,⁴¹ Os,⁴² Pt⁴³ and Au⁴⁴ have also been developed, albeit to a lesser extent. Among them, it should be highlighted the Pd-catalysts that have been used for the stereo- and chemoselective reduction of alkynes to alkenes under transfer hydrogenation conditions.⁴⁵

In summary, albeit there are many transition metals that are able to efficiently catalyze transfer hydrogenation reactions, the vast majority and the most efficient catalysts precursors are those based on ruthenium, rhodium and iridium modified with several ligand types (i.e. amino-alcohols, diamines, phosphines, ...). In recent years, research has been focused on the evaluation of carbene-type ligands, due to their highly adaptable steric and electronic properties. In the next sections I will discuss in more details the results obtained using metal-catalyst precursors containing classical N-heterocyclic and mesoionic carbene ligands.

4.1.2.1. N-Heterocyclic carbene catalyst

N-Heterocyclic carbenes (NHCs) are cyclic carbenes having at least one α -amino substituent.⁴⁶ The NHC ligand family has shortly triggered a true explosion of interest in coordination chemistry and organometallic catalysis.⁴⁷⁻⁵¹ This is due to their strong coordination ability as σ -donors and remarkable adjustability of the steric and electronic properties on the metal center, and almost infinite possibilities of topological modifications. NHC ligands were commonly incorporated into chelating, pincer, and chiral structures with mainly Ir, Ru and Rh catalysts and rarely Fe and Pd catalysts for transfer hydrogenation reactions.⁵² The first example of Rh-NHC catalyst for transfer

hydrogenation was $[\text{Rh}(\text{bis-NHC})\text{I}_2(\text{OAc})]$ (**25**; Figure 4.3) which was prepared by the groups of Prof. Crabtree and Prof. Peris in 2002.⁵³ These type of complexes showed good catalytic performance for TH of both ketones and imines but they were inactive in TH of alkenes. Some other rhodium complexes containing NHC ligands were also used in the TH of ketones (i.e. complex **26**; Figure 4.3).^{54,55}

Ru-NHC complexes have also been explored in TH reactions. A series of ruthenium complexes containing different donor substituent-functionalized NHCs were prepared in the group of Prof. Albrecht^{56,57} and among them the olefin-tethered NHC ruthenium complex **27** (Figure 4.3) was very efficient toward TH of olefins, alkynes, ketones, nitrobenzene, benzonitrile, and *N*-benzylideneaniline under various conditions.⁵⁶ Most of the Ru-NHC complexes, however, were applied in TH of ketones and imines.^{58,59} Nevertheless, Peris and coworkers reported the use of ruthenium complex containing bis-NHC **28** (Figure 4.3) for the transfer hydrogenation of carbone dioxide to formate.⁶⁰

Iridium/NHC complexes have also been successfully developed mostly for the transfer hydrogenation of carbonyl and imine compounds.⁶¹⁻⁶⁶ As representative examples, we can highlight the results achieved using the catalyst precursors **29** and **30** developed in the groups of Prof. Oro and Prof. Crabtree, respectively (Figure 4.3).

Few examples are available in the case of Pd-NHCs as some of them are not stable and therefore could not be isolated. As representative example, we should highlight the Pd-NHC complexes **31** (Figure 4.3) developed by Elsevier and coworkers in the TH of alkynes to alkenes.⁶⁷ Fe-NHC complexes, such as complex **32** (Figure 4.3), have also been reported for the TH albeit with a narrow substrate scope.⁶⁸

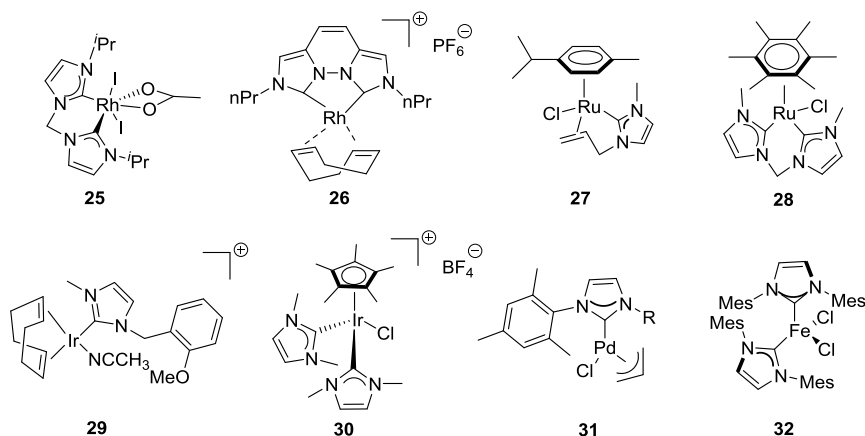


Figure 4.3. Representative TH metal catalyst precursors bearing NHC ligands.

4.1.2.2. Mesoionic carbene catalyst

Given the increasing interest in 1,2,3-triazol-5-ylidenes ligands in homogeneous metal-transition catalysis, the catalytic application of these ligands were also investigated in TH. Comparing the catalytic activity of the MIC containing metal catalyst precursors with the NHC analogues, we can see that metal-NHCs are superior in terms of activity, which it is not unexpected because the use of MIC ligands in catalysis has a shorter story than the NHCs.

TH with ruthenium complexes featuring a chelating triazolylidene ligand have appeared, and selected examples of complexes are gathered in Figure 4.4. The air- and moisture ruthenium(II) complex **33** bearing an unsymmetrical benzimidazole-benzotriazole-pyridine ligand has been shown to be a robust and highly active catalyst for the TH of ketones in refluxing 2-propanol, reaching final TOFs up to 176400 h^{-1} .⁶⁹ The authors demonstrated that the excellent catalytic performances resulted from the hemilabile unsymmetrical coordinating environment around the central metal and “N–H” effect. The two halfsandwich ruthenium complexes **34** and **35** containing a chelating 1,2,3-triazolyl or 1,2,4-triazolyl units also exhibited good catalytic behaviors in TH of carbonyls.^{69,70}

Selected examples of Rh-complexes are collected in Figure 4.4. The bidentate monovalent rhodium-cod complex **36** with square-planar geometry that contains tzNHC and an Arduengo-type NHC motif was successfully used as catalyst for the TH of carbonyls, imine, and diene using ⁱPrOH as the hydrogen source.⁷¹ More importantly, catalyst **36** was much more active than its analogue **37** in which the triazolyl moiety coordinates through a nitrogen donor. The complexes **38** having the N(2) atom of 1,2,3-triazole coordinated to the rhodium center have shown better activity in the TH of ketones than **39** in which N(3) is involved in ligation. Moreover, the reactivity with respect to the ligands is in the order Se > S.⁷² The mechanistic studies indicated that the Rh species that had lost the Cp* ligand was an intermediate in the catalytic cycle. The iridium analogues of complexes **36–39** were also synthesized and exhibited even better catalytic performances in TH reactions than these rhodium counterparts.^{71,72} Iridium complexes functionalized by pyridyltriazole **40**, bis-triazole **41**, or bis-abnormal carbene **42** with half-sandwich and piano-stool configuration were assayed in the catalytic TH of nitrobenzenes using ⁱPrOH providing aniline, azobenzene, and azoxybenzene compounds (Figure 4.4).⁷³ Investigations of ligand substitution, metal substitution (comparison with ruthenium counterparts containing each of the above-mentioned

triazolyl ligands), and temperature variation on the catalytic behavior indicated that the selectivity was moderately controlled by tuning the metals, ligands, and reaction conditions. In addition, the iridium-based catalysts provided higher conversion of nitrobenzenes than their ruthenium analogues.⁷³

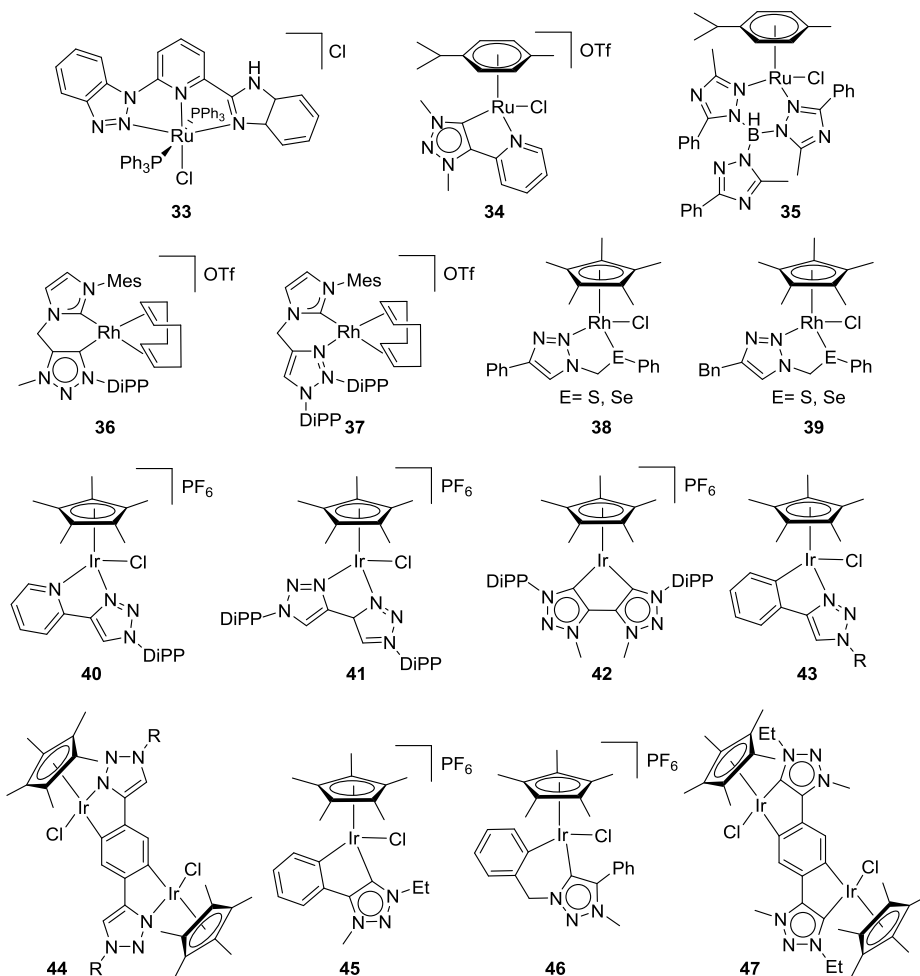


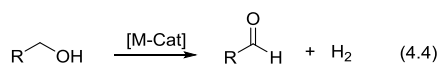
Figure 4.4. Selected metal-catalyst precursors containing triazolylidene ligands for TH.

The same research group reported a series of mono- and dinuclear orthometalated iridium complexes with both Cp* and triazolyl fragments either with C–N or with C–C donor sets to iridium centers with a central phenyl ring as C–H activation sites (compounds **43-47**; Figure 4.4).⁷⁴ All of these presynthesized complexes **43-47** were employed as catalysts for the TH of benzaldehyde and acetophenone revealing that the

dinuclear iridium complexes **44** and **47** produced faster reactions than their mononuclear counterparts. Moreover, the dinuclear cyclometalated iridium complex **47** with poly mesoionic carbene ligands gave the best catalytic performances.⁷⁴

4.2. Ir-catalyzed dehydrogenation of alcohols

One of the most fundamental technologies for organic synthesis is oxidation of organic compounds. Alcohols can be oxidized to their corresponding aldehydes and ketones. They are synthetically prevalent functional groups because of their outstanding versatility for derivatization.⁷⁵ Traditionally alcohols oxidation has been achieved using stoichiometric amounts of high-valent chromium (i.e. Cr₂O₃, pyridium chlorochromate ...) or manganese oxides.⁷⁶ Another well-known procedure is the Oppenauer-type oxidation via hydrogen transfer reaction using a sacrificial hydrogen acceptor (usually a ketone).⁷⁷ Other milder and often more selective methodologies have been more recently developed based on the use of hypervalent iodine⁷⁸ and the use of perruthenate as catalyst using N-oxides as terminal oxidant.⁷⁹ All these methodologies have as an important drawback the use of stoichiometric amounts of sacrificial oxidants, which led to low atom economy of the overall reactions due to the formation of high amounts of reduced (sometimes toxic) side-products. Due to this fact, it is not estrange that in recent years research has been focus on the use of more benign terminal oxidants (such as water peroxide and oxygen).⁸⁰ As alternative, the oxidant-free dehydrogenation of alcohols has been less studied although it is very attractive in terms of atom economy and waste (Eq (4.4)).

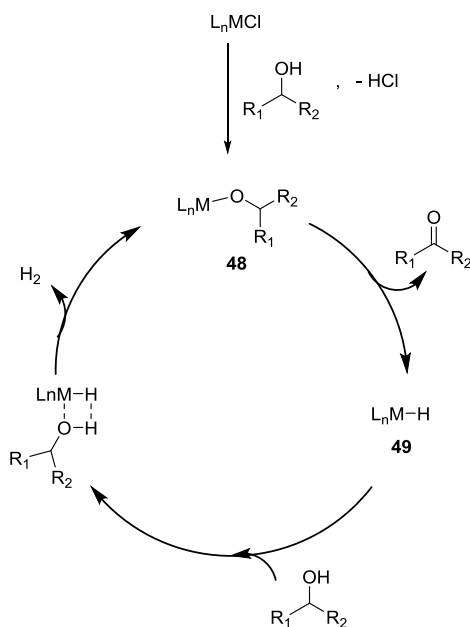


Another advantage of this process is that it generates molecular hydrogen as a useful side product that can be used as an alternative to fossil fuels, which has stimulated research in this area.⁸¹ In this context, the groups of Beller,⁸² Milstein⁸³, and Grützmacher⁸⁴ among others have developed ruthenium-catalyzed protocols for the dehydrogenation of primary and secondary alcohols. Other transition metals able to catalyze the dehydrogenation reactions include Pd,⁸⁵ Ir,⁸⁶ Cu⁸⁷ and Os.⁸⁸ In some cases, however, the formed product remains coordinated to the metal therefore it is predisposed for further coupling to produce esters and acetals.⁸⁹ Most of the catalysts,

however, require the addition of an external base to activate the catalysts. More research is therefore needed to achieve base- and oxidant-free dehydrogenation catalysts.⁹⁰

4.2.1. Mechanism

From the mechanistic point of view the dehydrogenation reaction is very similar to the transfer hydrogenation. The main difference can be found in the fact that acceptorless H_2 gas elimination (dehydrogenation) is more difficult than the transfer to another molecule (transfer hydrogenation) and therefore hardest reactions conditions are required for H_2 release. One of the possible simplest mechanism for dehydrogenation reaction is shown in Scheme 4.6. The first step of the reaction would involve the formation of alkoxo metal intermediate **48** by the reaction of metal complex with alcohol and liberation of HX ($X =$ labile ligand like Cl on the metal center) which would be accelerated by the addition of the base. β -Hydrogen elimination of **48** gives ketone as a dehydrogenated product and metal hydride species **49**. Then protonolysis of metal hydride **49** by the alcohol addition, which in most cases is ligand-assisted, takes place releasing hydrogen gas and regenerating species **48**.



Scheme 4.6. One of the possible accepted mechanisms for the oxidant-free dehydrogenative oxidation of alcohols.

4.2.2. Transition-metal catalysts

As it is mentioned in Section 4.2 several transition metal complexes have been applied for the dehydrogenation of alcohol such as Ru, Ir, Pd, Cu, Os, ... Among them the most used catalyst precursors are based on Ru and Ir catalysts. Pincer ligands have played a dominant role in the development of successful metal-catalyst precursors for the acceptorless alcohol dehydrogenation (AAD). Two of the most typical examples of this type of catalytic systems are the Ru-PNN **50**^{91a} and Ru-PNP **51**⁹² catalyst precursors developed by the groups of Milstein and Beller, respectively (Figure 4.5). The former have been successfully used in the oxidation of alcohols to the corresponding esters, while the latter has been used for the dehydrogenation of methanol to provide H₂ and CO₂. The groups of Gauvin and Koriz has also developed similar Ru-PNP **52**⁹³ and Ir-PCP **53**⁹⁴ for the oxidation of alcohols to the corresponding carboxylic acids (Figure 4.5). A common feature of most of these catalysts is that the addition of an external base is necessary to activate the catalyst. AAD catalysts that do not require the addition of base are rare. Most of the examples make use of metal ligand bifunctional catalyst, such as the Shvo's catalyst (Scheme 4.5), in which one of the sites of the ligand plays the role of base. Another selected example of base-free dehydrogenation catalysts is the IrCp* complex **54** (Figure 4.5) bearing hydroxypyridine ligand developed by Fuyita et al.⁹⁵

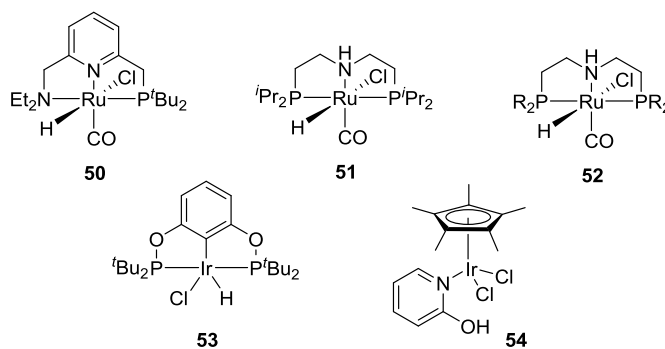


Figure 4.5. Representative examples metal catalysts precursors containing pincer and bifunctional ligands for the AAD.

As for the TH reactions, NHC's has also been successfully applied for the AAD, being the most widely used the ones bearing a bifunctional catalysts. In particular they have been useful in the β -alkylation⁹⁶ and N-alkylation⁹⁷ reactions of secondary

alcohols and amines with primary alcohols, respectively. β -Alkylation and N-alkylation reactions are tandem processes in which the first step is the alcohol dehydrogenation. Typical examples for these transformations are IrCp*-complexes **55**⁹⁸ and **56**⁹⁹ developed by the groups of Prof. Peris and Martín-Matute, respectively (Figure 4.6).

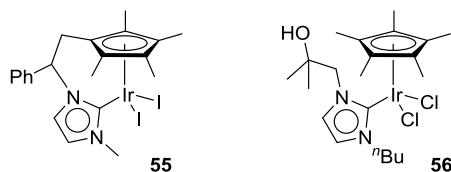


Figure 4.6. Representative examples of IrCp* catalyst precursors containing NHCs ligands for the AAD

More recently, metal complexes containing mesoionic triazolylidene ligands have also been successfully used in the AAD. This field of research was initiated by Peris and Albrecht et al.^{6g} They demonstrated that Ru-based catalyst precursor **57** (Figure 4.7), containing a monodentate triazolylidene ligand, was able to promote the oxidation not only of alcohols but also of amines. Later, Albrecht and coworkers further studied the effect of the nature of the triazolylidene substituents on AAD, by systematically replacing the ⁿBu substituents in **57** by other aryl and alkyl groups.^{6f} They found an important effect of them on catalytic activity. Thus, the presence of alkyl substituents has a positive effect on activity, while the presence of aryl groups induces much lower activity. The Albrecht group also studied the effect of introducing a second donor functionality. For that purpose they developed Ru-complexes containing a variety of C,X-bidentate triazolylidene ligands (complexes **34**, **58-60**; Figure 4.7).^{6j} Again they found an important effect of the nature of the second donor functionality on activity. The use of catalyst precursor **58**, containing the C,C-bidentate phenyl triazolyliedene ligand, therefore provided the highest activities, while the use of carboxylate or pyridine-complexes **34**, **59** and **60** provided very low activities. Interestingly, arene dissociation was observed as a potential catalyst deactivation pathway. In order to overcome this drawback, the same authors prepared Shvo's type Ru(0) complexes with triazolylidene ligands (**61**, Figure 4.7).¹⁰⁰ Nevertheless, low activities were achieved, though activity can be increased by adding cerium ammonium nitrate.

Ir-catalyst containing mesoionic ligands have also been applied in this transformation. Peris and coworkers demonstrated that IrCp*-complexes containing

abnormal carbenes can be applied for this transformation (catalyst precursor **62**; Figure 4.7).¹⁰¹ However, high amounts of the etherification products were observed. More recently, Albrecht and coworkers demonstrated that IrCp* complexes containing bidentate triazolylidene complexes are also effective for the AAD (compounds **63** and **64**; Figure 4.7). Again the presence of considerable amounts of etherification products were observed using compound **63**. Interestingly, the use of dimeric catalyst precursor **64** suppress completely the etherification products and led to the solely formation of the corresponding aldehyde or ketone. The different selectivities of monometallic complex **63** and the bimetallic one **64** has been rationalized by the significative differences observed of the electrochemical and spectroscopic analysis of both complexes.

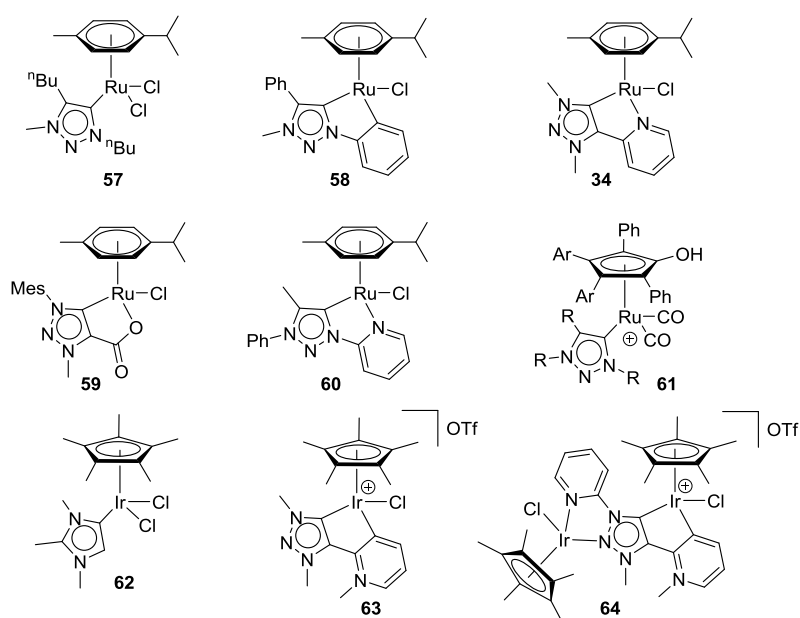


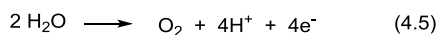
Figure 4.7. Representative metal-triazolylidene catalyst precursor developed for the acceptorless alcohol dehydrogenation.

4.3. Ir molecular catalysts for water oxidation

The sustainable production of clean energy from renewable sources is one of the most challenging scientific topics.¹⁰² Nowadays, the significant part of the global energy supply is provided by carbon-based energy sources, which is connected to several environmental problems such as air pollution and the greenhouse effect. Therefore, there is a strong demand for clean and environmentally friendly carbon-neutral

alternatives that have the potential to provide the needs of present and future generations.

The splitting of water into oxygen and hydrogen, inspired by nature's use of water and sunlight as environmentally abundant feedstocks, makes a particularly attractive approach towards addressing this issue. In nature, photosynthetic water fixation and splitting is a delicately balanced process, overcoming the energetic barrier of O-H bond cleavage and O-O bond formation by a stunning reaction cascade.¹⁰³ The complexity of the photosynthetic machinery requires alternative approaches for artificial photosynthesis.¹⁰⁴ This process requires the coupling of the two half-reactions: (i) water oxidation to produce the reducing equivalents (electrons) and oxygen as the only byproduct and (ii) reduction of protons using the electrons of the former reaction to generate molecular hydrogen. Albeit, both reaction steps are crucial for the generation of hydrogen from water, water oxidation is considered to be the bottleneck in the sustainable production of hydrogen from water.¹⁰⁵ This is because water oxidation is both thermodynamically and kinetically unfavorable, resulting in slow kinetics without the use of a catalyst.¹⁰⁶ High redox flexibility of the active center constitutes a key element in the design of synthetic complexes for water oxidation, since the formation of O₂ from H₂O requires the transfer of four electrons (Eq (4.5)).



For decades, scientists have sought to understand and imitate nature, creating not only biomimetic water oxidation catalysts (WOCs), but also well-defined homogeneous and heterogeneous catalysts. The field of water oxidation have been dominated by Ru- and Mn-catalysts. The field of water oxidation have been dominated by Ru- and Mn-catalysts. The first homogeneous catalyst for water oxidation was reported by Meyer's group in 1982.¹⁰⁷ This was the dinuclear μ -oxo-bridged ruthenium complex **65** (Figure 4.8), *cis,cis*-[(bpy)₂(H₂O)Ru(μ -O)Ru(H₂O)(bpy)₂]⁴⁺, known as the "blue dimer" because of its characteristic blue color. Albeit both productivity (TON's up to 13) and activity (TOF's up to 0.004 s⁻¹) were moderate using cerium ammonium nitrate (CAN) as sacrificial one electron oxidant, this study settle the basis for further research. The development of Mn-catalysts was inspired by the presence of the Mn₄Ca cluster in the natural oxygen evolving system. In this context, Crabtree's group reported that Mn(II)-containing terpyridine or dipicolinate ligands (such as complex **66**; Figure 4.8) are able to promote water oxidation using potassium persulfate as sacrificial two electron oxidant.¹⁰⁸ Over the last decades, rapid improvements in both activity and productivity

of Ru- and Mn-based catalytic systems have been achieved as has been clearly illustrated by the groups of Llobet,¹⁰⁹ Åkermark¹¹⁰ and Sun¹¹¹ among others.¹¹² Thus, for instance, the use of Ru-catalyst precursor **67** (Figure 4.8) led to TOF's up to 50000 s⁻¹ at pH=10000.^{109d} In recent years, however, cobalt,¹¹³ iron¹¹⁴ and iridium¹¹⁵ based catalysts have also given promising results.

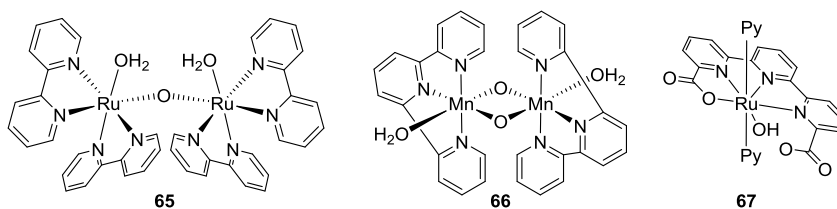
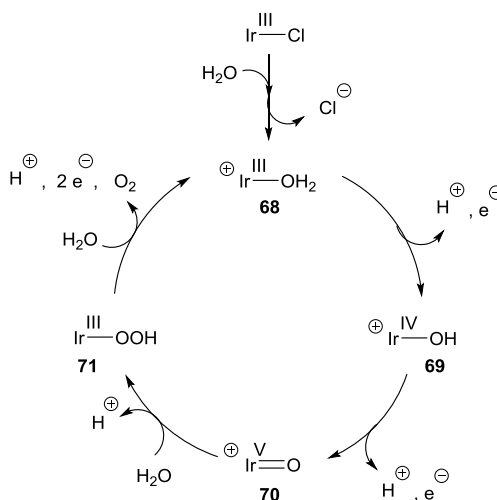


Figure 4.8. Representative examples of Ru- and Mn-based WOCs

4.3.1. Mechanism

The accepted reaction mechanism for iridium-catalyzed water oxidation is shown in Scheme 4.7. With a neutral chloro catalyst, the chloro ligand is replaced by a molecule of H₂O yielding a cationic Ir(III) aqua complex **68**. Complex **68** is then oxidized (i.e. using CAN as sacrificial oxidant) to form the Ir(IV)-hydroxo intermediate **69** liberating one proton and one electron. Further oxidation of **69** provides Ir(V) oxo complex **70**, which is a key intermediate species in the formation of the O-O bond by reacting with water. Complex **70** reacts with water to afford the Ir(III)-peroxo species **71**. The oxidation of **71** produces molecular oxygen O₂, and the species **68** is regenerated by coordination of H₂O.¹¹⁶



Scheme 4.7. Proposed reaction mechanism for iridium-catalyzed water oxidation.

4.3.2. Ir-catalysts for water oxidation

Iridium complexes applicable in water oxidation process can be classified in three categories based on the type of the coordinated ligand to Ir center.

4.3.2.1.1. Cyclometalated iridium complexes

A vital finding in the field of water oxidation catalysis was published by Bernhard and coworkers in 2008.¹¹⁷ This group showed that cyclometalated Ir(III) complexes bearing unsubstituted or substituted 2-phenylpyridine (ppy) ligands (compounds **72**; Figure 4.9) could mediate water oxidation. The cyclometalated phenylpyridine was employed as a bidentate ligand and created strong carbon-iridium bond in the desired iridium complexes and afforded the robustness that is needed for H₂O oxidation. The Ir-complexes have two open sites in the first coordination sphere for binding water to the iridium center. A control experiment with [Ir(ppy)(bpy)]⁺, lacking free coordination sites, showed no activity, confirming a key role for these open coordination sites in binding and activation of water. Oxygen-evolution experiments confirmed essentially stoichiometric consumption of CAN to generate oxygen, albeit with low TOF's (up to 0.047 s⁻¹).

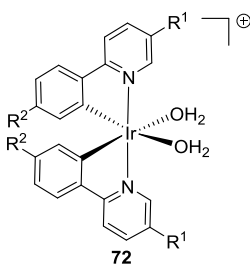


Figure 4.9. Cyclometalated iridium-based WOCs **72**.

4.3.2.1.2. Iridium complexes based on cyclopentadiene-type ligands

Inspired by the work of Bernhard, in 2009 Crabtree and Brudvig developed a new class of single-site iridium WOCs with a pentamethylcyclopentadiene (Cp*) ligand (complexes **73**; Figure 4.10).¹¹⁸ The Cp* ligand acts as an electron-donating ligand and probably this effect would result in more active catalysts. O₂ production with these type of catalysts was 1 order of magnitude faster than previously cyclometalated iridium catalysts **72**. Later the same groups studied the replacement of the cyclometalated

ligand by bipyridine, phenantroline, bipyrimidine, tetramethylenediamine and also phosphine and carbon monoxide ligands. Among these, the bipyridine-containing complex **73** (Figure 4.10) was the most active (TON's up to 320 and TOF's up to 0.24 s^{-1}) using CAN under highly acidic conditions.¹¹⁶

Crabtree and Brudvig also disclosed that these type of catalyst are also able to promote water oxidation under almost neutral pH media using sodium metaperiodate instead of CAN as sacrificial one electron oxidant. In particular they found that complex **75** is an efficient catalyst under these conditions (Figure 4.10).¹¹⁹ Experimental studies have confirmed that the cyclopentadiene ligand is degraded under reaction conditions and, therefore, **75** is readily transformed to dimeric species **76**, which are responsible for the catalytic activity (Figure 4.10).¹²⁰

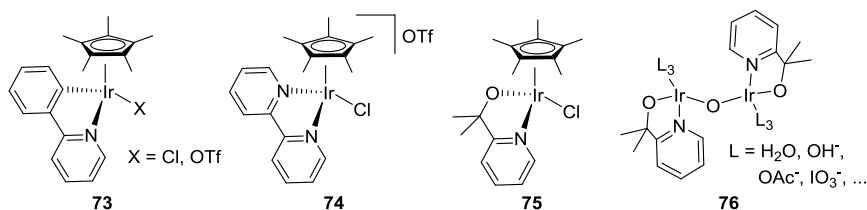


Figure 4.10. Representative iridium-based WOCs based on cyclopentadiene-type ligands.

4.3.2.1.3. Iridium complexes with N-heterocyclic carbene ligands

Crabtree and Brudvig also introduced NHC ligands into the iridium complexes to stabilize the iridium centers in the iridium WOCs in high oxidation states¹²¹ because NHCs are well known for binding tightly to metal centers and stabilizing them at high-valent states. As predicted, the use of Ir-NHC complex **77** (Figure 4.11) was able of oxidizing H_2O using CAN as oxidant under acidic conditions (TOF up to 0.13 s^{-1}) as well as using NaIO_4 as oxidant under almost neutral pH conditions (TOF up to 0.4 s^{-1}).¹²² Several modifications of these catalyst have been developed. Thus, for instance, while the replacement of the cyclometalated unit in **77** by another NHC fragment (complexes **78**; Figure 4.11) led to lower activities,¹²³ higher TOFs has been achieved by removing cyclometalated unit (complex **79**; Figure 4.11).¹²⁴

Bernhard and Albrecht took an interesting approach by using abnormal (mesoionic) carbene ligands.^{6e,7e,7j} The use of Ir-WOC containing pyridyl-triazolidene ligands has proved to be highly advantageous. For instance, compound **80** provided high turnover

numbers (up to 40000) in the CAN mediated water oxidation. Later, modification of the remote position of the carbene ligand (complexes **81** and **82**) led to a substantially increase in activity. It should be pointed out that the simple and counterintuitive introduction of more lipophilic n-octyl chain (complex **82**) led to one of the most active Ir-catalysts using acidic conditions (TOF's up to 2 s^{-1}). Nevertheless, activity substantially decrease when using sodium metaperiodate as sacrificial oxidant under nearly neutral media (pH 5.6). Thus, for instance, the activity of complex **82** dropped to TOF's up to 0.1 s^{-1} using NaIO_4 at pH = 5.6.

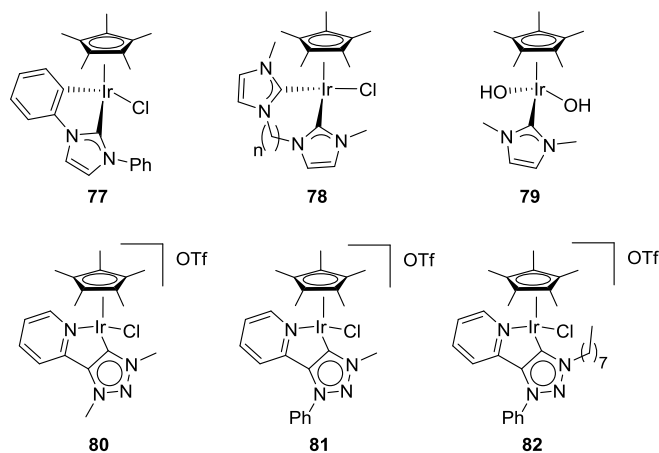


Figure 4.11. Representative iridium complexes bearing different type of carbene ligands applicable in water oxidation.

4.4. Pd-catalyzed asymmetric Heck reaction

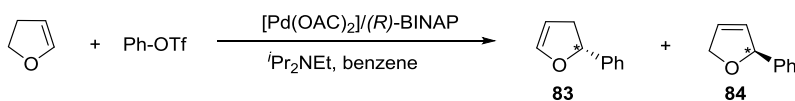
Catalytic enantioselective carbon-carbon bond formation is one of the most appealing goals in modern synthesis organic chemistry as they have a wide range of application in the synthesis of pharmaceuticals, natural products and functional materials. The Pd-catalyzed asymmetric Heck reaction (also known as Mizoroki-Heck), that is the coupling of an aryl or alkenyl halide or triflate to an alkene (Scheme 4.8) is one way to achieve this objective, as it was recognized with Nobel Prize in Chemistry in 2010. This reaction is so versatile for preparation of enantioenriched compounds due to its large functional group tolerance.¹²⁵ The extensive research dedicated to this process can give the erroneous impression that Heck Chemistry is a mature area.



Scheme 4.8. Pd-catalyzed Heck reaction. X = Halide or triflate.

Heck reaction was discovered more than 40 years ago¹²⁶ however, reports on the asymmetric version was not published until 1980, with most examples dealing with intramolecular reactions because the alkene regiochemistry and geometry in the product is easily controlled. They showed application of such an important transformation in the synthesis of natural compound.¹²⁷ Chiral bidentate phosphines such as (*R*)-BINAP are highly desired for asymmetric intramolecular reaction.¹²⁵

The first intermolecular asymmetric variant was reported by Hayashi and co-workers in 1991.¹²⁸ The number of examples about asymmetric intermolecular Heck reaction are less than their intramolecular counterparts due to the fact that regioselectivity is mostly a problem apart from enantioselectivity. For example, in the intermolecular Heck reaction of 2,3-dihydrofuran with phenyl triflate two products are generated, 2-phenyl-2,5-dihydro dihydrofuran **83** as an envisaged product and 2-phenyl-2,3-dihydrofuran **84** which is formed due to an isomerization process (Scheme 4.9).



Scheme 4.9. The first intermolecular asymmetric Heck reaction.

Nowadays various substrates in the intermolecular asymmetric Heck reactions which most of them are cyclic olefins and among them 2,3-dihydrofuran has been selected as benchmark substrate (Figure 4.12). A wide range of aryl or vinyl triflates have been used for the Heck coupling and phenyl triflate selected as standard. Zhou and Wu have recently solved a long-standing problem in asymmetric intermolecular Heck chemistry with the successful application of aryl halides in the enantioselective Heck arylation of cyclic alkenes.¹²⁹ Finally, the base is another important parameter which affects both activity and selectivity. *N,N*-diisopropylamine and proton sponge are the standard bases mostly applied in this type of reactions.¹²⁵

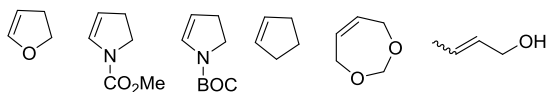
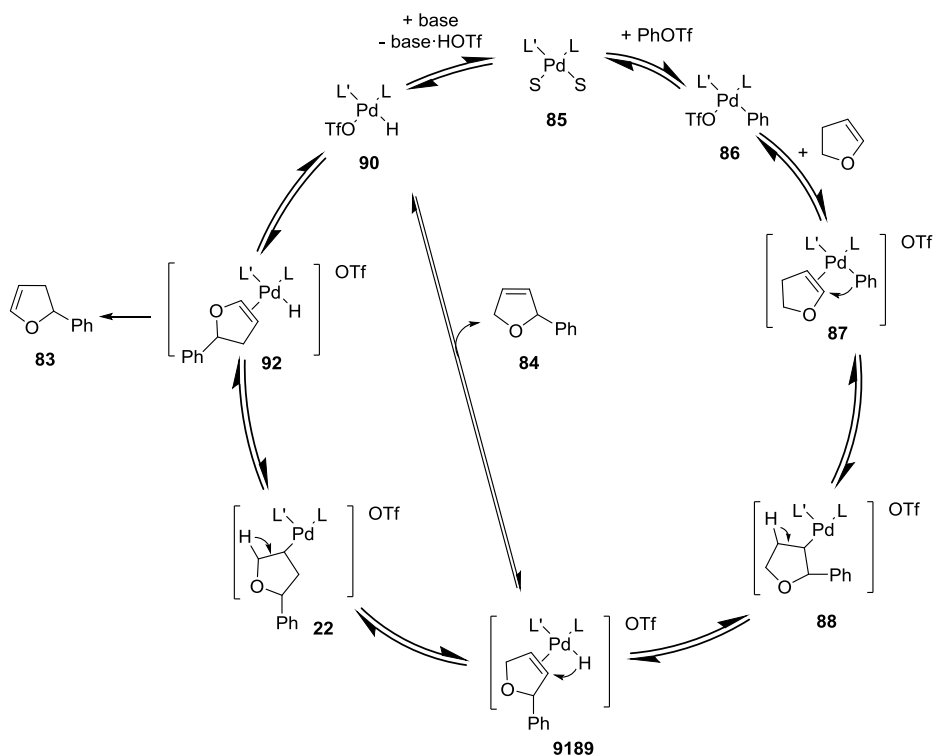


Figure 4.12. Most common substrates applied in the asymmetric Pd-Heck reaction.

4.4.1. Mechanism

Scheme 4.10 illustrates a proposed catalytic cycle for the phenylation of 2,3-dihydrofuran.¹²⁵ In the first step phenyl triflate oxidatively adds to the Pd(0) complex **85** to produce Pd(II) complex **86**. Since the triflate ligand is a good leaving group, coordination of 2,3-dihydrofuran on **86** enforces dissociation of the triflate ligand and makes a cationic palladium species **87** as a 16-electron square-planar complex, convenient for the subsequent enantioselective insertion of olefin. The alkyl Pd(II) complex **88** converts to the hydrido Pd(II) complex **89** by β -hydrogen elimination. Dissociation of olefin leads to the product **84** and hydrido Pd(II) complex **90**. Reductive elimination of HOTf which is happened by suitable base, regenerates Pd(0) complex **85** to continue the catalytic cycle. Depending on the ligands, catalyst precursor and reaction parameters, the Pd-complex **89** can also undergo re-insertion of the hydride to convert to the Pd(II) complex **91** and subsequently by β -hydrogen elimination constructs hydrido Pd(II) complex **92**. Dissociation of olefin leads to the product **83** and hydrido Pd(II) complex **90**. Again reductive elimination of HOTf regenerates active species **85**.



Scheme 4.10. Proposed mechanism for the Pd-catalyzed arylation of 2,3-dihydrofuran.

4.4.2. Ligand design

The first ligands developed for this process were diphosphines.^{125,128,130} Although Pd-diphosphine catalyst systems provided high enantioselectivities, there were still major problems of regioselectivity and activities.^{128,131} For instance, the diphosphine BINAP provided an enantioselectivity of 96% but the major product was the isomerized 2-phenyl-2,3-dihydrofuran (71% regioselectivity) and the reaction time was 9 days.

An important breakthrough in this area came with the report by Pfaltz et al., who showed that phosphine-oxazoline PHOX ligands minimize the double bond isomerization providing high regio- and enantioselectivity to the desired product.¹³² These ligands were successfully applied in the intermolecular Heck reaction of several substrates and triflate sources (Figure 4.13, ee's up to 98%). Results also indicate that the presence of a *tert*-butyl group in the oxazoline moiety was crucial for obtaining the highest levels of enantioselectivity. The main limitation of these catalytic systems was the long reaction times (reactions usually take 3-7 days to complete). In an attempt to reduce reaction times, Hallberg and coworkers decided to apply the benefits of

microwave irradiation in the Pd-catalyzed intermolecular Mizoroki-Heck reaction using PHOX ligands. They found that reaction times decreased considerably (from 4 days to 1 hour) but enantioselectivities were lower than those obtained under thermal conditions (from 97% ee to 90% ee).¹³³

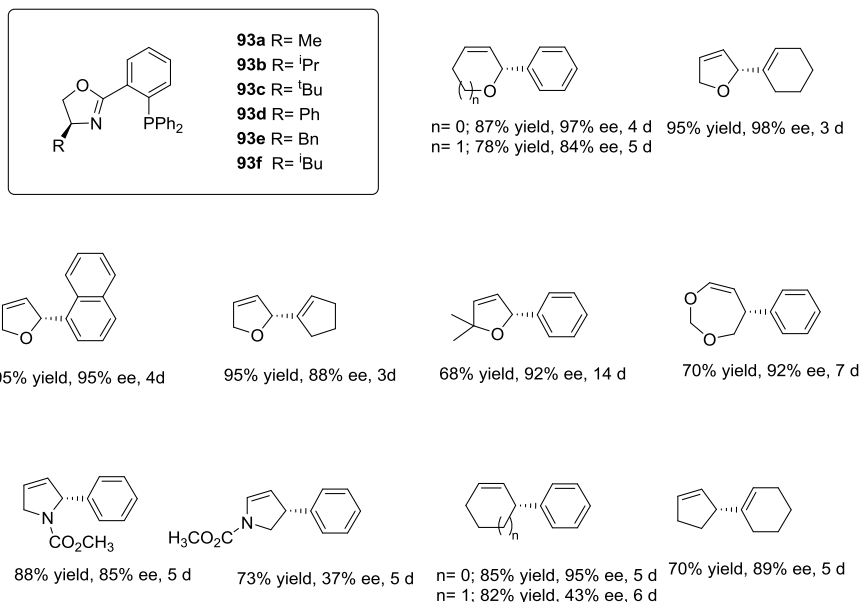


Figure 4.13. Phosphine-oxazoline PHOX type ligands **93**. Yields, enantioselectivities and reaction times using these Pd/**93** in the intermolecular Heck reaction are also shown.

4.4.2.1. Phosphine-oxazoline ligands

Since the initial report by Pfaltz, several other successful phosphine-oxazoline ligand libraries have been developed for this process. Figures 4.14 show the most representative phosphine-oxazoline ligands applied to this process.

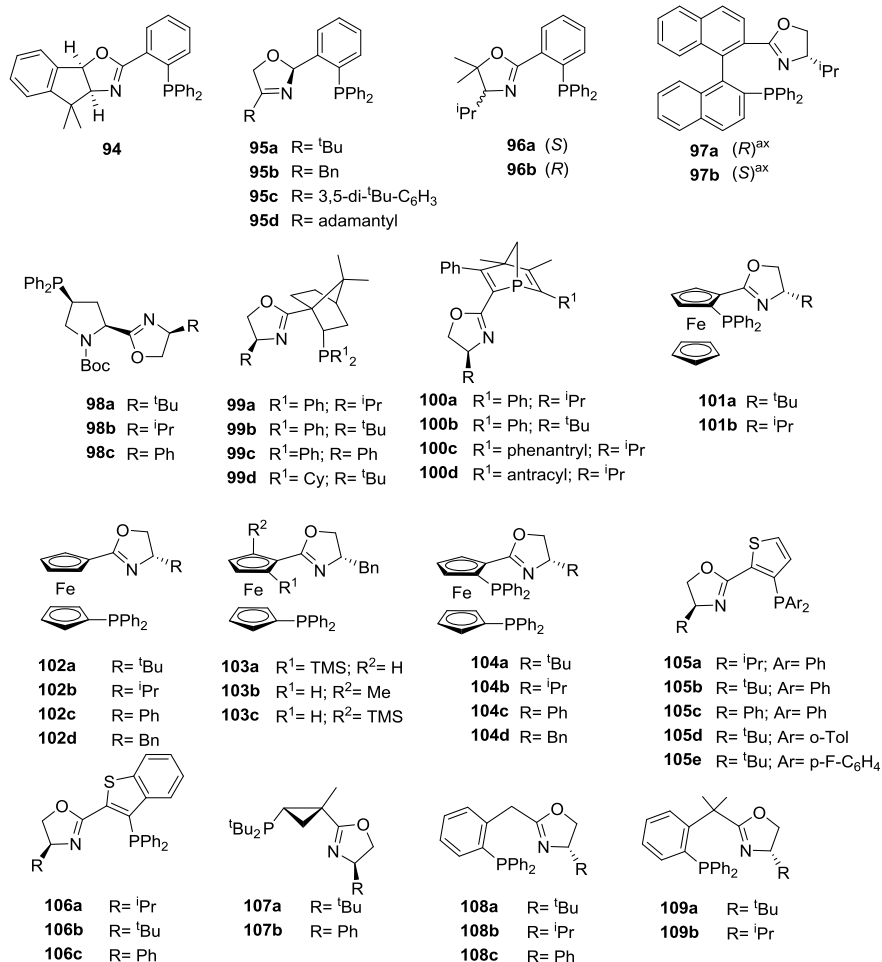


Figure 4.14. Selected phosphine-oxazoline ligands applied in the Pd-catalyzed intermolecular Heck reaction.

In 2000, Hayashi and coworkers reported a modification in the oxazoline moiety of the PHOX ligands with the development of an indano-fused ligand **94**.¹³⁴ This ligand was successfully investigated in the asymmetric arylation and cyclohexenylation of the standard substrate 2,3-dihydrofuran. The best result was obtained in the cyclohexenylation of 2,3-dihydrofuran showing conversions of up to 91% and enantiomeric excesses of up to 98%. More recently, other modifications in the oxazoline moiety of the PHOX ligand have also been performed. In this context, Zhang and coworkers developed ligands **95** achieving high yields and enantioselectivities (up to 94%) in the arylation of 2,3-dihydrofuran using ligand **95a** (that contains *tert*-butyl

groups at the oxazoline moiety).¹³⁵ Later in 2009, Paquin and coworkers reported ligand 5,5-(dimethyl)-ⁱPr-PHOX **96**, which behaves similarly in terms of enantioselectivity (ee's up to 92% in the phenylation of 2,3-dihydrofuran) to PHOX.¹³⁶

Hayashi's group also reported the synthesis of (*S,R*)- and (*S,S*)-2-[4-(isopropyl)oxazol-2-yl]-2'-diphenylphosphino-1,1'-binaphthyl ligands **97** and applied them in the Pd-catalyzed asymmetric arylation of 2,3-dihydrofuran, with a highest ee of 88% for product **84**.¹³⁷ Ligands **97**, with opposite configuration of their axial chirality on the binaphthyl backbone, induce opposite configurations in the product **83** respectively. These studies demonstrate that the axial chirality in ligands **97** regulates the chiral environment around the palladium center more strongly and has a greater influence on the stereochemical outcome than the central chirality in the corresponding oxazoline unit.

Gilbertson developed proline-derived phosphine-oxazoline **98** and bicyclic phosphine-oxazoline **99** and **100** ligands (Figure 4.14) that were screened in the Pd-catalyzed intermolecular Heck reaction of several substrates with several aryl- and alkenyltriflates (Figure 4.15).¹³⁸

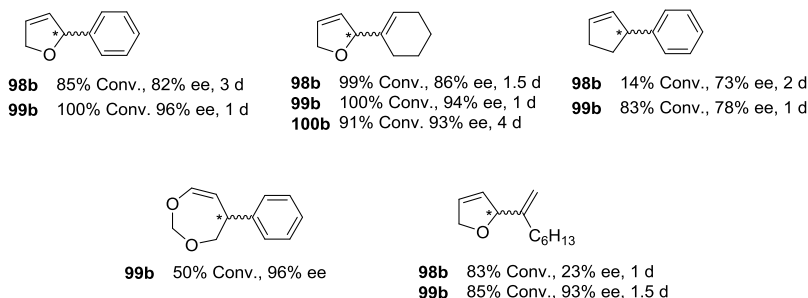


Figure 4.15. Summary of the best results obtained in the Pd-catalyzed Heck reaction using ligands **98-100**.

Several planar chiral ferrocene phosphine-oxazoline ligands **101-104** have been developed (Figure 4.14).¹³⁹ The results indicate: (a) that the position of the phosphine group is crucial for high activities and enantioselectivities, and (b) that the planar chirality is decisive in exerting control over both the absolute configuration and the enantiomeric excess of the product, which can be controlled by changing the size of the planar group and/or the configuration of the planar chirality. Therefore, results were best using ligands **103c** and **104a** in the arylation of 2,3-dihydrofuran (75% yield, 92% ee) and *N*-methoxycarbonyl-2-pyrroline (52% yield, 99% ee), respectively.

Interestingly, ligand **101a** provided excellent enantioselectivity (98% ee) in the phenylation of 2,2-dimethyl-2,3-dihydrofuran.

Guiry, Cozzi and coworkers reported the application of ligands **105** and **106**, in which the phenyl ring of the PHOX has been replaced by thiophene moieties, in the arylation and cyclohexenylation of 2,3-dihydrofuran.¹⁴⁰ Ligand **105d**, containing bulky substituents at both oxazoline and phosphine moieties, provided the best results for the arylation (ee's up to 96%) and cyclohexenylation (ee's up to 95%).

More recently two new studies on the development of new phosphine-oxazoline ligands have appeared. One of them reports the synthesis of a new type of PHOX ligand with a rigid chiral cyclopropyl backbone (ligands **107**, Figure 4.14).¹⁴¹ The introduction of this rigid cyclopropyl fragment lowered the degrees of freedom in the catalyst and led to an efficient Pd-**107b** catalyst, which demonstrates excellent enantioselectivities in the asymmetric arylation of dihydrofuran with various aryl triflates (yields up to 85 and ee's up to 99%). The second study reports the synthesis of the new phosphine-oxazoline ligands **108** and **109** (Figure 4.14) based on the PHOX ligands, in which the flat ortho-phenylene tether is replaced by benzylic type groups.¹⁴² The authors found that simply by changing the substituent of the benzylic group of the ligand backbone both enantiomers of the arylated products can be obtained in high regio- and enantioselectivities (ee's up to 95%).

4.4.2.2. Phosphine-nitrogen and phosphinite-oxazoline ligands

The effectiveness of phosphine-oxazoline ligands in the reactions discussed above suggested that it could be profitable to investigate related P,N-ligands further. In this respect, new heterodonor P,N-ligands in which the oxazoline and the phosphine moiety have been replaced by other nitrogen groups or a phosphinite group, respectively, have been developed (Figure 4.16).

Phosphine-pyridine ligands **110-112** (Figure 4.16) have been successfully applied to the phenylation of 2,3-dihydrofuran (regio's up to 98% and ee's up to 99%).¹⁴³ The results using ligands **110** and **111** showed that the structure of the remote silyl group has a small but significant influence on the enantioselectivity. Enantioselectivities (ee's up to 99%) were therefore best using ligands **110b** and **111b**, with a tert-butyldiphenylsilyl group. The reaction rates were similar to those observed with the above mentioned Pd-phosphine-oxazoline catalysts.

Guiry and coworkers developed new phosphine-amine ligands **113-114** (Figure 4.16) for the arylation and cycloalkenylation of the standard substrate 2,3-dihydrofuran but with little success.¹⁴⁴ These ligands proved to be considerably less reactive (<25% after several days) and enantioselective (ee's up to 17%) than analogous phosphine-oxazoline ligands.

Phosphine-phenylbenzoxazine **115** (Figure 4.16), in which the oxazoline group of the PHOX ligands has been replaced by an oxazine moiety, provided slightly lower enantioselectivities than those obtained using PHOX ligands in the phenylation and cycloalkenylation of 2,3-dihydrofuran (ee's up to 94%).¹⁴⁵

More recently, Andersson and coworkers successfully screened phosphine-thiazole **116** and phosphine-imidazole **117** (Figure 4.16) in the arylation of 2,3-dihydrofuran under microwave conditions (ee's up to 98%).¹⁴⁶ Results indicated that the presence of a bulky mesityl substituent at the thiazole group (**116e**) has a positive effect on selectivity. They also found that catalysts could be prevented from deteriorating with no decrease in selectivity by adding triphenylphosphine.^{146b}

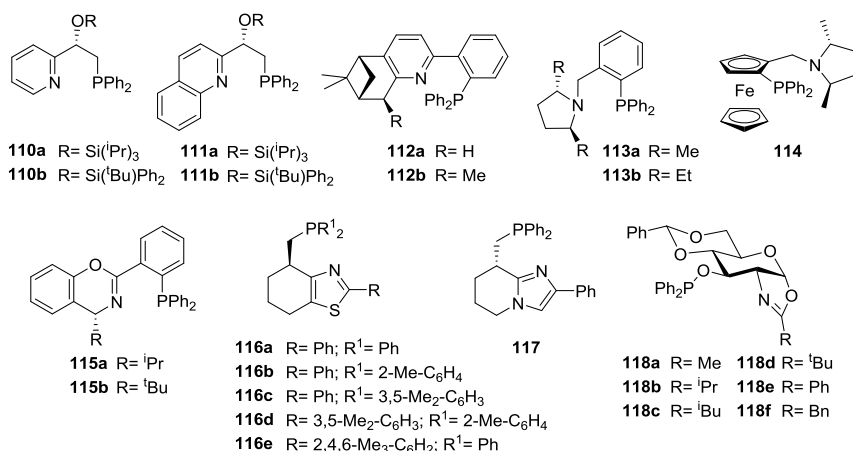


Figure 4.16. Selected phosphine-nitrogen and phosphinite-oxazoline ligands applied in the Pd-catalyzed intermolecular Heck reaction.

In 2000, Uemura and coworkers developed a new type of P,N-ligand for this process: the phosphinite-oxazoline **118** (Figure 4.16). These ligands, easily synthesized from readily available D-glucosamine, were successfully applied in the arylation of substrate 2,3-dihydrofuran (ee's up to 96%).¹⁴⁷ Results indicated that the oxazoline substituent has an important effect on selectivity. In contrast to the results obtained

using PHOX-type ligands and the vast majority of the phosphine-oxazoline ligands, results were best with a benzyl oxazoline substituent (**118f**). In addition, ligands **118** were also tested in the phenylation of *cis*- and *trans*-crotyl alcohols. This represented the first asymmetric Heck reaction of an acyclic alkene. Thus, the use of phenyl iodide resulted in good conversions (up to 76% after 3 days) albeit with low enantioselectivity (ee's up to 17%). It should be pointed out that the use of phenyl triflate did not give any coupling product after 3 days.

4.4.2.3. Mixed phosphine-phosphine oxide and phosphite-oxazoline ligands

Despite the important advances in ligand design there was still a problem of low reaction rates and substrate versatility. Therefore, it was very important to develop ligands that induced higher rates and selectivities (regio- and enantioselectivities) for several substrate types. For this purpose two main strategies have been used for ligand design. One, developed recently by Zhou's group, illustrates the power of mixed phosphine-phosphine oxides (Figure 4.17) which had been discarded in the Heck reaction for decades. Pd/phosphine-phosphine oxide^{129,148} systems were successfully applied in the intermolecular Heck reaction of several cyclic alkenes substrates with various aryl triflates and aryl halides.

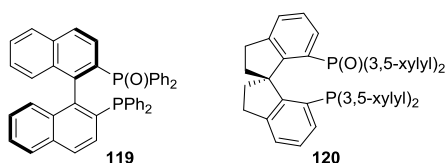


Figure 4.17. Representative phosphine-phosphine oxide ligands **119-120**.

The second strategy developed by our group was based on biaryl phosphite-oxazoline ligands. Their highly modular construction, facile synthesis from available alcohols and greater resistance to oxidation than the phosphines have proved to be highly advantageous. The application of two phosphite-oxazoline ligand libraries in the Heck reaction (Figure 4.18) led us to identify a Pd/phosphite-oxazoline **131a** catalyst that provided activities of 100% in only 10 min with excellent regio- (up to >99%) and enantioselectivities (up to >99% ee) in the coupling of several cyclic substrates and a variety of triflates.¹⁴⁹

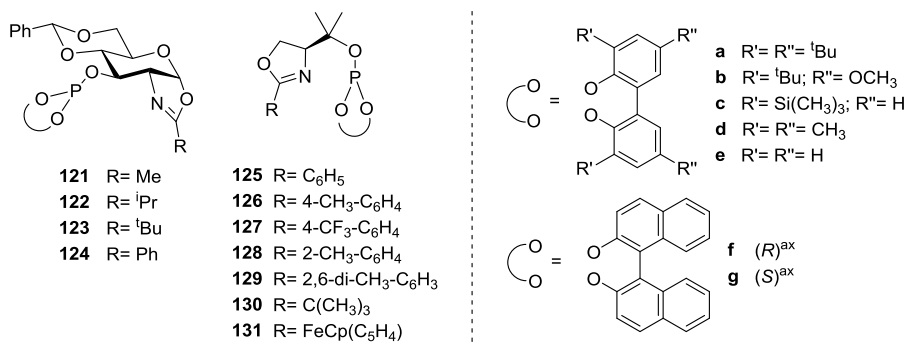


Figure 4.18. Selected phosphite-oxazoline ligands developed in Diéguez's group for Pd-catalyzed intermolecular Heck reaction.

4.5. References

- (a) van Leeuwen, P. W. N.M.; Chadwick, J. C. in *Homogeneous Catalysts*, Wiley-VCH, Weinheim, **2011**. (b) Börner, A.; Eds; *Phosphorus Ligands in Asymmetric Catalysis*; Wiley-VCH, Weinheim, **2008**.
- van Leeuwen, P. W. N. M.; Kamer, P. C. J.; Claver, C.; Pàmies, O.; Diéguez, M. *Chem. Rev.* **2011**, 111, 2077.
- See, for example: (a) Diéguez, M.; Pàmies, O. *Acc. Chem. Res.* **2010**, 43, 312. (b) Magre, M.; Pàmies, O.; Diéguez, M. *Chem. Rec.* **2016**, 16, 1578. (c) Pàmies, O.; Diéguez, M. *Chem. Rec.* **2016**, 16, 2460.
- (a) Hahn, F. E.; Jahnke, M. C. *Angew. Chem., Int. Ed.* **2008**, 47, 3122. (b) Arduengo, A. J.; Bertrand, G. *Chem. Rev.* **2009**, 109, 3209. (c) Bourissou, D.; Guerret, O.; Gabbai, F. P.; Bertrand, G. *Chem. Rev.* **2000**, 100, 39. (d) *N-Heterocyclic Carbenes in Transition Metal Catalysis*, ed. F. Glorius, *Topics in Organometallic Chemistry*, Springer, Berlin, **2007**. (e) Hopkinson, M. N.; Richter, C.; Schedler, M.; Glorius, F. *Nature*, **2014**, 510, 485. (f) Díez-González, S.; Marion, N.; Nolan, S. P. *Chem. Rev.* **2009**, 109, 3612. (g) Crudden, C. M.; Allen, D. P. *Coord. Chem. Rev.* **2004**, 248, 2247. (h) Crabtree, R. H. *Coord. Chem. Rev.* **2007**, 251, 595. (i) *N-Heterocyclic Carbenes: from Laboratory Curiosities to Efficient Synthetic Tools*, ed. S. Díez-González, RSC Publishing, Cambridge, **2011**. (j) *N-Heterocyclic Carbenes in Transition Metal Catalysis and Organocatalysis*, ed. C. S. J. Cazin, Springer, Berlin, **2011**.
- For reviews, see: (a) Donnelly, K. F.; Petronilho, A.; Albrecht, M. *Chem. Commun.* **2013**, 49, 1145. (b) Crabtree, R. H. *Coord. Chem. Rev.* **2013**, 257, 755. (c) Schulze, B.; Schubert, U. S. *Chem. Soc. Rev.* **2014**, 43, 2522.

6. For selected examples, see: (a) Canseco-Gonzalez, D.; Gniewek, A.; Szulmanowicz, M.; Müller-Bunz, H.; Trzeciak, A. M.; Albrecht, M. *Chem. Eur. J.* **2012**, *18*, 6055. (b) Hohloch, S.; Frey, W.; Su, C.-Y.; Sarkar, B. *Dalton Trans.* **2013**, *42*, 11355. (c) Keske, E. C.; Zenkina, O. V.; Wang, R.; Crudden, C. M. *Organometallics* **2012**, *31*, 456. (d) Keitz, B. K.; Bouffard, J.; Bertrand, G.; Grubbs, R. H. *J. Am. Chem. Soc.* **2011**, *133*, 8498. (e) Lalrempuia, R.; McDaniel, N. D.; Müller-Bunz, H.; Bernhard, S.; Albrecht, M. *Angew. Chem. Int. Ed.* **2010**, *49*, 9765. (f) Canseco-Gonzalez, D.; Albrecht, M. *Dalton Trans.* **2013**, *42*, 7424. (g) Prades, A.; Peris, E.; Albrecht, M. *Organometallics* **2011**, *30*, 1162. (h) Bolje, A.; Hohloch, S.; Urankar, D.; Pevec, A.; Gazvoda, M.; Sarkar, B.; Košmrlj, J. *Organometallics* **2014**, *33*, 2588. (i) Bolje, A.; Hohloch, S.; van der Meer, M.; Košmrlj, J.; Sarkar, B. *Chem. Eur. J.* **2015**, *21*, 6756. (j) Delgado-Rebollo, M.; Canseco-Gonzalez, D.; Hollering, M.; Müller-Bunz, H.; Albrecht, M. *Dalton Trans.* **2014**, *43*, 4462. (k) Nakamura, T.; Terashima, T.; Ogata, K.; Fukuzawa, S. *Org. Lett.* **2011**, *13*, 620. (l) Hohloch, S.; Sarkar, B.; Nauton, L.; Cisnetti, F.; Gautier, A. *Tetrahedron Lett.* **2013**, *54*, 1808.
7. (a) Bolje, A.; Košmrlj, J. *Org. Lett.* **2013**, *15*, 5084. (b) Bolje, A.; Urankar, D.; Košmrlj, J. *Eur. J. Org. Chem.* **2014**, 8167. (c) Bolje, A.; Hohloch, S.; Košmrlj, J.; Sarkar, B. *Dalton Trans.* **2016**, *45*, 15983. (d) Pretorius, R.; Mazloomi, Z.; Albrecht, M. *J. Organomet. Chem.* **2017**, <http://dx.doi.org/10.1016/j.jorganchem.2017.05.014>. (e) Corbucci, I.; Petronilho, A.; Müller-Bunz, H.; Rocchigiani, L.; Albrecht, M.; Macchioni, A. *ACS Catal.* **2015**, *5*, 2714. (f) Petronilho, A.; Woods, J. A.; Mueller-Bunz, H.; Bernhard, S.; Albrecht, M. *Chem. Eur. J.* **2014**, *20*, 15775. (g) Bernet, L.; Lalrempuia, R.; Ghattas, W.; Mueller-Bunz, H.; Vigara, L.; Llobet, A.; Albrecht, M. *Chem. Commun.* **2011**, *47*, 8058. (h) Pretorius, R.; Fructos, M. R.; Müller-Bunz, H.; A. Gossage, P. J. Pérez, M. Albrecht, *Dalton Trans* **2016**, *45*, 14591. (i) J. A. Woods, R. Lalrempuia, R.; Petronilho, A.; McDaniel, N. D.; Müller-Bunz, H.; Albrecht, M.; Bernhard, S. *Energy Environ. Sci.* **2014**, *7*, 2316.
8. (a) Meerwein, H.; Schmidt, R. *Liebigs Ann. Chem.* **1925**, *444*, 221. (b) Verley, A. *Bull. Soc. Fr.* **1925**, *37*, 537. (c) Ponndorf, W. *Angew. Chem.* **1926**, *39*, 138.
9. Oppenauer, R. V. *Recl. Trav. Chim. Pays-Bas.* **1937**, *56*, 137.
10. Gladiali, S.; Mestroni, G. in *Transition Metals for Organic Synthesis*. (Eds: Beller, M.; Bolmed, C.) Wiley-VCH **1998**, pp. 97-119.
11. Zheng, C.; You, S. L. *Chem. Soc. Rev.* **2012**, *41*, 2498.
12. Chen, S.-J.; Lu, G.-P.; Cai, C. *RSC Adv.* **2015**, *5*, 13208.

13. For recent reviews see: (a) Gladiali, S.; Alberico, E. in *Transition Metals for Organic Synthesis*. (Eds: Beller, M.; Bolmed, C.) Wiley-VCH **2004**, p. 145. (b) Clapham, S. E.; Hadzovic, A.; Morris, R. H. *Coord. Chem. Rev.* **2004**, 248, 2201. (c) Bäckvall, J. E. *J. Organomet. Chem.* **2002**, 652, 105.
14. Gladiali, S.; Mestroni, G. in *Transition Metals for Organic Synthesis*. (Eds: Beller, M.; Bolmed, C.) Wiley-VCH **2004**, p. 97.
15. (a) Hashiguchi, S.; Fujii, A.; Takehara, J.; Ikariya, T.; Noyori, R. *J. Am. Chem. Soc.* **1995**, 117, 7562. (b) Haack, K. J.; Hashiguchi, S.; Fujii, A.; Ikariya, T.; Noyori, R. *Angew. Chem., Int. Ed. Engl.* **1997**, 36, 285.
16. (a) Noyori, R.; Hashiguchi, S. *Acc. Chem. Res.* **1997**, 30, 97. (b) Haack, K.-J.; Hashiguchi, S.; Fujii, A.; Ikariya, T.; Noyori, R. *Angew. Chem., Int. Ed. Engl.* **1997**, 36, 285. (c) Matsumura, K.; Hashiguchi, S.; Ikariya, T.; Noyori, R. *J. Am. Chem. Soc.* **1997**, 119, 8738. (d) Casey, C. P.; Singer, S. W.; Powell, D. R.; Hayashi, R. K.; Kavana, M. *J. Am. Chem. Soc.* **2001**, 123, 1090.
17. (a) Pàmies, O.; Bäckvall, J.-E. *Chem. Eur. J.* **2001**, 7, 5052. (b) Laxmi, Y. R. S.; Bäckvall, J. E. *Chem. Commun.* **2000**, 611.
18. (a) Chowdhury, R. L.; Bäckvall, J.-E. *J. Chem. Soc. Chem. Commun.* **1991**, 1063. (b) Aranyos, A.; Csajnyik, G.; Szabo, K. J.; Bäckvall, J. E. *Chem. Commun.* **1999**, 351.
19. Haddad, Y. M. Y.; Henbest, H. B.; Husbands, J.; Mitchell, T. R. B. *Proc. Chem. Soc. London* **1964**, 361.
20. Trochagr, J.; Henbest, H. B. *Chem. Commun.* **1967**, 544.
21. McPartli, M.; Mason, R. *Chem. Commun.* **1967**, 545.
22. Sasson, Y.; Blum, J. *Tetrahedron Lett.* **1971**, 12, 2167.
23. Blum, J.; Sasson, Y.; Iflah, S. *Tetrahedron Lett.* **1972**, 13, 1015–1018.
24. Sasson, Y.; Blum, J. *J. Org. Chem.* **1975**, 40, 1887.
25. Chowdhury, R. L.; Bäckvall, J.-E. *J. Chem. Soc., Chem. Commun.* **1991**, 1063.
26. Zassinovich, G.; Mestroni, G.; Gladiali, S. *Chem. Rev.* **1992**, 92, 1051.
27. Bianchi, M.; Matteoli, U.; Menchi, G.; Frediani, P.; Pratesi, U.; Piacenti, F.; Botteghi, C. *J. Organomet. Chem.* **1980**, 198, 73.
28. Matteoli, U.; Frediani, P.; Bianchi, M.; Botteghi, C.; Gladiali, S. *J. Mol. Catal.* **1981**, 12, 265.
29. (a) Hashiguchi, S.; Fujii, A.; Takahara, J.; Ikariya, T.; Noyori, R. *J. Am. Chem. Soc.* **1995**, 117, 7562. (b) Fujii, A.; Hashiguchi, S.; Uematsu, N.; Ikariya, T.; Noyori, R.; *J. Am. Chem. Soc.* **1996**, 118, 2521.

30. Pugin, B.; Blaser, H.-U. *Top. Catal.* **2010**, *53*, 953.
31. Václavík, J.; Šot, P.; Vilhanová, B.; Pecháček, J.; Kuzma, M.; Kačer, P. *Practical Molecules* **2013**, *18*, 6804.
32. (a) Strassberger, Z.; Mooijman, M.; Ruijter, E.; Alberts, A. H.; de Graaff, C.; Orru, R. V. A.; Rothenberg, G. *Appl. Organometal. Chem.* **2010**, *24*, 142. (b) Monney, A.; Venkatachalam, G.; Albrecht, M. *Dalton Trans.* **2011**, *40*, 2716. (c) Akta, A.; Gök, Y. *Transition Met. Chem.* **2014**, *39*, 925. (d) Yasar, S.; Çekirdek, S.; Özdemir, I. *J. Coord. Chem.* **2014**, *67*, 1236. (e) DePasquale, J.; White, N. J.; Ennis, E. J.; Zeller, M.; Foley, J. P.; Papish, E. T. *Polyhedron* **2013**, *58*, 162. (f) Wdowik, T.; Samojłowicz, C.; Jawiczuk, M.; Malińska, M.; Wozniak, K.; Grela, K. *Chem. Commun.* **2013**, *49*, 674. (g) Yigit, B.; Yigit, M.; Özdemir, I.; Çetinkaya, E. *Transition Met. Chem.* **2012**, *37*, 297. (h) Witt, J.; Pöthig, A.; Kühn, F. E.; Baratta, W. *Organometallics* **2013**, *32*, 4042. (307) Aktas, A.; Gok, Y. *Catal. Lett.* **2015**, *145*, 631.
33. (a) Bartoszewicz, A.; Ahlsten, N.; Martín-Matute, *Chem. Eur. J.* **2013**, *19*, 7274. (b) Malacea, R.; Poli, R.; Manoury, E. *Coord. Chem. Rev.* **2010**, *254*, 729. (c) Wang, D.; Zhao, K.; Yang, S.; Ding, Y. *Z. Anorg. Allg. Chem.* **2015**, *641*, 400. (d) Jimenez, M. V.; Fernandez-Tornos, J.; Perez-Torrente, J. J.; Modrego, F. J.; García-Orduna, P.; Oro, L. *A. Organometallics* **2015**, *34*, 926.
34. Bata, P.; Notheisz, F.; Kluson, P.; Zsigmond, Á. *Appl. Organomet. Chem.* **2015**, *29*, 45.
35. Mikhailine, A. A.; Morris, R. H. *Inorg. Chem.* **2010**, *49*, 11039.
36. Zuo, W.; Morris, R. H. *Nat. Protoc.* **2015**, *10*, 241.
37. Dombay, T.; Helleu, C.; Darcel, C.; Sortais, J.-B. *Adv. Synth. Catal.* **2013**, *355*, 3358.
38. Jagadeesh, R. V.; Banerjee, D.; Arockiam, P. B.; Junge, H.; Junge, K.; Pohl, M. M.; Radnik, J.; Brückner, A.; Beller, M. *Green Chem.* **2015**, *17*, 898.
39. Zhang, G.; Hanson, S. K. *Chem. Commun.* **2013**, *49*, 10151.
40. Drost, R. M.; Bouwens, T.; van Leest, N. P.; de Bruin, B.; Elsevier, C. J. *ACS Catal.* **2014**, *4*, 1349.
41. Jiang, Y.; Blacque, O.; Fox, T.; Frech, C. M.; Berke, H. *Organometallics* **2009**, *28*, 5493.
42. Baratta, W.; Ballico, M.; Baldino, S.; Chelucci, G.; Herdtweck, E.; Siega, K.; Magnolia, S.; Rigo, P. *Chem. Eur. J.* **2008**, *14*, 9148.

43. Alonso, F.; Riente, P.; Rodriguez-Reinoso, F.; Ruiz-Martínez, J.; Sepúlveda-Escribano, A.; Yus, M. *J. Catal.* **2008**, 260, 113.
44. He, L.; Ni, J.; Wang, L.-C.; Yu, F.-J.; Cao, Y.; He, H.-Y.; Fan, K.-N. *Chem. Eur. J.* **2009**, 15, 11833.
45. Hauwert, P.; Maestri, G.; Sprengers, J. W.; Catellani, M.; Elsevier, C. *J. Angew. Chem., Int. Ed.* **2008**, 47, 3223.
46. For reviews on carbenes in general, see: (a) de Frémont, P.; Marion, N.; Nolan, S. P. *Coord. Chem. Rev.* **2009**, 253, 862. (b) Bourissou, D.; Guerret, O.; Gabbaï, F. P.; Bertrand, G. *Chem. Rev.* **2000**, 100, 39.
47. César, V.; Gade, L. H.; Bellemin-Lapponnaz, S. *In N-Heterocyclic Carbenes: From Laboratory Curiosities to Efficient Synthetic Tools*; Díez-González, S., Ed.; RSC Catalysis Series No. 6; Royal Society of Chemistry: Cambridge, **2011**.
48. Díez-González, S.; Marion, N.; Nolan, S. P. *Chem. Rev.* **2009**, 109, 3612.
49. Dupont, J.; Consorti, C. S.; Spencer, J. *Chem. Rev.* **2005**, 105, 2527.
50. van der Boom, M. E.; Milstein, D. *Chem. Rev.* **2003**, 103, 1759.
51. Albrecht, M.; van Koten, G. *Angew. Chem., Int. Ed.* **2001**, 40, 3750.
52. Peris, E.; Crabtree, R. H. *Coord. Chem. Rev.* **2004**, 248, 2239.
53. Albrecht, M.; Crabtree, R. H.; Mata, J.; Peris, E. *Chem. Commun.* **2002**, 32.
54. Gierz, V.; Urbanaite, A.; Seyboldt, A.; Kunz, D. *Organometallics* **2012**, 31, 7532.
55. Akıncı, P. A.; Gülcemal, S.; Kazheva, O. N.; Alexandrov, G. G.; Dyachenko, O. A.; Çetinkaya, E.; Çetinkaya, B. *J. Organomet. Chem.* **2014**, 765, 23.
56. Horn, S.; Albrecht, M. *Chem. Commun.* **2011**, 47, 8802.
57. Horn, S.; Gandolfi, C.; Albrecht, M. *Eur. J. Inorg. Chem.* **2011**, 2863.
58. Fernandez, F. E.; Puerta, M. C.; Valerga, P. *Organometallics* **2011**, 30, 5793.
59. Humphries, M. E.; Pecak, W. H.; Hohenboken, S. A.; Alvarado, S. R.; Swenson, D. C.; Domski, G. J. *Inorg. Chem. Commun.* **2013**, 37, 138.
60. Sanz, S.; Azua, A.; Peris, E. *Dalton Trans.* **2010**, 39, 6339.
61. Gülcemal, D.; Gökce, A. G.; Gülcemal, S.; Çetinkaya, B. *RSC Adv.* **2014**, 4, 26222.
62. Gülcemal, S.; Gökce, A. G.; Çetinkaya, B. *Dalton Trans.* **2013**, 42, 7305.
63. Gülcemal, S.; Gökce, A. G.; Çetinkaya, B. *Inorg. Chem.* **2013**, 52, 10601.
64. Jimenez, M. V.; Fernández-Tornos, J.; Pérez-Torrente, J. J.; Modrego, F. J.; Winterle, S.; Cunchillos, C.; Lahoz, F. J.; Oro, L. A. *Organometallics* **2011**, 30, 5493.

65. Hintermair, U.; Campos, J.; Brewster, T. P.; Pratt, L. M.; Schley, N. D.; Crabtree, R. H. *ACS Catal.* **2014**, *4*, 99.
66. Campos, J.; Hintermair, U.; Brewster, T. P.; Takase, M. K.; Crabtree, R. H. *ACS Catal.* **2014**, *4*, 973.
67. Drost, R. M.; Bouwens, T.; van Leest, N. P.; de Bruin, B.; Elsevier, C. J. *ACS Catal.* **2014**, *4*, 1349.
68. Hashimoto, T.; Urban, S.; Hoshino, R.; Ohki, Y.; Tatsumi, K.; Glorius, F. *Organometallics* **2012**, *31*, 4474.
69. Du, W.; Wu, P.; Wang, Q.; Yu, Z. *Organometallics* **2013**, *32*, 3083.
70. Kumar, M.; DePasquale, J.; White, N. J.; Zeller, M.; Papish, E. T. *Ruthenium Organometallics* **2013**, *32*, 2135.
71. Sluijter, S. N.; Elsevier, C. J. *Organometallics* **2014**, *33*, 6389.
72. Saleem, F.; Rao, G. K.; Kumar, A.; Mukherjee, G.; Singh, A. K. *Organometallics* **2014**, *33*, 2341.
73. Hohloch, S.; Suntrup, L.; Sarkar, B. *Organometallics* **2013**, *32*, 7376.
74. Maity, R.; Hohloch, S.; Su, C.-Y.; van der Meer, M.; Sarkar, B. *Chem. Eur. J.* **2014**, *20*, 9952.
75. (a) Leung, W.-H.; Che, C.-M. *Inorg. Chem.* **1989**, *28*, 4619. (b) Sato, K.; Aoki, M.; Takagi, J.; Noyori, R. *J. Am. Chem. Soc.* **1997**, *119*, 12386. (c) Nishimura, T.; Onoue, T.; Ohe, K.; Uemura, S. *Tetrahedron Lett.* **1998**, *39*, 6011. (d) Fung, W.-H.; Yu, W.-Y.; Che, C.-M. *J. Org. Chem.* **1998**, *63*, 2873. (e) Chatterjee, D.; Mitra, A.; Mukherjee, S. *Polyhedron* **1999**, *18*, 2659. (f) Gonsalvi, L.; Arends, I. W. C. E.; Sheldon, R. A. *Org. Lett.* **2002**, *4*, 1659. (g) Sheldon, R. A.; Arends, I. W. C. E.; Brink, G.-J. T.; Dijkman, A. *Acc. Chem. Res.* **2002**, *35*, 774. (h) Gonsalvi, L.; Arends, I. W. C. E.; Moilanen, P.; Sheldon, R. A. *Adv. Synth. Catal.* **2003**, *345*, 1321. (i) Cheung, W.-M.; Ng, H.-Y.; Williams, I. D.; Leung, W.-H. *Inorg. Chem.* **2008**, *47*, 4383. (j) Raja, M. U.; Gowri, N.; Ramesh, R. *Polyhedron* **2010**, *29*, 1175. (k) Raju, V. V.; Balasubramanian, K. P.; Jayabalakrishnan, C.; Chinnusamy, V. *Nat. Sci.* **2011**, *3*, 3542. (l) Trivedi, M.; Nagarajan, R.; Kumar, A.; Singh, N. K.; Rath, N. P. *J. Mol. Struct.* **2011**, *994*, 29. (m) Gunasekaran, N.; Remya, N.; Radhakrishnan, S.; Karvembu, R. *J. Coord. Chem.* **2011**, *64*, 491. (n) Tamizh, M. M.; Mereiter, K.; Kirchner, K.; Karvembu, R. *J. Organomet. Chem.* **2012**, *700*, 194.

76. (a) Bowden, K.; Heilbron, I. M.; Jones E. R. H.; Weedon, B. C. L. *J. Chem. Soc.* **1946**, 39. (b) Collins, J. C.; Hess, W. W.; Frank, F. J. *Tetrahedron Lett.* **1968**, 9, 3363. (c) Corey, E. J.; Suggs, J. W. *Tetrahedron Lett.* **1975**, 16, 2647.
77. (a) Ishihara, K.; Kurihara, H.; Yamamoto, H. *J. Org. Chem.* **1997**, 62, 5664. (b) Akamanchi, K. G.; Chaudhari, B. A. *Tetrahedron Lett.* **1997**, 38, 6925. (c) Ooi, T.; Otsuka, H.; Miura, T.; Ichikawa, H.; Maruoka, K. *Org. Lett.* **2002**, 4, 2669. (d) Suzuki, T.; Morita, K.; Tsuchida, M.; Hiroi, K. *J. Org. Chem.* **2003**, 68, 1601. (e) Kreis, M.; Palmelund, A.; Bunch, L.; Madsena, R. *Adv. Synth. Catal.* **2006**, 348, 2148. (f) Gabrielsson, A.; van Leeuwen, P.; Kaim, W. *Chem. Commun.* **2006**, 4926. (g) Levy, R.; Azerraf, C.; Gelman, D.; Braun, K. R.; Kapoor, P. N. *Catal. Commun.* **2009**, 11, 298. (h) Paul, P.; Richmond, M. G.; Bhattacharya, S. *J. Organomet. Chem.* **2014**, 751, 760.
78. Dess, D. B.; Martin, J. C. *J. Am. Chem. Soc.* **1991**, 113, 7277.
79. Ley, S. V.; Norman, J.; Griffith, W. P.; Marsden, S. P. *Synthesis*, **1994**, 639.
80. FOR REVIEWS SEE: (a) Sheldon, R. A.; I. Arends, W. C. E.; ten Brink, G. J.; Dijkstra, A. *Acc. Chem. Res.* **2002**, 35, 774. (b) Muzart, J.; *Tetrahedron* **2003**, 59, 5789. (c) Mallat, T.; Baiker, A. *Chem. Rev.* **2004**, 104, 3037. (d) Piera, J.; Bäckvall, J.-E. *Angew. Chem., Int. Ed.* **2008**, 47, 3506.
81. FOR REVIEWS, SEE: (a) Samec, J. S. M.; Bäckvall, J.-E.; Andersson, P. G.; Brandt, P. *Chem. Soc. Rev.* **2006**, 35, 237. (b) Nixon, T. D.; Whittlesey, M. K.; Williams, J. M. J. *Dalton Trans.* **2009**, 753. (c) Dobereiner, G. E.; Crabtree, R. H. *Chem. Rev.* **2010**, 110, 681. (d) Alonso, F.; Riente, P.; Yus, M. *Acc. Chem. Res.* **2011**, 44, 379.
82. See for example: (a) Sponholz, P.; Mellmann, D.; Cordes, C.; Alsabeh, P. G.; Li, B.; Li, Y.; Nielsen, M.; Junge, H.; Dixneuf, P.; Beller, M. *ChemSusChem* **2014**, 7, 2419. (b) Nielsen, M.; Kammer, A.; Cozzula, D.; Junge, H.; Gladiali, S.; Beller, M. *Angew. Chem., Int. Ed.* **2011**, 50, 9593. (c) Boddien, A.; Gartner, F.; Mellmann, D.; Sponholz, P.; Junge, H.; Laurency, G.; Beller, M. *Chimia* **2011**, 65, 214. (d) Nielsen, M.; Junge, H.; Kammer, A.; Beller, M. *Angew. Chem. Int. Ed.* **2012**, 51, 5711. *Angew. Chem.* **2012**, 124, 5809. (e) Junge, H.; Beller, M. *Tetrahedron Lett.* **2005**, 46, 1031.
83. (a) Zhang, J.; Leitus, G.; Ben-David, Y.; Milstein, D. *J. Am. Chem. Soc.* **2005**, 127, 12429. (b) Zhang, J.; Gandelman, M.; Shimon, L. J. W.; Rozenberg, H.; Milstein, D. *Organometallics* **2004**, 23, 4026.

84. (a) Zweifel, T.; Naubron, J. V.; Grützmacher, H. *Angew. Chem., Int. Ed.* **2009**, 48, 559. (b) Zweifel, T.; Naubron, J. V.; Büttner, T.; Ott, T.; Grützmacher, H. *Angew. Chem., Int. Ed.* **2008**, 47, 3245.
85. (a) Peterson, K. P.; Larock, R. C.; *J. Org. Chem.* **1998**, 63, 3185. (b) Stahl, S. S.; *Angew. Chem., Int. Ed.* **2004**, 43, 3400.
86. (a) Li, H.; Lu, G.; Jiang, J.; Huang, F.; Wang, Z.-X. *Organometallics* **2011**, 30, 2349. (b) Zeng, G.; Sakaki, S.; Fujita, K.-i.; Sano, H.; Yamaguchi, R. *ACS Catal.* 2014, 4, 1010. (c) Gülcemal, S.; Gülcemal, D.; Whitehead, G. F. S.; Xiao, J. *Chem. Eur. J.* **2016**, 22, 10513. (d) Valencia, M.; Müller-Bunz, H.; Gossage, R. A.; Albrecht, M. *Chem. Commun.* **2016**, 52, 3344. (e) Jimenez, M. V.; Fernández-Tornos, J.; Modrego, F. J.; Pérez-Torrente, J. J.; Oro, L. A. *Chem. Eur. J.* **2015**, 21, 17877. (f) Ngo, A. H.; Adams, M. J.; Do, L. H. *Organometallics* **2014**, 33, 6742.
87. Hoover, J. M.; Stahl, S. S.; *J. Am. Chem. Soc.* **2011**, 133, 16901.
88. Baratta, W.; Bossi, G.; Putignano, E.; Rigo, P. *Chem. Eur. J.* **2011**, 17, 3474.
89. (a) Zhang, J.; Leitus, G.; Ben-David, Y.; Milstein, D. *J. Am. Chem. Soc.* **2005**, 127, 10840. (b) Gunanathan, C.; Ben-David, Y.; Milstein, D. *Science* **2007**, 317, 790. (c) Gunanathan, C.; Shimon, L. J. W.; Milstein, D. *J. Am. Chem. Soc.* **2009**, 131, 3146.
90. (a) Miera, G. G.; Martínez-castro, E.; Martín-Matute, Belén. *Organometallics* **2017**, DOI: 10.1021/acs.organomet.7b00220. (b) Canseco-Gonzalez, D.; Albrecht, M. *Dalton Trans.* **2013**, 42, 7424.
91. (a) Zhang, J.; Leitus, G.; Ben-David, Y.; Milstein, D. *J. Am. Chem. Soc.* **2005**, 127, 10840. (b) Gunanathan, C.; Ben-David, Y.; Milstein, D. *Science* **2007**, 317, 790. (c) Gunanathan, C.; Shimon, L. J. W.; Milstein, D. *J. Am. Chem. Soc.* **2009**, 131, 3146.
92. Nielsen, M.; Alberico, E.; Baumann, W.; Drexler, H. J.; Junge, H.; Gladiali, S.; Beller, M. *Nature* **2013**, 495, 85.
93. Zhang, L.; Nguyen, D. H.; Raffa, G.; Trivelli, X.; Capet, F.; Desset, S.; Paul, S.; Dumeignil, F.; Gauvin, R. M. *ChemSusChem* **2016**, 9, 1413.
94. Polukeev, A. V.; Petrovskii, P. V.; Peregodov, A. S.; Ezernitskaya, M. G.; Koridze, A. A. *Organometallics* **2013**, 32, 1000.
95. Fujita, K. -I.; Tanino, N.; Yamaguchi, R. *Org. Lett.* **2007**, 9, 109.
96. See for example: (a) Kim, B. K.; Kim, H. -S.; Kim, T. -J.; Shim, S. C. *Organometallics* **2003**, 22, 3608. (b) Martínez, R.; Ramón, R. J.; Yus, M. *Tetrahedron* **2006**, 62, 8982. (c) Viciano, M.; Sanau, M.; Peris, E. *Organometallics* **2007**, 26, 6050.

- (d) Fujita, K. -I.; Asai, C.; Yamaguchi, T.; Hanasaka, F.; Yamaguchi, R. *Org. Lett.* **2005**, 7, 4017.
97. See for example: (a) Malai Haniti, S. A. H.; Williams, J. M. J. *Chem. Commun.* **2007**, 725. (b) Fujita, K., Li, Z., Ozeki, N. and Yamaguchi, R. *Tet. Lett.* **2003**, 44, 2687. (c) Fujita, K. -I.; Fujii, T.; Yamaguchi, R. *Org. Lett.* **2004**, 6, 3525.
98. Pontes da Costa, A.; Viciano, M.; Sanaú, M.; Merino, S.; Tejada, J.; Peris, E.; Royo, B. *Organometallics* **2008**, 27, 1305.
99. Miera, G. G.; Martínez-castro, E.; Martín-Matute, Belén. *Organometallics* **2017**, DOI: 10.1021/acs.organomet.7b00220.
100. Cesari, C.; Mazzoni, R.; Müller-Bunz, H.; Albrecht, M. *J. Organomet. Chem.* **2015**, 793, 256.
101. Prades, A.; Corbern, R.; Poyatos, M.; Peris, E. *Chem. Eur. J.* **2008**, 14, 11474.
102. (a) Chow, J.; Kopp, R. J.; Portney, P. R. *Science* **2003**, 302, 1528. (b) Lewis, N. S.; Nocera, D. G. *Proc. Natl. Acad. Sci. USA* **2006**, 103, 15729. (c) Balzani, V.; Credi, A.; Venturi, M. *ChemSusChem* **2008**, 1, 26.
103. Rutherford, A.W.; Boussac, A. *Science* **2004**, 303, 1831.
104. For a sophisticated model of the enzymatic Mn₄ core, see: Limburg, J.; Vrettos, J. S.; Liable-Sands, L. M.; Rheingold, A. L.; Crabtree, R. H.; Brudvig, G.W. *Science* **1999**, 283, 1524.
105. See for example: (a) Sun, L.; Hammarström, L.; Åkermark, B.; Styring, S. *Chem. Soc. Rev.* **2001**, 30, 36. (b) Tachibana, Y.; Vayssieres, L.; Durrant, J. R. *Nat. Photonics* **2012**, 6, 511. (c) Karkäs, M. D.; Johnston, E. V.; Verho, O.; Åkermark, B. *Acc. Chem. Res.* **2014**, 47, 100. (d) Cook, T. R.; Dogutan, D. K.; Reece, S. Y.; Surendranath, Y.; Teets, T. S.; Nocera, D. G. *Chem. Rev.* **2010**, 110, 6474. (e) Brudvig, G. W. *Coord. Chem. Rev.* **2008**, 252, 231. (f) Eisenberg, R.; Gray, H. B. *Inorg. Chem.* **2008**, 47, 1697. (g) Hammarström, L.; Hammes-Schiffer, S. *Acc. Chem. Res.* **2009**, 42, 1859. (h) Tollefson, J. *Nature* **2011**, 473, 134. (i) Service, R. F. *Science* **2011**, 334, 925.
106. Blakemore, J. D.; Crabtree, R. H.; Brudvig, G. W. *Chem. Rev.* **2015**, 115, 12974.
107. (a) Gersten, S. W.; Samuels, G. J.; Meyer, T. J. *J. Am. Chem. Soc.* **1982**, 104, 4029. (b) Gilbert, J. A.; Eggleston, D. S.; Murphy, W. R., Jr.; Geselowitz, D. A.; Gersten, S. W.; Hodgson, D. J.; Meyer, T. J. *J. Am. Chem. Soc.* **1985**, 107, 3855.
108. Limburg, J.; Brudvig, G. W.; Crabtree, R. H. *J. Am. Chem. Soc.* **1997**, 119, 2761.
109. (a) *Molecular Water Oxidation Catalysis*; Ed. Llobet, A., Wiley, Chichester, **2005**. (b) Sens, C.; Romero, I.; Rodríguez, M.; Llobet, A.; Parella, T.; Benet-Buchholz, J. J.

- Am. Chem. Soc.* **2004**, 126, 7798. (c) Duan, L.; Bozoglian, F.; Mandal, S.; Stewart, B.; Privalov, T.; Llobet, A.; Sun, L. *Nat. Chem.* **2012**, 4, 418. (d) Matheu, R.; Ertem, M. Z.; Benet-Buchholz, J.; Coronado, E.; Batista, V. S.; Sala, X.; Llobet, A. *J. Am. Chem. Soc.* **2015**, 137, 10786. (e) Creus, J.; Matheu, R.; Peñafiel, I.; Moonshiram, D.; Blondeau, P.; Benet-Buchholz, J.; García-Antón, J.; Sala, X.; Godard, C.; Llobet, T. *Angew. Chem., Intl. Ed.* **2016**, 55, 15382. (f) Rigsby, M. L.; Mandal, S.; Nam, W.; Spencer, L. C.; Llobet, A.; Stahl, S. S. *Chem. Sci.* **2012**, 3, 3058. (g) Moonshiram, D.; Gimbert-Suriñach, C.; Guda, A.; Picon, A.; Lehmann, C. S.; Zhang, Z.; Doumy, G.; March, A. M.; Benet-Buchholz, J.; Soldatov, A.; Llobet, A.; Southworth, S. H. *J. Am. Chem. Soc.* **2016**, 138, 10586.
110. (a) Kärkäs, M. D.; Verho, O.; Johnston, E. V.; Åkermark, B. *Chem Rev.* **2014**, 114, 11863. (b) Kärkäs, M. D.; Åkermark, T.; Johnston, E. V.; Karim, S. R.; Laine, T. M.; Lee, B.-L.; Åkermark, T.; Privalov, T.; Åkermark, B. *Angew. Chem., Int. Ed.* **2012**, 51, 11589. (c) Xu, Y.; Fischer, A.; Duan, L.; Tong, L.; Gabrielsson, E.; Åkermark, B.; Sun, L. *Angew. Chem., Int. Ed.* **2010**, 49, 8934. (d) Anderlund, M. F.; Höglblom, J.; Shi, W.; Huang, P.; Eriksson, L.; Weihe, H.; Styring, S.; Åkermark, B.; Lomoth, R.; Magnuson, A. *Eur. J. Inorg. Chem.* **2006**, 5033. (e) Nyhlén, J.; Duan, L.; Åkermark, B.; Sun, L.; Privalov, T. *Angew. Chem., Int. Ed.* **2010**, 49, 1773.
111. (a) Duan, L.-L.; Xu, Y.-H.; Tong, L.-P.; Sun, L.-C. *ChemSusChem* **2011**, 4, 238. (b) Zhang, B.; Li, F.; Yu, F.; Wang, X.; Zhou, X.; Li, H.; Jiang, Y.; Sun, L. *ACS Catal.* **2014**, 4, 804.
112. (a) Zong, R.; Thummel, R. P. *J. Am. Chem. Soc.* **2005**, 127, 12802. (b) Zhang, G.; Zong, R.; Tseng, H.-W.; Thummel, R. P. *Inorg. Chem.* **2008**, 47, 990. (c) Yoshida, M.; Masaoka, S.; Sakai, K. *Chem. Lett.* **2009**, 38, 702. (d) Seidler-Egdal, R. K.; Nielsen, A.; Bond, A. D.; Bjerrum, M. J.; McKenzie, C. J. *Dalton Trans.* **2011**, 40, 3849. (e) Sameera, W. M. C.; McKenzie, C. J.; McGrady, J. E. *Dalton Trans.* **2011**, 40, 3859.
113. For representative examples, see: (a) Abe, T.; Nagai, K.; Kabutomori, S.; Kaneko, M.; Tajiri, A.; Norimatsu, T. *Angew. Chem., Int. Ed. Engl.* **2006**, 45, 2778. (b) Rigsby, M. L.; Mandal, S.; Nam, W.; Spencer, L. C.; Llobet, A.; Stahl, S. S. *Chem. Sci.* **2012**, 3, 3058. (c) Lv, H.; Song, J.; Geletii, Y. V.; Vickers, J. W.; Sumliner, J. M.; Musaev, D. G.; Kögerler, P.; Zhuk, P. F.; Bacsá, J.; Zhu, G.; Hill, C. L. *J. Am. Chem. Soc.* **2014**, 136, 9268. (d) Berardi, S.; La Ganga, G.; Natali, M.; Bazzan, I.; Puntoriero, F.; Sartorel, A.; Scandola, F.; Campagna, S.; Bonchio, M. *J. Am. Chem. Soc.* **2012**, 134, 11104. (e) Zhang, B.; Li, F.; Yu, F.; Wang, X.; Zhou, X.; Li, H.; Jiang, Y.; Sun, L. *ACS Catal.*

2014, 4, 804. f) Moonshiram, D.; Gimbert-Suriñach, C.; Guda, A.; Picon, A.; Lehmann, C. S.; Zhang, Z.; Doumy, G.; March, A. M.; Benet-Buchholz, J.; Soldatov, A.; Llobet, A.; Southworth, S. H. *J. Am. Chem. Soc.* **2016**, 138, 10586.

114. For representative examples, see: (a) Ellis, W. C.; McDaniel, N. D.; Bernhard, S.; Collins, T. J. *J. Am. Chem. Soc.* **2010**, 132, 10990. (b) Demeter, E. L.; Hilburg, S. L.; Washburn, N. R.; Collins, T. J.; Kitchin, J. R. *J. Am. Chem. Soc.* **2014**, 136, 5603. (c) Panda, C.; Debgupta, J.; Diaz Diaz, D.; Singh, K. K.; Sen Gupta, S.; Dhar, B. B. *J. Am. Chem. Soc.* **2014**, 136, 12273. (d) Fillol, J. L.; Codola, Z.; Garcia-Bosch, I.; Gomez, L.; Pla, J. J.; Costas, M. *Nat. Chem.* **2011**, 3, 807. (e) Chen, G.; Chen, L.; Ng, S.-M.; Man, W.-L.; Lau, T.-C. *Angew. Chem., Int. Ed.* **2013**, 52, 1789. (f) Coggins, M. K.; Zhang, M.-T.; Vannucci, A. K.; Dares, C. J.; Meyer, T. J. *J. Am. Chem. Soc.* **2014**, 136, 5531.

115. For representative examples, see: (a) McDaniel, N. D.; Coughlin, F. J.; Tinker, L. L.; Bernhard, S. *J. Am. Chem. Soc.* **2008**, 130, 210. (b) Hull, J. F.; Balcells, D.; Blakemore, J. D.; Incarvito, C. D.; Eisenstein, O.; Brudvig, G. W.; Crabtree, R. H. *J. Am. Chem. Soc.* **2009**, 131, 8730. (c) Savini, A.; Bellachioma, G.; Ciancaleoni, G.; Zuccaccia, C.; Zuccaccia, D.; Macchioni, A. *Chem. Commun.* **2010**, 46, 9218. (d) Lalrempuia, R.; McDaniel, N. D.; Müller-Bunz, H.; Bernhard, S.; Albrecht, M. *Angew. Chem., Int. Ed.* **2010**, 49, 9765. (e) Turlington, C. R.; White, P. S.; Brookhart, M.; Templeton, J. L. *J. Am. Chem. Soc.* **2014**, 136, 3981. (f) Grotjahn, D. B.; Brown, D. B.; Martin, J. K.; Marelus, D. C.; Abadjian, M.-C.; Tran, H. N.; Kalyuzhny, G.; Vecchio, K. S.; Specht, Z. G.; Cortes-Llamas, S. A.; Miranda-Soto, V.; van Niekerk, C.; Moore, C. E.; Rheingold, A. L. *J. Am. Chem. Soc.* **2011**, 133, 19024. (g) Parent, A. R.; Blakemore, J. D.; Brudvig, G. W.; Crabtree, R. H. *Chem. Commun.* **2011**, 47, 11745. (h) Codola, Z.; Cardoso, J. M. S.; Royo, B.; Costas, M.; Lloret-Fillol, J. *Chem. Eur. J.* **2013**, 19, 7203. (i) Navarro, M.; Li, M.; Mueller-Bunz, H.; Bernhard, S.; Albrecht, M. *Chem. Eur. J.* **2016**, 22, 6740. (j) Sharninghausen, L. S.; Sinha, S. B.; Shopov, D. Y.; Choi, B.; Mercado, B. Q.; Roy, X.; Balcells, D.; Brudvig, G. W.; Crabtree, R. H. *J. Am. Chem. Soc.* **2016**, 138, 15917.

116. Blakemore, J. D.; Schley, N. D.; Balcells, D.; Hull, J. F.; Olack, G. W.; Incarvito, C. D.; Eisenstein, O.; Brudvig, G. W.; Crabtree, R. H. *J. Am. Chem. Soc.* **2010**, 132, 16017.

117. McDaniel, N. D.; Coughlin, F. J.; Tinker, L. L.; Bernhard, S. *J. Am. Chem. Soc.* **2008**, 130, 210.

118. Hull, J. F.; Balcells, D.; Blakemore, J. D.; Incarvito, C. D.; Eisenstein, O.; Brudvig, G. W.; Crabtree, R. H. *J. Am. Chem. Soc.* **2009**, 131, 8730.
119. Parent, A. R.; Brewster, T. P.; Wolf, W. D.; Crabtree, R. H.; Brudvig, G. W. *Inorg. Chem.* **2012**, 51, 6147.
120. Sharninghausen, L. S.; Sinha, S. B.; Shopov, D. Y.; Choi, B.; Mercado, B. Q.; Roy, X.; Balcells, D.; Brudvig, G. W.; Crabtree, R. H. *J. Am. Chem. Soc.* **2016**, 138, 15917.
121. Brewster, T. P.; Blakemore, J. D.; Schley, N. D.; Incarvito, C. D.; Hazari, N.; Brudvig, G. W.; Crabtree, R. H. *Organometallics* **2011**, 30, 965.
122. Singh, A. K.; Balamurugan, V.; Mukherjee, R. *Inorg. Chem.* **2003**, 42, 6497.
123. Volpe, A.; Sartorel, A.; Tubaro, C.; Meneghini, L.; Di Valentin, M.; Graiff, C.; Bonchio, M. *Eur. J. Inorg. Chem.* **2014**, 665.
124. Hetterscheld, D. G. H.; Reek, J. N. H. *Chem. Commun.* **2011**, 47, 2712.
125. (a) Tietze, L. T.; Bell, H. II, H. P. *Chem. Rev.* **2004**, 104, 3453. (b) Dai, L. X.; Tu, T.; You, S. L.; Deng, W. P.; Hou, X. L. *Acc. Chem. Res.* **2003**, 36, 659. (c) Bolm, C.; Hildebrand, J. P.; Muniz, K.; Hermanns, N. *Angew. Chem.* **2001**, 113, 3382; *Angew. Chem. Int. Ed.* **2001**, 40, 3284. (d) Shibasaki, M.; Vogl E. M. *Comprehensive Asymmetric Catalysis* (Eds.: Jacobsen, E. N.; Pfaltz, A.; Yamamoto, H.), Springer, Heidelberg, 1999. (e) Loiseleur, O.; Hayashi, M.; Keenan, M.; Schemees, N.; Pfaltz, A. *J. Organomet. Chem.* **1999**, 576, 16. (f) Beller, M.; Riermeier, T. H.; Stark G. *Transition Metals for Organic Synthesis* (Eds.: Beller, M.; Bolm, C.), Wiley-VCH, Weinheim, 1998. (g) Coeffard V.; Guiry, P. J. *Curr. Org. Chem.* **2010**, 14, 212. (h) Oestreich M. *Mizoroki–Heck Reaction*. Wiley-VCH, Weinheim, 2009.
126. Heck, R. F. *J. Am. Chem. Soc.* **1968**, 90, 5518.
127. (a) Sato, Y.; Sodeoka, M.; Shibasaki, M. *J. Org. Chem.* **1989**, 54, 4738. (b) Carpenter, N. E.; Kucera, D. J.; Overman, L. E. *J. Org. Chem.* **1989**, 54, 5846.
128. Ozawa, F.; Kubo, A.; Hayashi, T. *J. Am. Chem. Soc.* **1991**, 113, 1417.
129. Wu, Ch.; Zhou, J (S). *J. Am. Chem. Soc.* **2014**, 136, 650.
130. (a) Trabesinger, G.; Albinati, A.; Feiken, N.; Kunz, R. W.; Pregosin P. S.; Tschoerner, M. *J. Am. Chem. Soc.* **1997**, 119, 6315. (b) Tschoerner, M.; Pregosin P. S.; Albinati, A. *Organometallics* **1999**, 18, 670. (c) Tietze, L. F.; Thede K.; Sannicola, F. *Chem. Commun.* **1999**, 1811. (d) Andersen, N. G.; Parvez M.; Keay, B. A. *Org. Lett.* **2000**, 2, 2817.
131. Ozawa, F.; Hayashi, T. *J. Organomet. Chem.* **1992**, 428, 267.

132. (a) Loiseleur, O.; Meier, P.; Pfaltz, A. *Angew. Chem.* **1996**, 108, 218; *Angew. Chem. Int. Ed.* **1996**, 35, 200. (b) Loiseleur, O.; Hayashi, M.; Schmees, N.; Pfaltz, A. *Synthesis* **1997**, 1338. (c) Hennessy, A. J.; Malone, Y. M.; Guiry, P. J. *Tetrahedron lett.* **1999**, 40, 9163. (D) Hennessy, A. J.; Connolly, D. J.; Malone, Y. M.; Guiry, P. J. *Tetrahedron lett.* **2000**, 41, 7757.
133. Nilsson, P.; Gold, H.; Larhed, M.; Hallberg, A. *Synthesis* **2002**, 1611.
134. Hashimoto, Y.; Horie, Y.; Hayashi, M.; Saigo, K. *Tetrahedron: Asymmetry* **2000**, 11, 2205.
135. Liu, D.; Dai, Q.; Zhang, X. *Tetrahedron* **2005**, 61, 6460.
136. Bélanger, E.; Pouliot, M. -F.; Paquin, J. -F. *Org. Lett.* **2009**, 11, 2201.
137. Ogasawara, M.; Yoshida, K.; Hayashi, T. *Heterocycles* **2000**, 52, 195.
138. (a) Gilbertson, S. R.; Xie, D.; Fu, Z. *J. Org. Chem.* **2001**, 66, 7240. (b) Gilbertson, S. R.; Fu, Z. *Org. Lett.* **2001**, 3, 161. (c) Gilbertson, S. R.; Genov, D. G.; Rheingold, A. L. *Org. Lett.* **2000**, 2, 2885.
139. (a) Deng, W. -P.; Hou, X. -L.; Dai, L. -X.; Dong, X. -W. *Chem. Commun.* **2000**, 1483. (b) Tu, T.; Deng, W. -P.; Hou, X. -L.; Dai, L. -X.; Dong, X. -C. *Chem. Eur. J.* **2003**, 9, 3073.
140. (a) Kilroy, T. G.; Cozzi, G. P.; End, P. J.; Guiry, P. J. *Synlett* **2004**, 106. (b) Kilroy, T. G.; Cozzi, G. P.; End, P. J.; Guiry, P. J. *Synthesis* **2004**, 1879. (c) Fitzpatrick, M. O.; Müller-Bunz, H.; Guiry, P. J. *Eur. J. Org. Chem.* **2009**, 1889. (d) McCartney, D.; Nottingham, Ch.; Müller-Bunz, H.; Guiry, P. *J. Org. Chem.* **2015**, 80, 10151.
141. (a) M. Robina, W. M. Rubin. *Organometallics.* **2008**, 27, 6393. (b) Rubina, M.; Sherrill, W. M.; Barkov, A. Y.; Rubin, M. *Beilstein J. Org. Chem.* **2014**, 10, 1536.
142. W. -Q. Wu, Q. peng, D. -X. Dong, X. -L. Hou, Y. -D. Wu. *J. Am. Chem. Soc.* **2008**, 130, 9717.
143. (a) Drury III, W. J.; Zimmermann, N.; Keenan, M.; Hayashi, M.; Kaiser, S.; Goddard, R.; Pfaltz, A. *Angew. Chem. Int. Ed.* **2004**, 116, 72; *Angew. Chem. Int. Ed.* **2004**, 43, 70. (b) Malkov, A. V.; Bella, M.; Stará, I. G.; Kocövsky, P. *Tetrahedron Lett.* **2001**, 42, 3045.
144. Kilroy, T. G.; Hennessy, A. J.; Connolly, D. J.; Malone, Y. M.; Farrell, A.; Guiry, P. J. *J. Mol. Cat. A: Chem.* **2003**, 196, 65.
145. Bernardinelli, G. H.; Kündig, E. P.; Meier, P.; Pfaltz, A.; Radkowski, K.; Zimmermann, N.; Neuburger-Zehnder, M. *Helv. Chim. Acta* **2001**, 84, 3233.

146. (a) Kaukoranta, P.; Källström, K.; Andersson, P. G. *Adv. Synth. Catal.* **2007**, *349*, 2595. (b) Henriksen, S. T.; Norrby, P. O.; Kaukoranta, P.; Andersson, P. G. *J. Am. Chem. Soc.* **2008**, *130*, 10414.
147. Yonehara, K.; Mori, K.; Hashizume, T.; Chung, K. -G.; Ohe, K.; Uemure, S. *J. Organomet. Chem.* **2000**, 603, 40.
148. (a) Wöste, T. H.; Oestreich, M. *Chem. Eur. J.* **2011**, *17*, 11914. (b) Hu, J.; Lu, Y.; Li Y.; Zhou, J (S). *Chem. Commun.* **2013**, 49, 9425. (c) Zhang, Q-S.; Wan, Sh-L.; Chen, D.; Ding, Ch-H.; Hou, X-L. *Chem. Commun.* **2015**, 51, 12235. (d) Oestreich, M. *Angew. Chem. Int. Ed.* **2014**, *53*, 2282.
149. (a) Mata, Y.; Pàmies, O.; Diéguez, M. *Org. Lett.* **2005**, *7*, 5597. (b) Mata, Y.; Diéguez, M.; Pàmies, O. *Chem. Eur. J.* **2007**, *13*, 3296. (c) Mazuela, J.; Pàmies, O.; Diéguez, M. *Chem. Eur. J.* **2010**, *16*, 3434. (d) Mazuela, J.; Tolstoy, P.; Pàmies, O.; Andersson, Ph. J.; Diéguez, M. *Org. Biomol. Chem.* **2011**, *9*, 941. (e) Diéguez, M.; Pàmies, O. *Isr. J. Chem.* **2012**, *52*, 572. (f) Diéguez, M.; Pàmies, O. *Carbohydrates-tools for estereoselective synthesis*. Ed. Boysen, M. M. K. Wiley-VCH Verlag GmbH & Co. KGaA, **2013**, Chapter 11, 245.

Chapter 5.

*Ru- and Ir-catalyzed transfer hydrogenation and
dehydrogenation reactions*

5.1. Synthesis, hemilability, and catalytic transfer hydrogenation activity of iridium(III) and ruthenium(II) complexes containing oxygen-functionalised triazolylidene ligands

Pretorius, R.; Mazloomi, Z.; Albrecht, M. *J. Organomet. Chem.* **2017**. doi:10.1016/j.jorganchem.2017.05.014

5.1.1. Introduction

Pincer complexes have made one of the most fundamental contributions to the development of modern organometallic chemistry.¹ In pioneering work, van Koten and coworkers explored the consequences of combining hard amine donor sites with soft metals such as iridium(I) and platinum(II) nuclei,² which lead to a plethora of fascinating applications.

Building on this fundamental design concept, we became interested in modifying N-heterocyclic carbenes (NHCs), a classic ligand scaffold of modern catalyst design as NHCs much like pincer ligands typically impart high thermal stability and countless options for synthetic modifications.³ Introducing functional groups on the ligand scaffold allows for imparting stability through chelation, or hemilability for catalyst activation, or even bifunctional catalysis in which both the ligand and the metal participate in the conversion of substrate.⁴ Prototypical examples of such functionalised catalysts include Shvo⁵ and Noyori's⁶ (de)hydrogenation catalysts, which have excellent activity in an extended range of applications.⁷ Several examples of O- and N-functionalised Arduengo-type carbene complexes have been developed that display cooperative behaviour and enhanced catalytic properties.⁸ Such functionalisation is even more versatile with 1,2,3-triazolylidene ligands,⁹ as the core heterocycle is generally assembled via functional group-tolerant "click" cycloaddition reaction of azides and alkynes.¹⁰

NI,N3-disubstituted triazolylidene ligands are mesoionic¹¹ and have shown to stabilize high and low metal oxidation states.¹² They impart excellent catalytic activity in numerous transformations including cross-coupling,¹³ and in particular redox transformation such as water oxidation,¹⁴ amine and alcohol oxidation¹⁵ and transfer hydrogenation.¹⁶

5.1.2. Objectives

While much recent work has been focusing on C,N-chelating triazolylidene complexes with imine donor sites, much less work has been directed towards understanding the catalytic implications of oxygen donors as functional groups at the triazolylidene ligand scaffold.¹⁷ Due to the demonstrated benefits of oxygen functional groups in close proximity to the metal centre, we have designed triazolylidene metal complexes with a potential C,O-bidentate bonding motif.^{8e,18} Herein we describe the synthesis of O-functionalised 1,2,3-triazolylidene iridium(III) and ruthenium(II) complexes and their catalytic activity in transfer hydrogenation. Specifically, we sought to introduce pendant oxygen-wingtip groups adjacent to the carbene, to investigate hemilabile coordination and potential metal-ligand cooperative behaviour in hydrogen transfer for (de)hydrogenation processes.

5.1.3. Results and discussion

5.1.3.1. Synthesis and characterisation of 1,2,3-triazolylidene iridium(III) complexes.

The hydroxyfunctionalised ligand precursor **L1H**·BF₄ was prepared by literature procedures (Scheme 5.1.1).^{18d} For the synthesis of the ether-functionalised triazolylidene precursor **L2H**·BF₄ a Williamson ether synthesis using NaH and MeI was applied at the triazole stage to install the methyl ether, followed by triazole N-alkylation with [Me₃O]BF₄, which afforded the triazolium salt **L2H**·BF₄ in high yields (74%). Conveniently, NaH was used as the commercially available oil dispersion without any negative impact on yield. The purity of the crude triazole intermediate was not an issue as any oil residues were readily washed off from the final triazolium product after subsequent N-alkylation. The iridium(III) complexes **132-134** were synthesised by transmetallation procedures from the corresponding triazolium salt **L1H**·BF₄ or **L2H**·BF₄, using Ag₂O (2 equiv) and Me₄NCl (1 equiv) to form the Ag-carbene intermediates and subsequent in situ transmetallation with [Ir(Cp*)Cl₂]₂ (0.38 equiv). This procedure yielded iridium complexes **132-133** when starting from the hydroxy-functionalised ligand precursor **L1H**·BF₄, and complexes **134a,b** when starting from triazolium salt **L2H**·BF₄ with ether wingtip group. All complexes were obtained in spectroscopically pure form after separation by column chromatography, except for regioisomers **133** and **133'**, which were not attempted to be separated any further.

133 and **133'** ($\delta_{\text{C}} = 148.4$ and 147.9) are well within the range reported for related triazolylidene iridium complexes.^{14,15,19}

Triazolylidene bonding in a monodentate or C,O-bidentate mode in complexes **132a/134a** and **132b/134b**, respectively, was identified by the distinct ^1H NMR spectroscopic characteristics of these complexes. The NCH_2 hydrogens of the monodentate coordinated triazolylidene in complexes **132a** and **134a** are diastereotopic and separated by ca. 1 ppm ($\delta_{\text{H}} = 4.93$ and 4.09 for **132a**, and multiplets centred at $\delta_{\text{H}} = 4.95$ and 4.09 for **134a**). In contrast, this group appears in the chelating triazolylidene complex **132b** as a broad singlet at $\delta_{\text{H}} = 4.45$, and in complex **134b** as two resonances with only 0.2 ppm shift difference (multiplets around $\delta_{\text{H}} = 4.5$ and 4.3 ppm). In addition the ^{13}C NMR signals due to the triazolylidene carbons appear at 3–9 ppm higher field in the monodentate triazolylidenes ($\delta_{\text{C}} = 145.5$ and 152.9 in **132a**, and 146.7 and 150.2 in **134a**) when compared to the chelating triazolylidene complexes ($\delta_{\text{C}} = 154.1$ and 157.2 in **132b**, and 151.5 and 153.0 in **134b**). This shift correlates with the lower donor properties of the O-functionalities in comparison to the chlorido ligand, resulting in a deshielding of the triazole carbons. Likewise, the ^{13}C resonances corresponding to the quaternary carbons of the tert-butyl group undergo a diagnostic shift upon chelation and appear at $\delta_{\text{C}} = 77.6$ and 81.5 ppm, for **132b** and **134b**, respectively (cf. 69.0 and 76.5 ppm, for **132a** and **134a**, respectively), in agreement with a reduced electron density on the oxygen atom upon coordination to the metal centre.²⁰

Chelation of the triazolylidene ligand in complexes **132b** and **134b** was further supported by chloride abstraction experiments performed with the monodentate triazolylidene complexes **132a** and **134a**. For example, reaction of these complexes with AgBF_4 (1 equiv) in CH_2Cl_2 solution yielded complexes **132b** and **134b**, as corroborated by ^1H NMR spectroscopy. Similarly, when NaBPh_4 was used as the chloride scavenging agent, highly diastereotopic NCH_2 hydrogens were observed that are characteristic for complexes **3b** and **5b**. In addition, a 1:1 ratio between the metal complex and the BPh_4^- counter ion indicates that alternative chlorido scavengers yield the same type of cationic chelate complexes.

Finally, the presence of the acidic OH protons in both **132a** and **132b** was confirmed by D_2O exchange experiments, which induced disappearance of the resonances at $\delta_{\text{H}} = 6.21$ and 3.39 ppm for **132a** and **132b** respectively (CD_2Cl_2 solution). Interestingly, monocationic complexes analogous to **132b** could not be synthesised from closely

related O-functionalised imidazolylidene iridium complexes (though MeCN was used as solvent in lieu of CH₂Cl₂).^{8e}

Unambiguous evidence for the proposed structures was obtained from single crystal X-ray analyses of complexes **132a,b** and **134a** (Figure 5.1.1, Table 5.1.1). The molecular structures show the typical piano-stool arrangement around iridium(III), and general metrics are unexceptional.^{14,15,19} Analysis of the monodentate triazolylidene complexes **132a** and **134a** reveals only slight deviations of bond lengths and angles between these complexes. Complex **132b**, in contrast, displays C,O-bidentate coordination of the triazolylidene through both an Ir–C_{carbene} and an Ir–O bond. The bond lengths vary only slightly upon chelation.

Table 5.1.1. Selected bond distances (Å) and angles (°) for complexes **132a**, **132b** and **134a**.

	132a (X = Cl ₂) ^d	132b (X = O)	134a (X = Cl ₂)
Ir–C1	2.077(3)	2.032(4)	2.082(3)
Ir–Cl1	2.4237(7)	2.3779(10)	2.4184(8)
Ir–X	2.4271(7)	2.225(3)	2.4448(9)
C1–C2	1.403(4)	1.380(5)	1.405(5)
Ir–Centroid	1.807	1.785	1.814
C1–Ir–X	89.43(7)	73.61(12)	89.22(10)
C1–Ir–Cl1	92.13(8)	86.29(10)	89.67(10)
Cl1–Ir–X	86.33(3)	86.46(9)	84.02(10)
Ir–C1–C2	136.7(2)	119.1(3)	136.0(3)
Ir–C1–N3	121.54(19)	138.1(3)	121.9(2)

^(d) Data only for one of the two (essentially identical) crystallographically independent molecules in the unit cell.

The Ir–C and Ir–Cl bonds are contracted by ca 0.04 Å in **132b** when compared to **132a** (e.g. Ir–C1 2.032(4) vs 2.077(3) Å), presumably as a consequence of the formally cationic nature of the metal centre in **132b**. Also, as a consequence of chelation, the Ir–C1–C2 angle in **132b** is smaller than the corresponding angle in **132a** (119.1(3) vs 136.7(2)°). This distortion is compensated by an inverse trend in the Ir–C1–N1 angle (increasing to 138.1(3)° in **3b** vs. 121.54(19)° in **132a**). Accordingly, the overall yaw angle is only marginally affected with 7.6° for **132a** and 9.0° for **132b**. Intramolecular H-bonding is observed in complex **132a** between the hydroxy functionality and the metal-bound chloride with a O–H...Cl donor-acceptor distance of 3.06 Å and a 166.2° hydrogen bond angle, thus forming a 7-membered metallacycle. Complex **132b** displays

H-bonding between the coordinated alcohol and the noncoordinating BF_4^- anion with a O–H...F donor-acceptor distance of 2.63 Å and an angle of 174°. These H...X interactions fall within the range expected for moderate-strength H-bonds.²¹ The Ir–O bond length in complex **132b** is 2.225(3) Å, slightly longer than the analogous bond distance in a related $[\text{Ir}(\text{Cp}^*)(\text{trz-py})(\text{OH}_2)]^{2+}$ complex (cf. 2.166(3) Å),^{19a} and at the upper end of related NHC iridium(III) complexes (Ir–O bond in 2.15–2.24 Å range).^{8e,22} The relatively long Ir–O bond in **3b** has been attributed to the high steric bulk of the *tert*-butyl wingtip group.

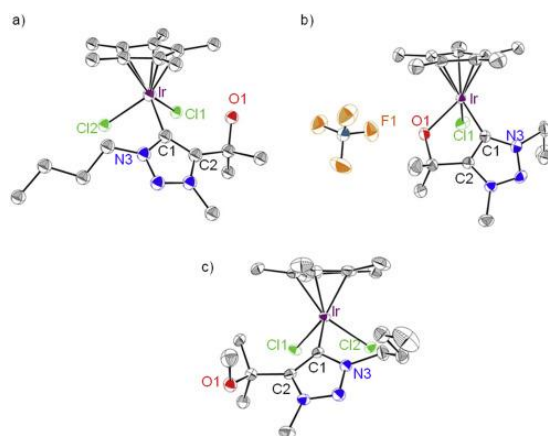
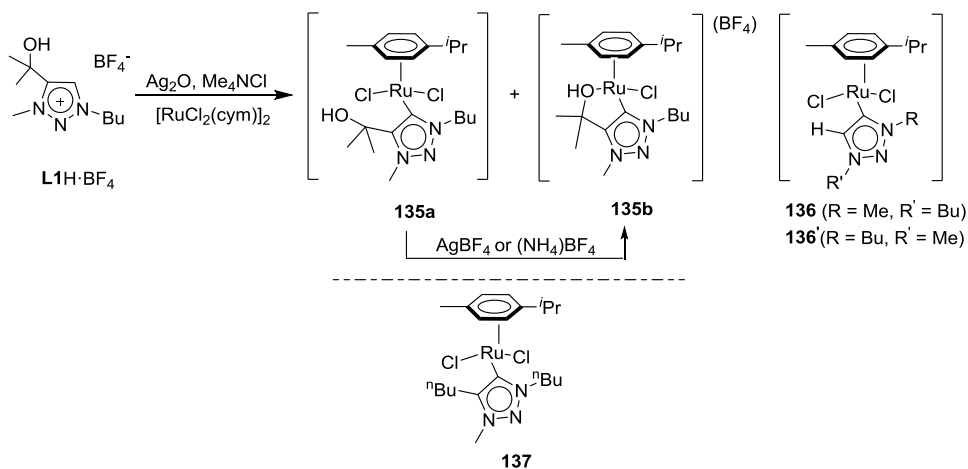


Figure 5.1.1. ORTEP representations of complex **132a** (a; only one of the two independent molecules shown), complex **132b** (b) and complex **134a** (c; all structures at 50% probability, disorder and hydrogen atoms omitted for clarity).

5.1.3.2. Synthesis and characterisation of O-functionalised 1,2,3-triazolylidene ruthenium(II) complexes.

The synthetic methodology developed for O-functionalised triazolylidene iridium(III) complexes was successfully extrapolated to prepare analogous ruthenium(II) complexes. Thus, ruthenium complexes **135** and **136** were synthesised from ligand precursor $\text{L1H}\cdot\text{BF}_4$ using $[\text{Ru}(\text{p-cymene})\text{Cl}_2]$ (0.3 equiv) instead of $[\text{Ir}(\text{Cp}^*)\text{Cl}_2]_2$ for transmetallation (Scheme 5.1.2). Purification by column chromatography yielded complexes **135a,b** and **136**. Alternatively, complex **135a** was isolated selectively in up to 60% yield through an aqueous extraction of the crude reaction mixture followed by salting out the complex into CH_2Cl_2 . This method of purification was applicable because in contrast to **135a**, complexes **136/136'** are insoluble in water. This difference in solubility is likely due to the presence of the

hydroxy functionality in **135a** and is an additional benefit of incorporating the alcohol functionality, as a wide solubility range increases the scope for potential catalytic applications. The synthesis of etherfunctionalised ruthenium complexes was probed using triazolium **L2H**·BF₄ in an analogous procedure. While ¹H NMR spectroscopy and specifically the diagnostic shifts of both the ligand and the *p*-cymene resonances suggest the formation of the product in the crude reaction mixture, the product was unstable and decomposed during purification, which prevented the isolation of a pure sample.



Scheme 5.1.2. Synthesis of 1,2,3-triazolylidene ruthenium(II) complexes **135** and **136**, and reference compound **137**.

In addition to complexes **135a,b**, the transmetalation procedure also yielded minor quantities of complexes **136** and **136'** as a result of the Ag-mediated degradation of the C4-wingtip group of triazolium salt **L1H**·BF₄, analogously to complexes **133**. The nature of these complexes was confirmed by NMR spectroscopy and elemental analysis. Two sets of resonances were observed in the ¹H and ¹³C spectra, confirming the presence of both regioisomers in a ca. 1:1 mixture. Purification by column chromatography provided pure complex **136** in small quantities, yet sufficient for unambiguous NMR characterisation of this complex. Consequently, this data in combination with NOESY experiments allowed also the ¹H and ¹³C resonances of complex **136'** to be assigned from the mixed sample. The ¹H NMR spectrum of complexes **136** and **136'** features two resonances at $\delta_{\text{H}} = 7.63$ and 7.59 ppm which are

diagnostic for the loss of the C4-wingtip group. The triazolylidene ^{13}C NMR resonances of complex **136** were slightly deshielded when compared to the isomer **136'** ($\delta_{\text{C}} = 166.0$ and 133.8 vs. 166.4 and 134.5). These data reflect the closely related structures of **136** and **136'** and the similar donor properties of the methyl and n-butyl groups.

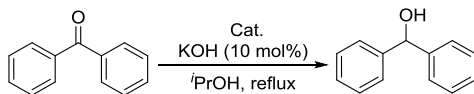
The monodentate triazolylidene complex **135a** and the C,O-bidentate triazolylidene ruthenium complex **135b** were readily distinguished by their $\text{C}_{\text{cym}}\text{H}$ resonances in the 5.9–4.5 ppm range, and in particular by the resonance of the NCH_2 group, which appears as a triplet at $\delta_{\text{H}} = 4.56$ in **6a**, while in **135b** this group gives rise to a multiplet at $\delta_{\text{H}} = 4.68$ – 4.52 . We note that the ^1H NMR spectrum of **135b** does not reveal diastereotopic resonances for the $\text{C}(\text{CH}_3)_2$ group of the *p*-cymene, even though the ruthenium(II) centre is stereogenic. The ^{13}C spectra revealed no distinct differences between **135a** and **135b**, and the carbenic resonances of these complexes are within the range reported for similar triazolylidene ruthenium complexes ($\delta_{\text{C}} = 164.8$ and 163.9 for **135a** and **135b** respectively).^{14a,15,16,23} NMR data was not sufficient to distinguish the structural motifs of **135a** and **135b**, and analogously to complexes **132** and **134** chloride scavenging reactions were used to identify the denticity of the triazolylidene ligand. Thus, addition of AgBF_4 (1 equiv, CH_2Cl_2) or NH_4BF_4 (1 equiv, acetone) to complex **135a** yielded **135b**, as evidenced by the diagnostic shift and splitting of the NCH_2 resonance in the ^1H NMR spectrum. When NaBPh_4 was used to abstract the chloride ligand from complex **135a**, the observed 1:1 ratio between the BPh_4^- anion and the ligand NMR resonances confirmed the monocationic nature of **135b**. Conversely, complex **135b** was converted to complex **135a** by the addition of brine to an aqueous solution of **135b** followed by extraction with CH_2Cl_2 . This methodology is analogous to the aqueous purification of the reaction mixture (see above), which yielded exclusively complex **135a**. Accordingly, the presence of excess chloride ions induces metallacycle ring opening and the transformation of the chelate ligand in **135b** to a monodentate bonding mode in **135a**. The reversible interconversion of **135a** and **135b** demonstrates that the hydroxy group provides a hemilabile ligand site. Finally, D_2O exchange experiments confirmed the presence of acidic OH groups in both complexes **135a** and **135b** by the disappearance of the ^1H NMR resonances at $\delta_{\text{H}} = 9.46$ and 9.34 , respectively (D_6 -DMSO solutions). These data confirm that the C,O-bidentate ligand in complex **135b** is formally neutral.

Transformation of **135b** to **135a** in aqueous media suggested that the chelating and the non-chelating triazolylidene binding mode may be interconvertible depending on the

polarity of the solvent. NMR spectroscopic investigations of pure complexes **135a** and **135b** revealed no equilibrium in CDCl_3 and CD_2Cl_2 and each complex displayed its own characteristic resonance pattern for the cymene and NCH_2 group (vide supra). In CD_3OD , the aromatic cymene resonances of complex **135a** are relatively broad, while the resolution was unaltered for complex **135b**. The broadening observed in complex **135a** may hint towards an exchange in the ruthenium coordination sphere and competitive MeOH coordination. In D_6 -DMSO, **135a** and **135b** have identical ^1H NMR spectra, indicating the formation of a cationic complex involving either C,O-bidentate triazolylidene chelation as in **135b**, or a Ru-DMSO bond formation by displacement of the chlorido and the chelating-hydroxy ligands of **135a** and **135b**, respectively. Further characterization of this species was prevented by the gradual decomposition of both **135a** and **135b** in DMSO solution, evidenced by the appearance of ^1H resonances corresponding to free *p*-cymene already within the first few min. When dissolved in CDCl_3 , CD_2Cl_2 , or CD_3OD , complexes **135a,b** exhibited better stability and *p*-cymene loss was only observed after extended time periods (ca. 24 h, i.e. when cymene loss was complete in DMSO). For comparative purposes, D_6 -DMSO solutions of a 1,4-dibutyl-triazolylidene ruthenium complex^{15a} as analogue of complexes **135a,b** displayed only ca. 2% free *p*-cymene even 2 days after sample preparation. Cymene loss is presumably promoted by the coordinating nature of the wingtip group, which is also corroborated by instability of related triazolylidene ruthenium(II) complexes containing an imine wingtip group.^{15b}

5.1.3.3. Catalytic transfer hydrogenation

The pendant O-functionalities in complexes **132**, **134** and **135** provide opportunities for cooperative metal-ligand interaction and proton-shuttling, which is particularly beneficial in hydrogen transfer reactions.^{4c,8,24} The catalytic activity of the novel iridium complexes **132-134** was therefore evaluated in transfer hydrogenation using standard reaction conditions, i.e. refluxing i PrOH as the sacrificial hydrogen source, KOH (10 mol% relative to the substrate) and benzophenone as model substrate.²⁵ An initial run with complex **3a** as catalyst precursor at 1 mol% loading produced the product alcohol in a moderate 67% yield after 8 h (Table 5.1.2, entry 1). Increasing the catalysts loading to 2 mol% enhanced the performance and gave quantitative conversions when using the Ofunctionalised iridium complexes **132a** and **132b** (entries 2,3).

Table 5.1.2. Catalytic transfer hydrogenation of benzophenone.

Entry	Cat.	mol%	time (h)/Conv. (%) ^b	time (h)/Conv. (%) ^b	TOF ₅₀ (h ⁻¹) ^c
1	132a	1	2/33	8/67	12
2	132a	2	2/46	8/96	12
3	132b	2	2/48	8/97	12
4	133/133'	2	2/13	8/35	2
5	134a	2	2/26	8/64	4
6	135a	1	0.5/78	1.5/97	210
7	135b	1	0.5/76	1.5/98	200
8	137	1	0.5/95	1.5/98	370

^(a) General reaction conditions: Benzophenone (0.5 mmol or 1.0 mmol), KOH (10 mol%), [Ir] (0.1 mmol), 2-propanol (5 ml), reflux temperature. ^(b) Conversions determined by ¹H NMR spectroscopy using mesitylene as internal standard, averaged 2 runs. ^(c) TOF₅₀ determined at 50% conversion.

A time conversion profile indicated no significant difference in performance of these two complexes (Figure 5.1.2), suggesting that the catalytically active species formed from **132a** and **132b** is identical. In comparison, complex **133** containing an unfunctionalised triazolylidene ligand only achieved 39% conversion within the same reaction time. This substantial reactivity difference emphasizes the beneficial role of the hydroxy functionality. Moreover, it indicates that the functional wingtip group is resistant to base-mediated degradation as observed in the presence of Ag₂O (cf formation of **133** during the metalation process). The presence of an ether functionality as triazolylidene wingtip group as in complex **134a** improves the activity of the iridium centre slightly when compared to the unfunctionalised ligand in **133** (65%, entry 4), though the performance is still significantly lower than in the presence of a hydroxy group. These data suggest that the hydroxyl group plays a distinct role, likely in the formation of a metal-bound alkoxide as an anionic C,O-bidentate chelate.²⁶ Such alkoxide formation increases the electron density at the iridium centre and therefore enhance its catalytic activity in transfer hydrogenation. Alternatively, the alkoxy group may facilitate formal dihydrogen abstraction from ⁱPrOH via an outer sphere mechanism, involving transfer of the hydride to the iridium centre and proton transfer to the ligand oxygen.^{8d,e} In stoichiometric experiments, reaction of **132b** with Cs₂CO₃ as a base indeed revealed formation of a new species with a ¹H resonance pattern distinct

from **132a** and **132b** (e.g. NCH_2 appears as a multiplet at 4.27–4.18 ppm), which has been assigned tentatively to the deprotonated alkoxide species.

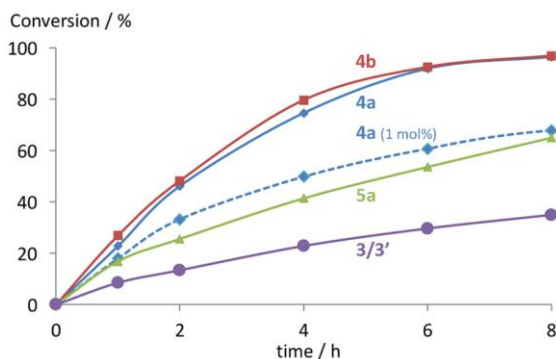


Figure 5.1.2. Time-dependent profile for the catalytic transfer hydrogenation of benzophenone with complexes 3-5 (solid lines: S/C/B ratio 50:1:5, 2 mol% complex; dashed lines: S/C/B ratio 100:1:10, 1 mol% complex).

The ruthenium complexes **135a,b** were considerably more active than their iridium analogues in transfer hydrogenation under otherwise identical conditions and reached full conversion within 1 h when used at 1 mol% loading (Table 5.1.2, entries 6,7). Again, both complexes showed a reactivity profile that is identical within standard errors. The analogous ruthenium complex **137** containing a 1,4-dibutyltriazolylidene ligand^{15a} was evaluated for comparison and reached 92% conversion within 15 min (cf. 51% for complexes **135a** and **135b**) and essentially complete conversion after 30 min (entry 8). The higher activity of complex **137** ($\text{TOF} > 370 \text{ h}^{-1}$ vs about 200 h^{-1} for complexes **135a,b**) indicates no beneficial role of the hydroxy group in the ruthenium system. These data are in agreement with an inner sphere monohydride mechanism,²⁷ in which the critical hydride species is formed via β -hydrogen elimination of metal-coordinated isopropoxide without any participation of ancillary ligands. Previous studies revealed that triazolylidene ruthenium(II) complexes are more active transfer hydrogenation catalysts than their iridium(III) analogues.^{16b,c} Likewise, ruthenium complex **135a** reaches nearly quantitative conversion within 1 h, and is more than an order of magnitude more active than its iridium analogue **132a** which reaches only 18% conversion in the same time ($\text{TOF} 210 \text{ h}^{-1}$ vs 12 h^{-1}). The different role of the hydroxy wingtip group in the iridium and ruthenium complexes suggests a different pathway for dihydrogen transfer from the $i\text{PrOH}$ donor to the catalyst, and due to the microscopic

reversibility, also from the catalyst to the substrate ketone. However, the hydrogen substituent of the triazolylidene in complex **133** may be susceptible to deprotonation thereby deactivating the catalyst. Therefore, it is clear that the catalytic activity of complexes **136/136'** or the iridium analogue of complex **137** is needed to make an unambiguous comparison between working modes of the iridium and ruthenium complexes with O-functionalised triazolylidene ligands, and will be included in future work. Finally, in comparison to other 1,2,3-triazolylidene complexes employed in transfer hydrogenation, the iridium complexes reported here perform only moderately, while the ruthenium complexes are comparable to other carbene-based systems.¹⁶

5.1.4. Conclusion

O-functionalised 1,2,3-triazolylidene iridium(III) and ruthenium(II) complexes were synthesized and applied in transfer hydrogenation. Ether- and hydroxy-substituted 1,2,3-triazolylidene iridium(III) complexes were isolated with the ligand both in mono- and bidentate coordination mode. Also, monodentate and C,O-bidentate, hydroxy-functionalised 1,2,3-triazolylidene ruthenium complexes are described. The monodentate complexes were converted to the chelating species by chloride abstraction and vice versa, the chelates were transformed into monodentate ligands in the presence of excess halide. Transfer hydrogenation studies revealed that pendant hydroxy-donors substantially enhance the catalytic activity of the triazolylidene iridium(III) catalyst while analogous hydroxy-functionalised triazolylidene ruthenium(II) complexes did not outperform analogous unfunctionalised complexes. Generally, activity was much higher for the ruthenium(II) complexes than the iridium(III) homologues, which hints towards diverging activation mechanisms. Caution is therefore required when generalizing beneficial ligand features. Future outlooks include a detailed investigation into the activity of the ruthenium complexes in transfer hydrogenation to conclusively determine the influence of the hydroxygroup. Also, applications in base free oxidations and N-alkylation reactions pose exciting avenues of research to determine the influence of O-functionality in other (de)hydrogenation processes.

5.1.5. Experimental section

5.1.5.1. General information

Ag₂O was used after regeneration by heating >160 °C under vacuum. [Ir(Cp*)Cl₂]₂,²⁸ 1-butyl-4-(CMe₂OH)-triazole,^{18d} **L1H**·BF₄,^{18d} and **137**^{15a} were prepared according to reported procedures. All other reagents were used as received from commercial suppliers. NMR spectra were recorded on Bruker and Varian spectrometers operating at room temperature. Chemical shifts (δ in ppm, coupling constants J in Hz) were referenced to residual solvent resonances and are given downfield from SiMe₄. Elemental analysis and mass spectrometry were carried out by the microanalytical services of University College Dublin and University of Bern.

5.1.5.2. Preparation of triazolium salt **L2H**·BF₄

Under a N₂ atmosphere, 1-butyl-4-(CMe₂OH)-triazole (0.914 g, 5.0 mmol) was dissolved in dry THF (20 mL) and cooled to 0 °C. To this solution, NaH (60% in mineral oil, 0.30 g, 7.5 mmol) was added in 3 portions. The temperature was maintained at 0 °C for 15 min, after which the reaction mixture was allowed to stir at room temperature for 1 h. Iodomethane (0.50 mL, 8.0 mmol) was added to the reaction mixture, which was stirred for a further 1 h. Then H₂O (100 mL) was slowly added and the mixture was stirred for 30 min. The reaction mixture was extracted with Et₂O (3 × 100 mL). The organic fractions were combined and washed with brine (2 × 100 mL), dried with Na₂SO₄, filtered and all volatiles removed under reduced pressure, yielding 1-butyl-4-(CMe₂OMe)-triazole as a pale yellow oil. This intermediate was purified by column chromatography (SiO₂; EtOAc/pentane, 2:1), however the crude form was suitable to be used for the next step. ¹H NMR (400 MHz, CDCl₃): δ = 7.43 (s, 1H, C_{triaz}H), 4.34 (t, ³J_{H-H} = 7.3 Hz, 2H, NCH₂), 3.14 (s, 3H, OCH₃), 1.95–1.83 (m, 2H, NCH₂CH₂), 1.61 (s, 6H, C(CH₃)₂), 1.43–1.30 (m, 2H, CH₂CH₃), 0.96 (t, ³J_{H-H} = 7.4 Hz, 3H, CH₂CH₃). ¹³C{¹H} NMR (101 MHz, CDCl₃): δ = 152.7 (C_{triaz}C), 120.4 (C_{triaz}H), 73.1 (C(CH₃)₂), 50.7 (OCH₃), 50.1 (NCH₂), 32.4 (NCH₂CH₂), 26.7 (C(CH₃)₂), 19.9 (CH₂CH₃), 13.6 (CH₂CH₃). The 1-butyl-4-(CMe₂OMe)-triazole was dissolved in dry CH₂Cl₂ (30 mL). Then Me₃OBF₄ (0.845 g, 5.0 mmol) was added and the suspension stirred for 20 h under a N₂ atmosphere. MeOH (5 mL) was added and stirring continued for 30 min. All volatiles were removed under reduced pressure and the residual brown oil was dissolved in a minimal amount of CH₂Cl₂ and precipitated by addition of

pentane (200 mL). The residue was collected by decantation and dried under reduced pressure. The solid was then dissolved in CH₂Cl₂ (50 mL) and stirred with activated carbon (100–325 mesh, 6 g) for 10 min. The suspension was filtered over Celite, and volatiles removed under reduced pressure. The residue was redissolved in a minimum amount of CH₂Cl₂ and added dropwise to cold Et₂O with vigorous stirring. The white precipitate was collected by decantation and thoroughly dried to yield the title product as a white solid (1.11 g, 74%). ¹H NMR (400 MHz, CDCl₃): δ = 8.60 (s, 1H, C_{uz}H), 4.60 (t, ³J_{H-H} = 7.5 Hz, 2H, NCH₂), 4.36 (s, 3H, NCH₃), 3.20 (s, 3H, OCH₃), 2.07–19.5 (m, 2H, NCH₂CH₂), 1.70 (s, 6H, C(CH₃)₂), 1.48–1.36 (m, 2H, CH₂CH₃), 0.98 (t, ³J_{H-H} = 7.4 Hz, 3H, CH₂CH₃). ¹³C{¹H} (101 MHz, CDCl₃): δ = 146.9 (C_{uz}C), 130.0 (C_{uz}H), 72.8 (C(CH₃)₂), 54.2 (NCH₂), 51.4 (OCH₃), 39.7 (NCH₃), 31.1 (NCH₂CH₂), 25.5 (C(CH₃)₂), 19.6 (CH₂CH₃), 13.4 (CH₂CH₃) HRMS (ESI +): m/z Found 212.1757 [M-BF₄]⁺ (calcd for C₁₁H₂₂N₃O, 212.1763) Anal. Calc. for C₁₁H₂₂BF₄N₃O: C, 44.17; H, 7.41; N, 14.05%. Found: C, 43.74, H, 7.27; N, 13.96%.

5.1.5.3. Preparation of complexes **132a**, **132b**, **133** and **133'**

A suspension of LIH·BF₄ (170 mg, 0.60 mmol), Me₄NCl (66 mg, 0.60 mmol), Ag₂O (280 mg, 1.2 mmol) in CH₂Cl₂/MeCN (1:1 v/v, 10 mL) was stirred protected from light for 16 h. The suspension was filtered through Celite, eluted with CH₂Cl₂ (100 mL), and [Ir(Cp*)Cl₂]₂ (180 mg, 0.23 mmol) added and the reaction mixtures stirred for 5 h protected from light. The reaction mixture was filtered over Celite, eluting with CH₂Cl₂ and the volatiles were removed under reduced pressure to yield the crude reaction mixture. Purification by column chromatography (SiO₂; CH₂Cl₂/MeOH gradient, 20:1 to 5:1) yielded complex **132a** (yellow solid, 120 mg, 43%), **132b** (yellow-brown solid, 58 mg, 20%) and complexes **133** and **133'** (1:1 mixture, hygroscopic yellow solid, 43 mg, 17%).

Complex 132a. ¹H NMR (400 MHz, CD₂Cl₂): δ = 6.21 (b, 1H, OH), 4.93 (b, 1H, NCH₂), 4.09 (s, 4H, NCH₃ and NCH₂), 2.04 (br s, 2H, NCH₂CH₂), 1.64 (s, 6H, C(CH₃)₂), 1.56 (s, 15H, CCpCH₃), 1.50–1.44 (m, 2H, CH₂CH₃), 1.00 (t, ³J_{H-H} = 7.4 Hz, 3H, CH₂CH₃) ¹³C{¹H} NMR (400 MHz, CD₂Cl₂): δ = 152.9 (C_{uz}), 145.5 (C_{uz}), 88.7 (CCp), 69.0 (C(CH₃)₂), 55.2 (NCH₂), 39.7 (NCH₃), 33.4 (NCH₂CH₂), 30.5 (br, C(CH₃)₂), 20.7 (CH₂CH₃), 14.2 (CH₂CH₃), 9.5 (CCpCH₃). HRMS (ESI+): m/z Found 560.2002 [M-Cl]⁺ (calcd for C₂₀H₃₄ON₃ClIr, 560.2014) Anal. Calcd for C₂₀H₃₄N₃Cl₂IrO: C, 40.33; H, 5.75; N, 7.05%; Cl, 40.04; Ir, 5.64; O, 6.95%.

Complex 132b. ^1H NMR (400 MHz, CD_2Cl_2): δ = 4.45 (b, 2H, NCH_2), 4.10 (s, 3H, NCH_3), 3.39 (b, 1H, OH), 2.05–1.93 (m, 2H, NCH_2CH_2), 1.73 (s, 15H, CCpCH_3), 1.65 (s, 6H, $(\text{C}(\text{CH}_3)_2)$), 1.47–1.33 (m, 2H, CH_2CH_3), 0.98 (t, $^3J_{\text{H-H}} = 7.4$ Hz, CH_2CH_3). $^{13}\text{C}\{^1\text{H}\}$ NMR (101 MHz, CD_2Cl_2): δ = 157.2 (C_{IrC}), 154.1 (C–Ir), 89.4 (CCp), 77.6 ($\text{C}(\text{CH}_3)_2$), 54.1 (NCH_2), 37.7 (NCH_3), 32.4 (NCH_2CH_2), 28.7 ($\text{C}(\text{CH}_3)_2$), 20.3 (CH_2CH_3), 13.9 (CH_2CH_3), 10.2 (CCpCH_3). HRMS (ESI+): m/z Found 524.2240 [M-H-Cl-BF_4] $^+$ (cald for $\text{C}_{20}\text{H}_{33}\text{ON}_3\text{Ir}$, 524.2247)

Complex 133. ^1H NMR (400 MHz, CD_2Cl_2): δ = 7.49 (s, ^1H , C_{IrH}), 4.50–4.46 (m, 2H, NCH_2), 4.05 (s, 3H, NCH_3), 2.09–1.98 (m, 2H, NCH_2CH_2), 1.59 or 1.58 (s, 15H, CpCH_3), 1.53–1.42 (m, 2H, CH_2CH_3), 0.99 (t, $^3J_{\text{H-H}} = 7.5$ Hz, 3H, CH_2CH_3). $^{13}\text{C}\{^1\text{H}\}$ NMR (101 MHz, CD_2Cl_2): δ = 148.4 (C_{IrC} –Ir), 134.8 (C_{IrC}), 88.3 (CCp), 53.7 (NCH_2), 38.8 (NCH_3), 31.9 (NCH_2CH_2), 20.2 (CH_2CH_3), 13.7 (CH_2CH_3), 9.13 or 9.12 (CCpCH_3).

Complex 133'. ^1H NMR (400 MHz, CD_2Cl_2): δ = 7.51 (s, 1H, C_{IrH}), 4.29 (t, 2H, $^3J_{\text{H-H}} = 7.3$ Hz, NCH_2), 4.25 (s, 3H, NCH_3), 2.09–1.98 (m, 2H, NCH_2CH_2), 1.59 or 1.58 ($2 \times$ s, 15H, CpCH_3), 1.42–1.30 (m, 2H, CH_2CH_3), 0.97 (t, $^3J_{\text{H-H}} = 7.4$ Hz, 3H, CH_2CH_3). $^{13}\text{C}\{^1\text{H}\}$ NMR (101 MHz, CD_2Cl_2): δ = 147.9 (C_{IrC} –Ir), 134.1 (C_{IrC}), 88.3 (CCp), 52.4 (NCH_2), 40.3 (NCH_3), 33.2 (NCH_2CH_2), 20.7 (CH_2CH_3), 14.2 (CH_2CH_3), 9.13 or 9.12 (CCpCH_3) HRMS (ESI+): m/z Found 502.1580 [M-Cl] $^+$ (cald for $\text{C}_{17}\text{H}_{28}\text{N}_3\text{ClIr}$, 502.1596).

5.1.5.4. Preparation of complexes 134a and 134b

A suspension of L2H-BF_4 (150 mg, 0.50 mmol), Me_4NCl (55 mg, 0.50 mmol), Ag_2O (233 mg, 1.0 mmol) in MeCN (10 mL) was stirred protected from light for 24 h. The suspension was then filtered through Celite, and the volatiles removed under reduced pressure. The residue was suspended in CH_2Cl_2 (20 mL) and $[\text{Ir}(\text{Cp}^*)\text{Cl}_2]_2$ (150 mg, 0.19 mmol) was added. The reaction mixture was stirred for 5 h protected from light, then filtered over Celite, and all volatiles were removed under reduced pressure to yield the crude products. Purification by column chromatography (SiO_2 ; $\text{CH}_2\text{Cl}_2/\text{MeOH}$ gradient, 20:1 to 10:1) yielded product **134a** (100 mg, 42%) and **134b** (62 mg, 23%) as orange solids.

Complex 134a. ^1H NMR (400 MHz, CD_2Cl_2): δ = 5.01–4.84 (m, 1H, NCH_2), 4.19 (s, 3H, NCH_3), 4.15–4.01 (m, 1H, NCH_2), 3.06 (s, 3H, OCH_3), 2.13–1.96 (m, 2H, NCH_2CH_2), 2.04 (s, 3H, $\text{C}(\text{CH}_3)_2$), 1.76 (s, 3H, $\text{C}(\text{CH}_3)_2$), 1.66–1.39 (m, 2H, CH_2CH_3),

1.53 (s, 15 H, C CpCH₃) 1.01 (t, 3H, CH₂CH₃). ¹³C{¹H} NMR (101 MHz, CD₂Cl₂): δ = 150.2 (C_{trz}C), 144.7 (C_{trz}-Ir), 88.4 (CCp), 76.5 (C(CH₃)₂), 56.1 (NCH₂), 50.0 (OCH₃), 41.0 (NCH₃), 33.6 (NCH₂CH₂), 28.6, 25.3 (C(CH₃)₂), 20.8 (CH₂CH₃), 14.3 (CH₂CH₃), 9.70 (CCpCH₃) HRMS (ESI+): m/z Found 574.2161 [M-Cl]⁺ (cald for C₂₁H₃₆ON₃ClIr, 574.2171). Anal. Calcd for C₂₁H₂₆N₃Cl₂IrO: C, 41.37; H, 5.95; N, 6.89%; C, 41.43; H, 5.95; N, 6.74%.

Complex 134b. ¹H NMR (400 MHz, CD₂Cl₂): δ = 4.57–4.49, 4.37–4.27 (2 × m, 1H, NCH₂), 4.13 (s, 3H, NCH₃), 3.70 (s, 3H, OCH₃), 2.02–1.85 (m, 2H, NCH₂CH₂), 1.67 (s, 15H, CCpCH₃), 1.61, 1.60 (2 × s, 3H, C(CH₃)₂), 1.41–1.30 (m, 2H, CH₂CH₃), 0.95 (t, ³J_{H-H} = 7.4 Hz, 3H, CH₂CH₃). ¹³C{¹H} NMR (101 MHz, CD₂Cl₂): δ = 153.0 (C_{trz}-Ir), 151.5 (C_{trz}C), 89.9 (CCp), 81.5 (C(CH₃)₂), 54.8 (OCH₃), 54.3 (NCH₂), 38.3 (NCH₃), 32.3 (NCH₂CH₂), 25.2, 24.6 (2 × C(CH₃)₂), 20.2 (CH₂CH₃), 13.9 (CH₂CH₃), 10.2 (CCpCH₃) HRMS (ESI+): m/z Found 574.2158 [M-BF₄]⁺ (cald for C₂₁H₃₆ON₃ClIr, 574.2171).

5.1.5.5. Preparation of complexes 135a, 135b, 136 and 136'

A suspension of L1H·BF₄ (170 mg, 0.60 mmol), Me₄NCl (66 mg, 0.60 mmol), Ag₂O (280 mg, 1.2 mmol) in CH₂Cl₂/MeCN (1:1 v/v, 10 mL) was stirred protected from light for 16 h. The suspension was filtered through Celite, eluted with CH₂Cl₂ (100 mL), and [Ru(p-cymene)Cl₂]₂ (110 mg, 0.18 mmol) added. The reaction mixture was stirred for 2 h protected from light, filtered over Celite, evaporated to dryness under reduced pressure. The crude reaction mixture was purified by column chromatography (SiO₂; CH₂Cl₂/MeOH gradient, 20:1 to 5:1), which yielded complex **135a** (50 mg, 28%) and complex **135b** (57 mg, 28%) both as a red-brown, hygroscopic solids, and complexes **136** and **136'** in a 1:1 mixture as a brown, hygroscopic solid (22.5 mg, 14%). Alternately complex **135a** was isolated selectively by applying an alternative purification procedure. The crude reaction mixture was suspended in CH₂Cl₂ (100 mL) and extracted with H₂O (100 mL). CH₂Cl₂ (100 mL) was added to the aqueous phase followed by brine (200 mL) and the mixture extracted. The organic phase was dried over Na₂SO₄, filtered and the volatiles were removed under reduced pressure. Residual [Ru(p-cymene)Cl₂]₂ was removed from this residue by washing a CH₂Cl₂ (100 mL) solution of the product with copious amounts of saturated NH₄Cl_{aq} until the aqueous phase was colourless. The crude product was purified by column chromatography

(SiO₂; CH₂Cl₂/MeOH, 10:1-5:1 gradient), yielding **135a** as a red-brown, hygroscopic solid (104 mg, 57%).

Complex 135a. ¹H NMR (400 MHz, CD₂Cl₂): δ = 5.82, 5.73, 5.68, 5.18 (4 × br s, 1H, H_{cym}), 4.56 (t, ³J_{H-H} = 7.4 Hz, NCH₂), 3.97 (s, 3H, NCH₃), 2.81–2.66 (m, 1H, CHMe₂), 2.14 (s, 3H, C_{cym}CH₃), 2.11–1.99 (m, 2H, NCH₂CH₂), 1.62, 1.54 (2 × br s, 3H, C(CH₃)₂), 1.52–1.38 (m, 2H, CH₂CH₃), 1.17 (d, ³J_{H-H} = 6.7 Hz, 6H, CH(CH₃)₂), 1.01 (t, ³J_{H-H} = 7.4 Hz, CH₂CH₃). ¹³C{¹H} NMR (101 MHz, CD₂Cl₂): δ = 164.8 (C_{trz}-Ru), 152.3 (C_{trz}C), 104.5 (C_{cym}CH), 100.7 (C_{cym}CH₃), 86.5, 82.0, 79.0 (4 × C_{cym}H), 76.1 (C(CH₃)₂), 54.3 (NCH₂), 37.1 (NCH₃), 32.3 (NCH₂CH₂), 31.5 (CHMe₂), 29.3, 28.9 (2 × C(CH₃)₂), 23.3, 22.3 (2 × CH(CH₃)₂), 20.5 (CH₂CH₃), 19.3 (C_{cym}CH₃), 13.9 (CH₂CH₃). HRMS(ESI⁺): m/z Found 468.1342 [M-Cl]⁺ (calcd. for C₂₀H₃₃ON₃ClRu, 468.1350) Anal. Calcd for C₂₀H₃₃N₃Cl₂ORu C, 47.71; H, 6.61; N, 8.35%; C, 48.37; H, 6.18; N, 8.35%.

Complex 135b. ¹H NMR (400 MHz, CD₂Cl₂): δ = 5.85–5.79 (m, 2H, H_{cym}), 5.49 (d, ³J_{H-H} = 6.0 Hz, 1H, H_{cym}), 5.18 (d, ³J_{H-H} = 5.9 Hz, 1H, H_{cym}), 4.68–4.52 (m, 2H, NCH₂), 4.01 (s, 3H, NCH₃), 2.79–2.64 (m, 1H, CHMe₂), 2.16 (s, 3H, C_{cym}CH₃), 2.09–1.96 (m, 2H, NCH₂CH₂), 1.58 (s, 6H, C(CH₃)₂), 1.51–1.36 (m, 2H, CH₂CH₃), 1.21 (d, ³J_{H-H} = 6.6 Hz, 6H, CH(CH₃)₂), 1.01 (t, ³J_{H-H} = 7.3 Hz, 3H, CH₂CH₃). ¹³C{¹H} NMR (101 MHz, CD₂Cl₂): δ = 163.9 (C_{trz}-Ru), 149.0 (C_{trz}C), 106.4 (C_{cym}CH₃), 100.8 (C_{cym}CH), 86.3, 82.0, 80.5, 79.0 (4 × C_{cym}H), 77.5 (C(CH₃)₂), 54.6 (NCH₂), 37.5 (NCH₃), 32.2 (NCH₂CH₂), 31.7 (CHMe₂), 28.5, 28.3 (2 × C(CH₃)₂), 23.1, 22.2 (2 × CH(CH₃)₂), 20.5 (CH₂CH₃), 19.3 (C_{cym}CH₃), 13.9 (CH₂CH₃) HRMS (ESI⁺): m/z Found 468.1342 [M-BF₄]⁺ (calcd. for C₂₀H₃₃ON₃ClRu, 468.1350).

Complex 136. ¹H NMR (400 MHz, CD₂Cl₂): δ = 7.63 (s, 1H, C_{trz}H), 5.28 (d, ³J_{H-H} = 5.9 Hz, 2H, H_{cym}), 5.14 (d, ³J_{H-H} = 5.8 Hz, 2H, H_{cym}), 4.32–4.24 (m, 5H, NCH₃ and NCH₂), 2.65 (hept, ³J_{H-H} = 6.9 Hz, 1H, CHMe₂), 2.09 (s, 3H, C_{cym}CH₃), 1.96–1.86 (m, 2H, NCH₂CH₂), 1.45–1.31 (m, 2H, CH₂CH₃), 1.19 (d, ³J_{H-H} = 6.9 Hz, 6H, CH(CH₃)₂), 0.97 (t, 3H, ³J_{H-H} = 7.4 Hz, CH₂CH₃). ¹³C{¹H} NMR (101 MHz, CD₂Cl₂): δ = 166.0 (C_{trz}-Ru), 133.8 (C_{trz}H), 104.1 (C_{cym}CH), 100.7 (C_{cym}CH₃), 84.8, 84.3 (2 × C_{cym}H), 52.3 (NCH₂), 41.0 (NCH₃), 31.9 (NCH₂CH₂), 31.3 (CHMe₂), 22.6 (CH(CH₃)), 20.2 (CH₂CH₃), 18.7 (C_{cym}CH₃), 13.7 (CH₂CH₃).

Complex 136'. ¹H NMR (400 MHz, CD₂Cl₂): δ = 7.59 (s, 1H, C_{trz}H), 5.27 (d, ³J_{H-H} = 5.9 Hz, 2H, H_{cym}), 5.12 (d, ³J_{H-H} = 6.1 Hz, 2H, H_{cym}), 4.58–4.49 (m, 2H, NCH₂), 4.04 (s, 3H, NCH₃), 2.76–2.66 (m, 1H, CHMe₂), 2.08 (s, 3H, C_{cym}CH₃), 2.07–1.96 (m, 2H,

NCH₂CH₂), 1.55–1.44 (m, 2H, CH₂CH₃), 1.20 (d, ³J_{H-H} = 7.0 Hz, 6H, CH(CH₃)₂), 1.01 (t, ³J_{H-H} = 7.4 Hz, 3H, CH₂CH₃). ¹³C{¹H} NMR (101 MHz, CD₂Cl₂): δ = 166.4 (C_{trz}-Ru), 134.5 (C_{trz}H), 104.3 (C_{cym}CH), 99.6 (C_{cym}CH₃), 84.9, 84.5 (2 × C_{cym}H), 52.3 (NCH₂), 38.8 (NCH₃), 33.8 (NCH₂CH₂), 31.2 (CHMe₂), 22.6 (CH(CH₃)₂), 20.7 (CH₂CH₃), 18.7 (C_{cym}CH₃), 14.2 (CH₂CH₃) HRMS (ESI+): m/z Found 410.0929 [M-Cl]⁺ (calcd for C₁₇H₂₇N₃ClRu, 410.0932) Anal. Calcd for C₁₇H₂₇N₃Cl₂Ru: C, 45.84; H, 6.11; N, 9.43%; C, 45.85; H, 6.09; N, 9.03%.

5.1.5.6. Chelation of monodentate ligand

AgBF₄ as Chlorido Scavenging Agent. To a solution of the corresponding metal complex (1 equiv) in CH₂Cl₂ (2 mL) was added AgBF₄ (1 equiv) followed by CH₂Cl₂ (3 mL). The reaction mixture was stirred for 15 min while protected from light, filtered over Celite and the volatiles were removed under reduced pressure. Further purification included gradient column chromatography (SiO₂; CH₂Cl₂ to MeOH). Alternatively, a solution of the metal complex (1 equiv) in acetone (2 mL) was treated with NaBF₄ or NaBPh₄ (1 equiv) in acetone (3 mL). The reaction mixture was stirred for 18 h, all volatiles were removed under reduced pressure, and the residue was suspended in CH₂Cl₂ and filtered over Celite. All volatiles were removed under reduced pressure and the residue purified by gradient column chromatography (SiO₂; CH₂Cl₂ to MeOH).

5.1.5.7. General procedure for catalytic transfer hydrogenation

In a one-necked round bottom flask metal complex (1.0 mmol), 2-propanol (5 mL) and mesitylene (0.36 mmol or 0.72 mmol) were mixed and KOH (2.0 M, 0.05 mmol or 0.1 mmol, 10 mol% relative to substrate) added and the mixture heated to a vigorous reflux for 10 minutes. Benzophenone (0.5 mmol or 1.0 mmol) was added, and aliquots (0.1 mL) were taken and directly dissolved in CDCl₃ (0.7 mL) and analysed by ¹H NMR spectroscopy, using mesitylene as internal standard.

5.1.5.8. Crystal structure determination

Crystal data of **132a**, **132b**, and **134a** were collected on a *Oxford Diffraction SuperNova* area-detector diffractometer using mirror optics monochromated Mo K α radiation ($\lambda = 0.71073 \text{ \AA}$) and Al filtered. Data reduction was performed using the *CrysAlisPro* program.²⁹ The intensities were corrected for Lorentz and polarization

effects, and an absorption correction based on the multi-scan method using SCALE3 ABSPACK in *CrysAlisPro*²⁹ was applied. The structure was solved by direct methods using *SHELXT*,³⁰ which revealed the positions of all nonhydrogen atoms of the title compound. The non-hydrogen atoms were refined anisotropically. All H atoms were placed in geometrically calculated positions and refined using a riding model. Refinement of the structure was carried out on F^2 using full-matrix least-squares procedures, which minimized the function $\Sigma w(F_o^2 - F_c^2)^2$. The weighting scheme was based on counting statistics and included a factor to downweight the intense reflections. All calculations were performed using the *SHELXL-2014/7* program.³¹ Crystallographic data for the structures of all compounds reported in this paper have been deposited with the Cambridge Crystallographic Data Centre (CCDC) as supplementary publication numbers 1537332 (**132a**), 1537334 (**132b**), and 1537333 (**134a**).

5.1.6. References

1. (a) Morales-Morales, D.; Jensen C.M. (Eds.), *The Chemistry of Pincer Compounds*, Elsevier, Amsterdam, 2007. (b) van Koten, G.; Milstein D. (Eds.), *Organometallic Pincer Chemistry*, Springer, 2013. (c) Szabo, K. J.; Wendt O. F. (Eds.), *Pincer and Pincer-type Complexes: Applications in Organic Synthesis and Catalysis*, Wiley-VCH, 2014. (d) Van Koten, G.; Gossage R. A. (Eds.), *The Privileged Pincer-Metal Platform: Coordination Chemistry & Applications*, Springer, 2017. (e) Albrecht, M. Van Koten, G. *Angew. Chem. Int. Ed.* 2001, 40, 3750. (f) Van der Boom, M.E.; Milstein, D. *Chem. Rev.* **2003**, 103, 1759.
2. (a) Van Koten, G.; Timmer, K.; Noltes, J. G.; Spek, A. L.; *J. Chem. Soc., Chem. Commun.* **1978**, 250. (b) Van Koten, G.; Jastrzebski, J. T. B. H.; Noltes, J. G.; Spek, A. L.; Schoone, J. C. *J. Organomet. Chem.* **1978**, 148, 233.
3. (a) Diez-Gonzalez, S. (Ed.), *N-Heterocyclic Carbenes – From Laboratory Curiosities to Efficient Synthetic Tools*, RSC Catalysis Series No 27, Cambridge, 2017. (b) Cazin, C. S. J. (Ed.), *N-Heterocyclic Carbenes in Transition Metal Catalysis and Organocatalysis*, Springer, 2011. (c) Melaimi, M.; Soleilhavoup, M.; Bertrand, G.; *Angew. Chem. Int. Ed. Engl.* **2010**, 49, 8810. (d) Diez-Gonzalez, S.; Marion, N.; Nolan, S.P. *Chem. Rev.* **2009**, 109, 3612. (e) Liddle, S. T.; Edworthy, I. S.; Arnold, P. L. *Chem. Soc. Rev.* **2007**, 36, 1732. (f) Hopkinson, M. N.; Richter, C.; Schedler, M.; Glorius, F. *Nature* **2014**, 510, 485. (g) Poyatos, M.; Mata, J.A.; Peris, E.; *Chem. Rev.* **2009**, 109,

3677. (h) Schuster, O.; Yang, L.; Raubenheimer, H.G.; Albrecht, M. *Chem. Rev.* **2009**, 109, 3445.
4. (a) Kühn, O. *Chem. Soc. Rev.* **2007**, 36, 592. (b) Normand, A. T.; Cavell, K. J.; *Eur. J. Inorg. Chem.* **2008**, 2781. (c) Ramasamy, B.; Ghosh, P. *Eur. J. Inorg. Chem.* **2016**, 1448. (d) Hameury, S.; de Frémont, P.; Braunstein, P. *Chem. Soc. Rev.* **2017**, 46, 632. (e) Peris, E. *Chem. Rev.* **2017**, acs.chemrev.6b00695.
5. (a) Shvo, Y.; Czarkie, D.; Rahamim, Y.; Chodosh, D. F. *J. Am. Chem. Soc.* **1986**, 108, 7400. (b) Conley, B. L.; Pennington-Boggio, M. K.; Boz, E.; Williams, T. J. *Chem. Rev.* **2010**, 110, 2294.
6. (a) Noyori, R.; Yamakawa, M.; Hashiguchi, S. *J. Org. Chem.* **2001**, 66, 7931. (b) Ohkuma, T.; Utsumi, N.; Tsutsumi, K.; Murata, K.; Sandoval, C.; Noyori, R. *J. Am. Chem. Soc.* **2006**, 128, 8724.
7. (a) Zweifel, T.; Naubron, J. V.; Grützmacher, H. *Angew. Chem. Int. Ed.* **2009**, 48, 559. (b) Gunanathan, C.; Milstein, D. *Acc. Chem. Res.* **2011**, 44, 588. (c) Grotjahn, D. B. *Chem. Eur. J.* **2005**, 11, 7146.
8. (a) García, N.; Jaseer, E. A.; Munarriz, J.; Sanz Miguel, P. J.; Polo, V.; Iglesias, M.; Oro, L. A. *Eur. J. Inorg. Chem.* **2015**, 4388. (b) Saha, B.; Wahidur Rahaman, S. M.; Daw, P.; Sengupta, G.; Bera, J. K. *Chem. Eur. J.* **2014**, 20, 6542. (c) MacNair, A. J.; Millet, C. R. P.; Nichol, G. S.; Ironmonger, A.; Thomas, S. P. *ACS Catal.* **2016**, 6, 7217. (d) Bartoszewicz, A.; Marcos, R.; Sahoo, S.; Inge, A. K.; Zou, X.; Martín-Matute, B. *Chem. Eur. J.* **2012**, 18, 14510. (e) Bartoszewicz, A.; González Miera, G.; Marcos, R.; Norrby, P. -O.; Martín-Matute, B. *ACS Catal.* **2015**, 5, 3704. (f) Türkmen, H.; Pape, T.; Hahn, F. E.; Çetinkaya, B. *Eur. J. Inorg. Chem.* **2008**, 5418. (g) Jiménez, M.V.; Fernández-Tornos, J.; Modrego, F. J.; Pérez-Torrente, J. J.; Oro, L. A. *Chem. Eur. J.* **2015**, 21, 17877. (h) Jacques, B.; Hueber, D.; Hameury, S.; Braunstein, P.; Pale, P.; Blanc, A.; de Frémont, P. *Organometallics* **2014**, 33, 2326. (i) Jacques, B.; Hueber, D.; Hameury, S.; Braunstein, P.; Pale, P.; Blanc, A.; de Frémont, P. *Organometallics* **2014**, 33, 2326. (j) Peñafiel, I.; Pastor, I. M.; Yus, M.; Esteruelas, M. A.; Oliván, M. *Organometallics* **2012**, 31, 6154. (k) Wylie, W. N. O.; Lough, A. J.; Morris, R. H. *Organometallics* **2013**, 32, 3808. (l) Wylie, W. N. O.; Morris, R. H. *ACS Catal.* **2013**, 3, 32. (m) Strydom, I.; Guisado-Barrios, G.; Fernández, I.; Liles, D.C.; Peris, E.; Bezuidenhout, D. I. *Chem. Eur. J.* **2017**, 23, 1393. (n) Samantaray, M. K.; Shaikh, M. M.; Ghosh, P. *Organometallics* **2009**, 28, 2267.

9. (a) Mathew, P.; Neels, A.; Albrecht, M. *J. Am. Chem. Soc.* **2008**, 130, 13534. (b) Guisado-Barrios, G.; Bouffard, J.; Donnadiou, B.; Bertrand, G. *Angew. Chem. Int. Ed.* **2010**, 49, 4759. (c) Crowley, J. D.; Lee, A. -L.; Kilpin, K. J.; *Aust. J. Chem.* **2011**, 64, 1118. (d) Donnelly, K. F.; Petronilho, A.; Albrecht, M. *Chem. Commun.* **2013**, 49, 1145. (e) Schweinfruth, D.; Hettmanczyk, L.; Suntrup, L.; Sakar, B. *Z. Anorg. Allg. Chem.* In press (doi:10.1002/zaac.20170030).
10. (a) Bock, V. D.; Hiemstra, H.; Van Maarseveen, J. H.; *European J. Org. Chem.* **2006**, 51. (b) Meldal, M.; Tomoe, C. W. *Chem. Rev.* **2008**, 108, 2952. (c) Kolb, H. C.; Finn, M. G.; Sharpless, K. B. *Angew. Chem. Int. Ed.* **2001**, 40, 2004. (d) Schulze, B.; Schubert, U. S. *Chem. Soc. Rev.* **2014**, 43, 2522.
11. (a) Crabtree, R. H. *Coord. Chem. Rev.* **2013**, 257, 755. (b) Albrecht, M. *Adv. Organomet. Chem.* **2014**, 62, 111.
12. (a) Cesari, C.; Mazzoni, R.; Müller-Bunz, H.; Albrecht, M. *J. Organomet. Chem.* **2015**, 793, 256. (b) Petronilho, A.; Llobet, A.; Albrecht, M. *Inorg. Chem.* **2014**, 53, 12896. (c) Leigh, V.; Ghattas, W.; Lalrempuia, R.; Müller-Bunz, H.; Pryce, M. T.; Albrecht, M. *Inorg. Chem.* **2013**, 52, 5395.
13. (a) Inomata, S.; Hiroki, H.; Terashima, T.; Ogata, K.; Fukuzawa, S. I. *Tetrahedron* **2011**, 67, 7263. (b) Karthikeyan, T.; Sankararaman, S. *Tetrahedron Lett.* **2009**, 50, 5834. (c) Canseco-Gonzalez, D.; Gniewek, A.; Szulmanowicz, M.; Müller-Bunz, H.; Trzeciak, A.M.; Albrecht, M. *Chem. Eur. J.* **2012**, 18, 6055. (d) Keske, E. C.; Zenkina, O. V.; Wang, R.; Crudden, C. M. *Organometallics* **2012**, 31, 6215. (e) Mitsui, T.; Sugihara, M.; Tokoro, Y.; Fukuzawa, S. I. *Tetrahedron* **2015**, 71, 1509. (f) Modak, S.; Gangwar, M. K.; Nageswar Rao, M.; Madasu, M.; Kalita, A. C.; Dorcet, V.; Shejale, M. A.; Butcher, R. J.; Ghosh, P. *Dalton Trans.* **2015**, 44, 17617. (g) Mendoza-Espinosa, D.; González-Olvera, R.; Negrón-Silva, G.E.; Angeles-Beltrán, D.; Suárez-Castillo, O.R.; Álvarez-Hernández, A.; Santillan, R. *Organometallics* **2015**, 34, 4529.
14. (a) Bernet, L.; Lalrempuia, R.; Ghattas, W.; Mueller-Bunz, H.; Vigara, L.; Llobet, A.; Albrecht, M. *Chem. Commun.* **2011**, 47, 8058. (b) Petronilho, A.; Rahman, M.; Woods, J. A.; Al-Sayyed, H.; Müller-Bunz, H.; Don MacElroy, J. M.; Bernhard, S.; Albrecht, M. *Dalton Trans.* **2012**, 41, 13074. (c) Woods, J. A.; Lalrempuia, R.; Petronilho, A.; McDaniel, N. D.; Müller-Bunz, H.; Albrecht, M.; Bernhard, S. *Energy Environ. Sci.* **2014**, 7, 2316. (d) Lalrempuia, R.; McDaniel, N. D.; Müller-Bunz, H.; Bernhard, S.; Albrecht, M. *Angew. Chem. Int. Ed.* **2010**, 49, 9765. (e) Corbucci, I.; Petronilho, A.; Müller-Bunz, H.; Rocchigiani, L.; Albrecht, M.; Macchioni, A. *ACS*

Catal. **2015**, *5*, 2714. (f) Petronilho, A.; Woods, J. A.; Muller. Bunz, H.; Bernhard, S.; Albrecht, M. *Chem. Eur. J.* **2014**, *20*, 15775.

15. (a) Prades, A.; Peris, E.; Albrecht, M. *Organometallics* **2011**, *30*, 1162. (b) Bolje, A.; Hohloch, S.; Urankar, D.; Pevec, A.; Gazvoda, M.; Sarkar, B.; Košmrlj, J. *Organometallics* **2014**, *33*, 2588. (c) Delgado-Rebollo, M.; Canseco-Gonzalez, D.; Hollering, M.; Mueller-Bunz, H.; Albrecht, M. *Dalton Trans.* **2014**, *43*, 4462. (d) Hohloch, S.; Hettmanczyk, L.; Sarkar, B. *Eur. J. Inorg. Chem.* **2014**, *2014*, 3164. (e) Bagh, B.; McKinty, A. M.; Lough, A. J.; Stephan, D.W. *Dalton Trans.* **2014**, *43*, 12842. (f) Donnelly, K. F.; Segarra, C.; Shao, L. -X.; Suen, R.; Müller-Bunz, H.; Albrecht, M. *Organometallics* **2015**, *34*, 4076. (g) Sabater, S.; Müller-Bunz, H.; Albrecht, M. *Organometallics* **2016**, *35*, 256. (h) Valencia, M.; Müller-Bunz, H.; Gossage, R. A.; Albrecht, M. *Chem. Commun.* **2016**, *52*, 3344. (i) Canseco-Gonzalez, D.; Albrecht, M. *Dalton Trans.* **2013**, *42*, 7424.

16. (a) Sluijter, S. N.; Elsevier, C. J. *Organometallics* **2014**, *33*, 6389. (b) Bolje, A.; Hohloch, S.; Van der Meer, M.; Košmrlj, J.; Sarkar, B. *Chem. Eur. J.* **2015**, *21*, 6756. (c) Bolje, A.; Hohloch, S.; Košmrlj, J.; Sarkar, B.; *Dalton Trans.* **2016**, *45*, 15983. (d) Hollering, M.; Albrecht, M.; Kühn, F. E. *Organometallics* **2016**, *35*, 2980. (e) Maity, R.; Hohloch, S.; Su, C.-Y.; Van der Meer, M.; Sarkar, B. *Chem. Eur. J.* **2014**, *20*, 9952. (f) Maity, R.; Mekić, A.; Van der Meer, M.; Verma, A.; Sarkar, B. *Chem. Commun.* **2015**, *51*, 15106.

17. For some examples, see. (a) Saravanakumar, R.; Ramkumar, V.; Sankararaman, S. *J. Organomet. Chem.* **2013**, *736*, 36. (b) Modak, S.; Gangwar, M. K.; Nageswar Rao, M.; Madasu, M.; Kalita, A. C.; Dorcet, V.; Shejale, M. A.; Butcher, R. J.; Ghosh, P. *Dalton Trans.* **2015**, *44*, 17617.

18. (a) Mendoza-Espinosa, D.; González-Olvera, R.; Osornio, C.; Negrón-Silva, G. E.; Santillan, R. *New J. Chem.* **2015**, *39*, 1587. (b) Wei, Y.; Liu, S. -X.; Mueller-Bunz, H.; Albrecht, M. *ACS Catal.* **2016**, *6*, 8192. (c) Mendoza-Espinosa, D.; González-Olvera, R.; Osornio, C.; Negrón-Silva, G. E.; Álvarez-Hernández, A.; Bautista-Hernández, C. I.; Suárez-Castillo, O. R. *J. Organomet. Chem.* **2016**, *803*, 142. (d) Pretorius, R.; Fructos, M. R.; Müller-Bunz, H.; Gossage, R. A.; Pérez, P. J.; Albrecht, M. *Dalton Trans.* **2016**, *45*, 14591. (e) Mendoza-Espinosa, D.; Rendón-Nava, D.; Alvarez-Hernández, A.; Angeles-Beltrán, D.; Negrón-Silva, G. E.; Suárez-Castillo, O. R. *Chem. Asian J.* **2017**, *12*, 203.

19. (a) Petronilho, A.; Woods, J. A.; Mueller-Bunz, H.; Bernhard, S.; Albrecht, M. *Chem. Eur. J.* **2014**, *20*, 15775. (b) Petronilho, A.; Woods, J. A.; Bernhard, S.; Albrecht, M. *Eur. J. Inorg. Chem.* **2014**, 708. (c) Maity, R.; Van der Meer, M.; Hohloch, S.; Sarkar, B. *Organometallics* **2015**, *34*, 3090. (d) Farrell, K.; Müller-Bunz, H.; Albrecht, M. *Dalton Trans.* **2016**, *45*, 15859. (e) Hohloch, S.; Kaiser, S.; Duecker, F. L.; Bolje, A.; Maity, R.; Košmrlj, J.; Sarkar, B. *Dalton Trans.* **2015**, *44*, 686. (f) Donnelly, K. F.; Lalrempuia, R.; Müller-Bunz, H.; Clot, E.; Albrecht, M. *Organometallics* **2015**, *34*, 858. (g) Maity, R.; Tichter, T.; Van der Meer, M.; Sarkar, B.; *Dalton Trans.* **2015**, *44*, 18311. (h) Baschieri, A.; Monti, F.; Matteucci, E.; Mazzanti, A.; Barbieri, A.; Armaroli, N.; Sambri, L. *Inorg. Chem.* **2016**, *55*, 7912.
20. Of note, the ^1H and ^{13}C NMR resonances for complex **132a** and **132b** displayed natural peak broadening when compared to complexes **133/133'** and **134a,b**. This broadening was especially evident for **132a**, for which high concentrations (ca. 60 mg in 0.7 mL CD_2Cl_2) were required to identify the chemical shifts the quaternary carbons in ^{13}C NMR spectroscopy (extended relaxation times ($t_1 = 10$ sec.) and scan numbers (5000) did not improve the quality of the spectra, albeit at lower concentrations ca. 15 mg).
21. Steiner, T. *Angew. Chem. Int. Ed.* **2002**, *41*, 48.
22. (a) Albrecht, M.; Miecznikowski, J. R.; Samuel, A.; Faller, J. W.; Crabtree, R. H.; *Organometallics* **2002**, *21*, 3596. (b) Feng, Y.; Jiang, B.; Boyle, P. A.; Ison, E. A.; *Organometallics* **2010**, *29*, 2857. (c) Iglesias, M.; Pérez-Nicolás, M.; Miguel, P. J. S.; Polo, V.; Fernández-Alvarez, F. J.; Pérez-Torrente, J. J.; Oro, L. A. *Chem. Commun.* **2012**, *48*, 9480. (d) Aliaga-Lavrijsen, M.; Iglesias, M.; Cebollada, A.; Garcés, K.; García, N.; Sanz Miguel, P. J.; Fernández-Alvarez, F. J.; Pérez-Torrente, J. J.; Oro, L. A. *Organometallics* **2015**, *34*, 2378. (e) Zhu, X. H.; Cai, L. H.; Wang, C. X.; Wang, Y. N.; Guo, X. Q.; Hou, X. F. *J. Mol. Catal. A Chem.* **2014**, *393*, 134.
23. (a) Ogata, K.; Inomata, S.; Fukuzawa, S. *Dalton Trans.* **2013**, *42*, 2362. (b) Bagh, B.; Stephan, D. W. *Dalton Trans.* **2014**, *43*, 15638. (c) Suntrup, L.; Hohloch, S.; Sarkar, B. *Chem. Eur. J.* **2016**, *22*, 18009.
24. (a) Jiménez, M. V.; Fernández-Tornos, J.; Pérez-Torrente, J. J.; Modrego, F. J.; Winterle, S.; Cunchillos, C.; Lahoz, F. J.; Oro, L. A. *Organometallics* **2011**, *30*, 5493. (b) Musa, S.; Shaposhnikov, I.; Cohen, S.; Gelman, D. *Angew. Chem. Int. Ed.* **2011**, *50*, 3533. (c) Musa, S.; Fronton, S.; Vaccaro, L.; Gelman, D. *Organometallics* **2013**, *32*, 3069. (d) Silantyev, G. A.; Filippov, O. A.; Musa, S.; Gelman, D.; Belkova, N. V.;

- Weisz, K.; Epstein, L.M.; Shubina, E.S. *Organometallics* **2014**, 33, 5964. (e)
- Khusnutdinova, J. R.; Milstein, D. *Angew. Chem. Int. Ed.* **2015**, 54, 12236.
25. (a) Wang, D.; Astruc, D. *Chem. Rev.* **2015**, 115, 6621. (b) Zassinovich, G.; Mestroni, G.; Gladiali, S. *Chem. Rev.* **1992**, 92, 1051.
26. Samec, J. S. M.; Bäckvall, J. -E.; Andersson, P. G.; Brandt, P. *Chem. Soc. Rev.* **2006**, 35, 237.
27. (a) Clapham, S. E.; Hadzovic, A.; Morris, R. H. *Coord. Chem. Rev.* **2004**, 248 2201. (b) Gladiali, S.; Alberico E. in *Transition Metals for Organic Synthesis* Vol 2 (Eds. Beller, M.; Bolm C.), Wiley-VCH, Weinheim, Germany, 2004, pp. 145.
28. Ball, R. G.; Graham, W. A. G.; Heinekey, D. M.; Hoyano, J. K.; McMaster, A. D.; Mattson, B. M.; Michel, S. T. *Inorg. Chem.* **1990**, 29, 2023.
29. Oxford Diffraction **2010**. CrysAlisPro (Version 1.171.38.41). Oxford Diffraction Ltd., Yarnton, Oxfordshire, UK. 24
30. G.M. Sheldrick, *Acta Cryst. A71* **2015**, 3.

5.2. Ir-complexes containing mesoionic carbenes for the highly efficient and versatile transfer hydrogenation of C=O, C=N and C=C functionalities and for dehydrogenation of alcohols

Mazloomi, Z.; Petrorius, R.; Pàmies, O.; Albrecht, M.; Diéguez, M. Manuscript to be submitted.

5.2.1. Introduction

Sustainable production is one of the important challenges our society is facing and catalysis is leading the developments in this process. With small amounts of catalysts, large quantities of compounds can be produced with fewer reaction steps and fewer byproducts than in non-catalyzed approaches. Undoubtedly, the research for improved activity and selectivity of the catalysts is at the core of sustainable processes, reduction of costs and continuous growth. The performance of catalytic reactions depends, to a large extent, on the adequate selection of the ligands, in which an electronically and sterically well defined scaffold is the most important factor. In this context, thousands of homo- and hetero-donor ligands, mainly P- and N-containing ligands with either C_2 - or C_1 -symmetry, have been developed although only a few of them have a general scope.¹ Among them, heterodonor ligands (P-N, P-S, P-P', etc.) equipped with strong and weak donor heteroatom pairs have made some of the most fundamental contributions to the development of catalysis. Our groups have contributed with improved generations of modular heterodonor P-X ligand libraries, obtained from readily available starting materials and easy to handle.² Among them, P-N ligand libraries containing in total more than 300 systematic structural variations were synthesized from unexpensive reagents (e.g., sugars) and containing mainly oxazoline, oxazole and thiazole moiety in the nitrogen functionality.^{2d-e}

In the last two decades N-heterocyclic carbenes (NHCs) have emerged as powerful ligands in catalysis. Owing to their strong σ -donation ability, air stability and low toxicity they have become practical alternatives to the most commonly used phosphines.³ A large number of transformations are known to proceed only with NHC-based catalysts. For that reason, exploring new classes of NHCs is a very important goal in recent organometallic chemistry. 1,2,3-Triazol-5-ylidenes are a relevant subclass of

NHCs possessing a mesoionic carbene (MIC) structure.⁴ The pioneering work of Albrecht^{5a} and Bertrand,^{5b} among others,⁶ with mesoionic carbene ligands recently put the focus on these type of ligands and spurred their development. Several reactions have therefore been explored where triazolylidene-based metal complexes are equally or more efficient compared to their NHC analogues, such as cross-coupling reactions, olefin metathesis, oxidative transformations, transfer hydrogenation catalysis, and the click reaction.⁷ The triazole framework adds the advantages of increased σ -donation compared to classical NHCs and the ability to potentially stabilize different metal oxidation states. In addition, they are accessible via synthetically highly efficient and modular nature of "click reaction". The click reaction tolerates a wide variety of functional groups in the azide and in the alkyne reactant. These features facilitate preparing series of modular heterodonor MIC-containing ligands, with different steric and electronic properties, in the quest to maximize catalytic performance.⁴ Despite this, the development of heterodonor 1,2,3-triazol-5-ylidene-containing ligands have been scarcely explored. Most of the reported complexes possessing 1,2,3-triazol-5-ylidene ligands have a monodentate coordination mode. Only a few MIC complexes with a bidentate coordination mode have been reported in the literature recently. To our knowledge the 1,2,3-triazol-5-ylidene carbene moiety has only been combined with pyridine/pyrimidine and hydroxyl groups.^{7e,i,8} More research is therefore still needed to explore new classes of chelating 1,2,3-triazolylidene based ligands.

5.2.2. Objectives

Inspired by the pioneering work on catalysis using 1,2,3-triazol-5-ylidenes based-carbenes and the success of oxazole/thiazole containing ligands in homogeneous catalysis a combination of these scaffolds is a logical field for investigation. Consequently, we here report the first examples of mixed oxazole/thiazole-MIC ligands (**L3H**·OTf and **L4H**·OTf, Figure 5.2.1). For comparison purposes we also synthesized the ether-functionalized 1,2,3-triazolylidene ligand **L2H**·BF₄ (Figure 5.2.1).^{8d} We used these ligands to generate the corresponding Ir(I) and Ir(III) oxazole/thiazole/ether-appended MIC complexes **134**, **138-142** (Figure 5.2.1). The coordination was achieved by a transmetallation protocol and the corresponding complexes were fully characterized by ¹H and ¹³C spectroscopies, high resolution mass spectrometry, elementary analysis and X-ray diffraction. Apart from synthetic and structural aspects, we also present the application of these complexes in transfer hydrogenation of a broad

range of substrates (ketones, aldehydes, imines, ...) and also the more challenging mono-, di- and trisubstituted olefins and in the base-free dehydrogenation reactions of alcohols. We also discuss some mechanistic insights for both transformations.

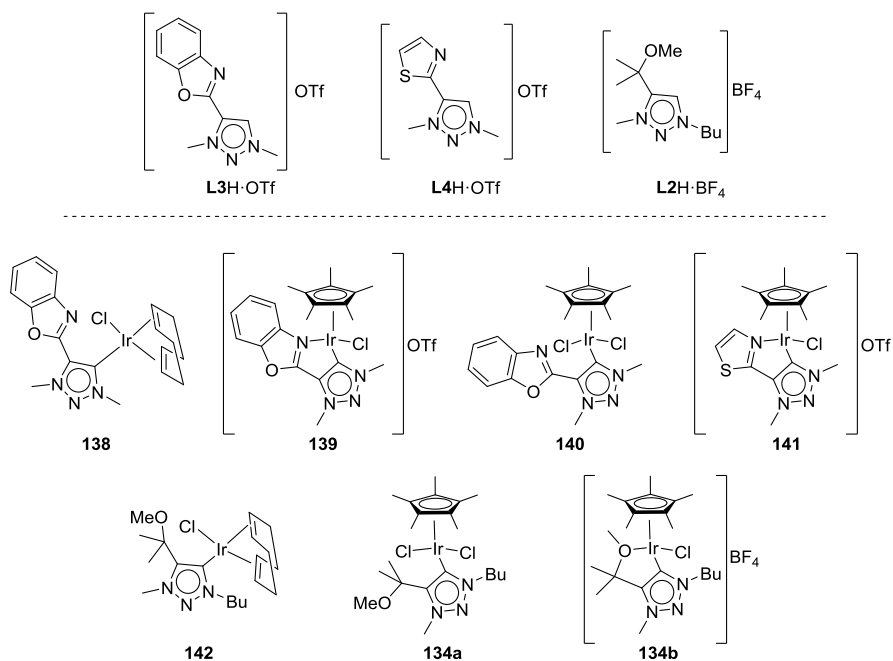


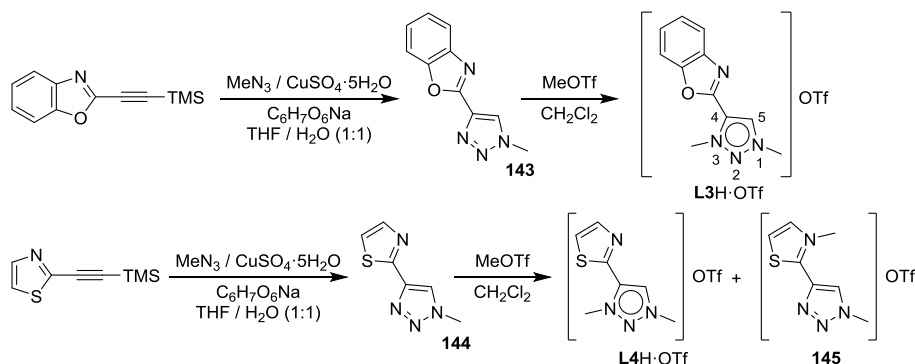
Figure 5.2.1. Heterodonor benzoxazole/thiazole/ether-1,2,3-triazol-5-ylidene **L2H**·BF₄, **L3**-**L4H**·OTf ligands and their Ir(I)/Ir(III) complexes **134**, **138**-**142** used in this work.

5.2.3. Results and discussion

5.2.3.1. Synthesis and characterization of ligands and complexes

The triazolium-benzoxazole/thiazole salts **L3H**·OTf and **L2H**·OTf used as ligand precursors were prepared via conventional copper-catalyzed [3+2] of the methyl azide and the corresponding functionalized trimethylsilyl-protected alkyne, followed by the methylation at the triazole N3 position as illustrated in (Scheme 5.2.1). This procedure yielded the desired triazolium-benzoxazole salt **L3H**·OTf as a sole product when starting from the benzoxazole protected alkyne but a mixture of triazolium-thiazole salts (desired ligand **L4H**·OTf and compound **145**) when starting from the thiazole protected alkyne. The unselective methylation that leads to the formation of the mixture of triazolium salts is attributed to the similar pK_a of the triazole N3 position and of the thiazole group. Fortunately, pure triazolium-thiazole salts **L4H**·OTf and **145** were

obtained after separation by column chromatography. The formation of ligand precursors **L3H**·OTf and **L4H**·OTf was confirmed by ^1H and ^{13}C NMR spectroscopy and mass spectrometry (see experimental section for characterization details). For ligand **L3H**·OTf single crystals suitable for XR-diffraction analysis were obtained which further confirm its formation (Figure 5.2.2). The triazolium-ether salt **L2H**·BF₄ was prepared as previously reported by Albrecht's group.^{8d}



Scheme 5.2.1. Synthesis of triazolium-benzoxazole/thiazole salts **L3-L4H**·OTf.

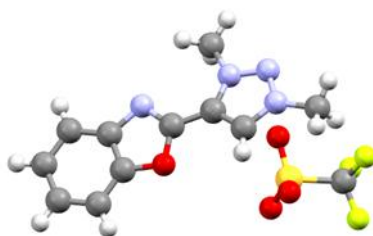
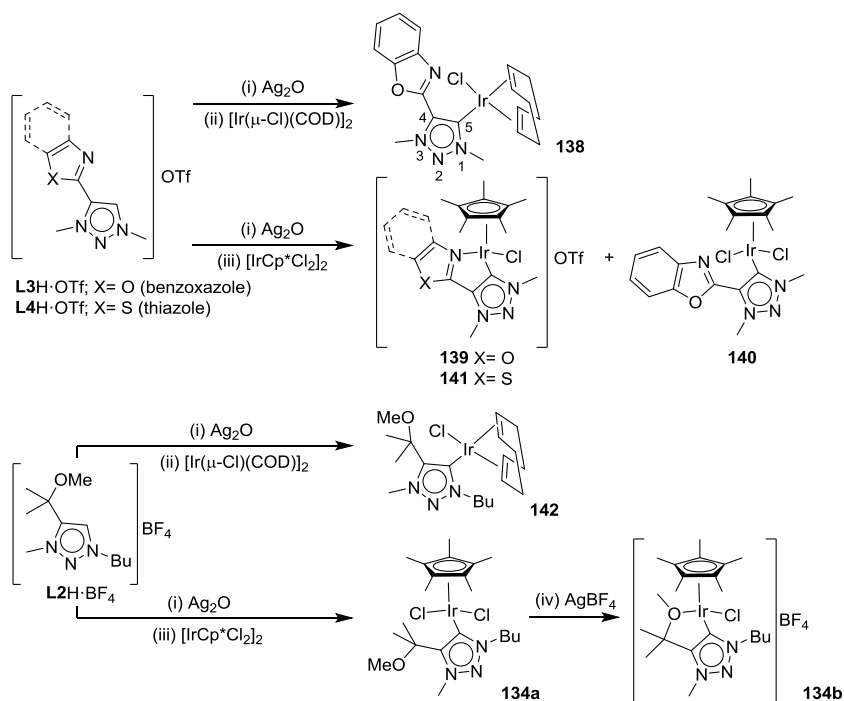


Figure 5.2.2. X-Ray structure of triazolium-benzoxazole salt **L3H**·OTf.

Iridium complexes **134**, **138-142** were obtained by a one-pot reaction from the corresponding triazolium salts **L2H**·BF₄ and **L3-L4H**·OTf using Ag₂O and Me₄NCl to form the desired Ag-carbene intermediates, and subsequent in situ transmetalation with either [Ir(μ -Cl)(COD)]₂ or [Ir(Cp*)Cl₂]₂ (Scheme 5.2.2). Note that under the applied reaction conditions the analogue [IrCl(**L4**)(COD)] complex with the triazolium-thiazole salt could not be reached. On the other hand, in the case of the triazolium-benzoxazole salt, a mixture of Ir (III) compounds **139** (with bidentated coordination of **L3**) and **140** (with monodentated coordination of **L3**) in a ratio 3:1, was obtained. Both complexes,

139 and **140**, were obtained in pure form after separation by column chromatography. The Ir(III) complexes **134a** and **134b** were synthesized as previously described.^{8d}



Scheme 5.2.2. Synthesis of benzoxazole/thiazole/ether-appended 1,2,3-triazol-5-ylidene iridium complexes **134**, **138-142**.

All complexes were obtained as air stable solids and were fully characterized by ^1H and ^{13}C NMR spectroscopy, elemental analysis, mass spectroscopy and X-ray diffraction. In all complexes, coordination of **L2-L4** through the 1,2,3-triazol-5-ylidene group was confirmed by the disappearance of the H-5 proton signal in the ^1H NMR spectra and by the strong downfield shift of the C-5 carbon signal in the ^{13}C NMR spectra (see Table 5.2.1). In the $[\text{IrCl}(\text{L3})(\text{COD})]$ **138** and **142** complexes, monocoordination of ligands **L3** and **L2** through the 1,2,3-triazol-5-ylidene group was also confirmed by the unfolding of the signals of the methinic hydrogens and carbons of the cyclooctadiene group. Therefore, two sets of signals at significantly different chemical shifts were observed for methinic protons (around 4.5 ppm and 2.8 ppm in the ^1H NMR) and carbons (around 80 ppm and 50 ppm in the ^{13}C NMR), see Table 5.2.1, which are characteristic of methinic protons trans to chloro and trans to the carbene

group, respectively. In the case of Ir(III)-complexes, the ability of ligands **L3** and **L4** to coordinate in a mono- or bidentated fashion was easily confirmed by ^{13}C NMR spectra where the signals from the quaternary O-C=N group were downfield shifted when the ligands were coordinated in a bidentated fashion (Table 5.2.1). Thus for instance, while the signal of O-C=N in **L3** appears at 154.5 ppm in complex **139** with a bidentated coordination of **L3**, for complex **140**, with a monodentated coordination mode of **L3**, this signal appears at 151.9 ppm, similar to the chemical shift of the free ligand.

Table 5.2.1. Selected ^1H and ^{13}C NMR signals for complexes **138-142** and ligands **L2H·BF₄** and **L3-L4H·OTf**.^a

Compound	^{13}C				^1H
	C-5	C-4	O-C=N	CH= (COD)	CH= (COD)
138	176.7	133.3	154.4	83.3; 82.9 52.1; 51.7	4.62 (bs); 4.51 (bs) 2.88 (bs); 2.8b (bs)
139	161.1	136.4	154.5	-	-
140	152.0	135.5	151.9	-	-
141	158.4	145.7	158.4	-	-
142	169.0	146.7	-	81.3; 79.8 51.3; 51.1	4.55 (m); 4.44 (m) 2.68-2.82 (m)
L3H·OTf	132.3	132.6	151.2	-	-
L4H·OTf	131.0	136.9	150.3	-	-
L2H·BF₄ ^{6d}	146.9	130.0	-	-	-

^(a) Otherwise noted all signals are singlets. Abbreviations used: bs= broad singlet; m= multiplet.

Suitable crystals for single-crystal X-ray diffraction analysis were obtained for all complexes by slow diffusion of pentane into a dichloromethane solution of the complexes (Figure 5.2.3). The results provide further evidence for the proposed structures of complexes **138-142**. The molecular structures show the expected square-planar and piano-stool arrangements for Ir(I) and Ir(III)-complexes, respectively. By comparing the structures of Ir(III) complexes **139** and **140**, containing the benzoxazole-MIC ligand **L3**, we can observe a small contraction of the Ir-C5 and Ir-Cl bonds upon

chelation which can be attributed to the cationic nature of complex **139**, with the ligand coordinated in a bidentated fashion (Table 5.2.2).

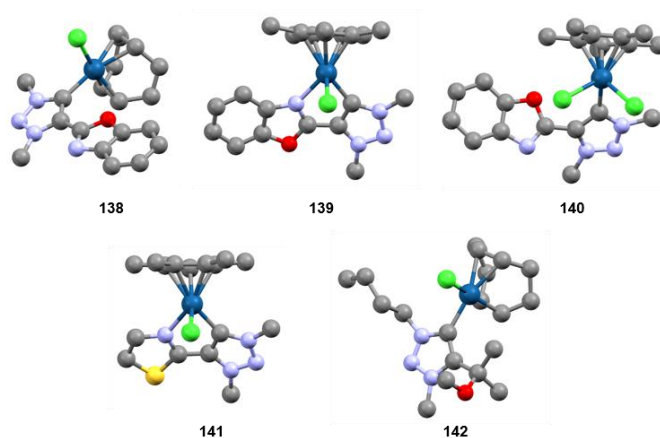


Figure 5.2.3. X-Ray structure of Ir(I) and Ir(III) complexes **138-142**. H and anions are omitted for clarity.

Coordination of **L3** as bidentated is also responsible for the Ir-C5-C4 angle in complex **139** that is lower than in **140**. This distortion is compensated by the increase of the reverse angle Ir-C5-N1 (Table 5.2.2). Comparison between the structures of Ir(III) complexes **139** and **141** (containing ligands **L3** and **L4** coordinated in a bidentated mode, respectively), we can observe a small contraction of the Ir-N4 bond in complex **141** and almost no deviation of the C5-Ir-N4 angle (Table 5.2.2). This distortion is compensated by a substantial increase of the Cl-Ir-N4 and C5-Ir-Cl angles. Comparison between the structures of Ir(I) complexes **138** and **142**, we can detect that the Ir-C5 bond is longer in complex **142** than in **138**, while almost no deviation of Ir-Cl bond is observed (Table 5.2.2). On the other hand, the C5-Ir-Cl angle is bigger in complex **138** than in **142**. Finally, if we compare Ir-complexes **139** and **141** with the analogous complex containing a pyridine group instead of a benzoxazole or a thiazole moiety (named as complex **146**⁸ⁱ in Table 5.2.2), we found that the Ir-N4 bond is smaller in **146** than in **141** and **139**. This confirms that the coordination ability of the three groups is Py > thiazole > benzoxazole.

Table 5.2.2. Selected bond distances (Å) and angles (o) for complexes **138-142**.

	138	139	140	141	142	146^{vi}
Ir-Cl	2.3587(16)	2.3949(11)	2.4150(4) 2.4205(5)	2.4260(9)	2.3635(11)	2.4220
Ir-C5	2.035(5)	2.027(4)	2.046(2)	2.022(4)	2.063(4)	2.017
Ir-N4	-	2.159(4)	-	2.141(3)	-	2.129
C5-C4	1.399(8)	1.380(6)	1.401(3)	1.387(5)	1.396(6)	1.389
C5-Ir-N4	-	76.07(16)	-	75.56(13)	-	76.07
Cl-Ir-N4	-	86.38(11)	-	90.35(8)	-	87.79
C5-Ir-Cl	91.8 (2)	84.97(13)	87.87(5) 88.06(6)	88.69(10)	91.39(12)	89.56
Ir-C5-C4	132.9(4)	117.8(3)	131.76(14)	117.2(3)	135.7(3)	116.76
Ir-C5-N1	126.1(4)	140.9(4)	126.92(14)	140.5(3)	121.3(3)	140.25

5.2.3.2. Ir-catalyzed transfer hydrogenation reactions

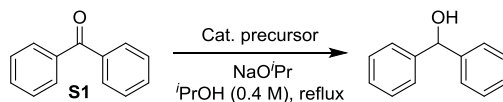
Catalytic transfer hydrogenation (TH) of unsaturated bonds is, nowadays, one of the most investigated hydrogenation reactions. It is a sustainable, efficient and mild method that is operationally simpler and significantly safer than direct hydrogenation with molecular hydrogen. Ru-, Rh- and Ir-catalysts bearing NHC ligands have been widely used for TH with results comparable to the Noyori-type catalysts for some substrates. For other substrates, such as heteroaromatic ketones, imines and alkenes, selectivity and turnover frequencies are not optimal yet for TH to be competitive with conventional hydrogenation. For these reasons, efforts are focused to extend the range of applicable substrates by improving the ligand design. In contrast to classical NHC containing complexes, few successful examples using complexes with MIC ligands of the triazolylidene type can be found in the literature and they are limited in substrate scope.^{7i,8c,11} In addition, these examples needed high amount of base (up to 20 mol%) and of hydrogen donor (usually 0.1 M of substrate in 2-propanol).

5.2.3.2.1. Transfer hydrogenation of benzophenone **S1**. Catalyst precursors screening.

In a first set of experiments the catalytic properties of our Ir(I) and Ir(III) complexes **134**, **138-142** were evaluated in the transfer hydrogenation of benzophenone **S1** as model substrate, using 2-propanol as both hydrogen donor and solvent, and NaOⁱPr as a base to activate the hydrogen donor. In all cases no induction period was observed from the time-conversion profiles (see supporting information for profiles details). The

results, which are summarized in Table 5.2.3, indicate that activity is highly dependent on the nature of the catalyst precursors. Thus, Ir(I)-catalyst precursors provided much higher activity than Ir(III)-counterparts (i.e. entry 1 vs 2-4; and entry 5 vs 6 and 7). A plausible explanation is that the higher electron density on the metal center of Ir(I)-catalyst precursors than of Ir(III)-analogues facilitates the formation of the metal-hydride species. We also found that **134a,d** and **142** catalyst precursors, which contain ligand **L2**, provide higher activity than the analogous **138-141** with heterodonor benzoxazole/thiazole-MIC ligands **L3-L4**. This can be attributed to the higher coordination ability of the benzoxazole and thiazole moieties (ligands **L3** and **L4**, respectively) compared to the methoxy group in **L2**. Moreover, the different time conversion profiles (see Supporting Information) and TOFs obtained with complexes **139** and **140**, with the benzoxazole-MIC ligand coordinated in a monodentate and bidentate mode, suggests that the catalytically active species are different.

Table 5.2.3. Transfer hydrogenation of benzophenone **S1** using complexes **134**, **138-142**.^a



Entry	Cat (mol %)	NaO ^{<i>i</i>} Pr (mol %)	TOF ^b	%Yield ^c (min)
1	138 (1)	5	252	84 (60)
2	139 (1)	5	12	8 (60)
3	140 (1)	5	24	29 (60)
4	141 (1)	5	60	58 (60)
5	142 (1)	5	780	97 (30)
6	134a (1)	5	96	62 (60)
7	134b (1)	5	72	54 (60)
8	142 (1)	10	840	97 (30)
9	142 (1)	2.5	48	97 (400)
10	142 (1)	1	24	96 (720)
11	142 (1)	5	985	96 (30)
12	142 (1)	5	816	85 (60)
13	142 (1)	5	1080	98 (150)

^(a) Reaction conditions: 0.4 M benzophenone **S1** in 2-propanol, catalyst precursor (0.1-1 mol%), NaO^{*i*}Pr (1-10 mol%). ^(b) TOF in mol **S1** × (mol cat × h)⁻¹ measured after 5 min. ^(c) Yield measured by ¹H NMR using mesitylene as internal standard.

We then performed several experiments with different amounts of base and catalyst precursor using **142**, which had provided the best result. The amount of base had a dramatic impact on activity (Table 5.2.3, entries 5 and 8-10): decreasing it to 2.5 mol% had an extremely negative effect (entry 9 *vs* 5) while a higher amount did not increase activity substantially (entries 5 and 8). The best trade-off between amount of base and activity was therefore achieved with 5% mol NaO^tPr. On the other hand, the amount of the catalyst precursor had little impact on activity (Table 5.2.3, entries 5 and 11-13). In summary, high activity with TOF's up to 1080 mol **S1** × (mol **142** × h)⁻¹ were achieved using 5 mol% of base and only 0.1 mol% of catalyst. This result surpasses the ones reported in the literature with Ir-containing MIC catalysts.¹¹

5.2.3.2.2. Transfer hydrogenation of several substrate types. Scope and limitations

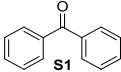
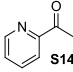
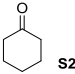
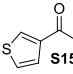
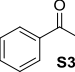
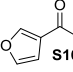
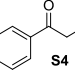
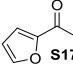
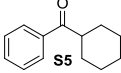
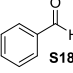
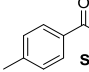
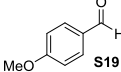
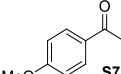
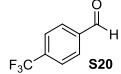
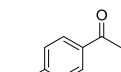
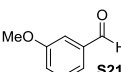
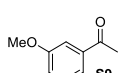
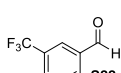
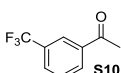
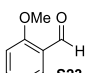
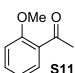
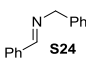
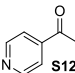
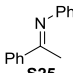
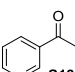
Encouraged by the previous results, we next studied [IrCl(**L2**)(COD)] (**142**), which had provided the best results, in the reduction of a broad range of substrates bearing other unsaturated groups such as ketones (**S1-S17**), aldehydes (**S18-S23**), imines (**S24-S25**), olefins (**S26-S37**), α,β -unsaturated ketones (**S38-S40**) and allylic alcohols (**S41-S42**). In all the cases, the reactions were performed using 0.5 mol% of catalyst precursor **5** and only 5 mol% of base.

We first investigated the reduction of 18 ketones with different steric and electronic properties including challenging heteroaromatic ketones (**S1-S17**). The results, which are collected in Table 5.2.4 (entries 1-17), indicate that the catalytic activity depends on both the steric and electronic demands of the substrate, being the highest TOF's of this series (up to 2100 mol × (mol × h)⁻¹) achieved in the reduction of less sterically demanding cyclohexenone **S2** and electron-poor 4-(trifluoromethyl)acetophenone **S8**. In the reduction of aryl ketones with increasingly sterically demanding alkyl substituents (**S1** and **S3-S5**), activity diminished when the steric demands of the alkyl substituent increased (i.e. entry 5 *vs* 3). However, catalytic activity was hardly affected by the steric factors on the aryl moiety of the substrate. Positively, ortho-substituted aryl ketones were somewhat more reactive than the non-substituted ones (i.e. entry 3 *vs* 11). The results using several para-substituted aryl ketones (**S3**, **S6-S8**) indicated that the catalytic activity increases when electronic withdrawing groups are present at the para position (i.e. entry 8 *vs* 7 and 6). Finally, the transfer hydrogenation of meta-substituted aryl ketones (**S9-S10**) provided high activities similar to **S3** (Table 5.2.4, entry 3 *vs* 9 and 10).

We next considered the transfer hydrogenation of heteroaromatic ketones. The reduction of these substrates is more puzzling because the coordination of the heteroaromatic group of the substrate to the metal often reduces the activity of the catalyst drastically. There are therefore very few catalytic systems able to reduce this substrate class under transfer hydrogenation conditions. To our best knowledge the reduction of these substrates has not been reported with NHC and MIC-containing complexes. We were pleased to find out that again heteroaromatic ketones (**S12-S17**, Table 5.2.4, entries 12-17) could be reduced in high activities (TOF's up to $1500 \text{ mol} \times (\text{mol} \times \text{h})^{-1}$). Activity, however, was dependent on the type of heteroaromatic moiety and on its substitution pattern. Regarding the effect of the type of heteroaromatic group, we found that furyl-based ketones (**S16** and **S17**) provided somewhat higher activities (TOF's up to $1500 \text{ mol} \times (\text{mol} \times \text{h})^{-1}$) than the non-heteroaromatic substrates (e.g., entries 16 and 17 *vs* 3). The lowest activity was achieved using thienyl-based ketone **S15** (TOF's up to $100 \text{ mol} \times (\text{mol} \times \text{h})^{-1}$; entry 15). The reduction of pyridyl-based ketones (**S12-S14**, entries 12-14) was dependent on the heteroaromatic ring substitution pattern. While similar high activities (TOF's up to $510 \text{ mol} \times (\text{mol} \times \text{h})^{-1}$) were achieved with 3- and 4-acetylpyridines **S12** and **S13**, lower TOF's (up to $260 \text{ mol} \times (\text{mol} \times \text{h})^{-1}$) were achieved with 2-acetylpyridine **S14**, which tends to coordinate more effectively than the *meta* and *para* counterparts.

Catalytic system **142** also proved to be highly efficient in the TH of several aldehydes (Table 5.2.4, entries 18-23). In general the results follow the trend observed in the reduction of ketones, albeit the electronic effect is less pronounced than in the reduction of ketones (TOF's in the range of 1400 for **S19** and 2300 for **S20**; entries 19 and 20 *vs* 7 and 8, respectively). Therefore, a broad range of aryl aldehydes with electron-withdrawing or electron-donating substituents in the *para* position as well as *ortho*- and *meta*-substituted aldehydes were reduced with comparable high activities than those achieved with ketones.

Table 5.2.4. Transfer hydrogenation of ketones, aldehydes and imines using Ir-complex **142**.^a

Entry	Substrate	TOF	%Conv (min)	Entry	Substrate	TOF	%Conv (min)
1		990	96 (30)	14		260	99 (180)
2		1800	97 (5)	15		100	84 (240)
3		1200	98 (30)	16		1500	96 (30)
4		1300	96 (15)	17		1400	93 (30)
5		500	89 (60)	18		1900	98 (10)
6		1300	99 (30)	19		1400	97 (15)
7		770	88 (30)	20		2300	99 (5)
8		2100	98 (5)	21		1500	96 (15)
9		1300	96 (30)	22		1600	94 (15)
10		1200	95 (30)	23		1200	98 (30)
11		1400	98 (30)	24		770	99 (30)
12		510	92 (60)	25		30	100 (24)
13		480	81 (60)				

^(a) Reaction conditions: 0.4 M substrate in 2-propanol, **142** (0.5 mol%), NaO^tPr (5 mol%), reflux. ^(b) TOF in mol substrate × (mol × h)⁻¹ measured after 5 min. ^(c) Yield measured by ¹H NMR using mesitylene as internal standard or by GC using dodecane as internal standard.

Furthermore, we investigated the reduction of imines (Table 5.2.4; entries 24 and 25). Imines are known to be more difficult to reduce than ketones and aldehydes and they usually require higher catalyst loading and much longer reaction times. Notably, the transfer hydrogenation of aldimine **S24** proceeded smoothly, under our mild reaction conditions, with TOF up to $770 \text{ mol} \times (\text{mol} \times \text{h})^{-1}$). Catalyst precursor **142** could also reduce ketimine **S25**, although with a low TOF (up to $30 \text{ mol} \times (\text{mol} \times \text{h})^{-1}$), as expected for this more sterically difficult substrate. It should be noted that for both substrates, the reduction proceeded cleanly providing the desired amines as the sole products as observed in the ^1H NMR.

In summary, $[\text{IrCl}(\mathbf{L2})(\text{COD})]$ (**142**) catalyst precursor is able to reduce a wide range of ketones, including the most challenging heteroaromatic ones, aldehydes and aldimines in high activities (TOF's up to $2300 \text{ mol} \times (\text{mol} \times \text{h})^{-1}$). Although there are some metal-carbene species, mainly Ru-NHC complexes, able to promote these transformations more efficiently, our results compete favorably with known Ir-MIC catalytic systems.^{7i,8c,11a,c,d,f}

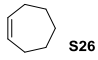
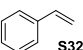
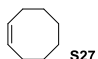
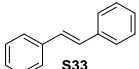
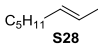
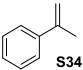
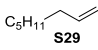
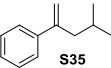
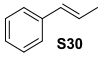
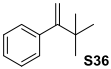
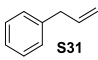
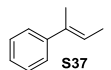
To further study the substrate scope, we next focused on the transfer hydrogenation of olefins. Olefins are challenging substrates because they are reduced at a much lower rate than ketones. So far only a few reports using NHC or MIC containing complexes with a limited in substrate scope have been published.^{8c,10a,d,11d,15} Two of these cases reported by the groups of Nolan^{10d} and Albrecht^{10a} et al. showed that Ir- and Ru- N-heterocyclic carbene complexes could efficiently reduce a small selection of olefins. More recently the groups of Elsevier^{11d} and Sarkar^{8c} showed that cyclooctene could be reduced using Ir-NHC and Ru/Ir-MIC complexes. They needed, however, long reaction times (20 hours with a 50% of Conv. with Ir-NHC and 24 hours with 80% and >99% of convs. with Ir and Ru-MIC, respectively), high catalyst loading (1 mol%) and high amount of base (up to 20 mol%) and hydrogen donor (0.1 M of substrate in 2-propanol).

Our results (Table 5.2.5) indicate that a broad range of olefins can be efficiently reduced using catalyst precursor **142** in milder reaction conditions. We found that the catalytic performance is relatively insensitive to the olefins substitution pattern and to the geometry of the double bond. Similar high activities were therefore achieved for a range of linear mono-, 1,2-di- and 1,1-disubstituted olefins as well as for cyclic olefins (TOF's up to $260 \text{ mol} \times (\text{mol} \times \text{h})^{-1}$).

We also found that activities are influenced by steric effects (compare entries 9-11). In this way, the transfer hydrogenation of 1,1-disubstituted olefins **S34-S36** with an

increasingly sterically demanding alkyl substituents proceeded with lower activities (Table 5.2.5, entries 9-11). Similarly, the reduction of sterically more hindered trisubstituted olefin **S37** proceed with the lowest activity of the series. In summary, [IrCl(**L2**)(COD)] (**142**) catalyst precursor is one of the rare examples of catalyst able to efficiently reduce such a range of olefins

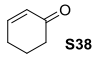
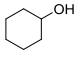
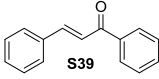
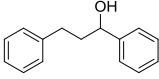
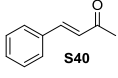
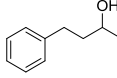
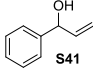
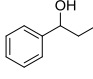
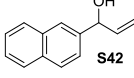
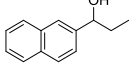
Table 5.2.5. Transfer hydrogenation of olefins using Ir-complex **142**.^a

Entry	Substrate	TOF	%Conv (h)	Entry	Substrate	TOF	%Conv (h)
1	 S26	170	88 (4)	7	 S32	190	91 (4)
2	 S27	130	93 (6)	8	 S33	240	94 (41)
3	 S28	170	95 (6)	9	 S34	200	97 (4)
4	 S29	160	94 (6)	10	 S35	190	90 (4)
5	 S30	260	96 (4)	11	 S36	110	87 (6)
6	 S31	260	99 (4)	12	 S37	80	89 (12)

^(a) Reaction conditions: 0.4 M substrate in 2-propanol, **142** (0.5 mol%), NaO^tPr (5 mol%), reflux. ^(b) TOF in mol substrate x (mol 5 x h)⁻¹ measured after 10 min. ^(c) Yield measured by ¹H-NMR using mesitylene as internal standard or by GC using dodecane as internal standard.

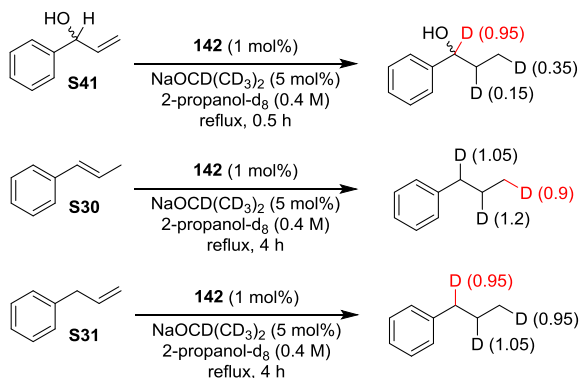
Finally, this novel set of catalysts was studied in the reduction of α,β -unsaturated ketones and allylic alcohols (Table 5.2.6). Again [IrCl(**L2**)(COD)] was able to efficiently reduce these important substrate classes to the corresponding saturated alcohols (full conversions in less than 1 hour). The extremely high activity achieved with substrates **S38-S42** (similar to the corresponding simple ketones) make us believe that the reaction proceeded via a tandem isomerization/transfer hydrogenation reaction rather than via the direct reduction of the ketone and the olefin as observed by Elsevier et al. using similar Ir(I) complexes containing chelating 1,2,3-triazolylidene-NHC ligands.^{11d} To prove this, we performed the transfer deuteration of α -vinylbenzyl alcohol **S41** using 2-propanol- d_8 as a deuterium source and sodium isopropoxide- d_7 as a base (Scheme 5.2.3).

Table 5.2.6. Reduction of α,β -unsaturated ketones and allylic alcohols using Ir-complex **142** under transfer hydrogenation conditions.^a

Entry	Substrate	Product	%Yield (min) ^b
1	 S38		96 (15)
2	 S39		94 (60)
3	 S40		96 (60)
4	 S41		92 (60)
5	 S42		96 (60)

^(a) Reaction conditions: 0.4 M substrate in 2-propanol, **142** (0.5 mol%), NaOPr (5 mol%), reflux. ^(b) Yield measured by ¹H NMR using mesytilene as internal standard or by GC using dodecane as internal standard.

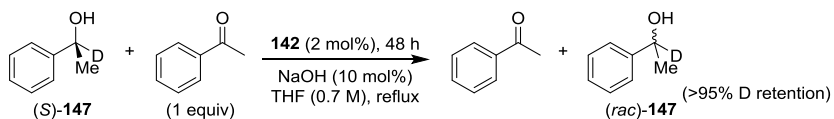
The formed product contained deuterium not only at the double bond (as expected) but also at the allylic position which agrees with a competing isomerization pathway.¹⁶ This was supported by the mass spectra of the corresponding deuterated products showing species with more than two deuterium atoms incorporated. To study how fast the alkene double bond was isomerized we run similar transfer deuterogenation experiments using *trans*- β -methylstyrene **S30** and allylbenzene **S31**. Again the results show that deuterium is added at both the double bond and the allylic position. Furthermore, the GC and ¹H NMR spectra over time indicate that the isomerization is faster than the reduction of olefins. Thus, after 10 minutes the allylbenzene **S31** was fully isomerized to the internal olefin **S30** under TH conditions. These results confirmed that the reduction of α,β -unsaturated ketones and allylic alcohols proceeded via a tandem isomerization/transfer hydrogenation reaction.



Scheme 5.2.3. Deuterium labeling experiments of olefins **S30** and **S31** and allylic alcohol **S41** using Ir-catalyst precursor **142**. The percentage of incorporation of deuterium atoms is shown in brackets. The results of the indirect addition of deuterium due to the isomerization process are shown in red.

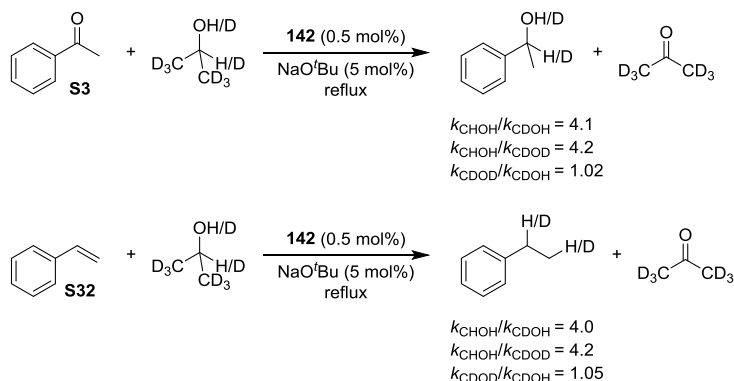
5.2.3.3 Mechanistic insights

Initially, the mechanism of the Ir-catalyzed transfer hydrogenation with complex $[\text{IrCl}(\text{L}2)(\text{COD})]$ (**142**) was studied using the racemization of (*S*)-1-phenylethan-1-d-1-ol in the presence of acetophenone **S3** (Scheme 5.2.4). This simple experiment has been previously used to elucidate the nature of the metal-hydride species responsible of the catalytic activity. Thus, while a selective carbon-to-carbon hydrogen transfer is indicative of metal-monohydride species responsible for the catalytic activity, a non-selective hydrogen transfer (involving both oxygen-to-carbon and carbon-to-carbon H-transfer) reveals the involvement of metal-dihydride species. $[\text{IrCl}(\text{L}2)(\text{COD})]$ showed a high degree of retention of deuterium in the α -position (>95%) after full racemization. This clearly indicates that the Ir-H species are responsible for the catalytic activity.



Scheme 5.2.4. Deuterium content in 1-phenylethan-1-d-1-ol after racemization of (*S*)-1-phenylethan-1-d-1-ol using Ir-catalyst precursor **142**.

Further mechanistic insights into the rate determining step of the reaction were obtained by studying the kinetic isotope effects (KIE) of the transfer hydrogenation of acetophenone **S3** and styrene **S32** (Scheme 5.2.5). We carried out several experiments using isopropanol, isopropanol- d_7 and isopropanol- d_8 . In these experiments we used sodium tert-butoxide instead of sodium isopropoxide to avoid potential problems with H/D scrambling. The reactions were monitored over time by GC analysis. For both substrate types, significant KIE for the hydrogen transfer reaction were obtained ($k_{\text{CHOH}}/k_{\text{CDOH}} \approx k_{\text{CHOH}}/k_{\text{CDOD}} \approx 4$; $k_{\text{CDOD}}/k_{\text{CDOH}} \approx 1$). These results clearly indicate that of the two processes involved in the transfer hydrogenation reactions (the hydride transfer and the proton transfer), the hydride transfer is the rate-limiting step for both substrate types.



Scheme 5.2.5. Kinetic isotope effects of the transfer hydrogenation of ketones (acetophenone **S3** as example) and olefins (styrene **S32** as example) using Ir-catalyst precursor **142**.

To know which of the two possible hydride transfer steps determined the rate (the one from the hydrogen donor to the metal to form the metal-hydride, or the one from the metal-hydride to the substrate), we compared the activity of catalytic system **142** for different para substituted acetophenones (**S3**, **S7-S8**) against the Hammett σ values of the substrates (Figure 5.2.4). The positive σ value ($\sigma = 0.52$) indicates that the electron density increases in the rate determining step. Moreover, the fact that the Hammett parameter affects the rate indicates that the substrate should also participate in the rate determining step. These facts, together with the observed KIE, agree with the hypothesis that the rate determining step is the C=O insertion on the M-H bond.

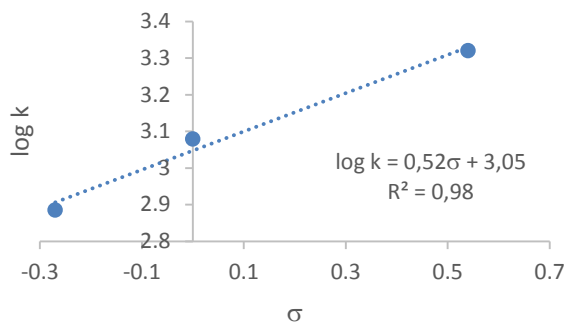


Figure 5.2.4. Hammett plot showing the effect of substituents on the transfer hydrogenation using catalytic system **142**.

5.2.3.4 Base-free Ir-catalyzed dehydrogenation reactions

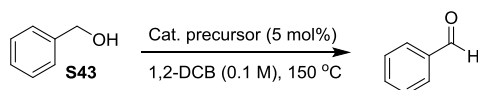
Available procedures for the oxidation of alcohols range from the use of high-valent oxo metal species, the Oppenauer-type oxidation and the use of hypervalent iodine among others,²⁰ to biomimetic approaches using more benign oxidants such as hydrogen peroxide or oxygen.²¹ The alternative oxidant-free dehydrogenation of alcohols has been less studied although it is very attractive in terms of atom economy and reduced waste. This process generates molecular hydrogen as a side product that can be used as an alternative to fossil fuels. Research in this area has rapidly moved from phosphine ligands to NHC ligands, including triazolylidene-based ligands for Ru- and Ir-catalysts. One of the drawbacks of the oxidant-free dehydrogenation of alcohols is that the product can remain in the coordination sphere and be subsequently transformed into undesired ethers and acetals. In this respect, the work with iridium triazolylidene-based catalysts has shown that monomeric species favor the etherification of the carbonyl product while dimeric species suppress this transformation.²²

5.2.3.4.1. Dehydrogenation of benzyl alcohol **S43**. Catalyst precursors screening

In a first set of experiments, benzyl alcohol **S43** was used as the benchmark substrate to study the effectiveness of the Ir(I)- and Ir(III)-complexes **134**, **138-142** in the oxidant-free dehydrogenation. For comparison, we evaluated them using the optimal conditions found in previous studies with Ir-MIC compounds.²² Reaction were therefore carried out without base, using a catalyst loading of 5 mol% in 1,2-dichlorobenzene.

Benzaldehyde formation was monitored over time (see Supporting Information) and conversions after 12 and 72 h are compiled in Table 5.2.7. For all complexes, the time-conversion profiles showed no significant activation time. Interestingly, only the formation of the desired benzaldehyde was observed in the ^1H NMR. This behavior contrasts with that above mentioned fact that Ir-monomeric species favored the etherification of the carbonyl product, which could be suppressed with dimeric species.²² As observed in the transfer hydrogenation reaction, we found that activity is highly dependent on the catalyst precursor (Table 5.2.7). As expected and in contrast to TH, cationic Ir(III) catalyst precursors provided much higher activity than the Ir(I) counterparts (Table 5.2.7: i.e. entry 1 vs 2-4; and entry 5 vs 6 and 7). The latter tended to readily deactivate under reaction conditions, leading to low conversions (entries 1 and 5). The results using Ir(III)-complexes also show that deactivation takes place except for complexes **139** and **141** (entries 2 and 4 vs 3, 6 and 7). This can be attributed to the higher coordination ability of the benzoxazole and thiazole moieties (compounds **139** and **141**) compared to that of the methoxy group in complex **6**. In summary, the best results were obtained with complexes **139** and **141** with a bidentate coordination mode of the benzoxazole/thiazole-1,2,3-triazol-5-ylidne ligands **L3** and **L4**.

Table 5.2.7. Oxidant-free dehydrogenation of benzyl alcohol **S43** using complexes **134**, **138-142**.^a



Entry	Cat precursor	% Yield (12 h)	% Yield (72 h)
1	138	30	33
2	139	33	99
3	140	18	34
4	141	28	94
5	142	30	38
6	134a	54	60
7	134b	36	55

^(a) Reaction conditions: 0.1 M benzyl alcohol **S43** in 1,2-dichlorobenzene, catalyst precursor (5 mol%). ^(b) Yield measured by ^1H NMR using hexamethylbenzene as internal standard.

5.2.3.4.2. Dehydrogenation of other primary and secondary alcohols. Mechanistic insights

Encouraged by the excellent selectivities provided by Ir(III) complexes **139** and **141**, we decided to further assess their efficiency with a range of benzylic alcohols **S43-S46** and secondary alcohols **S47-S50**. The results (Table 5.2.8) indicate that a range of alcohols can be dehydrogenated to the corresponding carbonyl compounds with good-to-excellent selectivities.

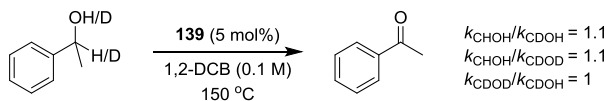
Table 5.2.8. Dehydrogenation of alcohols using Ir-complexes **139** and **141**.^a

Entry	Substrate	Cat. Precursor	% Yield (h)	I/II Ratio
1		139	99 (72)	>20/1
2		141	94 (72)	>20/1
3		139	100 (72)	4/1
4		141	99 (72)	10/1
5		139	85 (72)	>20/1
6		141	64 (72)	>20/1
7		139	97 (72)	3.3/1
8		141	84 (72)	8/1
9		139	94 (12)	>20/1
10		139	100 (12)	>20/1
11		139	35 (12)	>20/1
12		139	84 (12)	>20/1

^(a) Reaction conditions: 0.1 M substrate in 1,2-dichlorobenzene, Ir-cat (5 mol%). ^(b) Yield measured by ¹H NMR using mesitylene as internal standard or by GC using dodecane as internal standard. ^(c) Selectivity measured by ¹H NMR.

While the substituents of the substrate do not significantly affect the selectivity for secondary alcohols (entries 9-12), they do for benzylic alcohols (entries 1-8). Thus, while the excellent selectivity towards the desired carbonyl compounds is maintained when using electron-poor benzylic alcohol **S45**, methyl groups at meta and para positions (substrates **S44** and **S46**) reduce selectivity (entry 5 vs 3 and 7). Fortunately, the formation of the undesired corresponding ethers can be minimized by using catalyst precursor **141** instead of **139** (entries 4 and 8 vs 3 and 7). Activity, depends on the substrate structure and are in general best for secondary alcohols (entries 9-12 vs 1-8) and are positively affected by electron-donating groups at the para position (e.g., entry 3 vs 5 and 10 vs 11).

In order to get some insight into the reaction mechanism, we firstly determined the kinetic isotope effects (KIE) of the dehydrogenation reaction by conducting experiments using 1-phenylethanol, 1-phenylethan-1-d-1-ol and 1-phenylethan-1-d-1-ol-d (Scheme 5.2.6). The reactions were monitored over time by GC analysis. In contrast to the transfer hydrogenation reaction, very small KIE were obtained ($k_{\text{CHOH}}/k_{\text{CDOH}} \approx k_{\text{CHOH}}/k_{\text{CDOD}} \approx 1.1$; $k_{\text{CDOD}}/k_{\text{CDOH}} \approx 1$). These low values indicate that neither the C-H nor the O-H cleavages are the rate determining step. To gain further insight about the rate determining step, we compared the activity of catalytic system **139** for different *para* substituted benzyl alcohols (**S43-S45**) against the Hammett σ values¹⁹ of the substrates (Figure 5.2.5). The negative ρ value ($\rho = -0.61$) indicates that the electron density decreases in the rate determining step. All these results may indicate that substrate coordination to the metal center is the rate determining step.



Scheme 5.2.6. Kinetic isotope effects of the dehydrogenation of alcohols using Ir-catalyst precursor **139**.

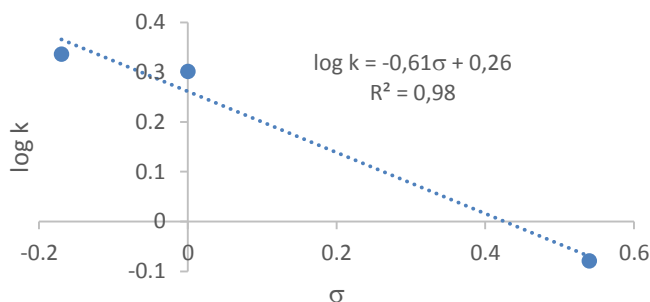


Figure 5.2.5. Hammett plot showing the effect of substituents on the dehydrogenation using catalytic system **139**.

5.2.4. Conclusions

In summary, we prepared new triazolium-benzoxazole/thiazole salts as ligands **L3H**·BF₄ and **L4H**·BF₄ and also their corresponding complexes (**138-142**) which were fully characterized. The new Ir-complexes were successfully applied as catalysts in transfer hydrogenation of different C=O, C=N and C=C functionalities. Encouraged by the results, the Ir-complexes were utilized for oxidation of primary and secondary alcohols and in this case pleasant results were achieved as well. Kinetic isotope effect was studied in both case to have ideas about the mechanism pathway.

5.2.5. Experimental section

5.2.5.1. General information

All reactions were carried out using standard Schlenk techniques under an atmosphere of argon. Solvents were purified and dried by standard procedures. Compounds 2-((trimethylsilyl)ethynyl)benzo[*d*]oxazole and 2-((trimethylsilyl)ethynyl)thiazole;²³ ligand **L2H**·BF₄;^{8d} Ir complexes **134a** and **134b**;^{8d} substrates **S25**,²⁴ **S35**,²⁵ **S36**,²⁶ **S37**,²⁷ **S41**,²⁸ **S42**²⁸ and (*S*)-1-phenylethan-1-d-1-ol;^{17b} and propan-d7-2-ol²⁹ were prepared as previously described. All other commercially available reagents and substrates were used as received. ¹H, ¹³C{¹H}, and ¹⁹F NMR spectra were recorded using a 400 MHz spectrometer. Chemical shifts are relative to that of SiMe₄ (¹H and ¹³C) as internal standard. ¹H and ¹³C assignments were made on the basis of ¹H-¹H gCOSY, ¹H-¹³C gHSQC and ¹H-¹³C gHMBC experiments.

5.2.5.2. Preparation of ligands and complexes

5.2.5.2.1. General procedure for the preparation of triazoles 143 and 144

A suspension of MeI (0.21 ml, 3.30 mmol) and NaN_3 (644 mg, 9.90 mmol) in $\text{H}_2\text{O}/\text{THF}$ (14 mL; 1:1 v/v) was stirred at room temperature for 48 h. $\text{CuSO}_4 \cdot 5\text{H}_2\text{O}$ (49.5 mg, 0.198 mmol), sodium ascorbate (393 mg, 1.98 mmol) and the corresponding functionalized trimethylsilyl-protected alkyne (3.96 mmol) were added subsequently and the mixture was stirred in the oil bath at 70 °C for 36 h. The organic solvent (THF) was removed under reduced pressure and the residue was suspended in CH_2Cl_2 (30 mL) and washed with water (2×50 mL), and brine (2×50 mL). After drying over MgSO_4 , charcoal was added to the solution and stirred for 30 min to further purify the compound. The suspension filtered off through celite, washed with CH_2Cl_2 (20 mL) and evaporated to obtain the desired triazol as an off-white powder.

2-(1-Methyl-1*H*-1,2,3-triazol-4-yl)benzo[*d*]oxazole (143). Yield: 383 mg (70%). ^1H NMR (400 MHz, CD_3CN): δ = 8.45 (s, 1H, H-5), 7.81 – 7.72 (m, 1H, CH=), 7.72 – 7.65 (m, 1H, CH=), 7.47 – 7.36 (m, 2H, CH=), 4.16 (s, 3H, CH_3 -N). $^{13}\text{C}\{^1\text{H}\}$ NMR (101 MHz, CD_3CN): δ = 157.4 (C=N), 151.2 (C), 142.5 (C), 137.6 (C-4), 127.7 (C-5), 126.4 (CH=), 125.7 (CH=), 120.7 (CH=), 111.7 (CH=), 37.5 (CH_3 -N). MS HR-ESI [found 223.0592 (M-Na) $^+$, $\text{C}_{10}\text{H}_8\text{N}_4\text{O}$ requires 223.0590].

2-(1-Methyl-1*H*-1,2,3-triazol-4-yl)thiazole (144). Yield: 394 mg (60%). ^1H NMR (400 MHz, CDCl_3): δ = 8.05 (s, 1H, H-5), 7.84 (d, $^3J_{\text{H-H}} = 3.2$ Hz, 1H, CH=), 7.36 (d, $^3J_{\text{H-H}} = 3.2$ Hz, 1H, CH=), 4.17 (s, 3H, CH_3 -N). $^{13}\text{C}\{^1\text{H}\}$ NMR (101 MHz, CDCl_3): δ = 159.4 (C=N), 143.8 (C-4), 143.3 (CH=), 121.9 (C-5), 119.1 (CH=), 37.1 (CH_3 -N). MS HR-ESI [found 189.0205 (M-Na) $^+$, $\text{C}_6\text{H}_6\text{N}_4\text{S}$ requires 189.0205].

5.2.5.2.2. Preparation 2-(1,3-dimethyl-1*H*-1,2,3- λ^4 -triazol-4-yl)benzo[*d*]oxazole trifluoromethanesulfonate (L3H·OTf)

A suspension of 2-(1-methyl-1*H*-1,2,3-triazol-4-yl)benzo[*d*]oxazole (400 mg, 2.00 mmol) and MeOTf (249 μL , 2.20 mmol, 1.1 equiv) in CH_2Cl_2 (6 mL) was stirred at -12 °C for 20 h (the reaction was monitored by TLC). Et_2O was added in order to precipitate out the product. All volatiles were evaporated under reduced pressure. The precipitate was washed with Et_2O three times to obtain **L3H·BF₄** as a white solid (400 mg, 55%). ^1H NMR (400 MHz, CD_3CN): δ = 9.05 (s, 1H, CH=_{tr}), 7.93 (d, $^3J_{\text{H-H}} = 7.9$ Hz, 1H, CH=), 7.80 (d, $^3J_{\text{H-H}} = 8.2$ Hz, 1H, CH=), 7.59 (m, 2H, CH=), 4.66 (s, 3H, CH_3 -N), 4.38 (s, 3H, CH_3 -N). $^{13}\text{C}\{^1\text{H}\}$ NMR (101 MHz, CD_3CN): δ = 151.2 (C=N), 150.1 (C),

141.4 (C), 132.6 (C-4), 132.3 (C-5), 129.0 (CH=), 127.1 (CH=), 122.0 (q, $^1J_{C-F} = 320.8$, CF₃), 122.0 (CH=), 112.4 (CH=), 41.8 (CH₃-N), 41.57 (CH₃-N). ¹⁹F NMR (377 MHz, CD₃CN): $\delta = -79.39$ (s). MS HR-ESI [found 215.0927 (M-OTf)⁺, C₁₁H₁₁N₄O requires 215.0925]. Suitable crystals for X-ray diffraction were achieved by slow diffusion of pentane to acetonitrile solution.

5.2.5.2.3. Preparation of 2-(1,3-dimethyl-1H-1,2,3 λ^4 -triazol-4-yl)thiazole trifluoromethanesulfonate (L4H·OTf)

A suspension of 2-(1-methyl-1H-1,2,3-triazol-4-yl)thiazole (597.43 mg, 3.30 mmol) and MeOTf (411 μ L, 3.63 mmol, 1.1 equiv) in CH₂Cl₂ (15 mL) was stirred at -12 °C for 36 h (the reaction was monitored by TLC). All volatiles were evaporated under reduced pressure. The residue was washed with Et₂O. Analysis of the crude product by ¹H NMR spectroscopy showed a mixture of the desired L4H·BF₄ and 3-methyl-2-(1-methyl-1H-1,2,3-triazol-4-yl)-3 λ^4 -thiazole trifluoromethanesulfonate (**145**) in approximately a 1:3 ratio. Purification by column chromatography (SiO₂, CH₂Cl₂/MeOH gradient 20:1 to 0:1) yielded L4H·BF₄ in the first fraction (120 mg, 11%) and **145** in the second fraction (240 mg, 33%) as waxy pale yellow solids.

2-(1,3-Dimethyl-1H-1,2,3 λ^4 -triazol-4-yl)thiazole trifluoromethanesulfonate (L4H·OTf). ¹H NMR (400 MHz, CD₃CN): $\delta = 8.84$ (s, 1H, H-5), 8.14 (d, $^3J_{H-H} = 3.2$ Hz, 1H, CH=), 7.96 (d, $^3J_{H-H} = 3.2$ Hz, 1H, CH=), 4.50 (s, 3H, CH₃-N), 4.31 (s, 3H, CH₃-N). ¹³C{¹H} NMR (101 MHz, CD₃CN): $\delta = 150.3$ (C=N), 145.9 (CH=), 136.9 (C-4), 131.0 (C-5), 125.7 (CH=), 121.5 (q, $^1J_{C-F} = 319.32$, CF₃), 41.2 (CH₃-N), 41.20 (CH₃-N). ¹⁹F NMR (377 MHz, CD₃CN): $\delta = -79.38$ (s). MS HR-ESI [found 181.544 (M-OTf)⁺, calcd for C₇H₉N₄S requires 181.0542].

3-Methyl-2-(1-methyl-1H-1,2,3-triazol-4-yl)-3 λ^4 -thiazole trifluoromethanesulfonate (145). ¹H NMR (400 MHz, CD₃CN): $\delta = 8.74$ (s, 1H, H-5), 8.09 (d, $^3J_{H-H} = 4.0$ Hz, 1H, CH=), 7.99 (d, $^3J_{H-H} = 4.0$ Hz, 1H, CH=), 4.23 (s, 3H, CH₃-N), 4.21 (s, 3H, CH₃-N). ¹³C{¹H} NMR (101 MHz, CD₃CN): $\delta = 162.7$ (C=N), 140.0 (CH=), 135.2 (C-4), 128.7 (C-5), 123.4 (CH=), 121.7 (q, $^1J_{C-F} = 320.33$, CF₃), 42.1 (CH₃-N), 37.9 (CH₃-N). ¹⁹F NMR (377 MHz, CD₃CN): $\delta = -79.38$ (s). MS HR-ESI [found 181.0545 (M-OTf)⁺, C₇H₉N₄S requires 181.0542].

5.2.5.2.4. Preparation of [IrCl(L3)(COD)] (138)

A suspension of L3H·OTf (107 mg, 0.30 mmol), Me₄NCl (33 mg, 0.30 mmol), Ag₂O (140 mg, 0.6 mmol) in MeCN (8 mL) was stirred protected from light for 16 h. The suspension was then filtered through celite, and the volatiles removed under reduced pressure. The residue was suspended in CH₂Cl₂ (8 mL) and [Ir(μ-Cl)(COD)]₂ (100 mg, 0.15 mmol, 0.5 equiv) was added. The reaction mixture was stirred for 1 h protected from light, then filtered over celite, and all volatiles were removed under reduced pressure to yield the crude products. The compound triturated with pentane yielded product **138** as a light brown solid (90 mg, 55%). ¹H NMR (400 MHz, CD₂Cl₂): δ = 7.87 – 7.72 (m, 2H, CH=), 7.46 (m, 2H, CH=), 4.62 (bs, 1H, CH=, COD), 4.51 (bs, 1H, CH=, COD), 4.49 (s, 3H, CH₃-N), 4.43 (s, 3H, CH₃-N), 2.88 (bs, 1H, CH=, COD), 2.80 (bs, 1H, CH=, COD), 2.34 (bs, 1H, CH₂, COD), 2.19 (bs, 3H, CH₂, COD), 1.76 (bs, 2H, CH₂, COD), 1.58 (bs, 2H, CH₂, COD). ¹³C{¹H} NMR (101 MHz, CD₂Cl₂): δ = 176.7 (C-5), 154.4 (C=N), 150.7 (C), 141.7 (C), 133.3 (C-4), 126.6 (CH=), 125.5 (CH=), 120.6 (CH=), 111.4 (CH=), 83.3 (CH=, COD), 82.9 (CH=, COD), 52.1 (CH=, COD), 51.7 (CH=, COD), 42.4 (CH₃-N), 40.3 (CH₃-N), 34.3 (CH₂, COD), 33.7 (CH₂, COD), 30.2 (CH₂, COD). MS HR-ESI [found 515.1417 (M-Cl)⁺, C₁₉H₂₂IrN₄O requires 515.1410]. Anal. Calcd for C₁₉H₂₂ClIrN₄O: C, 41.49; H, 4.03; N, 10.19%. Found: C, 41.13; H, 3.87; N, 9.89%. Suitable crystals for X-ray diffraction were achieved by slow diffusion of pentane to dichloromethane solution.

5.2.5.2.5. Preparation of [IrCp*Cl(L3)]OTf (139) and [IrCp*Cl₂(L3)] (140)

A suspension of L3H·OTf (107 mg, 0.30 mmol), Me₄NCl (33 mg, 0.30 mmol), Ag₂O (140 mg, 0.6 mmol) in MeCN (8 mL) was stirred protected from light for 16 h. The suspension was then filtered through celite, and the volatiles removed under reduced pressure. The residue was suspended in CH₂Cl₂ (8 mL) and [Ir(Cp*)Cl₂]₂ (90 mg, 0.11 mmol, 0.4 equiv) was added. The reaction mixture was stirred for 5 h protected from light, then filtered over celite, and all volatiles were removed under reduced pressure to yield the crude products. Purification by column chromatography (neutral Al₂O₃; CH₂Cl₂/MeCN gradient, 3:1 to 0:1) yielded product [IrCp*Cl(L3)]OTf (**139**) in the first fraction (70 mg, 32%) and [IrCp*Cl₂(L3)] (**140**) in the second fraction (25 mg, 14%) as yellow and orange solids, respectively.

[IrCp*Cl(L3)]OTf (**139**). ¹H NMR (400 MHz, CD₂Cl₂): δ = 7.86 – 7.78 (m, 1H, CH=), 7.77 – 7.70 (m, 1H, CH=), 7.66 – 7.56 (m, 2H, CH=), 4.58 (s, 3H, CH₃-N), 4.37

(s, 3H, CH₃-N), 1.92 (s, 15H, CH₃, Cp*). ¹³C{¹H} NMR (101 MHz, CD₂Cl₂): δ = 161.1 (C-5), 160.4 (C=N), 152.0 (C), 137.3 (C), 136.3 (C-4), 128.1 (CH=), 127.4 (CH=), 121.2 (q, ¹J_{C-F} = 321.27, CF₃), 117.6 (CH=), 113.4 (CH=), 91.5 (C, Cp*), 40.6 (CH₃-N), 39.3 (CH₃-N), 10.4 (CH₃, Cp*). ¹⁹F NMR (377 MHz, CD₂Cl₂): δ = -78.92 (s). MS HR-ESI [found 577.1338 (M-OTf)⁺, C₂₁H₂₅ClIrN₄O requires 577.1340]. Anal. Calcd for C₂₂H₂₅ClF₃IrN₄O₄S: C, 36.39; H, 3.47; N, 7.72%. Found: C, 36.43; H, 3.58; N, 7.65%. Suitable crystals for X-ray diffraction were achieved by slow diffusion of pentane to dichloromethane solution.

[IrCp*Cl₂(L3)] (140). ¹H NMR (400 MHz, CDCl₃): δ = 7.80 – 7.74 (m, 1H, CH=), 7.57 – 7.51 (m, 1H, CH=), 7.42 – 7.34 (m, 2H, CH=), 4.46 (s, 3H, CH₃-N), 4.26 (s, 3H, CH₃-N), 1.74 (s, 15H, CH₃, Cp*). ¹³C{¹H} NMR (101 MHz, CDCl₃): δ = 152.0 (C-5), 151.9 (C=N), 149.7 (C), 140.4 (C), 135.5 (C-4), 125.1 (CH=), 123.9 (CH=), 119.8 (CH=), 110.0 (CH=), 87.6 (C, Cp*), 40.5 (CH₃-N), 37.6 (CH₃-N), 8.4 (CH₃, Cp*). MS HR-ESI [found 577.1341 (M-Cl)⁺, C₂₁H₂₅ClIrN₄O requires 577.1341]. Anal. Calcd for C₂₁H₂₅Cl₂IrN₄O with one molecule of H₂O: C, 40.00; H, 4.32; N, 8.89%. Found: C, 39.51; H, 3.72; N, 8.47%. Suitable crystals for X-ray diffraction were achieved by slow diffusion of pentane to dichloromethane solution.

5.2.5.2.6. Preparation of [IrCp*Cl(L4)]OTf (141)

A suspension of L4H-OTf (100 mg, 0.30 mmol), Me₄NCl (33 mg, 0.30 mmol), Ag₂O (140 mg, 0.6 mmol) in MeCN (8 mL) was stirred protected from light for 21 h. The suspension was then filtered through celite, and the volatiles removed under reduced pressure. The residue was suspended in CH₂Cl₂ (8 mL) and [Ir(Cp*)Cl₂]₂ (90 mg, 0.11 mmol, 0.4 equiv) was added. The reaction mixture was stirred for 20 h protected from light, then filtered over celite, and all volatiles were removed under reduced pressure to yield the crude products. Purification by column chromatography (neutral Al₂O₃; CH₂Cl₂/MeCN gradient, 3:1 to 0:1) yielded product **141** as yellow solid (70 mg, 37%). ¹H NMR (400 MHz, CDCl₃): δ = 7.98 (d, ³J_{H-H} = 3.5 Hz, 1H, CH=), 7.75 (d, ³J_{H-H} = 3.5 Hz, 1H, CH=), 4.50 (s, 3H, CH₃-N), 4.35 (s, 3H, CH₃-N), 1.86 (s, 16H, CH₃, Cp*). ¹³C{¹H} NMR (101 MHz, CDCl₃): δ = 158.5 (C-5), 158.3 (C=N), 145.7 (C-4), 140.7 (CH=), 122.9 (CH=), 120.7 (q, ¹J_{C-F} = 320.06, CF₃), 90.8 (C, Cp*), 39.9 (CH₃-N), 38.7 (CH₃-N), 9.7 (CH₃, Cp*). ¹⁹F NMR (377 MHz, CDCl₃): δ = -78.53 (s). MS HR-ESI [found 543.0961 (M-OTf)⁺, C₁₇H₂₃ClIrN₄S requires 543.0950]. Anal. Calcd for C₁₈H₂₃ClF₃IrN₄O₃S₂: C, 31.23; H, 3.35; N, 8.09; S, 9.26%. Found: C, 31.41;

H, 3.00; N, 7.77; S, 9.77%. Suitable crystals for X-ray diffraction were achieved by slow diffusion of pentane to dichloromethane solution.

5.2.5.2.7. Preparation of [IrCl(L2)(COD)] (142)

A suspension of L2H·BF₄ (90 mg, 0.30 mmol), Me₄NCl (33 mg, 0.30 mmol), Ag₂O (140 mg, 0.6 mmol) in MeCN/CH₂Cl₂ (10 mL 1:1 v/v) was stirred protected from light for 15 h. The suspension was then filtered through celite, and the volatiles removed under reduced pressure. The residue was suspended in CH₂Cl₂ (10 mL) under Ar atmosphere and [Ir(μ-Cl)(COD)]₂ (100 mg, 0.15 mmol, 0.5 equiv) was added. The reaction mixture was stirred for 1 h protected from light, then filtered over celite, and all volatiles were removed under reduced pressure. The crude product dissolved in Et₂O in order to precipitate out the remaining ligand. Purification by column chromatography (SiO₂; CH₂Cl₂/MeOH 20:1) yielded product **142** as a yellow solid (57 mg, 35%). ¹H NMR (400 MHz, CDCl₃): δ = 4.88 – 4.72 (m, 2H, CH₂-N), 4.55 (m, 1H, CH=, COD), 4.44 (m, 1H, CH=, COD), 4.14 (s, 3H, CH₃-N), 3.11 (s, 3H, CH₃-O), 2.82 – 2.68 (m, 2H, CH=, COD), 2.26 – 2.11 (s, 5H, CH₂, COD and CH₂), 2.04 (s, 3H, CH₃, CMe₂), 2.01 – 1.91 (m, 1H, CH₂, COD), 1.86 (s, 3H, CH₃, CMe₂), 1.74 – 1.58 (m, 2H, CH₂), 1.40 – 1.43 (m, 4H, CH₂, cod), 1.03 (t, ³J_{H-H} = 7.4 Hz, 3H, CH₃). ¹³C{¹H} NMR (101 MHz, CDCl₃): δ = 169.0 (C-5), 146.7 (C-4), 81.3 (CH=, COD), 79.8 (CH=, COD), 74.6 (CMe₂), 55.7 (CH₂-N), 51.3 (CH=, COD), 51.2 (CH₃-O), 51.1 (CH=, COD), 38.8 (CH₃-N), 33.6 (CH₂, COD), 33.4 (CH₂, COD), 30.0 (CH₂), 29.5 (CH₂, COD), 29.3 (CH₃, CMe₂), 28.9 (CH₃, CMe₂), 20.2 (CH₂, COD), 13.8 (CH₃). MS HR-ESI [found 548.2014 (M-Cl)⁺, C₁₉H₃₃IrN₃O requires 548.2006]. Anal. Calcd for C₁₉H₃₃ClIrN₃O: C, 41.71; H, 6.08; N, 7.68%. Found: C, 41.71; H, 6.10; N, 7.72%. Suitable crystals for X-ray diffraction were achieved by slow diffusion of pentane to dichloromethane solution.

5.2.5.2.8. Typical procedure for the transfer hydrogenation

The desired catalyst precursor (0.025 mmol), were treated under vacuum for 10 min. Under argon, propan-2-ol (2.5 mL), NaO^{*i*}Pr (0.1 M in ^{*i*}PrOH, 0.25 mL, 0.025 mmol) and the corresponding internal standard (0.166 mmol; mesytilene for ¹H NMR or dodecane for GC) were sequentially added and stirred at reflux for 10 minutes. The reaction was initiated by adding the substrate (0.5 mmol). Aliquotes were taken and were analyzed either by ¹H NMR or by GC.

5.2.5.2.9. Typical procedure for the base-free dehydrogenation of alcohols

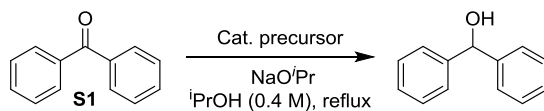
A mixture of substrate alcohol (0.1 mmol) and the iridium complex (0.005 mmol, final alcohol/Ir concentration always 20:1) in 1,2-dichlorobenzene (1 mL) was heated at 150 °C in a closed vial. Aliquots were taken at specific times, diluted with CDCl₃ and then analyzed by ¹H NMR spectroscopy. Hexamethylbenzene (0.0165 mmol) was used in all cases as internal standard in order to accurately determine the percentage conversions and yields.

5.2.5.2.10. Crystal Structure Determination

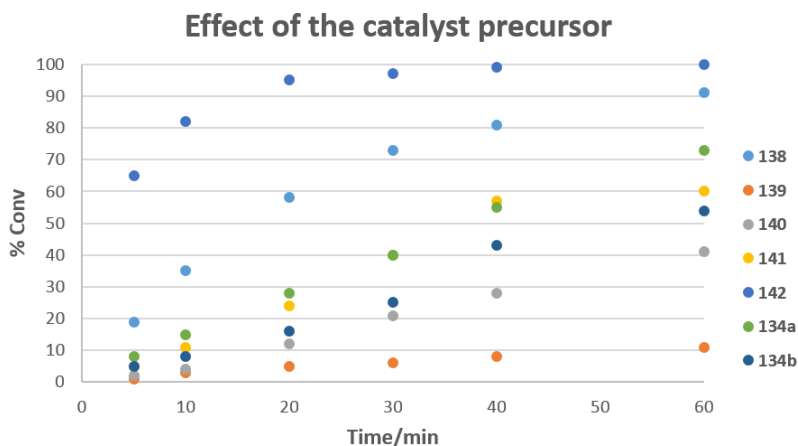
Crystal data for all compounds were collected on a Oxford Diffraction SuperNova area-detector diffractometer using mirror optics monochromated Mo K α radiation ($\lambda = 0.71073 \text{ \AA}$) and Al filtered. Data reduction was performed using the CrysAlisPro program.³⁰ The intensities were corrected for Lorentz and polarization effects, and an absorption correction based on the multi-scan method using SCALE3 ABSPACK in CrysAlisPro³⁰ was applied. The structure was solved by direct methods using SHELXT,³¹ which revealed the positions of all nonhydrogen atoms of the title compound. The non-hydrogen atoms were refined anisotropically. All H atoms were placed in geometrically calculated positions and refined using a riding model. Refinement of the structure was carried out on F² using full-matrix least-squares procedures, which minimized the function $\Sigma w(\text{Fo}^2 - \text{Fc}^2)^2$. The weighting scheme was based on counting statistics and included a factor to downweight the intense reflections. All calculations were performed using the SHELXL-2014/7 program.³² Further crystallographic details are compiled in the Supporting Information..

5.2.6. Supporting information

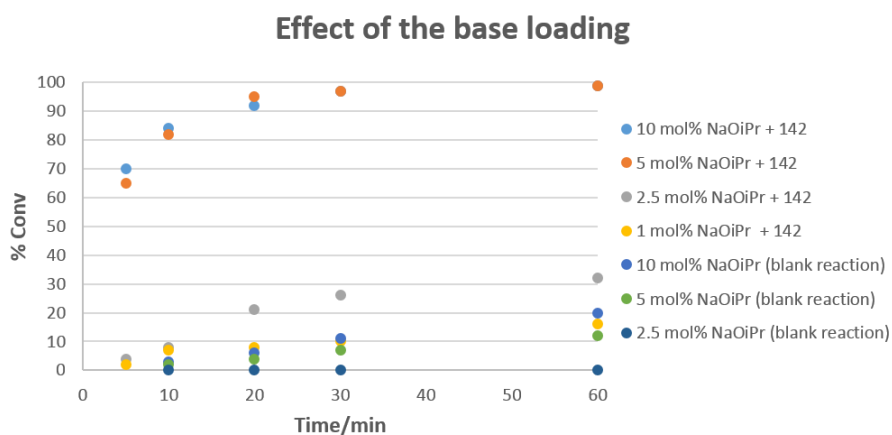
5.2.6.1. Conversion vs time plots of the TH of S1. Effect of the catalyst precursor, base loading and catalysts loading.



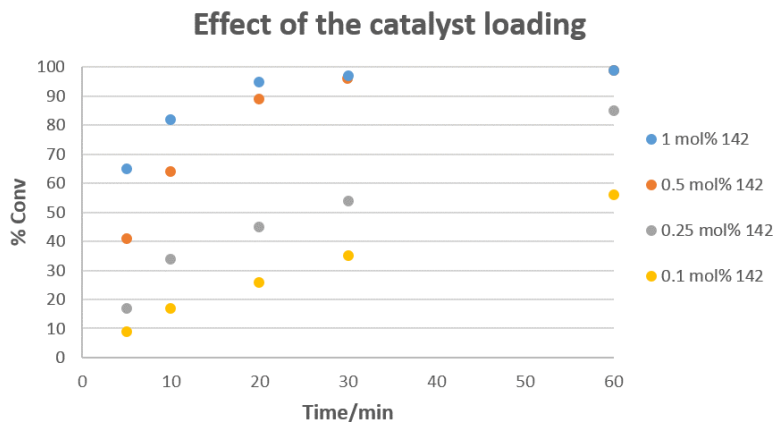
- **Effect of the catalyst precursor.** Conditions: 0.5 mol% cat precursor, 5 mol% base.



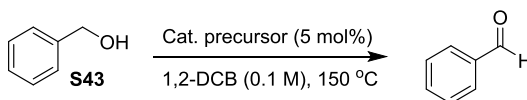
- **Effect of the base loading.** Conditions: 0.5 mol% of 142.



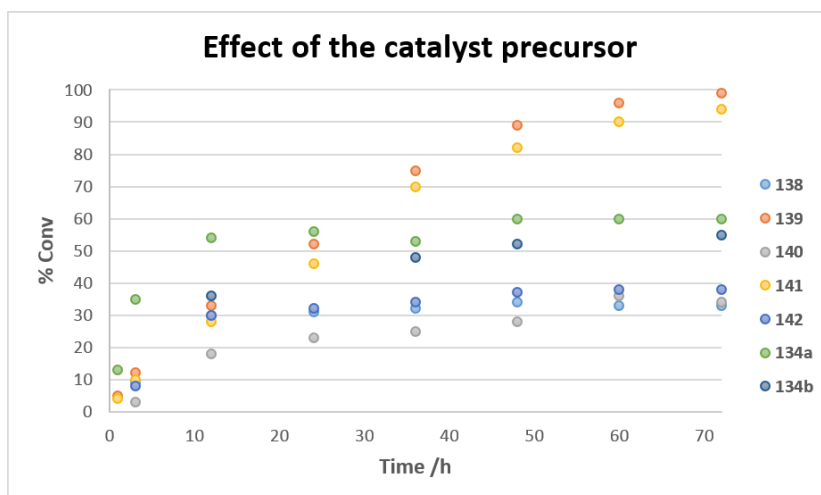
- **Effect of the catalyst loading.** Conditions: 5 mol% of base.



5.2.6.2. Conversion vs time plots of the dehydrogenation of S43. Effect of the catalyst precursors.

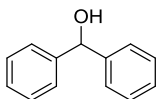


-**Effect of the catalyst precursor.** Conditions: 5 mol% cat precursor.

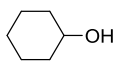


5.2.6.3. Characterization details and methods yield determination of TH and dehydrogenation products.

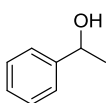
Diphenylmethanol.³³ ^1H NMR (CDCl_3): $\delta = 2.19$ (d, 1H, CH_3 , $J=4.0$ Hz), 5.86 (d, 1H, OH, $J=4.0$ Hz), 7.27 (m, 2H, CH=), 7.34 (m, 4H, CH=), 7.39 (m, 4H). Yield determined by ^1H -NMR using mesitylene as internal standard.



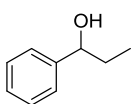
Cyclohexanol. ^1H NMR (CDCl_3): $\delta = 1.21$ (m, 4H, CH_2), 1.52 (m, 2H, CH_2), 1.70 (m, 2H, CH_2), 1.83 (m, 2H, CH_2), 2.23 (b, 1H, OH), 3.59 (m, 1H, CH). Yield determined by ^1H -NMR using mesitylene as internal standard.



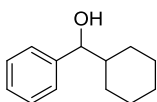
1-Phenylethan-1-ol.³³ ^1H NMR (CDCl_3): $\delta = 1.51$ (d, 3H, CH_3 , $J=6.8$ Hz), 1.80 (d, 1H, OH, $J=3.2$ Hz), 4.91 (dq, 1H, CH, $J=6.8$, $J=3.2$ Hz), 7.31-7.24 (m, 1H, CH=), 7.41-7.33 (m, 4H). Yield determined by GC using Chiralsil-Dex CB column (80 kPa H_2 , Hold 110 $^\circ\text{C}$ for 15 min, rate 10 $^\circ\text{C}/\text{min}^{-1}$ to 180 $^\circ\text{C}$ and hold for 20 min). t_{R} 14.9 min (*R*); t_{R} 16.0 min (*S*).



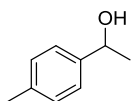
1-Phenylpropan-1-ol.³³ ^1H NMR (CDCl_3): $\delta = 0.92$ (t, 3H, $J=7.6$ Hz, CH_3), 1.80 (m, 2H, CH_2), 4.61 (d, 1H, CH, $J=6.8$ Hz), 7.30 (m, 5H, CH=). Yield determined by GC using Chiralsil-Dex CB column (80 kPa H_2 , Hold 110 $^\circ\text{C}$ for 15 min, rate 10 $^\circ\text{C}/\text{min}^{-1}$ to 180 $^\circ\text{C}$ and hold for 20 min). t_{R} 18.9 min (*R*); t_{R} 19.1 min (*S*).



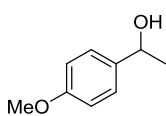
Cyclohexyl(phenyl)methanol.³⁴ ^1H NMR (CDCl_3): $\delta = 0.91$ –1.24 (m, 5H, CH_2), 1.29–1.35 (m, 1H, CH_2), 1.59-1.65 (m, 3H, CH_2), 1.74-1.86 (m, 2H, CH_2), 1.97-2.00 (m, 1H, CH), 4.37 (d, 1H, $J=6.9$ Hz), 7.24-7.35 (m, 5H, CH=). Yield determined by ^1H -NMR using mesitylene as internal standard.



1-(*p*-Tolyl)ethan-1-ol.³⁴ ^1H NMR (CDCl_3): $\delta = 1.48$ (d, 3H, $J=6.4$ Hz), 1.79 (b, 1H, OH), 2.34 (s, 3H, CH_3), 4.82-4.92 (m, 1H, CH), 7.16 (d, 2H, CH=, $J=7.8$ Hz), 7.27 (d, 2H, CH=, $J=7.8$ Hz). Yield determined by GC using Chiralsil-Dex CB column (80 kPa H_2 , Hold 110 $^\circ\text{C}$ for 15 min, rate 10 $^\circ\text{C}/\text{min}^{-1}$ to 180 $^\circ\text{C}$ and hold for 20 min). t_{R} 14.2 min (*R*); t_{R} 15.3 min (*S*).

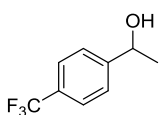


1-(4-Methoxyphenyl)ethan-1-ol.³⁴ ¹H NMR (CDCl₃): δ = 1.48 (d, 3H, *J*=6.2 Hz), 1.73



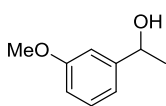
(b, 1H, OH), 3.81 (s, 3H, CH₃), 4.82-4.91 (m, 1H, CH), 6.88 (d, 2H, CH=, *J*=7.8 Hz), 7.30 (d, 2H, CH=, *J*=7.8 Hz, 2H). Yield determined by GC using Chiralsil-Dex CB column (80 kPa H₂, Hold 110 °C for 15 min, rate 10 °C/min⁻¹ to 180 °C and hold for 20 min). t_R 21.9 min (*R*); t_R 22.1 min (*S*).

1-(4-(Trifluoromethyl)phenyl)ethan-1-ol.³⁴ ¹H NMR (CDCl₃): δ = 1.47 (d, 3H, CH₃,



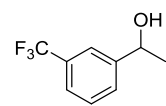
J=6.6 Hz), 2.43 (b, 1H, OH), 4.87-4.96 (m, 1H, CH), 7.45 (d, 2H, CH=, *J*=8.0 Hz), 7.58 (d, 2H, CH=, *J*=7.6 Hz). Yield determined by GC using Chiralsil-Dex CB column (80 kPa H₂, Hold 110 °C for 15 min, rate 10 °C/min⁻¹ to 180 °C and hold for 20 min). t_R 16.1 min (*R*); t_R 18.3 min (*S*).

1-(3-Methoxyphenyl)ethan-1-ol.³⁴ ¹H NMR (CDCl₃): δ = 1.48 (d, 3H, CH₃, *J*=6.2



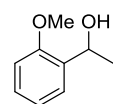
Hz), 1.73 (b, 1H, OH), 3.81 (s, 3H, CH₃), 4.82-4.91 (m, 1H, CH), 6.88 (d, 2H, CH=, *J*=7.8 Hz), 7.30 (d, 2H, CH=, *J*=7.8 Hz). Yield determined by GC using Chiralsil-Dex CB column (80 kPa H₂, Hold 110 °C for 15 min, rate 10 °C/min⁻¹ to 180 °C and hold for 20 min). t_R 22.0 min (*R*); t_R 22.2 min (*S*).

1-(3-(Trifluoromethyl)phenyl)ethan-1-ol.³⁴ ¹H NMR (CDCl₃): δ = 1.52 (d, 3H, CH₃,



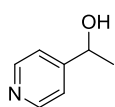
J=6.6 Hz), 1.90 (b, 1H, OH), 4.93-5.02 (m, 1H, CH), 7.43-7.51 (m, 1H, CH=), 7.51-7.61 (m, 2H, CH=), 7.65 (s, 1H, CH=). Yield determined by GC using Chiralsil-Dex CB column (100 kPa H₂, Hold 110 °C for 15 min, rate 10 °C/min⁻¹ to 180 °C and hold for 20 min). t_R 5.6 min (*R*); t_R 6.4 min (*S*).

1-(2-Methoxyphenyl)ethan-1-ol.³⁴ ¹H NMR (CDCl₃): δ = 1.51 (d, 3H, CH₃, *J*=6.2



Hz), 2.66 (b, 1H, OH), 3.87 (s, 3H, CH₃), 5.05-5.14 (m, 1H, CH), 6.88 (d, 1H, CH=, *J*=8.0 Hz), 6.93-7.00 (m, 1H, CH=), 7.21-7.28 (m, 1H, CH=), 7.31-7.37 (m, 1H, CH=). Yield determined by GC using Chiralsil-Dex CB column (80 kPa H₂, Hold 110 °C for 15 min, rate 10 °C/min⁻¹ to 180 °C and hold for 20 min). t_R 21.2 min (*R*); t_R 21.5 min (*S*).

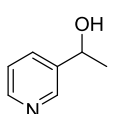
1-(Pyridin-4-yl)ethan-1-ol.³⁴ ¹H NMR (CDCl₃): δ = 1.46 (d, 3H, CH₃, J =6.4 Hz), 4.13



(s, 1H, OH), 4.86 (q, 1H, CH, J =6.4 Hz), 7.27 (d, 2H, J =4.5 Hz, CH=), 8.42 (d, 1H, J =4.5 Hz, OH). Yield determined by GC using Chiraldex β -DM column (100 kPa H₂, Hold 110 °C for 25 min, rate 3 °C/min⁻¹ to 180

°C and hold for 5 min). t_R 22.8 min (*R*); t_R 23.6 min (*S*).

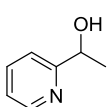
1-(Pyridin-3-yl)ethan-1-ol.³⁴ ¹H NMR (CDCl₃): δ = 1.44 (d, 3H, CH₃, J =6.4 Hz), 4.6



(b, 1H, OH), 4.85 (q, 1H, CH, J =6.4 Hz), 7.15-7.24 (m, 1H, CH=), 7.64-7.75 (m, 1H, CH=), 8.29 (dd, 1H, CH=, J =1.3 Hz, J =4.6 Hz), 8.38 (d, 1H, CH=, J =2.4 Hz). Yield determined by ¹H-NMR using mesitylene as

internal standard.

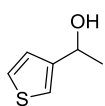
1-(Pyridin-2-yl)ethan-1-ol.³³ ¹H NMR (CDCl₃): δ = 1.51 (d, 3H, CH₃, J =6.4 Hz), 4.7



(b, 1H, OH), 4.91 (q, 1H, CH, J =6.4 Hz), 7.15-7.23 (m, 1H, CH=), 7.34 (d, 1H, CH=, J =8.0 Hz), 7.69 (m, 1H, CH=), 8.51 (d, 1H, CH=, J =4.0 Hz).

Yield determined by ¹H-NMR using mesitylene as internal standard.

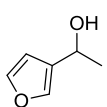
1-(Thiophen-3-yl)ethan-1-ol.³⁴ ¹H NMR (CDCl₃): δ = 1.52 (d, 1H, CH₃, J =6.8 Hz),



1.89 (s, 1H, OH), 4.97 (q, 1H, CH, J =6.8 Hz), 7.09-7.10 (m, 1H, CH=), 7.29-7.31 (m, 1H, CH=), 7.18-7.20 (m, 1H, CH=). Yield determined by ¹H-

NMR using mesitylene as internal standard.

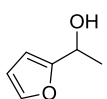
1-(Furan-3-yl)ethan-1-ol.³⁴ ¹H NMR (CDCl₃): δ = 1.54 (d, 3H, CH₃, J =6.8 Hz), 2.30



(b, 1H, OH), 4.88 (q, 1H, CH, J =6.4 Hz), 6.22 (d, 1H, CH=, J =3.2 Hz), 6.32 (dd, 1H, CH=, J =3.2 Hz, J =1.2 Hz), 7.35-7.40 (m, 1H, CH=). Yield

determined by ¹H-NMR using mesitylene as internal standard.

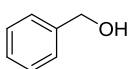
1-(Furan-2-yl)ethan-1-ol.³³ ¹H NMR (CDCl₃): δ = 1.54 (d, 3H, CH₃, J =6.4 Hz), 1.99



(b, 1H, OH), 4.88 (q, 1H, CH, J =6.4 Hz), 6.22 (d, 1H, CH=, J =3.2 Hz), 6.32 (dd, 1H, CH=, J =3.2 Hz, J =2.0 Hz), 7.37 (d, 1H, CH=, J =2.0 Hz).

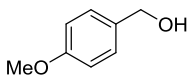
Yield determined by ¹H-NMR using mesitylene as internal standard.

Benzyl alcohol.³³ ¹H NMR (CDCl₃): δ = 2.62 (b, 1H, OH), 4.59 (s, 2H, CH₂), 7.28 (m,

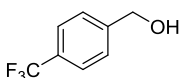


5H, CH=). Yield determined by ¹H-NMR using mesitylene as internal standard.

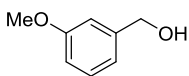
(4-Methoxyphenyl)methanol.³⁸ ¹H NMR (CDCl₃): δ = 2.57 (b, 1H), 3.77 (s, 3H, CH₃O), 4.53 (s, 2H, CH₂), 6.85 (d, 2H, CH=, J = 8.6 Hz), 7.23 (d, 2H, CH=, J = 8.6 Hz). Yield determined by ¹H-NMR using mesitylene as internal standard.



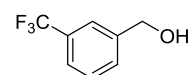
(4-(Trifluoromethyl)phenyl)methanol.³³ ¹H NMR (CDCl₃): δ = 1.93 (b, 1H), 4.58 (d, 2H, CH₂, J = 4.8 Hz), 7.55 (d, 2H, CH=, J = 8.4 Hz), 8.23 (d, 2H, CH=, J = 8.4 Hz). Yield determined by ¹H-NMR using mesitylene as internal standard.



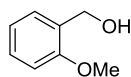
(3-Methoxyphenyl)methanol.³³ ¹H NMR (CDCl₃): δ = 2.67 (b, 1H), 3.83 (s, 3H, CH₃O), 4.66 (s, 2H, CH₂), 6.89 (m, 2H, CH=), 7.26 (m, 2H, CH=). Yield determined by ¹H-NMR using mesitylene as internal standard.



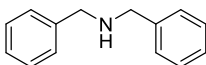
(3-(Trifluoromethyl)phenyl)methanol.³³ ¹H NMR (CDCl₃): δ = 1.91 (b, 1H), 4.76 (b, 2H, CH₂), 7.47 (t, 1H, CH=, J = 7.4 Hz), 7.55 (m, 2H, CH=), 7.64 (s, 1H, CH=). Yield determined by ¹H-NMR using mesitylene as internal standard.



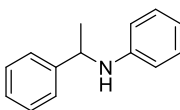
(2-Methoxyphenyl)methanol.³⁹ ¹H NMR (CDCl₃): δ = 2.52 (b, 1H), 3.73 (s, 3H, CH₃O), 4.6 (d, 2H, CH₂, J = 4.6 Hz), 6.80 (m, 2H, CH=), 7.16 (m, 2H, CH=). Yield determined by ¹H-NMR using mesitylene as internal standard.



Dibenzylamine. ¹H NMR (CDCl₃): δ = 1.60 (b, 1H, NH), 3.78 (s, 4H, CH₂), 7.2-7.4 (m, 10H, CH=). Yield determined by GC using HP-5 column (150 kPa H₂, Hold 200 °C for 0 min, rate 10 °C/min⁻¹ to 280 °C and hold for 100 min). t_R 3.1 min.



***N*-(1-Phenylethyl)aniline.**³³ ¹H NMR (CDCl₃): δ = 1.51 (d, 3H, CH₃, J = 6.8 Hz), 4.00 (b, 1H, NH), 4.48 (q, 1H, CH, J = 6.8 Hz), 6.50 (d, 2H, CH=, J = 8.0 Hz), 6.63 (t, 1H, CH=, J = 7.2 Hz), 7.08 (t, 2H, CH=, J = 8.0 Hz), 7.23 (m, 1H, CH=), 7.33 (m, 4H, CH=). Yield determined by ¹H-NMR using mesitylene as internal standard.



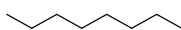
Cycloheptane. $^1\text{H NMR}$ (CDCl_3): $\delta = 1.55$ (s, 14H, CH_2). Yield determined by $^1\text{H-NMR}$ using mesitylene as internal standard.



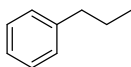
Cyclooctane. $^1\text{H NMR}$ (CDCl_3): $\delta = 1.52$ (s, 16H, CH_2). Yield determined by $^1\text{H-NMR}$ using mesitylene as internal standard.



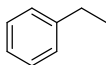
Octane.⁴³ $^1\text{H NMR}$ (CDCl_3): $\delta = 0.89$ (m, 6H, CH_3), 1.27 (b, 12H, CH_2). Yield determined by GC using HP-5 column (100 kPa H_2 , Hold 50 °C for 10 min, rate 3 °C/min⁻¹ to 180 °C and hold for 20 min). t_R 5.2 min.



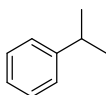
Propylbenzene.³³ $^1\text{H NMR}$ (CDCl_3): $\delta = 0.91$ (t, 3H, CH_3 , $J=6.8$ Hz), 1.91 (m, 2H, CH_2), 2.49 (m, 2H, CH_2), 7.0-7.4 (m, 5H, CH=). Yield determined by GC using HP-5 column (100 kPa H_2 , Hold 80 °C for 10 min, rate 3 °C/min⁻¹ to 120 °C and hold for 20 min). t_R 5.4 min.



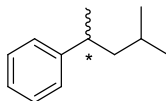
Ethylbenzene.⁴³ $^1\text{H NMR}$ (CDCl_3): $\delta = 1.22$ (t, 3H, CH_3 , $J=6.4$ Hz), 2.63 (q, 2H, CH_2 , $J=6.4$ Hz), 7.0-7.5 (m, 5H, CH=). Yield determined by GC using HP-5 column (100 kPa H_2 , Hold 80 °C for 10 min, rate 3 °C/min⁻¹ to 120 °C and hold for 20 min). t_R 3.8 min.



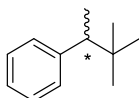
Cumene. $^1\text{H NMR}$ (CDCl_3): $\delta = 1.21$ (d, 6H, CH_3 , $J=7.2$ Hz), 2.82 (sp, 1H, CH , $J=7.2$ Hz), 7.1-7.40 (m, 5H, CH=). Yield determined by $^1\text{H-NMR}$ using mesitylene as internal standard using mesitylene as internal standard.



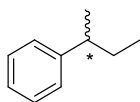
(4-Methylpentan-2-yl)benzene.³³ $^1\text{H NMR}$ (CDCl_3): $\delta = 0.84$ (d, 3H, $J = 6.8$ Hz), 0.87 (d, 3H, $J = 6.8$ Hz), 1.21 (d, 3H, $J = 7.2$ Hz), 1.36 (m, 2H), 1.45 (m, 1H), 2.79 (m, 1H), 7.19 (m, 2H), 7.29 (m, 3H). Yield determined by GC using Chiradex B-DM column (100 kPa H_2 , 60 °C for 30 min, 3 °C/min until 175 °C). t_R 27.9 min (*S*); t_R 29.5 min (*R*).



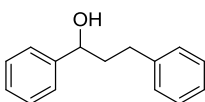
(3,3-Dimethylbutan-2-yl)benzene.³³ $^1\text{H NMR}$ (CDCl_3): $\delta = 0.83$ (s, 9H), 1.24 (d, 3H, $J=6.8$ Hz), 2.54 (q, 1H, $J=6.8$ Hz), 7.1-7.3 (m, 5H). Yield determined by GC using Chiradex B-DM column (100 kPa H_2 , 60 °C for 30 min, 3 °C/min until 175 °C). t_R 47.2 min (*S*); t_R 47.8 min (*R*).



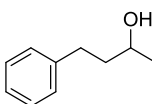
sec-Butylbenzene.³³ ¹H NMR (CDCl₃): δ = 0.80 (t, 3H, *J* = 7.6 Hz), 1.22 (d, 3H, *J* = 6.4 Hz), 1.61 (m, 2H), 2.60 (m, 1H), 7.18 (m, 3H), 7.33 (m, 2H). Yield determined by GC using Chiradex B-DM column (100 kPa H₂, 50 °C for 30 min, 2 °C/min until 175 °C). t_R 20.4 min (S); t_R 20.8 min (R).



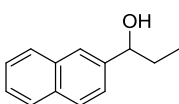
1,3-Diphenylpropan-1-ol.³³ ¹H NMR (CDCl₃): δ = 1.97-2.11 (m, 1H, CH₂), 2.12-2.17 (m, 1H, CH₂), 2.64-2.71 (m, 1H, CH₂), 2.72-2.78 (m, 1H, CH₂), 4.70 (dd, 1H, CH, *J* = 8.0 Hz, *J* = 5.6 Hz), 7.17 (m, 3H, CH=), 7.21-7.28 (m, 3H, CH=), 7.30-7.37 (m, 4H, CH=). Yield determined by ¹H-NMR using mesytilene as internal standard.



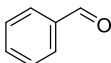
4-Phenylbutan-2-ol.³³ ¹H NMR (CDCl₃): δ = 1.21 (d, 3H, CH₃, *J* = 6.0 Hz), 1.73 (m, 2H, CH₂), 2.65 (m, 1H, CH₂), 2.74 (m, 1H, CH₂), 3.82 (m, 1H, CH), 7.12 (m, 3H, CH=), 7.25 (m, 2H, CH=). Yield determined by ¹H-NMR using mesytilene as internal standard.



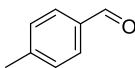
1-(Naphthalen-2-yl)propan-1-ol.³⁵ ¹H NMR (CDCl₃): δ = 0.94 (t, 3H, *J* = 8.0 Hz, CH₃), 1.82-1.91 (m, 2H, CH₂), 4.75 (t, 1H, CH, *J* = 6.4 Hz), 7.48 (m, 3H, CH=), 7.77 (s, 1H, CH=), 7.82 (m, 3H, CH=). Yield determined by GC using Chiralsil-Dex CB column (80 kPa H₂, Hold 110 °C for 15 min, rate 10 °C/min⁻¹ to 180 °C and hold for 20 min). t_R 30.9 min (R); t_R 31.3 min (S).



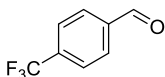
Benzaldehyde. ¹H NMR (CDCl₃): δ = 7.52 (m, 2H, CH=), 7.63 (m, 1H, CH=), 7.89 (m, 2H, CH=), 10.02 (s, 1H, CHO). Yield determined by ¹H-NMR using mesytilene as internal standard.



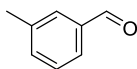
4-Methylbenzaldehyde.³³ ¹H NMR (CDCl₃): δ = 2.41 (s, 3H, CH₃), 7.30 (d, 2H, CH=, *J* = 7.4 Hz), 7.75 (d, 2H, CH=, *J* = 7.4 Hz), 10.03 (s, 1H, CHO). Yield determined by ¹H-NMR using mesytilene as internal standard.



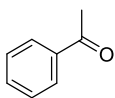
4-Trifluoromethylbenzaldehyde. ¹H NMR (CDCl₃): δ = 7.81 (d, 2H, CH=, *J* = 7.8 Hz), 7.99 (d, 2H, CH=, *J* = 7.8 Hz), 10.10 (s, 1H, CHO). Yield determined by ¹H-NMR using mesytilene as internal standard.



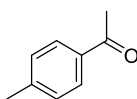
3-Methylbenzaldehyde. $^1\text{H NMR}$ (CDCl_3): $\delta = 2.50$ (s, 3H, CH_3), 7.46 (m, 2H, $\text{CH}=\text{O}$), 7.64 (m, 1H, $\text{CH}=\text{O}$), 9.93 (s, 1H, CHO). Yield determined by $^1\text{H-NMR}$ using mesitylene as internal standard.



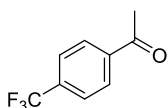
Acetophenone. $^1\text{H NMR}$ (CDCl_3): $\delta = 2.54$ (s, 3H, CH_3), 7.45 (m, 2H, $\text{CH}=\text{O}$), 7.63 (m, 1H, $\text{CH}=\text{O}$), 7.92 (m, 2H, $\text{CH}=\text{O}$). Yield determined by GC using Chiralsil-Dex CB column (80 kPa H_2 , Hold 110 $^\circ\text{C}$ for 15 min, rate 10 $^\circ\text{C}/\text{min}^{-1}$ to 180 $^\circ\text{C}$ and hold for 20 min). t_R 4.2 min.



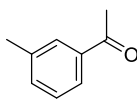
1-(*p*-Tolyl)ethan-1-one. $^1\text{H NMR}$ (CDCl_3): $\delta = 2.40$ (s, 3H, CH_3), 2.56 (s, 3H, CH_3), 7.21 (d, 2H, $\text{CH}=\text{O}$, $J=7.8$ Hz), 7.85 (d, 2H, $\text{CH}=\text{O}$, $J=7.8$ Hz). Yield determined by GC using Chiralsil-Dex CB column (100 kPa H_2 , Hold 110 $^\circ\text{C}$ for 15 min, rate 10 $^\circ\text{C}/\text{min}^{-1}$ to 180 $^\circ\text{C}$ and hold for 20 min). t_R 4.4 min.



1-(4-(Trifluoromethyl)phenyl)ethan-1-one. $^1\text{H NMR}$ (CDCl_3): $\delta = 2.66$ (s, 3H, CH_3), 7.73 (d, 2H, $\text{CH}=\text{O}$, $J=8.0$ Hz), 8.04 (m, 1H, $\text{CH}=\text{O}$, $J=8.0$ Hz). Yield determined by GC using Chiralsil-Dex CB column (80 kPa H_2 , Hold 110 $^\circ\text{C}$ for 15 min, rate 10 $^\circ\text{C}/\text{min}^{-1}$ to 180 $^\circ\text{C}$ and hold for 20 min). t_R 3.8 min.

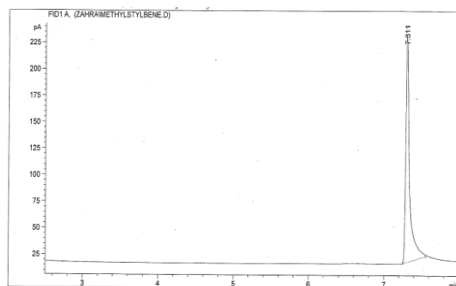


1-(*m*-Tolyl)ethan-1-one. $^1\text{H NMR}$ (CDCl_3): $\delta = 2.40$ (s, 3H, CH_3), 2.57 (s, 3H, CH_3), 7.32 (m, 3H, $\text{CH}=\text{O}$), 7.75 (m, 2H, $\text{CH}=\text{O}$). Yield determined by GC using Chiralsil-Dex CB column (80 kPa H_2 , Hold 110 $^\circ\text{C}$ for 15 min, rate 10 $^\circ\text{C}/\text{min}^{-1}$ to 180 $^\circ\text{C}$ and hold for 20 min). t_R 4.3 min.

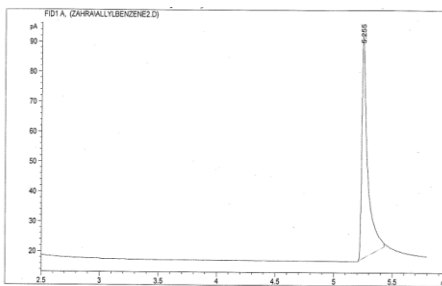


5.2.6.4 GC's, ¹H-NMR and mass spectra of transfer hydrogenation and transfer deuteration experiments of substrates S30 and S31

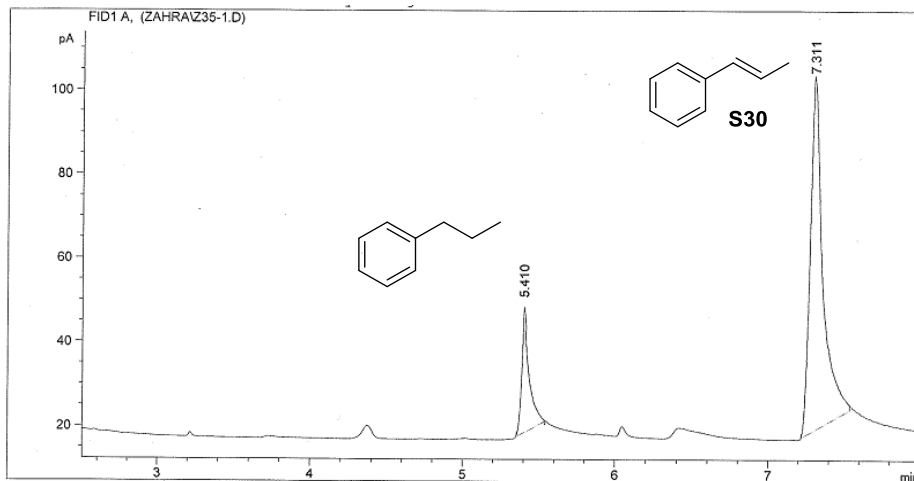
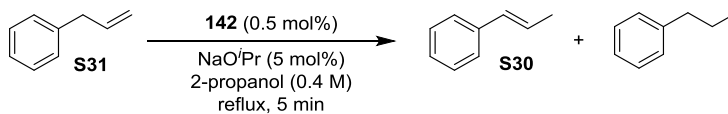
GC of S30



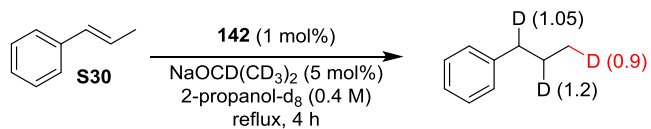
GC of S31



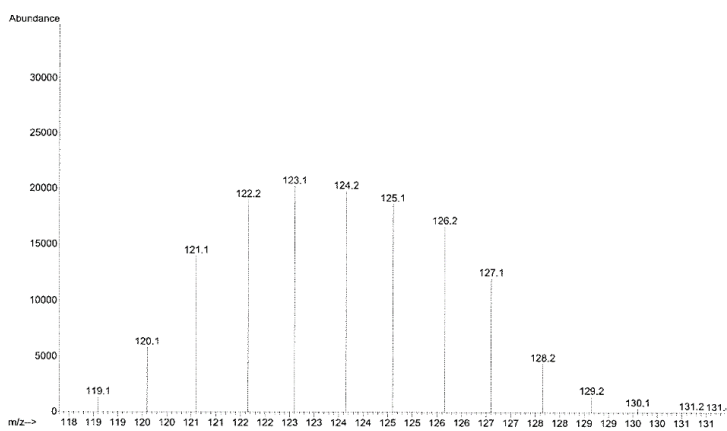
GC of TH of S31 after 5 min



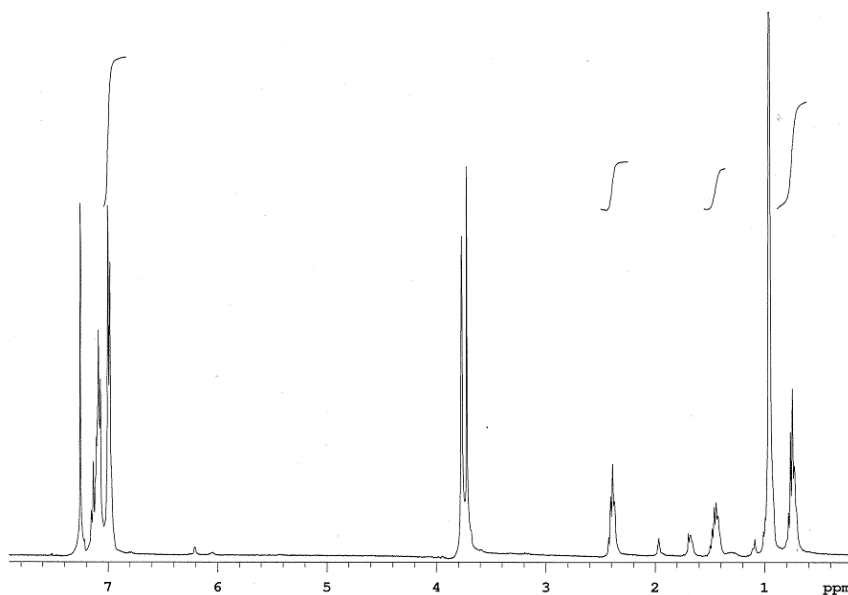
Mass spectrum and $^1\text{H-NMR}$ of transfer deuteration of S30



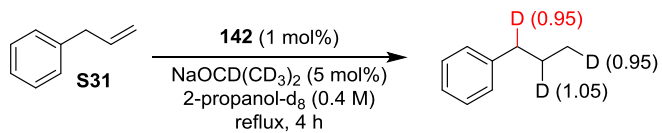
Mass spectra of the deuterated final product



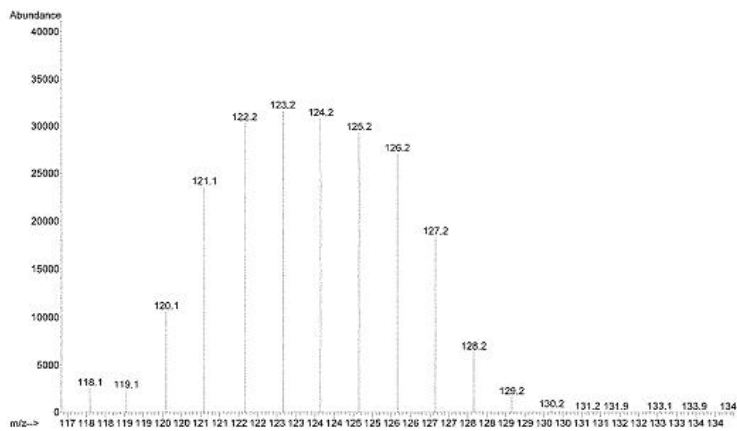
$^1\text{H-NMR}$ of the deuterated final product



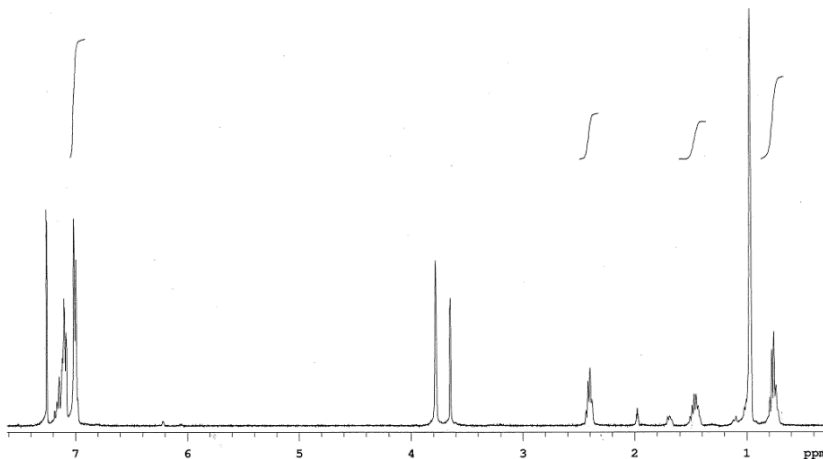
Mass spectrum and ¹H-NMR of transfer deuterogenation of S31



Mass spectra of the deuterated final product



¹H-NMR of the deuterated final product



5.2.6.5. Crystal data and structure refinement for ligand L3H·OTf and Ir-complexes 138-142.

- Crystal data and structure refinement for ligand L3H·OTf

Empirical formula	C ₁₂ H ₁₁ F ₃ N ₄ O ₄ S
Formula weight	364.31
Temperature	173(2) K
Wavelength	0.71073 Å
Crystal system	Monoclinic
Space group	P 2 ₁ /n
Unit cell dimensions	a = 10.49444(10) Å α = 90°. b = 8.65841(7) Å β = 93.2254(8)°. c = 16.56110(15) Å γ = 90°.
Volume	1502.44(2) Å ³
Z	4
Density (calculated)	1.611 Mg/m ³
Absorption coefficient	0.277 mm ⁻¹
F(000)	744
Crystal size	0.367 x 0.228 x 0.073 mm ³
Theta range for data collection	2.242 to 26.369°.
Index ranges	-13<=h<=13, -10<=k<=10, -20<=l<=20
Reflections collected	25549
Independent reflections	3066 [R(int) = 0.0284]
Completeness to theta = 25.242°	100 %
Absorption correction	Semi-empirical from equivalents
Max. and min. transmission	1 and 0.80197
Refinement method	Full-matrix least-squares on F ²
Data / restraints / parameters	3066 / 0 / 219
Goodness-of-fit on F ²	1.059
Final R indices [I>2σ(I)]	R1 = 0.0331, wR2 = 0.0862
R indices (all data)	R1 = 0.0377, wR2 = 0.0896
Largest diff. peak and hole	0.351 and -0.32 e.Å ⁻³

- **Crystal data and structure refinement for [IrCl(L3)(COD)] (138).**

Empirical formula	C ₁₉ H ₂₂ Cl Ir N ₄ O
Formula weight	550.05
Temperature	173(2) K
Wavelength	0.71073 Å
Crystal system	Orthorhombic
Space group	P n a 21
Unit cell dimensions	a = 21.2461(2) Å α = 90°. b = 7.15410(10) Å β = 90°. c = 12.48750(10) Å γ = 90°.
Volume	1898.06(4) Å ³
Z	4
Density (calculated)	1.925 Mg/m ³
Absorption coefficient	7.191 mm ⁻¹
F(000)	1064
Crystal size	0.301 x 0.215 x 0.022 mm ³
Theta range for data collection	1.917 to 26.371°.
Index ranges	-26<=h<=26, -8<=k<=8, -15<=l<=15
Reflections collected	25483
Independent reflections	3856 [R(int) = 0.0343]
Completeness to theta = 25.242°	100 %
Absorption correction	Gaussian
Max. and min. transmission	0.857 and 0.324
Refinement method	Full-matrix least-squares on F ²
Data / restraints / parameters	3856 / 5 / 250
Goodness-of-fit on F ²	1.083
Final R indices [I>2sigma(I)]	R1 = 0.0186, wR2 = 0.0401
R indices (all data)	R1 = 0.0214, wR2 = 0.0415
Absolute structure parameter	-0.022(10)
Largest diff. peak and hole	0.647 and -0.472 e.Å ⁻³

- **Crystal data and structure refinement for [IrCp*Cl(L3)]OTf (139).**

Empirical formula	C ₂₂ H ₂₅ Cl F ₃ Ir N ₄ O ₄ S
Formula weight	726.17
Temperature	173(2) K
Wavelength	0.71073 Å
Crystal system	Triclinic
Space group	P -1
Unit cell dimensions	a = 8.4198(3) Å α = 70.626(4)° b = 10.8029(4) Å β = 77.463(4)° c = 15.3887(8) Å γ = 80.308(3)°
Volume	1281.91(10) Å ³
Z	2
Density (calculated)	1.881 Mg/m ³
Absorption coefficient	5.451 mm ⁻¹
F(000)	708
Crystal size	0.365 x 0.253 x 0.083 mm ³
Theta range for data collection	2.009 to 28.269°.
Index ranges	-11 ≤ h ≤ 11, -14 ≤ k ≤ 14, -20 ≤ l ≤ 20
Reflections collected	64250
Independent reflections	6374 [R(int) = 0.0319]
Completeness to theta = 25.242°	100 %
Absorption correction	Gaussian
Max. and min. transmission	0.648 and 0.248
Refinement method	Full-matrix least-squares on F ²
Data / restraints / parameters	6374 / 279 / 405
Goodness-of-fit on F ²	1.111
Final R indices [I > 2σ(I)]	R1 = 0.0344, wR2 = 0.0818
R indices (all data)	R1 = 0.0351, wR2 = 0.0823
Largest diff. peak and hole	9.196 and -0.954 e.Å ⁻³

- **Crystal data and structure refinement for [IrCp*Cl₂(L3)] (140).**

Empirical formula	C ₂₁ H ₂₅ Cl ₂ Ir N ₄ O
Formula weight	612.55
Temperature	100(2) K
Wavelength	0.71073 Å
Crystal system	Monoclinic
Space group	P2(1)/c
Unit cell dimensions	a = 8.4361(6)Å α = 90°. b = 16.4263(11)Å β = 103.6862(14)°. c = 16.0490(10)Å γ = 90°.
Volume	2160.8(3) Å ³
Z	4
Density (calculated)	1.883 Mg/m ³
Absorption coefficient	6.446 mm ⁻¹
F(000)	1192
Crystal size	0.20 x 0.15 x 0.10 mm ³
Theta range for data collection	1.801 to 30.595°.
Index ranges	-12<=h<=11, -23<=k<=23, -22<=l<=21
Reflections collected	21761
Independent reflections	6354[R(int) = 0.0235]
Completeness to theta =30.595°	95.5%
Absorption correction	Multi-scan
Max. and min. transmission	0.565 and 0.402
Refinement method	Full-matrix least-squares on F ²
Data / restraints / parameters	6354/ 0/ 269
Goodness-of-fit on F ²	1.034
Final R indices [I>2sigma(I)]	R1 = 0.0174, wR2 = 0.0403
R indices (all data)	R1 = 0.0201, wR2 = 0.0411
Largest diff. peak and hole	1.341 and -0.747 e.Å ⁻³

- **Crystal data and structure refinement for [IrCp*Cl(L4)] (141).**

Empirical formula	C ₁₈ H ₂₃ Cl F ₃ Ir N ₄ O ₃ S ₂
Formula weight	692.17
Temperature	100(2) K
Wavelength	0.71073 Å
Crystal system	Monoclinic
Space group	P2(1)/n
Unit cell dimensions	a = 8.5926(17) Å α = 90°. b = 16.579(3) Å β = 99.975(5)°. c = 16.372(3) Å γ = 90°.
Volume	2297.0(8) Å ³
Z	4
Density (calculated)	2.002 Mg/m ³
Absorption coefficient	6.164 mm ⁻¹
F(000)	1344
Crystal size	0.50 x 0.02 x 0.01 mm ³
Theta range for data collection	1.762 to 34.957°.
Index ranges	-13<=h<=11, -12<=k<=26, -11<=l<=25
Reflections collected	18301
Independent reflections	9156[R(int) = 0.0422]
Completeness to theta =34.957°	90.7%
Absorption correction	Multi-scan
Max. and min. transmission	0.941 and 0.724
Refinement method	Full-matrix least-squares on F ²
Data / restraints / parameters	9156/ 237/ 368
Goodness-of-fit on F ²	0.984
Final R indices [I>2sigma(I)]	R1 = 0.0384, wR2 = 0.0679
R indices (all data)	R1 = 0.0678, wR2 = 0.0769
Largest diff. peak and hole	2.223 and -1.677 e.Å ⁻³

- **Crystal data and structure refinement for [IrCl(L2)(COD)] (142).**

Empirical formula	C ₁₉ H ₃₃ Cl Ir N ₃ O
Formula weight	547.13
Temperature	123(2) K
Wavelength	0.71073 Å
Crystal system	Monoclinic
Space group	P 2 ₁ /n
Unit cell dimensions	a = 9.21700(10) Å α = 90°. b = 12.4893(2) Å β = 97.311(2)°. c = 17.9919(5) Å γ = 90°.
Volume	2054.28(7) Å ³
Z	4
Density (calculated)	1.769 Mg/m ³
Absorption coefficient	6.641 mm ⁻¹
F(000)	1080
Crystal size	0.1341 x 0.0993 x 0.0287 mm ³
Theta range for data collection	1.990 to 28.209°.
Index ranges	-12 ≤ h ≤ 12, -16 ≤ k ≤ 14, -23 ≤ l ≤ 22
Reflections collected	19216
Independent reflections	4654 [R(int) = 0.0464]
Completeness to theta = 25.000°	100.0 %
Absorption correction	Gaussian
Max. and min. transmission	0.83 and 0.472
Refinement method	Full-matrix least-squares on F ²
Data / restraints / parameters	4654 / 1 / 243
Goodness-of-fit on F ²	1.051
Final R indices [I > 2σ(I)]	R1 = 0.0317, wR2 = 0.0629
R indices (all data)	R1 = 0.0413, wR2 = 0.0670
Extinction coefficient	n/a
Largest diff. peak and hole	2.243 and -1.671 e.Å ⁻³

5.2.7. References

1. (a) Yoon, T. P.; Jacobsen, E. N. *Science* **2003**, 299, 1691. (b) *Privileged Chiral Ligands and Catalysts*; Ed. Q.-L. Zhou; Wiley-VCH: Weinheim, Germany, 2011. (c) Börner, A., Eds; *Phosphorus Ligands in Asymmetric Catalysis*; Wiley-VCH, Weinheim, 2008.
2. For recent reviews, see: (a) Diéguez, M.; Pàmies, O.; Claver, C. *Chem. Rev.* **2004**, 104, 3189. (b) Diéguez, M.; Pàmies, O. *Acc. Chem. Res.* **2010**, 43, 312. (c) van Leeuwen, P. W. N. M.; Kamer, P. C. J.; Claver, C.; Pàmies, O.; Diéguez, M. *Chem. Rev.* **2011**, 111, 2077. (d) Magre, M.; Pàmies, O.; Diéguez, M. *Chem. Rec.* **2016**, 16, 1578. (e) Pàmies, O.; Diéguez, M. *Chem. Rec.* **2016**, 16, 2460. (f) Margalef, J.; Pàmies, O.; Diéguez, M. *Tetrahedron* **2016**, 72, 2623.
3. (a) Hahn, F. E.; Jahnke, M. C. *Angew. Chem., Int. Ed.* **2008**, 47, 3122. (b) Arduengo, A. J.; Bertrand, G. *Chem. Rev.* **2009**, 109, 3209. (c) Bourissou, D.; Guerret, O.; Gabbai, F. P.; Bertrand, G. *Chem. Rev.* **2000**, 100, 39. (d) *N-Heterocyclic Carbenes in Transition Metal Catalysis*, ed. F. Glorius, *Topics in Organometallic Chemistry*, Springer, Berlin, 2007. (e) Hopkinson, M. N.; Richter, C.; Schedler, M.; Glorius, F. *Nature*, **2014**, 510, 485. (f) Díez-González, S.; Marion, N.; Nolan, S. P. *Chem. Rev.* **2009**, 109, 3612. (g) Crudden, C. M.; Allen, D. P. *Coord. Chem. Rev.* **2004**, 248, 2247. (h) Crabtree, R. H. *Coord. Chem. Rev.* **2007**, 251, 595. (i) *N-Heterocyclic Carbenes: from Laboratory Curiosities to Efficient Synthetic Tools*, ed. Díez-González, S. RSC Publishing, Cambridge, 2011. (j) *N-Heterocyclic Carbenes in Transition Metal Catalysis and Organocatalysis*, ed. Cazin, C. S. J. Springer, Berlin, 2011.
4. For reviews, see: (a) Donnelly, K. F.; Petronilho, A.; Albrecht, M. *Chem. Commun.* **2013**, 49, 1145. (b) Crabtree, R. H. *Coord. Chem. Rev.* **2013**, 257, 755. (c) Schulze, B.; Schubert, U. S. *Chem. Soc. Rev.* **2014**, 43, 2522.
5. (a) Mathew, P.; Neels, A.; Albrecht, M. *J. Am. Chem. Soc.* **2008**, 130, 13534. (b) Guisado-Barríos, G.; Bouffard, J.; Donnadieu, B.; Bertrand, G. *Angew. Chem. Int. Ed.* **2010**, 49, 4759.
6. See for example: (a) Aizpurua, J. M.; Fratila, R. M.; Monasterio, Z.; Perez-Esnaola, N.; Andreieff, E.; Irastorza, A.; Sagartzazu-Aizpurua, M. *New J. Chem.* **2014**, 38, 474. (b) Crowley, J. D.; Lee, A.; Kilpin, K. J. *Aust. J. Chem.* **2011**, 64, 1118. (c) Schweinfurth, D.; Deibel, N.; Weisser, F.; Sarkar, B. *Nachr. Chem.* **2011**, 59, 937. (d) Brown, D. G.; Schauer, P. A.; Bureau-Garcia, J.; Fancy, B. R.; Berlinguette, C. P. *J. Am. Chem. Soc.* **2013**, 135, 1692. (e) Sinn, S.; Schulze, B.; Friebe, C.; Brown, D. G.; Jäger,

M.; Kübel, J.; Dietzek, B.; Berlinguette, C. P.; Schubert, U. S. *Inorg. Chem.* **2014**, 53, 1637. (f) Sinn, S.; Schulze, B.; Friebe, C.; Brown, D. G.; Jäger, M.; Altuntas, E.; Kübel, J.; Guntner, O.; Berlinguette, C. P.; Dietzek, B.; Schubert, U. S. *Inorg. Chem.* **2014**, 53, 2083.

7. For selected examples, see: (a) Canseco-Gonzalez, D.; Gniewek, A.; Szulmanowicz, M.; Müller-Bunz, H.; Trzeciak, A. M.; Albrecht, M. *Chem. Eur. J.* **2012**, 18, 6055. (b) Hohloch, S.; Frey, W.; Su, C.-.; Sarkar, B. *Dalton Trans.* **2013**, 42, 11355. (c) Keske, E. C.; Zenkina, O. V.; Wang, R.; Crudden, C. M. *Organometallics* **2012**, 31, 456. (d) Keitz, B. K.; Bouffard, J.; Bertrand, G.; Grubbs, R. H. *J. Am. Chem. Soc.* **2011**, 133, 8498. (e) Lalrempuia, R.; McDaniel, N. D.; Müller-Bunz, H.; Bernhard, S.; Albrecht, M. *Angew. Chem. Int. Ed.* **2010**, 49, 9765. (f) Canseco-Gonzalez, D.; Albrecht, M. *Dalton Trans.* **2013**, 42, 7424. (g) Prades, A.; Peris, E.; Albrecht, M. *Organometallics* **2011**, 30, 1162. (h) Bolje, A.; Hohloch, S.; Urankar, D.; Pevec, A.; Gazvoda, M.; Sarkar, B.; Košmrlj, J. *Organometallics* **2014**, 33, 2588. (i) Bolje, A.; Hohloch, S.; van der Meer, M.; Košmrlj, J.; Sarkar, B. *Chem. Eur. J.* **2015**, 21, 6756. (j) Delgado-Rebollo, M.; Canseco-Gonzalez, D.; Hollering, M.; Müller-Bunz, H.; Albrecht, M. *Dalton Trans.* **2014**, 43, 4462. (k) Nakamura, T.; Terashima, T.; Ogata, K.; Fukuzawa, S. *Org. Lett.* **2011**, 13, 620. (l) Hohloch, S.; Sarkar, B.; Nauton, L.; Cisnetti, F.; Gautier, A. *Tetrahedron Lett.* **2013**, 54, 1808.

8. (a) Bolje, A.; Košmrlj, J. *Org. Lett.* **2013**, 15, 5084. (b) Bolje, A.; Urankar, D.; Košmrlj, J. *Eur. J. Org. Chem.* **2014**, 8167. (c) Bolje, A.; Hohloch, S.; Košmrlj, J.; Sarkar, B. *Dalton Trans.* **2016**, 45, 15983. (d) Pretorius, R.; Mazloomi, Z.; Albrecht, M. *J. Organomet. Chem.* **2017**, <http://dx.doi.org/10.1016/j.jorganchem.2017.05.014>. (e) Corbucci, I.; Petronilho, A.; Müller-Bunz, H.; Rocchigiani, L.; Albrecht, M.; Macchioni, A. *ACS Catal.* **2015**, 5, 2714. (f) Petronilho, A.; Woods, J. A.; Mueller-Bunz, H.; Bernhard, S.; Albrecht, M. *Chem. Eur. J.* **2014**, 20, 15775. (g) Bernet, L.; Lalrempuia, R.; Ghattas, W.; Mueller-Bunz, H.; Vigara, L.; Llobet, A.; Albrecht, M. *Chem. Commun.* **2011**, 47, 8058. (h) Pretorius, R.; Fructos, M. R.; Müller-Bunz, H.; Gossage, R. A.; Pérez, P. J.; Albrecht, M. *Dalton Trans* **2016**, 45, 14591. (i) Woods, J. A.; Lalrempuia, R.; Petronilho, A.; McDaniel, N. D.; Müller-Bunz, H.; Albrecht, M.; Bernhard, S. *Energy Environ. Sci.* **2014**, 7, 2316.

9. (a) *Modern Reduction Methods*; (Eds. Andersson, P. G.; Munslow, I. J.); Wiley-VCH, Weinheim, 2008. (b) Gladiali, S.; Alberico, E. *Chem. Soc. Rev.* **2006**, 35, 226. (c)

Samec, J. S. M.; Bäckvall, J.-E.; Andersson, P. G.; Brandt, P. *Chem. Soc. Rev.* **2006**, *35*, 237.

10. For selected examples, see: (a) Horn, S.; Albrecht, M. *Chem. Commun.* **2011**, *47*, 8802. (b) Gnanamgari, D.; Sauer, E. L. O.; Schley, N. D.; Butler, C.; Incarvito, C. D.; Crabtree, R. H. *Organometallics* **2009**, *28*, 321. (c) Gürbüz, N.; Özcan, E. O.; Özdemir, I.; Cetinkaya, B.; Sahin, O.; Büyükgüngör, O. *Dalton Trans.* **2012**, *41*, 2330. (d) Hillier, A. C.; Lee, H. M.; Stevens, E. D.; Nolan, S. P. *Organometallics* **2001**, *20*, 4246.

11. (a) Maity, R.; Hohloch, S.; Su, C.-Y.; van der Meer, M.; Sarkar, B. *Chem. Eur. J.* **2014**, *20*, 9952. (b) Hollering, M.; Albrecht, M.; Kühn F. E. *Organometallics* **2016**, *35*, 2980. (c) Hohloch, S.; Suntrup, L.; Sarkar, B. *Organometallics* **2013**, *32*, 7376. (d) Sluijter, S. N.; Elsevier, C. J. *Organometallics* **2014**, *33*, 6389. (e) Farrell, K.; Melle, P.; Gossage, R. A.; Müller-Bunza, H.; Albrecht, M. *Dalton Trans.* **2016**, *45*, 4570. (f) Maity, R.; Mekic, A.; van der Meer, M.; Verma, A.; Sarkar, B. *Chem. Commun.* **2015**, *51*, 15106.

12. The blank experiments carried out without catalyst and under different reaction conditions are shown in the supporting information.

13. For successful applications in the ATH of heteroaromatic ketones, see: (a) Everaere, K.; Mortreux, A.; Bulliard, M.; Brussee, J.; van der Gen, A.; Nowogrocki, G.; Carpentier, J.-F. *Eur. J. Org. Chem.* **2001**, 275. (b) Letondor, C.; Pordea, A.; Humbert, N.; Ivanova, A.; Mazurek, S.; Novic, M.; Ward, T. R. *J. Am. Chem. Soc.* **2006**, *128*, 8320. (c) Coll, M.; Pàmies, O.; Diéguez, M. *Adv. Synth. Catal.* **2014**, *356*, 2293. (d) Matharu, D. S.; Martins, J. E. D.; Wills, M. *Chem. Asian J.* **2008**, *3*, 1374. (e) Wu, X.; Li, X.; Zanotti-Gerosa, A.; Pettman, A.; Liu, J.; Mills, A. J.; Xiao, J. *Chem. Eur. J.* **2008**, *14*, 2209. (f) Baratta, W.; Chelucci, G.; Magnolia, S.; Siega, K.; Rigo, P. *Chem. Eur. J.* **2009**, *15*, 726. (g) Ito, M.; Watanabe, A.; Shibata, Y.; Ikariya, T. *Organometallics* **2010**, *29*, 4584. (h) Buitrago, E.; Lundberg, H.; Andersson, H.; Ryberg, P.; Adolffson, H. *ChemCatChem* **2012**, *4*, 2082. (i) Margalef, J.; Slagbrand, T.; Tinnis, F.; Adolffson, H.; Diéguez, M.; Pàmies, O. *Adv. Synth. Catal.* **2016**, *358*, 4006.

14. (a) Albrecht, M.; Miecznikowski, J. R.; Samuel, A.; Faller, J. W.; Crabtree, R. H. *Organometallics* **2002**, *21*, 3596. (b) Miecznikowski, J. R.; Crabtree, R. H. *Polyhedron* **2004**, *23*, 2857. (c) Albrecht, M.; Crabtree, R. H.; Mata, J.; Peris, E. *Chem. Commun.* **2002**, *32*. (d) McGuinness, D. S.; Cavell, K. J.; Skelton, B. W.; White, A. H. *Organometallics* **1999**, *18*, 1596.

15. (a) Fekete, M.; Joó, F. *Collect. Czech. Chem. Commun.* **2007**, 72, 1037. (b) Gnanamgari, D.; Moores, A.; Rajaseelan, E.; Crabtree, R. H. *Organometallics* **2007**, 26, 1226.
16. It has been suggested that this isomerization process can proceed via the formation of Ir- π -allyl intermediates, see: ref 10a.
17. (a) Pàmies, O.; Bäckvall, J.-E. *Chem. Eur. J.* **2001**, 7, 5052. (b) Laxmi, Y. R. S.; Bäckvall, J.-E. *Chem. Commun.* **2000**, 611.
18. The values of these KIE's are within the range of those obtained for other TH catalytic systems. See, for instance: (a) Casey, C. P.; Singer, S. W.; Powell, D. R.; Hayashi, R. K.; Kavana, M. *J. Am. Chem. Soc.* **2001**, 123, 1090. (b) Wettergren, J.; Buitrago, E.; Ryberg, P.; Adolfsson, H. *Chem. Eur. J.* **2009**, 15, 5709.
19. Hansch, C.; Leo, A.; Taft, R. W. *Chem. Rev.* **1991**, 91, 165.
20. See, for instance: (a) Corey, E. J.; Suggs, J. W. *Tetrahedron Lett.* **1975**, 16, 2647. (b) Djerassi, C. *Org. React.* **1951**, 6, 207. (c) Dess, D. B.; Martin, J. C. *J. Am. Chem. Soc.* **1991**, 113, 7277. (d) Ley, S. V.; Norman, J.; Griffith, W. P.; Marsden, S. P. *Synthesis* **1994**, 639.
21. See, for example: (a) Sheldon, R. A.; Arends, I. W. C. E.; ten Brink, G. J.; Dijkman, A. *Acc. Chem. Res.* **2002**, 35, 774. (b) Mallat, T.; Baiker, A. *Chem. Rev.* **2004**, 104, 3037. (c) Piera, J.; Bäckvall, J.-E. *Angew. Chem., Int. Ed.* **2008**, 47, 3506.
22. Valencia, M.; Müller-Bunz, H.; Gossage, R. A.; Albrecht, M. *Chem. Commun.* **2016**, 52, 3344.
23. (a) Aslanian, R. G. Patent WO2012051036, **2012**. (b) Geronikaki, A.; Vasilevsky, S.; Hadjipavlou-Litina, D.; Lagunin, A.; Poroikov, B. V. *Chemistry of Heterocyclic Compounds*, **2006**, 42, 675.
24. Khasanov, A. B.; Ramirez-Weinhouse, M. M.; Webb, Th. R.; Thiruvazhi, M. *J. Org. Chem.* **2004**, 69, 5766.
25. Limmert, M. E.; Roy, A. H.; Hartwig, J. F. *J. Org. Chem.* **2005**, 70, 9364.
26. Baciocchi, E.; Ruzziconi, R. *J. Org. Chem.* **1991**, 56, 4772.
27. Barton, D. H. R.; Bohe, L.; Lusinchi, X. *Tetrahedron* **1990**, 46, 5273.
28. Slagbrand, T.; Lundberg, H.; Adolfsson, H. *Chem. Eur. J.* **2014**, 20, 16102.
29. Casey, Ch. P.; Johnson, J. B. *J. Org. Chem.* **2003**, 68, 1998.
30. Oxford Diffraction (2010). CrysAlisPro (Version 1.171.34.44). Oxford Diffraction Ltd., Yarnton, Oxfordshire, UK.
31. Sheldrick, G. M. *Acta Cryst.* **2015**, A71, 3-8.

32. Sheldrick, G. M. *Acta Cryst.* **2015**, C71, 3-8.
33. Kuriyama, K.; Shimazawa, R.; Shirai, R. *J. Org. Chem.* **2008**, 73, 1597.
34. Coll, M.; Pàmies, O.; Diéguez, M. *Adv. Synth. Catal.* **2014**, 356, 2293.
35. Slagbrand, T.; Lunderg, H.; Adolfsson, H. *Chem. Eur. J.* **2014**, 20, 16102.
36. Bhattacharya, P.; Krause, J. A.; Guan, H. *Organometallics* **2011**, 30, 4720.
37. Coombs, T. C.; Lee, M. D.; Wong, H.; Armstrong, M.; Cheng, B.; Chen, W.; Moretto, A. F.; Liebeskind, L. S. *J. Org. Chem.* **2008**, 73, 882.
38. Cano, R.; Yus, M.; Siego, Ramón, D. J. *Tetrahedron* **2011**, 67, 8079.
39. Zhang, L.; Wang, S.; Zhou, S.; Yang, G.; Sheng, E. *J. Org. Chem.* **2006**, 71, 3149.
40. Moiseev, D. V.; James, B. R.; Hu, T. Q. *Inorg. Chem.* **2006**, 45, 10338.
41. Zhang, C.-P.; Cai, J.; Zhou, C.-B.; Wang, X.-P.; Zheng, X.; Gu, Y.-C.; Xiao, J.-C. *Chem. Commun.* **2011**, 47, 9516.
42. Liang, S.; Hammond, L.; Xu, B.; Hammond, G. B. *Adv. Synth. Catal.* **2016**, 358, 3313.
43. Eisch, J. J.; Dutta, S. *Organometallics* **2005**, 24, 3355.
44. Ohta, T.; Ikegami, H.; Miyake, T.; Takaya, H. *J. Organomet. Chem.* **1995**, 502, 169.
45. Källström, K.; Hedberg, C.; Brandt, P.; Bayer, P.; Andersson, P. G. *J. Am. Chem. Soc.* **2004**, 126, 14308.
46. Ohta, T.; Ikegami, H.; Miyake, T.; Takaya, H. *J. Organomet. Chem.* **1995**, 502, 169.
47. Barsamian, A. L.; Wu, Z.; Blakemore, P. R. *Org. Biom. Chem.* **2015**, 13, 3781.
48. Query, I. P.; Squier, P. A.; Larson, E. M.; Isley, N. A.; Clark, T. B. *J. Org. Chem.* **2011**, 76, 6452.
49. Hong, B.-C.; Tseng, H.-C.; Chen, S.-H. *Tetrahedron* **2007**, 63, 2840.

Chapter 6.

*Iridium molecular catalysts for catalytic water
oxidation*

6.1. Benzoxazole/thiazole-triazolidene iridium complexes as new efficient molecular catalysts for water oxidation

Mazloomi, Z.; Gil, M.; Albrecht, M.; Salas, X.; Pàmies, O.; Diéguez, M.
Manuscript in prepration.

6.1.1. Introduction

Nowadays, the major part of the global energy supply is provided by carbon-based energy sources, which are connected to severe environmental issues, such as the greenhouse effect and air pollution. Consequently, exist a strong social demand for clean and environmentally friendly carbon-free alternatives to fossil fuels. However, the sustainable production of clean energy constitutes one of the most important scientific challenges.¹

One of the potential alternatives to fossil fuels is water splitting to produce hydrogen as fuel.² This process requires the coupling of the two half-reactions: (i) water oxidation to produce the reducing equivalents (electrons) and oxygen as the only byproduct and (ii) reduction of protons using the electrons of the former reaction to generate molecular hydrogen. Albeit, both reaction steps are crucial for the generation of hydrogen from water, water oxidation is considered to be the bottleneck in the sustainable production of hydrogen from water.³ This is because water oxidation is both thermodynamically and kinetically unfavorable, resulting in slow kinetics without the use of a catalyst.^{3b} The development of powerful and stable water oxidation catalysts is therefore of great importance. For decades, scientists have sought to understand and imitate nature, creating not only biomimetic water oxidation catalysts, but also well-defined homogeneous^{3a-c} and heterogeneous^{3d} catalysts. One of the key features that water oxidation catalysts need to fulfill is the high redox flexibility of the metal center because the formation of molecular oxygen from water requires the transfer of four electrons. The field of water oxidation have been dominated by Mn-⁴ and Ru-⁵ catalysts, albeit in recent years cobalt,⁶ iron⁷ and iridium⁸ based catalysts have also given promising results.

The redox behavior of the metal center can be modulated by the coordinated ligands. In this respect mesoionic carbenes (MIC), such as 1,2,3-triazol-5-ylidenes, facilitate the stabilization of different metal oxidation states mainly because of the large

contributions from zwitterionic resonance forms and also because they can serve as a transient reservoir of both negative and positive charge.^{8d} Such advantages have been used mainly by the groups of Bernhard and Albrecht to develop a new class of efficient Ir-complexes containing pyridyl-triazolidene ligands for water oxidation (Figure 6.1.1).^{8d,9} For instance, compound **80** provided high turnover numbers (up to 40000) in the cerium ammonium nitrate ((NH₄)₂Ce(NO₃)₆, CAN) mediated water oxidation. Later, modification of the remote position of the carbene ligand (complexes **81** and **82**) led to a substantially increase in activity. It should be pointed out that the simple and counterintuitive introduction of more lipophilic n-octyl chain (complex **82**) led to one of the most active Ir-catalysts. Nevertheless, activity substantially decrease when using sodium metaperiodate as sacrificial oxidant under nearly neutral media (pH 5.6). Thus, for instance, the activity of complex **82** dropped from TOF's up to 2 s⁻¹ using CAN at pH = 1 to TOF's up to 0.1 s⁻¹ using NaIO₄ at pH = 5.6.

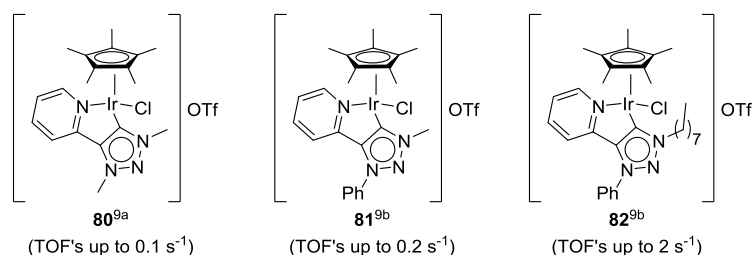


Figure 6.1.1. Representative pyridine-triazolidene iridium water oxidation catalyst precursors. TOF measured in the CAN-mediated water oxidation at pH = 1.

6.1.2. Objectives

We have recently shown that the replacement of the pyridyl group in Ir-complexes containing pyridyl-triazolidene ligands by other robust nitrogen or oxygen groups, such as benzoxazole and thiazole, is highly advantageous in hydrogen transfer reactions (both transfer hydrogenation and dehydrogenation reactions, see Chapter 5). Having in mind the large effect observed using simple and sometimes counterintuitive modifications in the pyridyl-triazolidene scaffold for Ir-catalyzed water oxidation, the decision was made to study the effect of varying the pyridine group by a benzoxazole and a thiazole moiety (complexes **139** and **141**; Figure 6.1.2). We also would like to study the effect of the nature of catalyst precursors, from cationic to neutral complexes, by means of complexes **139** and **140** (Figure 6.1.2). Furthermore, we also seek to

evaluate complex **148** (Figure 6.1.2), without an extra coordinative group rather than the triazolidene moiety, to prove if the presence of bidentated ligands is crucial for high activities and, more importantly, if ligand chelation is key to avoid the decomposition of the homogeneous system to form IrO_x nanoparticles, which are also active water oxidation catalysts.

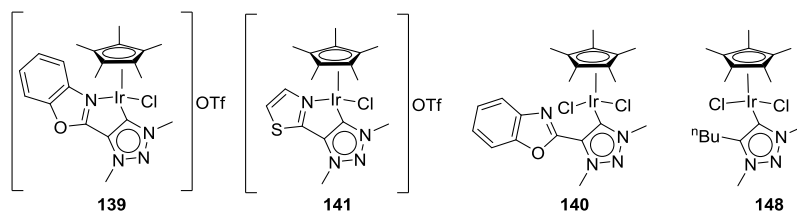
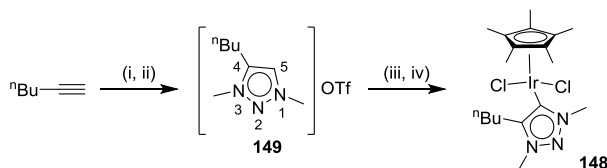


Figure 6.1.2. Ir catalyst precursors **139-141** and **148** for water oxidation using both CAN and NaIO_4 as sacrificial one-electron oxidants.

6.1.3. Results and discussion

6.1.3.1. Synthesis and characterization of Ir-complexes

Complexes **139-141** were prepared as previously reported in Chapter 5. The new Ir-complex **148** was prepared by a one-pot reaction from the corresponding triazolium salt **149**, using Ag_2O and Me_4NCl to form the desired Ag-carbene intermediate, and subsequent in situ transmetalation with $[\text{Ir}(\text{Cp}^*)\text{Cl}_2]_2$ (Scheme 6.1.1). Triazolium salt **149** was prepared via conventional copper-catalyzed [3+2] of the methyl azide and 1-hexyne, followed by the methylation at the triazole N3 position as illustrated in Scheme 6.1. Complex **148** was obtained as air stable solid and was fully characterized by ^1H and ^{13}C NMR spectroscopy and mass spectroscopy. Coordination of **148** through the 1,2,3-triazol-5-ylidene group was confirmed by the disappearance of the H-5 proton signal in the ^1H -NMR spectra and by the strong downfield shift of the C-5 carbon signal in the ^{13}C -NMR spectra.



Scheme 6.1.1. Synthesis of 1,2,3-triazol-5-ylidene iridium complex **148**. (i) MeN_3 , $\text{CuSO}_4 \cdot 5\text{H}_2\text{O}$, $\text{C}_6\text{H}_7\text{O}_6\text{Na}$, $\text{THF}/\text{H}_2\text{O}$. (ii) MeOTf , CH_2Cl_2 . (iii) Ag_2O , Me_4NCl , $[\text{IrCp}^*\text{Cl}_2]_2$, CH_2Cl_2 .

6.1.3.2. Electrochemical analysis

To examine the oxidation behavior of complexes **139** and **141** we studied the electrocatalytic properties in a non-protic solvent (dichloromethane) as well as in aqueous solutions in acidic (pH = 1) and an almost neutral (pH = 5.6) media.

Cyclic voltammetry (CV) and differential pulse voltammetry (DPV) in dichloromethane shows a redox couple at 1.61 V vs SVE for **4** and at 1.55 V vs SVE for **5** (Figure 6.1.3).

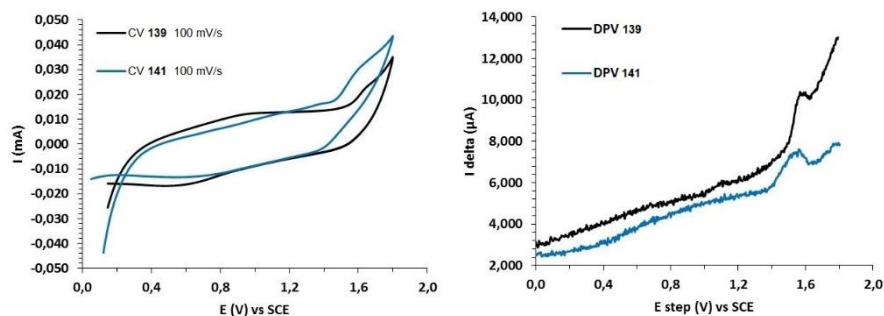


Figure 6.1.3. (Left) Cyclic Voltammetry of **139** and **141** in DCM (0.1 M TBAP) with a scan rate of 100 mV/s. (Right) Differential Pulse Voltammetry of **139** and **141** in DCM (0.1 M TBAP) recorded using pulse amplitudes of 0.05 V, pulse widths of 0.05 s, sampling widths of 0.02 s, pulse periods of 0.1 s, and quiet times of 2 s.

Cyclic voltammograms of aqueous solutions of **139** and **141**, however, showed different behaviors in acidic and an almost neutral media (Figure 6.1.4). Under acid conditions, complexes **139** and **141** show waves at 1.24 V and 1.29 V vs SCE, which can be assigned to Ir(III)/Ir(IV), and strong irreversible waves at a higher potentials due to the electrocatalytic water oxidation. An unassigned redox process at ca. 0.25-0.3 V was also observed. Under almost neutral pH conditions, the Ir(III)/Ir(IV) event shifted to 1.08 V and 1.05 V vs SCE for complexes **139** and **141**, respectively. As expected, the potential at which the water oxidation appear increased substantially as did the current at the highest applied voltage at elevated pH.

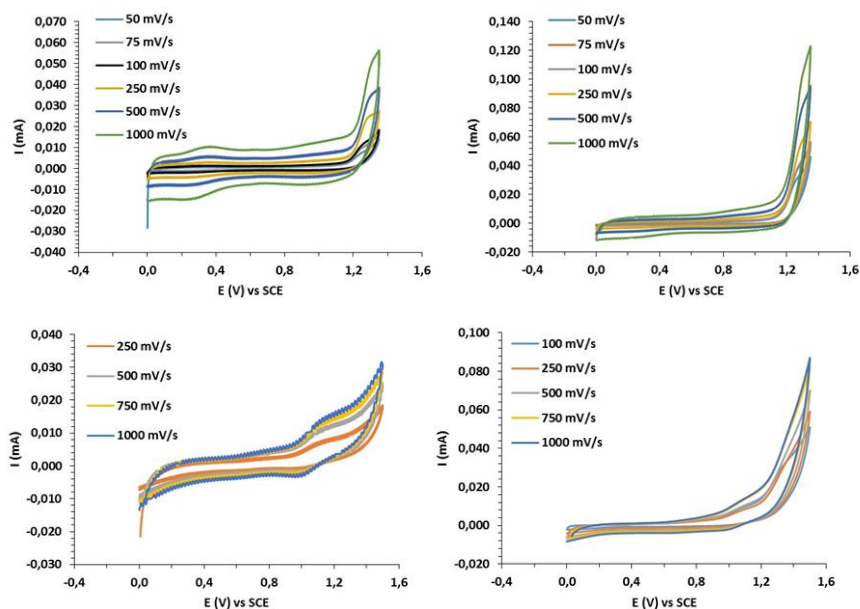


Figure 6.1.4. Top: cyclic voltammeteries of **139** (left) and **141** (right) at different scan rates at pH = 1. Conditions: 1mM concentration of both complexes in a pH = 1 aqueous solution (0.1M triflic acid). Bottom: cyclic voltammeteries of **139** (left) and **141** (right) at different scan rates at pH = 5.6. Conditions: 1mM concentration of both complexes in a pH = 5.6 aqueous solution (NaOAc buffer).

The stability of the both complexes at a different pH conditions was studied using consecutive CV experiments (Figure 6.1.5). Again, the results using complexes **139** and **141** showed different behaviors in acidic and an almost neutral media. Under acidic conditions, a significant decrease in the current of the waves at 1.24 and 1.29 V was observed after 10 consecutive potential cycles (Figure 6.1.5). The decrease on intensity of such waves is attributed to passivation of the electrode surface. A plausible explanation is the degradation of the molecular complexes at highly positive potentials and subsequent formation of IrO_x heterogeneous materials that cover the electrode.¹² To confirm the electrodeposition of IrO_x , the electrodes after the consecutive CVs were washed with water, acetone and methanol, and were placed in neat triflic acid. The CV of the recovered electrode material show clear electrocatalytic water oxidation waves in both complexes (Figure 6.1.6), which clearly indicates the presence of catalytically active heterogeneous materials on the surface of both electrodes.

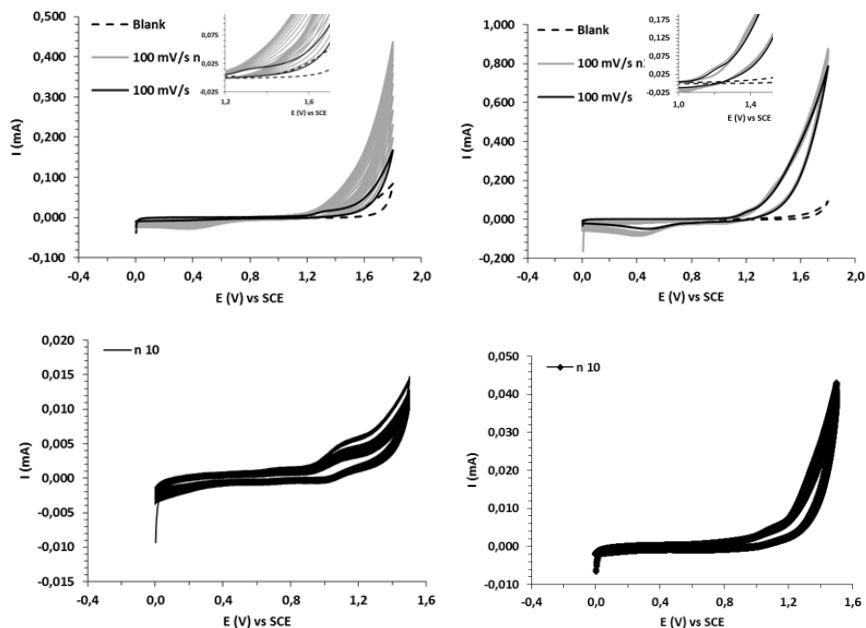


Figure 6.1.5. Top: consecutive cyclic voltammeteries of **139** (left) and **141** (right) with a scan rate of 100 mV/s (black line), 100 mV/s during 11 cycles (grey line) and blank (dashed line) in a pH = 1 aqueous solution (0.1M triflic acid). Bottom: consecutive cyclic voltammeteries of **139** (left) and **141** (right) with a scan rate of 100 mV/s in a pH = 5.6 aqueous solution (NaOAc buffer).

On the other hand, at almost neutral pH conditions, no signs of electrodeposition, and therefore of decomposition, on the surface of the electrode were observed for both complexes **139** and **141** (Figure 6.1.5).

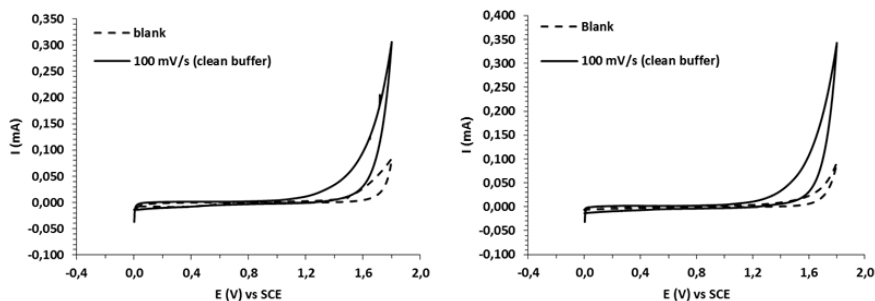
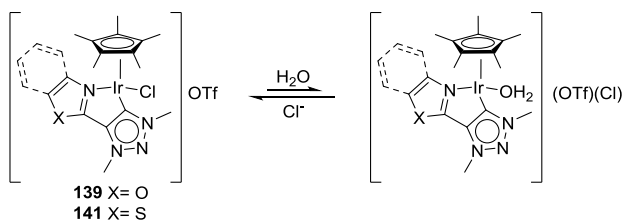


Figure 6.1.6. Cyclic voltammeteries of **139** (left) and **141** (right) after washing the electrode with water, acetone and MeOH (black line) and blank (dashed line).

6.1.3.3. Reactivity of complexes **139-141** towards water

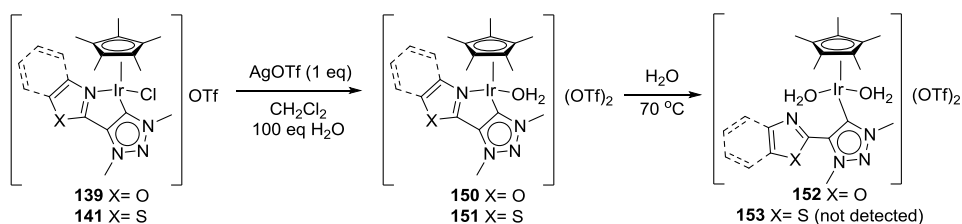
In order to investigate the Cl⁻/H₂O ligand exchange propensity of complexes **139** and **141** in solution, their behavior in D₂O was studied by ¹H-NMR (Scheme 6.1.2). Interestingly, different behavior was observed for both complexes. Complex **139** is very robust and no detectable ligand exchange was observed by ¹H-NMR even after 4 days. However, for complex **141** two compounds at a ratio of ca 9:1 were observed when performing the ¹H-NMR in D₂O. Thus, for instance, two set of the thiazole signals were observed. The major compound presents two doublets at 8.00 ppm and at 8.16 ppm, whereas the corresponding signals of the minor compound are downfield shifted to 8.07 ppm and 8.29 ppm, respectively. The downfield shift of the thiazole signals in the minor compound is indicative of the formation of the corresponding dicationic aquo complex, which is in equilibrium with the major compound **141**.



Scheme 6.1.2. Cl⁻/H₂O ligand exchange equilibria of complexes **139** and **141**.

To provide further evidence of the formation of the dicationic aquo complexes, we prepared such species by irreversible abstraction of the chloride anion with silver triflate in the presence of water (Scheme 6.1.3). In line with the different behavior in aqueous solution of complexes **139** and **141** previously observed, the formation of dicationic aquo complex **150** requires longer reaction times (2 days) than for thiazole analogue **151** (12 h). Under this reaction conditions, chloride abstraction of dichloro complex **140** affords complex **139** instead of the corresponding aquo complexes after 12 hours reaction. Complexes **150** and **151** were characterized by ¹H and ¹³C NMR spectroscopy and mass spectroscopy. To date, we have been unable to achieve crystals of sufficient quality to make X-ray diffraction measurements. As expected, for both complexes **150** and **151**, the benzoxazole and thiazole signals appear more downfield shifted than those of cationic chloro complexes **139** and **141**. The number of water molecules coordinated could not be determined by mass spectroscopy because, as expected, the HRMS-ESI spectra show the heaviest ions at m/z which correspond to the loss of the solvato

molecules and of the triflate anion. Nevertheless, the ^{13}C NMR spectra of complexes **150** and **151** also indicates that the signals from the quaternary X-C=N group were downfield shifted compared to the free ligand (i.e. 153.8 ppm for complex **150** and 151.2 ppm for benzoxazole-triazolylidene salt), which clearly indicates the coordination of the benzoxazole and thiazole moieties and that therefore only one water molecule is coordinated in complexes **150** and **151**. In the case of monoquo complex **150** is it possible to coordinate a second molecule of water if the reaction is carried in water as solvent and heated to 70 °C for more than 3 days (compound **152**). The coordination of the second water molecule is associated with the concomitant decoordination of the benzoxazole moiety, which is demonstrated by the deshielding of the ^1H -NMR signals of the benzoxazole unit (Figure 6.1.7). The coordination ability of the thiazole group is greater than the benzoxazole moiety. Therefore, the presence of diaquo complex **153** was not observed after 3 days of reaction.



Scheme 6.1.3. Preparation of dicationic water complexes **150-153**.

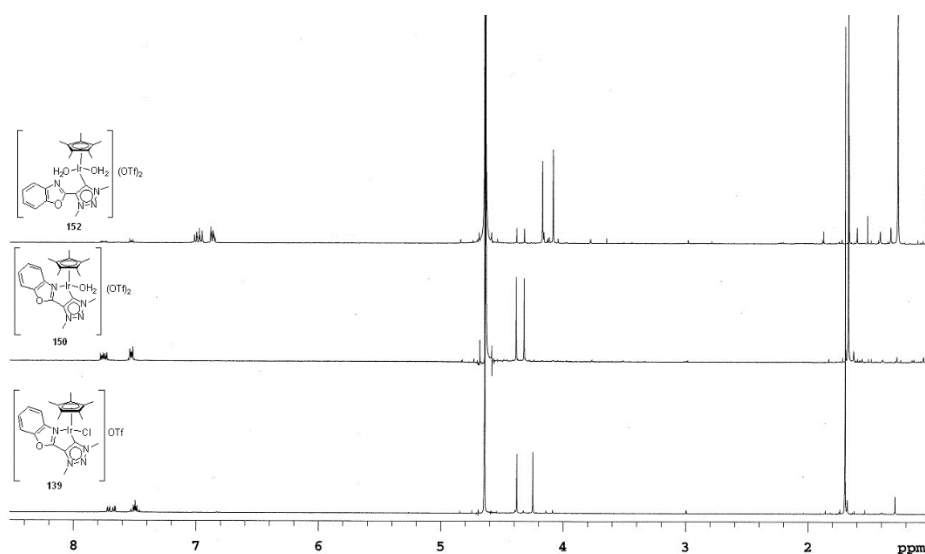


Figure 6.1.7. ^1H -NMR spectra of compounds **139**, **150** and **152** in D_2O .

6.1.3.4. Water oxidation catalysis

Complexes **139** and **141** were evaluated as water oxidation catalyst precursors using either cerium ammonium nitrate ($(\text{NH}_4)_2\text{Ce}(\text{NO}_3)_6$, CAN) or sodium metaperiodate (NaIO_4) as sacrificial one-electron oxidants. Catalytic activity was monitored by combining differential pressure manometry with a molecular oxygen selective Clark electrode. In a first set of experiments the ability to promote water oxidation of complexes **139** and **141** was evaluated using CAN as oxidant at $\text{pH} = 1$ (0.1 M HOTf). The reactions were carried out using 1 mM of Ir-catalysts and three consecutive additions of CAN (100 eq in each addition). For both catalyst precursors fast production of gas was observed after the addition of the sacrificial oxidant (Figure 6.1.8). Both catalyst showed similar catalytic behavior with TOF's ca 0.06 s^{-1} . It should be pointed out that no other gases rather than molecular oxygen were obtained in all the runs. As previously observed for other $\text{Cp}^*\text{Ir-MIC}$ complexes, considerable amounts of CAN were used to generate the active species rather than to be used as oxidant, which affects the TON in the first injection. We also carried out the reaction using 4000 equivalents of CAN, providing similar TOF's and TON around 1000 after 2.5 h runs (see Supporting Information).

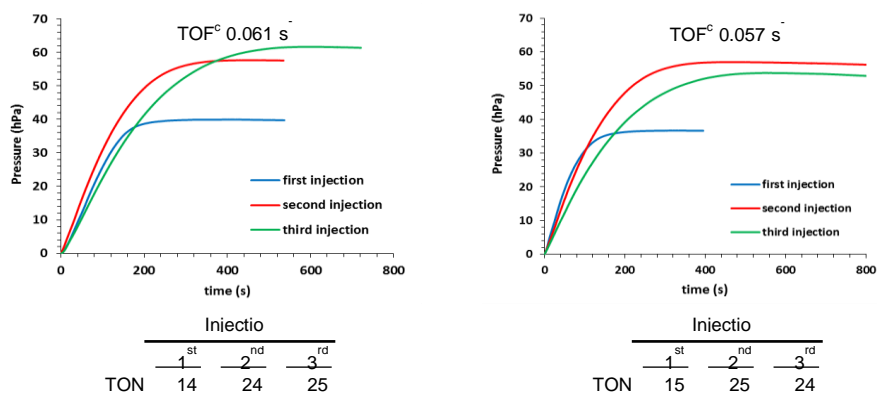


Figure 6.1.8. Manometric monitoring of gas evolution vs. time for complex **139** (left) and **141** (right) during three consecutive additions of CAN (100 eq). Conditions for each addition: 1 mM catalyst / $\text{pH} = 1$ (0.1M triflic acid) solution / 100 mM $(\text{NH}_4)_2\text{Ce}(\text{NO}_3)_6$. (a) TON measured from O_2 -selective clark-type electrode analysis of the reaction headspace. $\text{TON}_{\text{max}} = 25$. (b) $\text{O}_2\%$ in the total gas evolved by combining manometry (total gas) + O_2 -selective clark-type electrode analysis. (c) TOF values calculated after the first 5 min of catalysis.

Over the last years it has been a controversy whether the IrCp* catalyst precursors are stable under the presence of CAN,¹⁶ and therefore if the catalysis occurs in homogeneous or in heterogeneous phase. The presence of heterogenized catalysts (e.g. IrO_x nanoparticles) have been usually disclosed by in situ UV-VIS or by TEM analysis. However, these two methodologies have recently proved to be not fully reliable in WO catalysis. Thus, for instance the UV-VIS absorbance around 560 nm, which was attributed to the presence of IrO_x, could alternatively indicate the presence of homogeneous Ir(IV) species, as described by Crabtree, Brudvig et al.^{8g,17} On the other hand the high-energy of the electron beam in a TEM analysis can induce the formation of clusters and nanoparticles from homogeneous samples.¹⁸ As demonstrated by Crabtree and Brudvig, one of the simple ways to circumvent this problem is the use of dynamic light scattering (DLS).¹⁹ The DLS of the resulting purple solutions after catalysis indicate the presence of aggregates in the range of 0.78 – 0.92 nm (Figure 6.1.9), which rather than indicating the presence of Ir-NPs, it is in agreement with the estimated hydrodynamic volumes of the Crabtree's type dimeric iridium species [(C,N)X₂Ir(μ₂-X)₂IrX₂(C,N)] (X = O, OH),²⁰ which have been recently proposed to play a crucial role in the WOCs using CAN as oxidant.^{9b}

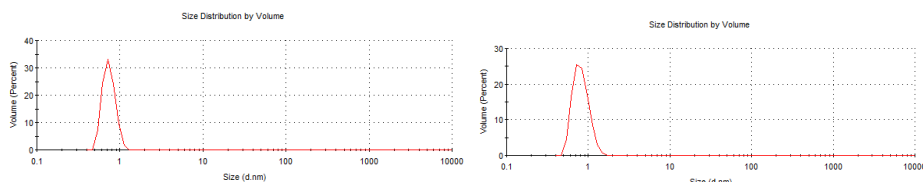


Figure 6.1.9. DLS measurements of solutions after catalysis using **139** (left) and **141** (right). Conditions: 1 mM of catalyts in a pH = 1.0 (0.1M triflic acid) aqueous solution in the presence of 100 mM (NH₄)₂Ce(NO₃)₆.

We have also evaluated the performance of complexes **139** and **141** as WOC using sodium periodate as sacrificial oxidant at pH = 5.6. The development of WOC able to work in almost neutral pH conditions instead of at highly corrosive low pH conditions is of great important for large-scale application. For the purpose of comparison, the experiments were carried out using the so-called “Crabtree’s conditions”: 20 mM NaIO₄ (4000 eq) in NaOAc buffer at pH = 5.6. As previously observed when CAN was used as oxidant, water oxidation began immediately after the addition of NaIO₄ to the catalyst (Figure 6.1.10). However, in contrast to CAN, complete consumption of NaIO₄ to form

molecular oxygen was observed for both **139** and **141** leading to efficiencies close to 100 % (TON's 996 and 998 for **139** and **141**, respectively). It should be highlighted the high activity of the catalytic systems (TOF's up to 0.58 s^{-1} and 0.21 s^{-1} for **139** and **141**, respectively). These results competes favorably with most of the Ir-catalyst developed (including other triazolylidene Cp^*Ir catalyst precursors),²¹ with the exception of Wilkinson's Ir acetate trimer (TOF's up to 0.8 s^{-1}).^{8g} The potential formation of Ir-NPs under these catalytic conditions was also examined by DLS. No evidence of NPs formation was obtained for neither **139** nor **141** in a 2 h analysis. Further indication of the homogeneous nature of the active species is the quick color change from the initially pale yellow of the catalyst precursors to the blue solution in both cases. Given the relative structural similarity of **139** and **141** with Crabtree's complexes the stable and highly active blue solutions observed could indicate the formation of similar dinuclear active species (Figure 6.1.11), which has been proposed to be resting state in WOC.^{8j}

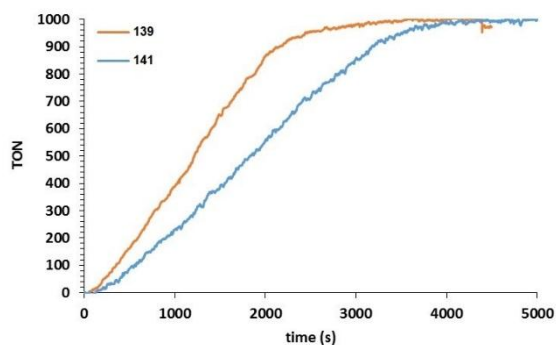


Figure 6.1.10. Monitoring of O_2 evolution vs. time using a Clark-type electrode for complexes **139** (orange line) and **141** (blue line) triggered by sodium periodate. Conditions: $5 \mu\text{M}$ catalyst, acetate buffer $\text{pH} = 5.6$, 4000 eq of NaIO_4 (TONmax = 1000).

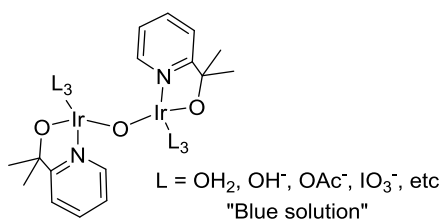


Figure 6.1.11. Structure of the catalytically active Ir "blue solution" formed from $\text{Cp}^*\text{Ir}(\text{pyalk})\text{OH}$ catalyst precursor in the presence of NaIO_4 .^{8j}

6.1.4. Conclusions

In this chapter we have disclosed the electrochemical properties of complexes **139** and **141** in a non-protic solvent as well as in aqueous solution at different pHs. We have also studied the Cl⁻/H₂O ligand exchange propensity of complexes **139** and **141** in water solution. More importantly, we have demonstrated that complexes **139** and **141** are able to promote water oxidation using both CAN and NaIO₄ as sacrificial oxidant. The molecular nature of the active species have been corroborated using both oxidants. Using CAN as oxidant at low pH, both catalyst precursors provided similar activities (TOF's ca 0.06s⁻¹) and lower than those achieved using parent pyridine complex **80**. However, excellent activities (much better than related pyridine analogues **80-82**; TOF's up to 0.58 s⁻¹) were achieved when using more appealing almost neutral conditions (pH = 5.6) and NaIO₄ as oxidant. Although the results using CAN can be simply rationalized by the lower donor abilities of the benzoxale and thiazole groups compared to the pyridine moiety,²² this explanation is in disagreement with the results using NaIO₄. The most probable explanation for the substantial rate enhancement using NaIO₄ instead of CAN can be found in the different nature of the active species formed by a specific aggregation process under different reaction conditions.^{9b} Work is still in progress to study the catalytic behavior of complexes **140** and **148** using CAN and NaIO₄ as sacrificial oxidants.

6.1.5. Experimental section

6.1.5.1. General information

All reactions for the synthesis of Ir-complexes were carried out using standard Schlenk techniques under an atmosphere of argon. Solvents were purified and dried by standard procedures. Ir-complexes **139-141** were prepared as previously described. All other commercially available reagents and substrates were used as received. ¹H, ¹³C{¹H}, and ¹⁹F NMR spectra were recorded using a 400 MHz spectrometer. Chemical shifts are relative to that of SiMe₄ (¹H and ¹³C) as internal standard. ¹H and ¹³C assignments were made on the basis of ¹H-¹H gCOSY, ¹H-¹³C gHSQC and ¹H-¹³C gHMBC experiments. Dynamic light scattering experiments (DLS) were carried out using a Zetazizer Nano ZS at 25 °C with an operating range of measurement from 0.3 nm to 10 microns.

6.1.5.2. Preparation of 4-butyl-1,3-dimethyl-1H-1,2,3-triazole trifluoromethanesulfonate (**149**)

A suspension of MeI (0.58 ml, 9.33 mmol) and NaN_3 (1.84 g, 28 mmol) in $\text{H}_2\text{O}/\text{THF}$ (32 mL 1:1 v/v) was stirred at room temperature for 48 h. $\text{CuSO}_4 \cdot 5\text{H}_2\text{O}$ (141 mg, 0.56 mmol), sodium ascorbate (1.12 g, 5.65 mmol) and 1-hexyne (1.33 g, 11.2 mmol) were added subsequently and the mixture was stirred in the oil bath at 55 °C for 48 hours. The organic solvent (THF) was removed under reduced pressure and the residue was suspended in CH_2Cl_2 (40 mL) and washed with water (2×50 mL), and brine (2×50 mL). After drying over MgSO_4 , charcoal was added to the solution and stirred for 30 min to further purify the compound. The suspension filtered off through celite, washed with CH_2Cl_2 (30 ml) and evaporated the solvent to obtain 4-butyl-1-methyl-1H-1,2,3-triazole as a white powder. The compound is suitable to be used for the next step. Yield: 750 mg (48%) ^1H NMR (400 MHz, CDCl_3): δ = 7.24 (s, 1H, H-5), 4.01 (s, 3H, $\text{CH}_3\text{-N}$), 2.69 – 2.63 (t, $^3J_{\text{H-H}} = 7.3$ Hz, 2H, $\text{CH}_2\text{-C}_4$), 1.60 (quintet, 2H, $\text{CH}_2\text{-CH}_2$), 1.33 (sextet, 2H, $\text{CH}_2\text{-CH}_3$), 0.88 (t, $^3J_{\text{H-H}} = 7.3$ Hz, 3H, CH_3 , n-Bu). $^{13}\text{C}\{^1\text{H}\}$ NMR (100 MHz, CDCl_3): δ = 148.8 (C-4), 121.7 (C-5), 36.5 ($\text{CH}_3\text{-N}$), 31.6 ($\text{CH}_2\text{-CH}_2$), 25.3 ($\text{CH}_2\text{-CH}_2$), 22.3 ($\text{CH}_2\text{-CH}_3$), 13.8 (CH_3 , n-Bu). MS HR-ESI [found 139.1116 (M-H) $^+$, $\text{C}_7\text{H}_{13}\text{N}_3$ requires 139.1109].

MeOTf (600 μL , 6.20 mmol, 1.2 equiv) was added to a solution of 4-butyl-1-methyl-1H-1,2,3-triazole (713 mg, 5.13 mmol) in CH_2Cl_2 (5 mL) at 0 °C then the solution kept to stir at 23 °C for 12 h (the reaction monitored by TLC). All volatiles were evaporated under reduced pressure. Purification by column chromatography (SiO_2 ; $\text{CH}_2\text{Cl}_2/\text{MeOH}$ 30:1) yielded product **149** as a pale yellow liquid. Yield: 1.00 g (64%). ^1H NMR (400 MHz, CDCl_3): δ 8.43 (s, 1H, H₅), 4.27 (s, 3H, $\text{CH}_3\text{-N}$), 4.16 (s, 3H, $\text{CH}_3\text{-N}$), 2.78 (t, 2H, $^3J_{\text{H-H}} = 15.96$, CH_2CH_2), 1.69 (quintet, 2H, CH_2CH_2), 1.42 (sextet, 2H, CH_2CH_3), 0.93 (t, $^3J_{\text{H-H}} = 7.3$ Hz, 3H, $\text{CH}_{3,\text{n-Bu}}$). $^{13}\text{C}\{^1\text{H}\}$ NMR (100 MHz, CDCl_3): δ = 144.9 (C-4), 129.3 (C-5), 120.6 (q, $^1J_{\text{C-F}} = 320.33$, CF_3), 40.0 ($\text{CH}_3\text{-N}$), 37.4 ($\text{CH}_3\text{-N}$), 28.7 ($\text{CH}_2\text{-CH}_2$), 23.0 ($\text{CH}_2\text{-CH}_2$), 22.1 ($\text{CH}_2\text{-CH}_3$), 13.5 ($\text{CH}_{3,\text{n-Bu}}$). ^{19}F NMR (377 MHz, CDCl_3), δ : -78.53. MS HR-ESI [found 154.1345 (M-OTf) $^+$, $\text{C}_8\text{H}_{16}\text{N}_3$ requires 154.1344].

6.1.5.3. Synthesis of [IrCp*Cl(149)]OTf (148)

Triazolium salt **149** (65 mg, 0.21 mmol), Me₄NCl (46 mg, 0.42 mmol), Ag₂O (97 mg, 0.42 mmol) and [Ir(Cp*)Cl₂]₂ (67 mg, 0.084 mmol, 0.4 equiv) were stirred in CH₂Cl₂ (10 ml) at 40 °C for 8 h. After cooling to rt, the suspension was filtered through celite and the solvent was removed under reduced pressure to yield the crude product. Purification by column chromatography (SiO₂; CH₂Cl₂/MeOH, 40:1) yielded product **148** as yellow solid (12 mg, 10%). ¹H NMR (400 MHz, CDCl₃): δ = ¹H NMR 4.27 (s, 3H, CH₃-N), 3.96 (s, 3H, CH₃-N), 2.95 (m, 2H, CH₂-CH₂), 2.01 – 1.74 (m, 1H, CH₂-CH₂), 1.61 (s, 15H, Cp*), 1.55 – 1.18 (m, 3H, CH₂-CH₂), 0.95 (t, ³J_{H-H} = 7.1 Hz, 3H). ¹³C{¹H} NMR (101 MHz, CDCl₃), δ: 148.9 (C-5), 144.4 (C-4), 87.8 (C, Cp*), 40.9 (CH₃-N), 36.3 (CH₃-N), 32.1 (CH₂), 29.8 (CH₂), 23.2 (CH₂), 14.0 (CH_{3,n-Bu}), 9.2 (CH₃, Cp*). MS HR-ESI [found 516.1718 (M-Cl)⁺, C₁₈H₃₀ClIr requires 516.1756]. Suitable crystals for X-ray diffraction were achieved by slow diffusion of pentane to dichloromethane solution.

6.1.5.4. Preparation of dicationic monoquo complexes **150** and **151**

To a solution of the corresponding [IrCp*Cl(L)]OTf (0.01 mmol) in dichloromethane (1.5 mL) was sequentially added water (18 μL, 1.1 mmol) and AgOTf (3.1 mg, 1.2 eq). The reaction was stirred for 48 h (compound **150**) or 12 h (for compound **151**) protected from light. Then the resulting suspension was filtered over celite, and all volatiles were removed under reduced pressure to yield the crude products.

[IrCp*(L3)(H₂O)](OTf)₂ (**150**). Yield: 7.7 mg, 88%. ¹H NMR (400 MHz, D₂O), δ: 7.73-7.78 (m, 2H, CH=), 7.52 (m, 2H, CH=), 4.38 (s, 3H, CH₃-N), 4.32 (s, 3H, CH₃-N), 1.67 (s, 15H, CH₃, Cp*). ¹³C{¹H} NMR (101 MHz, D₂O), δ: 156.8 (C-5), 151.5 (C=N), 135.9 (C-4), 128.1 (CH=), 127.3 (CH=), 120.0 (q, ¹J_{C-F} = 210.2, CF₃), 90.8 (C, Cp*), 40.8 (CH₃-N), 38.3 (CH₃-N), 9.2 (CH₃, Cp*). ¹⁹F NMR (377 MHz, D₂O), δ: -79.1 (s).

[IrCp*(L4)(H₂O)](OTf)₂ (**151**). Yield: 7.5 mg, 89%. ¹H NMR (400 MHz, D₂O), δ: 8.15 (d, ³J_{H-H} = 3.6 Hz, 1H, CH=), 7.93 (d, ³J_{H-H} = 3.6 Hz, 1H, CH=), 4.29 (s, 3H, CH₃-N), 4.28 (s, 3H, CH₃-N), 1.61 (s, 15H, CH₃, Cp*). ¹³C{¹H} NMR (101 MHz, D₂O), δ: 159.6 (C-5), 157.53 (C=N), 147.0 (C-4), 141.5 (CH=), 124.8 (CH=), 119.2 (q, ¹J_{C-F} = 320.0, CF₃), 90.3 (C, Cp*), 40.3 (CH₃-N), 37.9 (CH₃-N), 8.6 (CH₃, Cp*). ¹⁹F NMR

(377 MHz, D₂O), δ : -79.1 (s). MS HR-ESI [found 509.1351 (M-(OTf)₂-H₂O)⁺, C₁₇H₂₄IrN₄S requires 509.1345].

6.1.5.5. Preparation of dicationic diaquo complex 152

Monoaquo complexes [IrCp*(L3)(H₂O)](OTf)₂ (0.01 mmol) were dissolved in D₂O (1 mL) and allowed to stir at 70 C for 3 days.

[IrCp*(L3)(D₂O)₂](OTf)₂ (152). 85% yield by ¹H NMR. ¹H NMR (400 MHz, D₂O), δ : 6.98 (m, 2H, CH=), 6.86 (m, 2H, CH=), 4.17 (s, 3H, CH₃-N), 4.08 (s, 3H, CH₃-N), 1.27 (s, 15H, CH₃, Cp*). ¹³C{¹H} NMR (101 MHz, D₂O), δ : 166.6 (C-5), 149.9 (C=N), 144.4 (C-4), 136.4 (C), 128.0 (CH=), 127.2 (CH=), 126.5 (CH=), 119.2 (q, ¹J_{C-F} = 260.7, CF₃), 116.1 (CH=), 88.7 (C, Cp*), 39.6 (CH₃-N), 35.8 (CH₃-N), 8.1 (CH₃, Cp*). ¹⁹F NMR (377 MHz, D₂O), δ : -79.0 (s).

6.1.5.6. Electrochemistry

Cyclic voltammetry (CV) and differential pulse voltammetry (DPV) experiments were performed on a Biologic SP-150 potentiostat, using EC Lab software for data acquisition and data handling. Measurements were made using a standard three-electrode cell using glassy carbon disk electrode of 3.0 mm diameter as a working electrode, a Pt disk of 1 mm diameter as counter electrode and an aqueous saturated calomel electrode (SCE) as a reference electrode. All of the potentials are reported versus SCE isolated from the working electrode compartment by a salt bridge. Working electrodes were polished with 1 and 0.05 micron Alumina paste washed with distilled water and acetone and sonicated in acetone for 5 minutes before each measurement. The complexes were dissolved in DCM containing the necessary amount of ⁿBu₄NPF₆ (TBAPF₆) as supporting electrolyte to yield 0.1 M ionic strength solutions. For electrocatalytic experiments, complexes were dissolved in the corresponding water solutions (0.1 M triflic acid solution or acetate buffer pH 5.6). CV were recorded at different scan rates (50-1000 mV/s) and DPV were recorded using pulse amplitudes of 0.05 V, pulse widths of 0.05 s, sampling widths of 0.02 s, pulse periods of 0.1 s and quite times of 2 s. E₀ values reported in this work were estimated from DPV experiments. The error associated with the potential values is less than 5 mV.

6.1.5.7. Typical procedure for the water oxidation

Catalysis experiments were performed in a homemade thermostated glass cell ($V = 15$ mL) at 25 °C which was closed with a septum. The evolution of gases were monitored by on-line manometry with a differential pressure manometer (Testo 521), with an operating range of 0.1 – 10 kPa and accuracy within 0.5% , which was connected to a reference cell of approximately the same size, as well as by a gas phase oxygen sensor (Unisense Ox-N sensor) controlled by Unisense multimeter. The oxygen sensor was calibrated after each experiment by addition of known amounts of oxygen to the cell.

In a typical experiment, a solution of complex in 0.1 M triflic acid (pH 1) was degassed for 10 minutes using N_2 flow. After pressure equilibration between reference and measurement cell, baseline was recorded for 20-30 minutes and a solution of cerium ammonium nitrate (CAN) in 0.1 M Triflic acid was added to the reference and measurement cell. Resulting a final concentration of catalyst 1 mM and concentration of CAN 100 mM. For second and third injections, this procedure was carried out again adding 100 more equivalents of CAN in 0.1 M Triflic acid to the measurement and reference cells. Experiments with $NaIO_4$ were performed by using diluted degassed solutions of the complex in acetate buffer pH 5.6 in the same setup, resulting a final ratio Catalyst/Oxidant $1:4000$ and a final concentration 5 μ M for the catalyst and 20 mM for the $NaIO_4$.

TON was calculated from O_2 -selective clark-type electrode analysis of the reaction headspace and TOF values were calculated from the increase of TON in the initial 5 minutes after addition of oxidant. O_2 /Gas ratios were calculated dividing total oxygen produced detected by O_2 -selective clark probe by the total gas evolved obtained by manometric experiments.

6.1.6. References

1. International Energy Agency: World Energy Outlook, **2015**.
2. (a) Gray, H. B. *Nat. Chem.* **2009**, 1, 7. (b) Lewis, N. S.; Nocera, D. G. *Proc. Natl. Acad. Sci.* **2006**, 103, 15729. (c) Lewis, N. S.; Crabtree, G. *Basic Research Needs for Solar Energy Utilization: Report of the Basic Energy Sciences Workshop on Solar Energy Utilization*, Apr 18–21, 2005. US Department of Energy Office of Basic Energy Sciences, **2005**.

3. For recent reviews, see: (a) Kärkäs, M. D.; Verho, O.; Johnston, E. V.; Åkermark, B. *Chem Rev.* **2014**, 114, 11863. (b) Blakemore, J. D.; Crabtree, R. H.; Brudvig, G. W. *Chem. Rev.* **2015**, 115, 12974. (c) *Molecular Water Oxidation Catalysis*; Ed. Llobet, A., Wiley, Chichester, **2005**. (d) Hunter, B. M.; Gray, H. B.; Müller, A. M. *Chem. Rev.* **2016**, 116, 14120.

4. For representative examples, see: (a) Anderlund, M. F.; Höglblom, J.; Shi, W.; Huang, P.; Eriksson, L.; Weihe, H.; Styring, S.; Åkermark, B.; Lomoth, R.; Magnuson, A. *Eur. J. Inorg. Chem.* **2006**, 5033. b) Limburg, J.; Brudvig, G. W.; Crabtree, R. H. *J. Am. Chem. Soc.* **1997**, 119, 2761. (c) Limburg, J.; Vrettos, J. S.; Liable-Sands, L. M.; Rheingold, A. L.; Crabtree, R. H.; Brudvig, G. W. *Science* **1999**, 283, 1524. (d) Chen, H.; Faller, J. W.; Crabtree, R. H.; Brudvig, G. W. *J. Am. Chem. Soc.* **2004**, 126, 7345. (e) Herrero, C.; Hughes, J. L.; Quaranta, A.; Cox, N.; Rutherford, A. W.; Leibl, W.; Aukauloo, A. *Chem. Commun.* **2010**, 46, 7605. (f) Shimazaki, Y.; Nagano, T.; Takesue, H.; Ye, B.-H.; Tani, F.; Naruta, Y. *Angew. Chem., Int. Ed.* **2004**, 43, 98. (g) Naruta, Y.; Sasayama, M.-A.; Sasaki, T. *Angew. Chem., Int. Ed. Engl.* **1994**, 33, 1839. (h) Poulsen, A. K.; Rompel, A.; McKenzie, C. J. *Angew. Chem., Int. Ed.* **2005**, 44, 6916. (i) Brimblecombe, R.; Swiegers, G. F.; Dismukes, G. C.; Spiccia, L. *Angew. Chem., Int. Ed.* **2008**, 47, 7335. j) Brimblecombe, R.; Koo, A.; Dismukes, G. C.; Swiegers, G. F.; Spiccia, L. *J. Am. Chem. Soc.* **2010**, 132, 2892.

5. For representative examples, see: (a) Gersten, S. W.; Samuels, G. J.; Meyer, T. J. *J. Am. Chem. Soc.* **1982**, 104, 4029. (b) Sens, C.; Romero, I.; Rodríguez, M.; Llobet, A.; Parella, T.; Benet-Buchholz, J. *J. Am. Chem. Soc.* **2004**, 126, 7798. (c) Xu, Y.; Fischer, A.; Duan, L.; Tong, L.; Gabrielsson, E.; Åkermark, B.; Sun, L. *Angew. Chem., Int. Ed.* **2010**, 49, 8934. (d) Zong, R.; Thummel, R. P. *J. Am. Chem. Soc.* **2005**, 127, 12802. (e) Duan, L.-L.; Xu, Y.-H.; Tong, L.-P.; Sun, L.-C. *ChemSusChem* **2011**, 4, 238. (f) Kärkäs, M. D.; Åkermark, T.; Johnston, E. V.; Karim, S. R.; Laine, T. M.; Lee, B.-L.; Åkermark, T.; Privalov, T.; Åkermark, B. *Angew. Chem., Int. Ed.* **2012**, 51, 11589. (g) Duan, L.; Bozoglian, F.; Mandal, S.; Stewart, B.; Privalov, T.; Llobet, A.; Sun, L. *Nat. Chem.* **2012**, 4, 418. (h) Nyhlén, J.; Duan, L.; Åkermark, B.; Sun, L.; Privalov, T. *Angew. Chem., Int. Ed.* **2010**, 49, 1773. (i) Matheu, R.; Ertem, M. Z.; Benet-Buchholz, J.; Coronado, E.; Batista, V. S.; Sala, X.; Llobet, A. *J. Am. Chem. Soc.* **2015**, 137, 10786. (j) Creus, J.; Matheu, R.; Peñafiel, I.; Moonshiram, D.; Blondeau, P.; Benet-Buchholz, J.; García-Antón, J.; Sala, X.; Godard, C.; Llobet, T. *Angew. Chem., Intl. Ed.* **2016**, 55, 15382.

6. For representative examples, see: (a) Abe, T.; Nagai, K.; Kabutomori, S.; Kaneko, M.; Tajiri, A.; Norimatsu, T. *Angew. Chem., Int. Ed. Engl.* **2006**, 45, 2778. (b) Rigsby, M. L.; Mandal, S.; Nam, W.; Spencer, L. C.; Llobet, A.; Stahl, S. S. *Chem. Sci.* **2012**, 3, 3058. (c) Lv, H.; Song, J.; Geletii, Y. V.; Vickers, J. W.; Sumliner, J. M.; Musaev, D. G.; Kögerler, P.; Zhuk, P. F.; Bacsá, J.; Zhu, G.; Hill, C. L. *J. Am. Chem. Soc.* **2014**, 136, 9268. (d) Berardi, S.; La Ganga, G.; Natali, M.; Bazzan, I.; Puntoriero, F.; Sartorel, A.; Scandola, F.; Campagna, S.; Bonchio, M. *J. Am. Chem. Soc.* **2012**, 134, 11104. (e) Zhang, B.; Li, F.; Yu, F.; Wang, X.; Zhou, X.; Li, H.; Jiang, Y.; Sun, L. *ACS Catal.* **2014**, 4, 804. (f) Moonshiram, D.; Gimbert-Suriñach, C.; Guda, A.; Picon, A.; Lehmann, C. S.; Zhang, Z.; Doumy, G.; March, A. M.; Benet-Buchholz, J.; Soldatov, A.; Llobet, A.; Southworth, S. H. *J. Am. Chem. Soc.* **2016**, 138, 10586.

7. For representative examples, see: (a) Ellis, W. C.; McDaniel, N. D.; Bernhard, S.; Collins, T. J. *J. Am. Chem. Soc.* **2010**, 132, 10990. (b) Demeter, E. L.; Hilburg, S. L.; Washburn, N. R.; Collins, T. J.; Kitchin, J. R. *J. Am. Chem. Soc.* **2014**, 136, 5603. (c) Panda, C.; Debgupta, J.; Diaz Diaz, D.; Singh, K. K.; Sen Gupta, S.; Dhar, B. B. *J. Am. Chem. Soc.* **2014**, 136, 12273. (d) Fillol, J. L.; Codola, Z.; Garcia-Bosch, I.; Gomez, L.; Pla, J. J.; Costas, M. *Nat. Chem.* **2011**, 3, 807. (e) Chen, G.; Chen, L.; Ng, S.-M.; Man, W.-L.; Lau, T.-C. *Angew. Chem., Int. Ed.* **2013**, 52, 1789. (f) Coggins, M. K.; Zhang, M.-T.; Vannucci, A. K.; Dares, C. J.; Meyer, T. J. *J. Am. Chem. Soc.* **2014**, 136, 5531.

8. For representative examples, see: (a) McDaniel, N. D.; Coughlin, F. J.; Tinker, L. L.; Bernhard, S. *J. Am. Chem. Soc.* **2008**, 130, 210. (b) Hull, J. F.; Balcells, D.; Blakemore, J. D.; Incarvito, C. D.; Eisenstein, O.; Brudvig, G. W.; Crabtree, R. H. *J. Am. Chem. Soc.* **2009**, 131, 8730. (c) Savini, A.; Bellachioma, G.; Ciancaleoni, G.; Zuccaccia, C.; Zuccaccia, D.; Macchioni, A. *Chem. Commun.* **2010**, 46, 9218. (d) Lalrempuia, R.; McDaniel, N. D.; Müller-Bunz, H.; Bernhard, S.; Albrecht, M. *Angew. Chem., Int. Ed.* **2010**, 49, 9765. (e) Turlington, C. R.; White, P. S.; Brookhart, M.; Templeton, J. L. *J. Am. Chem. Soc.* **2014**, 136, 3981. (f) Grotjahn, D. B.; Brown, D. B.; Martin, J. K.; Marelius, D. C.; Abadjian, M.-C.; Tran, H. N.; Kalyuzhny, G.; Vecchio, K. S.; Specht, Z. G.; Cortes-Llamas, S. A.; Miranda-Soto, V.; van Niekerk, C.; Moore, C. E.; Rheingold, A. L. *J. Am. Chem. Soc.* **2011**, 133, 19024. (g) Parent, A. R.; Blakemore, J. D.; Brudvig, G. W.; Crabtree, R. H. *Chem. Commun.* **2011**, 47, 11745. (h) Codola, Z.; Cardoso, J. M. S.; Royo, B.; Costas, M.; Lloret-Fillol, J. *Chem. Eur. J.* **2013**, 19, 7203. (i) Navarro, M.; Li, M.; Mueller-Bunz, H.; Bernhard, S.; Albrecht, M. *Chem. Eur. J.* **2016**, 22, 6740. (j) Sharninghausen, L. S.; Sinha, S. B.; Shopov, D. Y.; Choi, B.;

- Mercado, B. Q.; Roy, X.; Balcells, D.; Brudvig, G. W.; Crabtree, R. H. *J. Am. Chem. Soc.* **2016**, 138, 15917.
9. (a) Woods, J. A.; Lalrempuia, R.; Petronilho, A.; McDaniel, N. D.; Müller-Bunz, H.; Albrecht, M.; Bernhard, S. *Energy Environ. Sci.* **2014**, 7, 2316. (b) Corbucci, I.; Petronilho, A.; Muller-Bunz, H.; Rocchigiani, L.; Albrecht, M.; Macchioni, A. *ACS Catal.* **2015**, 5, 2714.
10. Thomsen, J. M.; Sheehan, S. W.; Hashmi, S. M.; Campos, J.; Hintermair, U.; Crabtree, R. H.; Brudvig, G. W. *J. Am. Chem. Soc.* **2014**, 136, 13826.
11. This behavior contrast with that observed using Cp*IrPy-O complexes developed by Crabtree et al, see reference 10.
12. Schley, N. D.; Blakemore, J. D.; Subbaiyan, N. K.; Incarvito, C. D.; D'Souza, F.; Crabtree, R. H.; Brudvig, G. W. *J. Am. Chem. Soc.* **2011**, 133, 10473.
13. Similar behavior has been observed for related pyridyl-triazolidene complexes, see reference 9a.
14. The activities obtained using complexes **4** and **5** are lower than those obtained using parent pyridyl-triazolidene Ir catalyst precursor **1**, which is not unexpected due to the lower donor ability of the benzoxazole and thiazole moieties compared to those of the pyridine groups. However, activities can possibly be improved by introducing more lipophilic alkyl chain as previously observed, see reference 9b.
15. Most probably the other gas formed is carbon dioxide, most likely due to the decomposition cyclopentadienyl ring. The formation of degradation products such as formic acid, carbon dioxide and methanol have been reported from IrCp*-based catalysts in the presence of CAN. See reference 9b.
16. CAN is able to oxidize many organic groups, see: Nair, V.; Deepthi, A. *Chem. Rev.* **2007**, 107, 1862.
17. Parent, A. R.; Brewster, T. P.; De Wolf, T.; Crabtree, R. H.; Brudvig, G. W. *Inorg. Chem.* **2012**, 51, 6147.
18. (a) Crabtree, R. H. *Chem. Rev.* **2012**, 112, 1536. (b) Thomsen, J. M.; Sheehan, S. W.; Hashmi, S. M.; Campos, J.; Hintermair, U.; Crabtree, R. H.; Brudvig, G. W. *J. Am. Chem. Soc.* **2014**, 136, 13826.
19. This technique cannot reliable measure particles <1 nm and neither is efficient when the concentration is not high enough.
20. Hydrodynamic volumes between 0.65 and 0.95 have been recently calculated using similar Cp*Ir-MIC complexes. See reference 9b.

21. For representative examples, see: (a) DePasquale, J.; Nieto, I.; Reuther, L. E.; Herbst-Gervasoni, C. J.; Paul, J. J.; Mochalin, V.; Zeller, M.; Thomas, C. M.; Addison, A. W.; Papish, E. T. *Inorg. Chem.* **2013**, *52*, 9175-9183 (TOF's up to 0.16 s^{-1}). (b) reference 9b (TOF's up to 0.1 s^{-1}). For reviews, see: 3a-b.
22. The ligand donor ability is crucial to facilitate the oxidation of the Ir(III) to Ir(IV) and Ir(V) species.

Chapter 7.

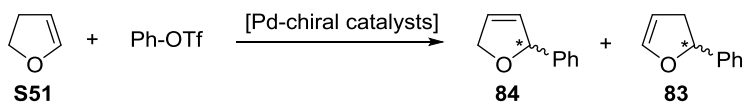
*Palladium-catalyzed asymmetric intermolecular
Heck reaction*

7.1. Air stable and simple phosphite-oxazoline ligands for Pd-intermolecular asymmetric Heck reaction. Mechanistic insights

Mazloomi, Z.; del Valle, E.; Pàmies, O.; Pericàs, M. A.; van Leeuwen, P. W. N. M.; Diéguez, M. Manuscript in preparation.

7.1.1. Introduction

The Pd-catalyzed Heck reaction (also known as Mizoroki-Heck), i.e., the coupling of an alkenyl, aryl halide or triflate to an alkene, is one of the most powerful C-C bond forming reactions, as it was recognized with the Nobel Prize in Chemistry in 2010.¹ Its applicability to highly functionalized substrates confers the reaction a large substrate scope and it is widely applied in the synthesis of pharmaceuticals, natural products and fine chemicals.¹ The extensive research dedicated to this process can give the erroneous impression that Heck chemistry is a mature area. Although the Heck reaction has been known since the late 1960s, its asymmetric version was not published until 1980, with most examples dealing with intramolecular reactions, where the alkene regiochemistry and geometry of the product can be easily controlled.¹ The asymmetric intermolecular Heck reaction was not published until 1991.² Although since then many research groups have devoted considerable efforts to the intermolecular version, it is still less developed than the intramolecular version and its synthetic utility remains limited. This is due in part to regioselectivity problems caused by the possible migration of the carbon-carbon double bond, which leads to mixtures of products. For example, in the Heck coupling of the model 2,3-dihydrofuran substrate (**S51**) with phenyl triflate (Scheme 7.1.1), both the desired 2-phenyl-2,5-dihydrofuran (**84**) and the undesired 2-phenyl-2,3-dihydrofuran (**83**) can be obtained.



Scheme 7.1.1. Model Pd-catalyzed Heck reaction of 2,3-dihydrofuran (**S51**) with phenyl triflate.

At the beginning, the research in the asymmetric intermolecular reaction focused in the development of diphosphine ligands, being BINAP the central ligand.¹ Although Pd-diphosphine catalysts provided high enantioselectivities, the regioselectivity and activity were less favorable (e.g., BINAP provided enantioselectivities up to 96% but the main product was **83**, in only 71% of regioselectivity, and the reaction time was 9 days)². This moved the research to other types of ligands. A breakthrough was the report by Pfaltz et al., who showed that phosphine-oxazoline PHOX ligands (**93c**, Figure 7.1.1) minimize the double bond isomerization providing high regio- and enantioselectivity to the desired product **84**, although still at low activity with long reaction times (3-7 days to achieve full conversion).³ Then, the follow up work for the intermolecular Heck reaction focused in Pd-catalysts modified with chiral phosphine-oxazoline ligands.^{4,5} Although many of these ligands were developed, only a few of them provided high selectivity (Figure 7.1.1) and the problems of low reaction rates and low substrate specificity remained. Although microwave irradiation considerably reduced the reaction times from weeks to days, it affected enantioselectivity – and sometimes regioselectivity – negatively.⁶ Additionally, the most successful phosphine-oxazoline ligands contained a *t*Bu group in the oxazoline and their synthesis required starting from the very expensive amino acid *tert*-leucine. Although alternative phosphine-oxazoline ligands, such as those incorporating geminal substituents at C-4 of *i*Pr-PHOX,^{4q} were developed to solve this limitation, they had lower substrate scope and/or required more reaction steps. A final limitation of phosphine-oxazoline ligands is that most of them are prone to oxidation.

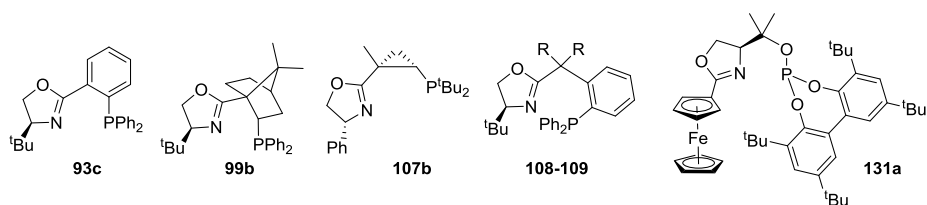


Figure 7.1.1. Representative privileged P-oxazoline ligands for Pd-catalyzed asymmetric intermolecular Heck reaction.

The search for efficient ligands prepared in only a few steps from inexpensive raw materials, easy to handle (i.e., solid, robust and air stable) and that induce higher rates and substrate scope has therefore attracted the attention of many researchers. For this purpose two main strategies have been used for ligand design. One, developed recently

by the groups of Oestrich and Zhou, illustrates the power of mixed phosphine-phosphine oxides which had been discarded in the Heck reaction for decades. Pd/phosphine-phosphine oxide systems were successfully applied in the intermolecular Heck reaction of several cyclic alkene substrates with various aryl triflates and aryl halides.⁷ The second strategy developed by our group was based on biaryl phosphite-oxazoline ligands. Phosphite-containing ligands are particularly useful for asymmetric catalysis.⁸ Their highly modular construction, facile synthesis from available alcohols and greater resistance to oxidation than the phosphines have proved to be highly advantageous. In this respect, our group has contributed with an improved generation of air stable phosphite-oxazoline ligand libraries for several asymmetric catalytic transformations.⁹ The application of two of these phosphite-oxazoline libraries in the Heck reaction lead us to identify a Pd/phosphite-oxazoline **131a** catalyst (Figure 7.1.1) that provided activities of 100% in only 10 min with excellent regio- and enantioselectivities in the coupling of several cyclic substrates and a variety of triflates.¹⁰ To the best of our knowledge no other phosphite-oxazoline ligands have been applied. Despite the mentioned developments, the use of the phosphite-oxazoline ligands in the intermolecular Heck reaction has unknowns that must be explored in the search of better catalysts. For example, no mechanistic studies have been made to discern the role of the ligand structure parameters that should lead to a conclusive reason of the higher activity of our chiral phosphite-oxazoline compared with their analogues phosphine-N ligands. Different from other C-C bond forming reaction such as Pd Tsuji-Trost reactions, most of the mechanistic studies in Heck reaction have focused on achiral systems.¹¹ For example, the rate determining step using achiral diphosphine Pd-catalysts is well determined.^{11b,c,f} Achiral phosphite ligands, however, have been less studied.^{11a,d,e} Moreover, the investigations of catalytic intermediates in asymmetric Heck reaction are still preliminary. No kinetic studies have been carried out and the very few mechanistic studies for specific ligands are mainly computational.^{40,5g,12} Experimental studies by NMR and kinetic studies are difficult because of the high reactivity and multifaceted aggregation behavior of Pd-precursor that gives unreactive Pd-black species. The experimental protocol to control the formation of Pd-black under reaction conditions must still be developed.

7.1.2. Objectives

The potential of phosphite containing-ligands in enantioselective Pd-catalyzed Heck reaction and the species responsible for the catalytic performance must be studied with new phosphite-oxazoline ligands. To address these points, we report a reduced but structurally valuable library of readily accessible phosphite-oxazoline ligands **L5-L9a-e** (Figure 7.1.2). These are based on privileged phosphine-oxazoline ligands **108-109**⁴⁰ (Figure 7.1.1) in which the phosphine moiety has been replaced by biaryl phosphite moieties that increase robustness and modularity (that allows a better control of the flexibility of the chiral pocket). In addition these ligands are solid and stable to air and other oxidizing agents. In a simple two or four step-procedure, that starts from commercially available materials, (Scheme 7.1.2) several ligand parameters can be easily tuned to maximize the catalyst performance. With this ligand library we systematically investigated the effect of changing the oxazoline substituents (Ph, ⁱPr and ^tBu) and their configuration, the substituents in the benzylic position (ligands **L5-L7a-e** with a hydrogen group and ligands **L8a-e** with a methyl group) and the substituents and configurations of the biaryl phosphite moiety (**a-e**). Interestingly, we found that the range of substrates and triflate sources that can be successfully coupled was higher than for the previous phosphine-oxazoline **108-109** counterparts, which have emerged as some of the most successful catalysts designed for this process. In addition, the phosphite-oxazoline ligands that provided the best selectivities contained the ⁱPr substituent in the oxazoline moiety instead of the pricy ^tBu substituent found in the related phosphine-oxazoline **108-109**. Finally, in this paper we have also successfully carried out mechanistic studies by combining in situ NMR of key intermediates and kinetics studies.

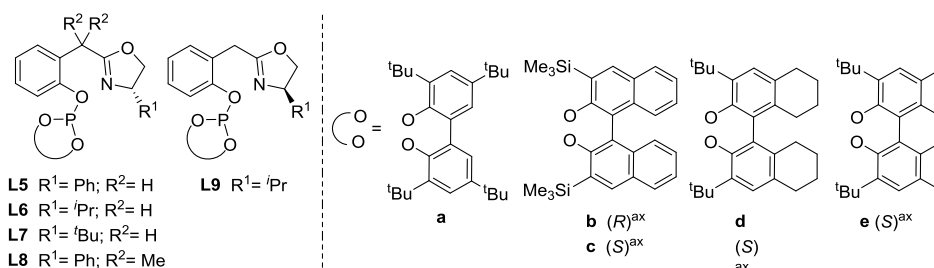
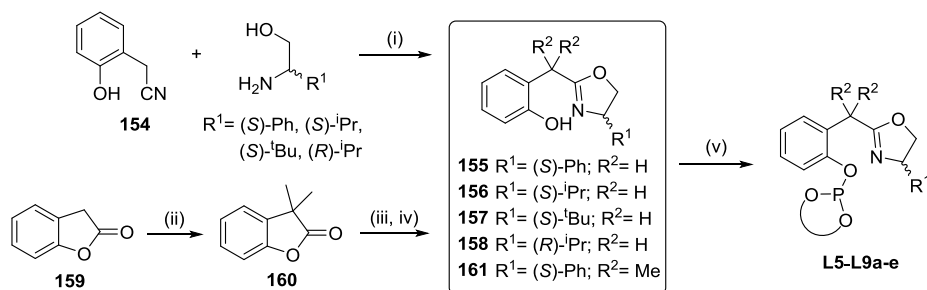


Figure 7.1.2. Phosphite-oxazoline ligand library (**L5-L9a-e**).

7.1.3. Results and discussion

7.1.3.1. Synthesis of ligands

The sequence of ligand synthesis is illustrated in Scheme 7.1.2. Phosphite-oxazoline ligands **L5-L9a-e** were synthesized very efficiently from the corresponding easily accessible hydroxyl-oxazolines **155-158** and **161**. Hydroxyl-oxazoline **155-158** were prepared, in only one step, as previously reported in the literature from readily available starting materials. Therefore, coupling of hydroxyl-cyanide **154** with the appropriate amino alcohol yielded the hydroxyl-oxazolines **155-158** with diverse oxazoline substituents (Scheme 7.1.2, step i).¹³ For the synthesis of the hydroxyl-oxazoline **161**, which differs from **155-158** in the presence of methyl groups on the benzylic position, the commercially available 2(3*H*)-benzofuranone **159** was converted into the corresponding benzofuranone **160** by treatment with methyl iodide and sodium hydride (step ii).¹⁴ Subsequent reaction of **160** with 3-amino-3-phenylpropan-1-ol (amino alcohol) followed by cyclization with *p*-TsCl afforded the desired hydroxyl-oxazoline **161** (steps iii and iv).



Scheme 7.1.2. Synthetic route for the synthesis of phosphite-oxazoline ligands **L5-L9a-e**. (i) amino alcohol, ZnCl_2 , $\text{C}_6\text{H}_5\text{Cl}$, reflux, 16 h (yields 68-78%);¹³ (ii) NaH, MeI, THF, -78°C to rt (43% yield);¹⁴ (iii) Aminoalcohol, NaH, MeOH, THF, 0°C to rt, 4 h, (75% yield). (iv) *p*-TsCl, NEt_3 , DMAP, CH_2Cl_2 , 0°C to rt, overnight (89% yield). (v) $\text{CIP}(\text{OR})_2$ ((OR)₂ = **a-e**), Py, toluene at rt for 18 h (40-78% yields).

The last step of the synthesis is common for all ligands (Scheme 7.1.2, step v). Condensation of the desired *in situ* formed phosphorochloridites ($\text{CIP}(\text{OR})_2$ (OR)₂ = **a-e**) with the corresponding hydroxyl-oxazoline **155-158** and **161** yielded phosphite-oxazoline ligands **L5-L9a-e**, with different biaryl phosphite groups. They were isolated as white solids in good-to-high yields. As mentioned earlier, **L5-L9a-e** can be

manipulated and stored in air. All ligands were characterized by $^{31}\text{P}\{^1\text{H}\}$, ^1H and $^{13}\text{C}\{^1\text{H}\}$ NMR spectra and mass spectrometry. All data were in agreement with assigned structures (see experimental and supporting information sections for details). The ^1H , ^{13}C , and ^{31}P NMR spectra showed the expected pattern for these C_1 -complexes. The VT-NMR spectra in CD_2Cl_2 (+35 to -85 °C) showed only one isomer in solution.

7.1.3.2. Asymmetric Heck reaction of 2,3-dihydrofuran (S1)

We first applied the ligands **L5–L9a-e** to the Pd-catalyzed phenylation of 2,3-dihydrofuran **S51**. For comparison, we evaluated them using the optimal reaction conditions reported in our previous studies with other phosphite-oxazoline ligands.¹⁰ Reactions were therefore performed in tetrahydrofuran, at 50°C, using 2.5 mol% of *in-situ* generated catalyst, by mixing the $[\text{Pd}_2(\text{dba})_3]\cdot\text{C}_6\text{H}_6$ ¹⁵ with the corresponding chiral ligand, and $i\text{Pr}_2\text{NEt}$ as base. The results are collected in Table 7.1.1. The catalytic performance was found to depend on the ligand structure, i.e., the substituents on the oxazoline ring and on the benzylic position and the substituents/configuration of the biaryl phosphite moiety.

The reactions that proceeded with the highest activities, regio- and enantioselectivities (e.g. entries 4-6 vs 1-3 and 9-11) had ligands containing the $i\text{Pr}$ oxazoline group (ligands **L6**). This contrasts with the oxazoline-substituent effect observed in the vast majority of successful P-oxazoline ligands (such as the $t\text{Bu}$ PHOX **93c** and the Gilberston phosphine-oxazoline ligand based on ketopinonic acid **99b**; see Figure 7.1.1) whose enantioselectivities are higher when *tert*-butyl groups are present. Interestingly, by comparing our results with those from the analogous Pd-phosphine-oxazoline systems **108-109**⁴⁰ (Figure 7.1.1, R=H) we found that the simple substitution of the phosphine by biaryl phosphite groups is advantageous since the ligands that provided the best selectivities contained the $i\text{Pr}$ substituent in the oxazoline moiety instead of the costly $t\text{Bu}$ substituent. We also found, as expected, that the sense of enantioselectivity is governed by the absolute configuration of the oxazoline substituent (entry 4 ligand **L6a** vs 15 ligand **L9a**). Both enantiomers of the phenylation product **84** can therefore be accessed by simple changing the absolute configuration of the oxazoline group.

Table 7.1.1. Pd-catalyzed enantioselective phenylation of 2,3-dihydrofuran **S51** using ligands **L5-L9a-e**.^a

Entry	Ligand	%Conv (84:83) ^b	%ee 84 ^c
1	L5a	94 (98:2)	67 (<i>R</i>)
2	L5b	50 (52:48)	81 (<i>R</i>)
3	L5c	92 (99:1)	75 (<i>R</i>)
4	L6a	100 (97:3) ^d	90 (<i>R</i>)
5	L6b	42 (58:42)	47 (<i>S</i>)
6	L6c	97 (96:4)	71(<i>R</i>)
7	L6d	99 (98:2) ^e	92 (<i>R</i>)
8	L6e	88 (97:3) ^f	92 (<i>R</i>)
9	L7a	20 (44:56)	85 (<i>R</i>)
10	L7b	47 (43:54)	10 (<i>S</i>)
11	L7c	85 (96:4)	81 (<i>R</i>)
12	L8a	48 (20:80)	4 (<i>R</i>)
13	L8b	5 (45:55)	15 (<i>R</i>)
14	L8c	13 (43:57)	20 (<i>R</i>)
15	L9a	100 (96:4) ^g	90 (<i>S</i>)
16 ^h	L6a	6 (89:11)	78 (<i>R</i>)
17 ⁱ	L6a	100 (97:3)	85 (<i>R</i>)
18 ^j	L6a	64 (87:13)	71 (<i>R</i>)

^(a) [Pd₂(dba)₃], benzene (1.25×10⁻² mmol), **S51** (2.0 mmol), phenyl triflate (0.5 mmol), ligand (2.8×10⁻² mmol), THF (3 ml), ⁱPr₂NEt (1 mmol), T = 50 °C, t = 24 h. ^(b) Conversion percentages determined by GC. ^(c) Enantiomeric excesses measured by GC. ^(d) 89% isolated yield. ^(e) 86% isolated yield. ^(f) 71% isolated yield. ^(g) 87% isolated yield. ^(h) Reaction carried out at 23 °C. ⁽ⁱ⁾ Reaction carried out at 70 °C. ^(j) Reaction carried out in benzene.

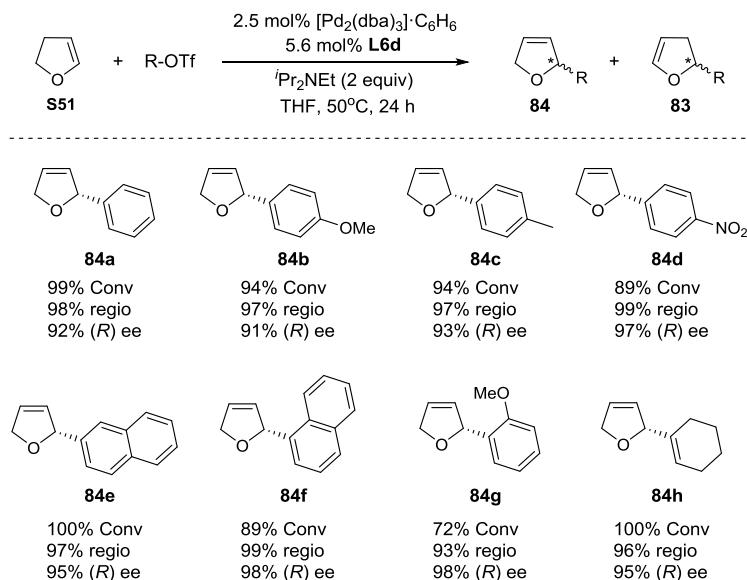
Concerning the effect of the biaryl phosphite group, we found that its configuration affected activity and selectivity. In general, ligands with an *S*-configuration of the biaryl phosphite moiety provided higher conversion, regio- and enantioselectivities than ligands with an *R*-configuration (Table 7.1.1, entries 6-8 vs 5) although ligand **L6a** with the aquiral biaryl phosphite group also provided high activities and selectivities (Table 7.1.1, entry 4). This ligand maintains the economic benefits of using an ⁱPr oxazoline substituent and has the added advantage that an achiral inexpensive biaryl phosphite moiety **a** is used. If we compare the results of **L6a** with those of the related enantiopure biaryl ligands **L6b** and **L6c**, (entry 4 vs 5 and 6), we can conclude that the

tropoisomeric biphenyl moiety in **L6a** adopts an *S*-configuration. We also found that the substituent of the biaryl phosphite moiety has an important effect on selectivity since ligands **L6d-e** provided higher selectivity than **L6c** (entries 7-8 vs 6). Finally, the introduction of methyl groups at the benzylic position had a negative effect on both activity and selectivity (Table 7.1.1, entries 12-14 vs 1-3). This contrasts with the results reported for related phosphine-oxazoline **108-109**⁴⁰ where the introduction of Me substituents at the benzylic position provided the reverse enantiomer although with somewhat lower enantioselectivity (from 93 % (*R*) with a H substituent to 81 % (*S*) with a Me substituent) and regioselectivity.

In summary, the highest regio- (up to 98%) and enantioselectivities (up to 92%) were achieved with phosphite-oxazoline ligands **L6a,d-e** and **L9a**. Moreover, both enantiomers of phenylation product **84** can be accessed in high regio- and enantioselectivity simply by changing the configuration of the oxazoline substituent. We next studied the effect of the temperature with one of the best ligands (entries 16-17). Lowering the temperature to 23 °C has a negative effect on both selectivity and activity (only 6% of conversion after two days). High temperature (70 °C) has also a negative effect on enantioselectivity whereas the good regioselectivity is maintained. Finally, we studied the effect of changing the solvent to benzene. Most of the successful ligands reported in the literature gave better catalytic performance using benzene instead of THF.³ This was not the case with our ligands: activities and selectivities were lower with benzene (entry 18).

Other triflate sources. We next studied other triflate sources. The results (Scheme 7.1.3) follow the same trend, in terms of the effect of the ligand parameters, as the phenylation of **S51**. Again, the best results were obtained with **L6a,d-e** and **L9a**. As an example, Scheme 7.1.3 shows the results using ligand **L6d** which had provided one of the best results in the phenylation of **S51** (the full results are shown in the supporting information). Both enantiomers of the coupling products **84a-h** were accessible with high activity, regio- (up to 99%) and enantioselectivity (up to 98%). Improving results reported in the literature, we found that the catalytic performance was almost not affected by the steric and electronic properties of the aryl groups. Therefore, a variety of triflates with different electronic and steric properties (1- and 2-naphthyl, *p*-CH₃-C₆H₄, *p*-NO₂-C₆H₄, *p*-OMe-C₆H₄ and *o*-OMe-C₆H₄) reacted with **S51** in regio- and enantioselectivities as high as or higher than those obtained with phenyl triflate. Even the sterically demanding *o*-methoxyphenyl and 1-naphthyl triflates were cross-coupled

efficiently. Finally, it is also worth mentioning that the addition of the cyclohexenyl triflate that usually reacted with less regio- and enantioselectivity than the coupling of phenyl triflate proceeded with comparable high regio- and enantioselectivity. All these results are among the best that have been reported in the literature^{1c,n} and surpass the range of triflate sources that could be coupled with higher enantioselectivity than using the phosphine-oxazoline analogues **108-109**⁴⁰.

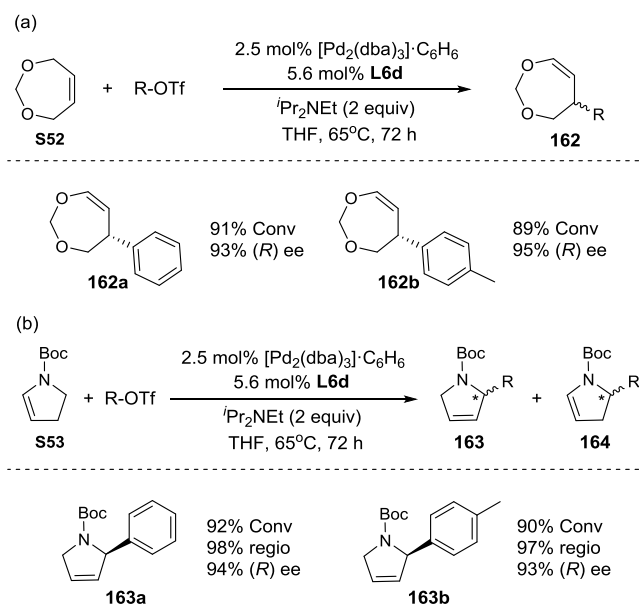


Scheme 7.1.3. Asymmetric Heck reaction of 2,3-dihydrofuran **S51**.

7.1.3.3. Asymmetric Heck reaction of other substrates

To further study the potential of **L5-L9a-e** ligands, we used them in the Pd-catalyzed Heck reaction of other challenging substrates. We initially studied the arylation of 4,7-dihydro-1,3-dioxepin **S52** with phenyl- and *p*-CH₃-C₆H₄ triflates (Scheme 7.1.4a). The enol ethers **162** resulting from these substrates are easily converted into chiral β-aryl-γ-butyrolactones, which are useful synthetic intermediates.¹⁶ Despite its relevance, the successful examples found in the literature are scarce and require long reaction times (typically 5-7 days).¹⁷ The results are summarized in Scheme 7.1.4a and followed the same trends as for the arylation of **S51**. Again, catalysts Pd/**L6a,d-e** and Pd/**L9a** provided both enantiomers of the arylation products **162a** and **162b** in high enantioselectivities (up to 95%) comparable to the best reported so far.

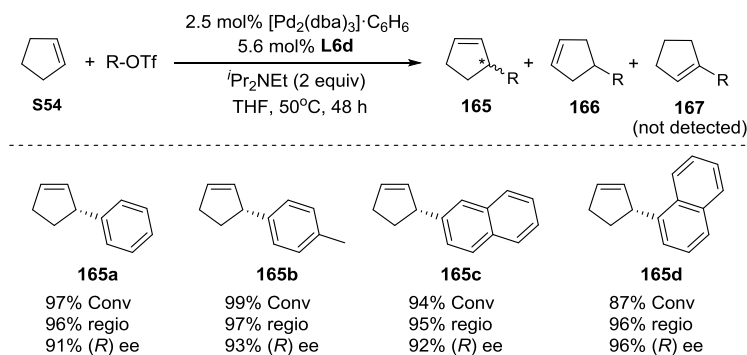
Dihydropyrroles are another important set of substrates which are widely present in biological compounds and have versatile synthetic applications.¹⁸ We investigated the asymmetric Heck reaction of *N*-Boc-2,3-dihydropyrrole **S53** with phenyl- and *p*-CH₃-C₆H₄ triflates (Scheme 7.1.4b). Although their Pd-catalyzed alkenylation has been studied before, the few reported examples had a limited success.¹ Again, ligands **L6a,d-e** and **L9a** that contain the *i*Pr substituent in the oxazoline moiety (see the complete results in the Supporting Information section) provided the best results with activities, regio- (up to 98%) and enantioselectivities (up to 94%) comparable to the best one reported in the literature.¹



Scheme 7.1.4. Asymmetric Heck reaction of (a) 4,7-dihydro-1,3-dioxepin **S52** and (b) *N*-Boc-2,3-dihydropyrrole **S53**.

We finally turned our attention to the asymmetric alkenylation of cyclopentene **S54** (Scheme 7.1.5). Due to extensive double-bond migration, the selectivity is more difficult to control in this substrate than in functionalized alkenes, such as **S51** and **S53**.¹ Most of the catalysts fail to control the regioselectivity and, in addition to the desired product **165**, the corresponding achiral regioisomers **166** and **167** can be obtained. Therefore, the reported catalysts for the Pd-catalyzed arylation of this substrate are fewer than for the arylation of functionalized alkenes.¹ Our Pd/**L6a,d-e** and Pd/**L9a**

catalytic systems turned out to be efficient in the alkenylation of **S54** using four triflate sources with different electronic and steric proprieties (Scheme 7.1.5). In all cases high activities, regio- and enantioselectivities in both enantiomers of the arylation products **165a-d** were achieved without the formation of the undesired achiral product **167**.



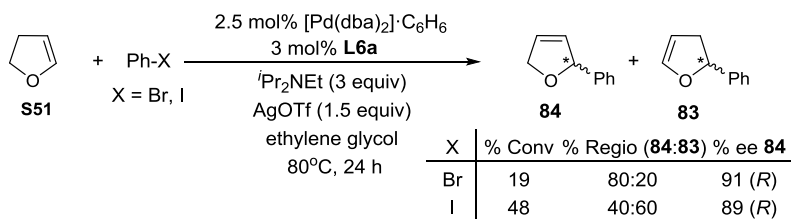
Scheme 7.1.5. Asymmetric Heck reaction of cyclopentene **S54**.

In summary, the replacement of the phosphine by a phosphite group in the phosphine-oxazoline ligands **108-109** extended the range of substrates and triflate sources that could be successfully coupled with regio- and enantioselectivities that were among the best reported so far.¹ In addition, the ligands that provided the best enantioselectivities contained the ^tPr substituent in the oxazoline moiety instead of the expensive ^tBu substituent.

7.1.3.4. Asymmetric Heck reaction of 2,3-dihydrofuran with aryl halides

Carbon electrophiles in the asymmetric intermolecular Heck reaction have been mostly restricted to aryl or vinyl triflates, thus limiting the synthetic value of intermolecular coupling. To date, only a few successful examples using aryldiazonium salts,^{5h} arylboronic acids¹⁹ and benzylic electrophiles²⁰ and one using aryl halides^{7c} have been reported. With aryl halides, mixed phosphine-phosphine oxide ligands were found to be the best choice whilst BINAP and ^tBu-PHOX provided very low activities (less 10%) and BINAP also extremely low enantioselectivity (<5% *ee*). The success of this transformation also required the addition of 1 equiv. of additive (mainly *p*-NO₂PhCO₂H although silver salts such as AgOTf were also used) and ethylene glycol, MeOH or (CH₂OH)₂ as solvents (the more common toluene, ether and 1,4 dioxane led to poor results). In addition, most of the electrophiles were aryl bromides and only a few were

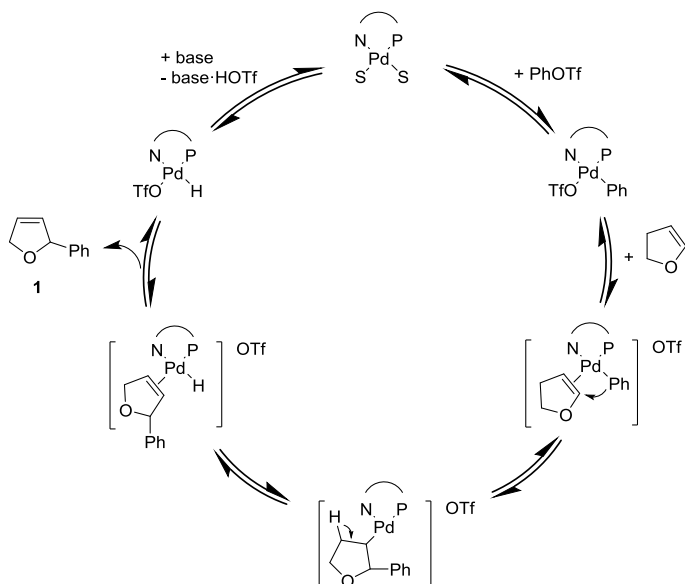
ArCl. Aryl iodides gave not only lower enantioselectivity but also a shift to the preferential formation of regioisomer **83** (i.e., the phenylation of **S51** afforded **84** and **83** at a 1:2 ratio). Under this reaction conditions, we test whether our ligands could do the same coupling (Scheme 7.1.6). The reaction of **S51** with phenyl bromide provided the desired regioisomer **84** as a major product in high enantioselectivity (91% *ee*). The use of phenyl iodide, led to similar levels of enantioselectivities albeit the formation of the isomer **83** is favored.



Scheme 7.1.6. Asymmetric Heck reaction of **S51** with aryl halides.

7.1.3.5. Mechanistic insights

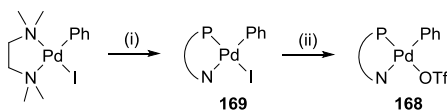
There are no mechanistic studies that give a conclusive reason for the chiral phosphite-oxazoline ligands giving a higher activity than most of the phosphine-oxazolines. Kinetic studies with achiral diphosphine ligands in the Pd-catalyzed coupling of iodobenzene with styrene showed that the rate limiting step is the oxidative addition.^{11b,c,f} Van Leeuwen and Kamer's kinetic studies with achiral monophosphite ligands showed that the rate determining step is not the oxidative addition but rather the alkene coordination or the migratory insertion, being the migratory insertion the most plausible choice as suggested, although not conclusively, by further electronic alkene effects.^{11a,e} So, we performed a kinetic study to discover the rate determining step in the Pd/phosphite-oxazoline catalysts reported in this manuscript. Scheme 7.1.7 presents the most accepted mechanism for the Heck coupling reaction that served as the basis for the kinetic study. The catalytic cycle is initiated by the oxidative addition of phenyl triflate to the Pd(0)-NP* complex resulting in the four coordinate aryl-Pd(II) complex which then reacts with the olefin to form the π -complex. Insertion of the olefin into the Pd-Ph bond leads to a Pd-alkyl species which undergoes β -hydride elimination, followed by dissociation to the product and a Pd-hydride complex. The catalytic cycle is completed by base-assisted reductive elimination of HOTf regenerating the catalytically active Pd(0) complex.



Scheme 7.1.7. Accepted mechanism for the asymmetric Pd-catalyzed Heck reaction of 2,3-dihydrofuran **S51**.

As a viable catalyst precursor for our kinetic study we used [Pd(Ph)(OTf)(**L6a**)] **168**. Using Pd₂(dba)₃/**L6a** or its [Pd(dba)(**L6a**)] analogues was discarded because the active species form too slowly under the employed conditions.²¹ [Pd(Ph)(OTf)(**L6a**)] **168** was synthesized in two steps (Scheme 7.1.8). First reaction of the [Pd(Ph)(I)(TMEDA)] (TMEDA= *N,N,N,N*-tetramethylethylenediamine)²² with one equiv of phosphite-oxazoline ligand **L6a** afforded the corresponding compound [Pd(Ph)(I)(**L6a**)] **169**. Then, iodine abstraction in **169** by treatment with AgOTf yielded the desired complex [Pd(Ph)(OTf)(**L6a**)]. Complexes **168** and **169** were characterized by ³¹P, ¹H and ¹³C NMR spectroscopies. The VT-NMR experiments (-78 to 30 °C) indicated the formation of a single stereoisomer. This is in agreement with the tropoisomerization of the biphenyl phosphite moiety being controlled by the ligand backbone upon coordination to the Pd-center observed in Table 7.1.1 (*vide supra*). The NMR data also indicated that, as previously observed for other P,N-containing complexes, the phenyl ligand is located *cis* to the phosphite moiety.^{5a} To prove the viability of **168** as a catalyst precursor, we first performed the stoichiometric reaction by adding 2 equivalents of **S51** and an excess of base. The regio- and enantioselectivity achieved were similar to those achieved using the catalytic conditions (95%

regioselectivity and 88% *ee*), which clearly indicated that [Pd(Ph)(OTf)(**L6a**)] is a viable intermediate.



Scheme 7.1.8. Preparation of [Pd(Ph)(OTf)(**L6a**)]. (i) **L6a**, C₆H₆ (66% yield); (ii) AgOTf, THF (90% yield).

The kinetic studies were performed using the classical approach, varying the concentration of each of the reagents involved in the catalysis and studying the reaction rate after 5 minutes (TOF_{ini}) vs the concentration. Deactivation of the molecular system due to the formation of inactive Pd-black was observed after 10-15 minutes. This contrasts with the stability observed in the catalytic runs using [Pd₂(dba)₃]/**L5-L9a-e** catalytic precursors (see *vide supra*) and suggest that although the dba does not participate in the catalytic cycle, it stabilizes the molecular species thus preventing the formation of the inactive Pd black.

The rate of the reaction between **S51** and phenyl triflate catalyzed by Pd-complex **168** was independent of the concentration of *N,N*-diisopropylethylamine (0.16-2.7 M; Figure 7.1.3a) and phenyl triflate (0.16-2 M; Figure 7.1.3b). The zero order dependence in phenyl triflate agrees with a rapid oxidative addition. The independence of the reaction rate on the concentration of *N,N*-diisopropylethylamine agrees with the fact that the elimination/reduction steps, that are base-assisted, are also fast. The effect of the Pd loading (2-16 mM) on activity (Figure 7.1.3c) indicates a first order-dependency, because the rate of product formation is proportional to the Pd concentration. Figure 7.1.3d shows a linear dependence of the initial turn over frequency (TOF_{ini}) on alkene concentration. The first-order rate dependence on the alkene concentration clearly shows that the substrate is involved in the turn-over limiting step of the catalytic cycle. This implies that either the alkene coordination to Pd or the subsequent insertion into the Pd-Ph bond must be the turn-over limiting step. However these two steps cannot be distinguished from our kinetic results. We therefore determined the initial reaction rates with several *para*-substituted phenyl triflate sources (*p*-R-C₆H₄OTf; R= OMe, Me, H, NO₂) using Pd-complex **168** under our reaction conditions. The Hammet plot (Figure 7.1.4) showed a linear correlation between the Hammett σ value and the relative reaction rates,²³ with a negative ρ value ($\rho = -0.89$). Therefore, the use of electronwithdrawing

aryl triflates led to lower reaction rates, exhibiting the order $p\text{-NO}_2 < p\text{-H} < p\text{-Me} < p\text{-OMe}$. This indicates that the electron density decreases in the rate determining step and confirms that the rate determining step is the migratory insertion of the aryl group to the olefin.

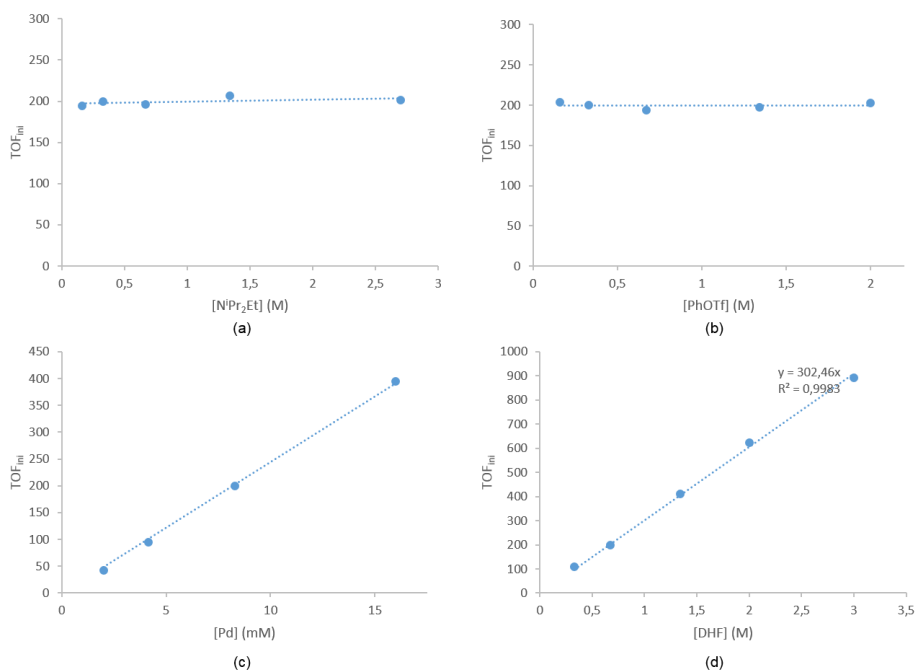


Figure 7.1.3. Kinetic measurements. Plots of TOF_{ini} versus (a) $[\text{N}^i\text{Pr}_2\text{Et}]$, (b) $[\text{PhOTf}]$, (c) $[\text{Pd}]$ and (d) **S51** for the reaction of **S51** with PhOTf in THF at 50°C catalyzed with complex $[\text{Pd}(\text{Ph})(\text{OTf})(\text{L6a})]$.

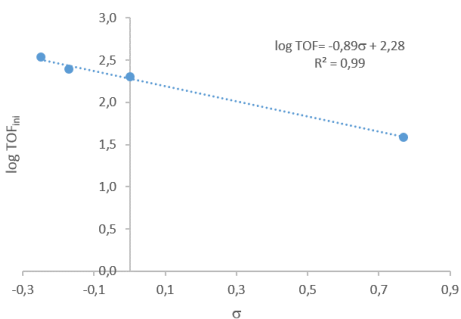


Figure 7.1.4. Hammett plot showing the effect of substituents on the Heck reaction using catalytic system Pd/**L6a**.

7.1.4. Conclusions

We have replaced the phosphine group with several biaryl phosphite moieties in one of the most successful phosphine-oxazoline ligand family **108-109** for the Pd-catalyzed intermolecular Heck reaction. With these simple modifications, the phosphite-based ligands not only had a more modular design than the source phosphine-oxazoline **108-109**, but also were air-stable solids with no increase in the number of synthetic steps. With a careful selection of the ligand components, (oxazoline substituent and its configuration, the substituents in the benzylic position and the substituents and configurations of the biaryl phosphite moiety) the new ligands were superior to the privileged phosphine-oxazolines **108-109**, extending the range of substrates and triflates sources than can be coupled with regio- and enantioselectivities comparable to the best ones reported. In addition, the phosphite-oxazoline ligands that provided the best selectivities contained the ⁱPr substituent in the oxazoline moiety instead of the expensive ^tBu substituent found in the related phosphine-oxazoline **108-109**. Finally, in this paper we have also carried out mechanistic investigations by combining kinetic studies and Hammet plots. The results indicates that the migratory insertion of the aryl group to the olefin is the rate determining step.

7.1.5. Experimental section

7.1.5.1. General information

All syntheses were performed with standard Schlenck techniques under argon atmosphere. The kinetic studies were performed using a glove box. Solvents were purified by standard procedures. All reagents were used as commercially available. Compounds **155-158**,¹³ **160**,¹⁴ phosphochloridites²⁴ and [Pd(Ph)(I)(TMEDA)]²² were prepared as previously reported. ¹H, ¹³C{¹H} and ³¹P{¹H} NMR spectra were recorded on a Varian Gemini 400 MHz spectrometer. The chemical shifts are referenced to tetramethylsilane (¹H and ¹³C) as internal standard or H₃PO₄ (³¹P) as external standard. The ¹H and ¹³C{¹H} NMR spectral assignments were determined by ¹H-¹H and ¹H-¹³C correlation spectra.

7.1.5.2. General procedure for the preparation of phosphite-oxazoline ligands (L5-L9a-e)

To a solution of in situ generated phosphochloridite (1.1 mmol) in dry toluene (6 mL), pyridine (0.16 mL, 2.0 mmol) was added. Then, this solution was placed in a -78 °C bath. After 2 min at that temperature, a solution of the corresponding alcohol oxazoline (1.0 mmol) and pyridine (0.16 mL, 2.0 mmol) in toluene (6 mL) was added drop wise at -78 °C. The mixture was left to warm to room temperature and stirred overnight at this temperature. The precipitate formed was filtered under argon and the solvent was evaporated under vacuum. The residue was purified by flash chromatography (under argon, using neutral alumina and dry toluene as eluent system) to afford the corresponding phosphite-oxazoline (**L5-L9a-e**) as white solids.

L5a. Yield: 449.7 mg (65%); ^{31}P NMR (161.9 MHz, C_6D_6): $\delta = 139.1$ ppm (s). ^1H NMR (400 MHz, C_6D_6): $\delta = 1.27$ (s, 9H, CH_3 , ^tBu), 1.28 (s, 9H, CH_3 , ^tBu), 1.51 (s, 9H, CH_3 , ^tBu), 1.52 (s, 9H, CH_3 , ^tBu), 3.6 (pt, 1H, CH-O, $J_{\text{H-H}} = 8.4$ Hz), 3.8 (s, 2H, CH_2), 4.73 (dd, 1H, CH-O, $^2J_{\text{H-H}} = 10.0$ Hz, $^3J_{\text{H-H}} = 8.0$ Hz), 4.9 (m, 1H, CH-N), 6.8-7.15 (m, 7H, CH=), 7.39 (m, 4H, CH=), 7.59 (m, 2H, CH=). $^{13}\text{C}\{^1\text{H}\}$ (100.6 MHz, C_6D_6): $\delta = 28.7$ (CH_2), 30.9 (CH_3 , ^tBu), 31.2 (CH_3 , ^tBu), 34.3 (C, ^tBu), 35.3 (C, ^tBu), 69.6 (CH-N), 74.1 ($\text{CH}_2\text{-O}$), 120.8-150.2 (aromatic carbons), 166.0 (C=N). MS HR-ESI [found 714.3679, $\text{C}_{44}\text{H}_{54}\text{NO}_4\text{P}$ (M-Na) $^+$ requires 714.3683].

L5b. Yield: 512.5 mg (72%); ^{31}P NMR (161.9 MHz, C_6D_6): $\delta = 144.2$ ppm (s). ^1H NMR (400 MHz, C_6D_6): $\delta = 0.4$ (s, 9H, CH_3 , SiMe_3), 0.6 (s, 9H, CH_3 , SiMe_3), 3.1 (pt, 1H, CHO, $J_{\text{H-H}} = 8.4$ Hz), 3.2 (d, 1H, CH_2 , $^2J_{\text{H-H}} = 16.0$ Hz) 3.36 (d, 1H, CH_2 , $^2J_{\text{H-H}} = 16.0$ Hz), 3.5 (dd, 1H, CH-O, $^2J_{\text{H-H}} = 10.0$ Hz, $^3J_{\text{H-H}} = 8.0$ Hz), 4.9 (m, 1H, CH-N), 6.91 (m, 4H, CH=), 7.02-7.23 (m, 7H, CH=), 7.43 (m, 4H, CH=), 7.78 (m, 2H, CH=), 8.16 (s, 1H, CH=), 8.27 (s, 1H, CH=). $^{13}\text{C}\{^1\text{H}\}$ (100.6 MHz, C_6D_6): $\delta = -0.5$ (d, CH_3 , SiMe_3 , $J_{\text{C-P}} = 4.6$ Hz), 0.1 (CH_3 , SiMe_3), 28.3 (CH_2), 69.6 (CH-N), 73.9 ($\text{CH}_2\text{-O}$), 120.3-152.4 (aromatic carbons), 165.7 (C=N). MS HR-ESI [found 734.2280, $\text{C}_{42}\text{H}_{42}\text{NO}_4\text{PSi}_2$ (M-Na) $^+$ requires 734.2282].

L5c. Yield: 555.3 mg (78%); ^{31}P NMR (161.9 MHz, C_6D_6): $\delta = 143.5$ ppm (s). ^1H NMR (400 MHz, C_6D_6): $\delta = 0.0$ (s, 9H, CH_3 , SiMe_3), 0.2 (s, 9H, CH_3 , SiMe_3), 3.1 (pt, 1H, CHO, $J_{\text{H-H}} = 8.4$ Hz), 3.2 (d, 1H, CH_2 , $^2J_{\text{H-H}} = 16.0$ Hz) 3.3 (d, 1H, CH_2 , $^2J_{\text{H-H}} = 16.0$ Hz), 3.5 (dd, 1H, CH-O, $^2J_{\text{H-H}} = 10.0$ Hz, $^3J_{\text{H-H}} = 8.0$ Hz), 4.4 (m, 1H, CH-N), 6.54 (m, 4H, CH=), 6.69-6.82 (m, 8H, CH=), 7.04 (m, 4H, CH=), 7.38 (m, 5H, CH=), 7.75 (s, 1H, CH=), 7.86 (s, 1H, CH=). $^{13}\text{C}\{^1\text{H}\}$ (100.6 MHz, C_6D_6): $\delta = -0.5$ (d, CH_3 , SiMe_3 , $J_{\text{C-}}$

$p = 4.6$ Hz), 0.0 (CH₃, SiMe₃), 28.3 (CH₂), 69.5 (CH-N), 73.9 (CH₂-O), 120.5-149.5 (aromatic carbons), 165.7 (C=N). MS HR-ESI [found 734.2279, C₄₂H₄₂NO₄PSi₂ (M-Na)⁺ requires 734.2282].

L6a. Yield: 394.72 mg (60%); ³¹P NMR (161.9 MHz, C₆D₆): $\delta = 139.2$ ppm (s). ¹H NMR (400 MHz, C₆D₆): $\delta = 0.71$ (d, 3H, CH₃, ⁱPr, ³J_{H-H} = 6.8 Hz), 0.90 (d, 3H, CH₃, ⁱPr, ³J_{H-H} = 6.4 Hz), 1.28 (s, 18H, CH₃, ^tBu), 1.5 (s, 18H, CH₃, ^tBu), 1.55 (m, 1H, CH, ⁱPr), 3.55 (m, 1H, CH-O), 3.64 (m, 1H, CH-O), 3.77 (m, 3H, CH₂, CH-N), 6.8-6.9 (m, 2H, CH=), 7.0-7.15 (m, 2H, CH=), 7.38 (m, 2H, CH=), 7.59 (m, 2H, CH=). ¹³C{¹H} (100.6 MHz, C₆D₆): $\delta = 19.0$ (CH₃, ⁱPr), 19.4 (CH₃, ⁱPr), 28.7 (CH₂), 31.6 (CH₃, ^tBu), 31.7 (CH₃, ^tBu), 31.9 (CH₃, ^tBu), 33.6 (CH, ⁱPr), 35.0 (C, ^tBu), 36.0 (C, ^tBu), 70.5 (CH₂-O), 73.2 (CHN), 121.5-150.8 (aromatic carbons), 165.1 (C=N). MS HR-ESI [found 680.3834, C₄₁H₅₆NO₄P (M-Na)⁺ requires 680.3839].

L6b. Yield: 467.8 mg (69%); ³¹P NMR (161.9 MHz, C₆D₆): $\delta = 143.7$ ppm (s). ¹H NMR (400 MHz, C₆D₆): $\delta = 0.3$ (s, 9H, CH₃, SiMe₃), 0.5 (s, 9H, CH₃, SiMe₃), 0.59 (d, 3H, CH₃, ⁱPr, ³J_{H-H} = 6.4 Hz), 0.78 (d, 3H, CH₃, ⁱPr, ³J_{H-H} = 6.8 Hz), 1.33 (m, 1H, CH, ⁱPr), 3.34 (pt, 1H, CH-O, J_{H-H} = 7.6 Hz), 3.4-3.6 (m, 4H, CH₂, CH-O, CH-N), 6.7-6.83 (m, 3H, CH=), 6.96-7.11 (m, 5H, CH=), 7.29 (m, 2H, CH=), 7.64 (d, 1H, CH=, ³J_{H-H} = 8.4 Hz), 7.68 (d, 1H, CH=, ³J_{H-H} = 8.4 Hz), 8.03 (s, 1H, CH=), 8.15 (s, 1H, CH=). ¹³C{¹H} (100.6 MHz, C₆D₆): $\delta = 0.2$ (d, CH₃, SiMe₃, J_{C-P} = 4.8 Hz), 0.7 (CH₃, SiMe₃), 18.9 (CH₃, ⁱPr), 19.3 (CH₃, ⁱPr), 29.3 (CH₂), 33.4 (CH, ⁱPr), 70.4 (CH₂-O), 73.0 (CH-N), 121.3-154.5 (aromatic carbons), 164.9 (C=N). MS HR-ESI [found 700.2435, C₃₉H₄₄NO₄PSi₂ (M-Na)⁺ requires 700.2439].

L6c. Yield: 508.4 mg (75%); ³¹P NMR (161.9 MHz, C₆D₆): $\delta = 143.3$ ppm (s). ¹H NMR (400 MHz, C₆D₆): $\delta = 0.33$ (s, 9H, CH₃, SiMe₃), 0.55 (s, 9H, CH₃, SiMe₃), 0.66 (d, 3H, CH₃, ⁱPr, ³J_{H-H} = 6.4 Hz), 0.85 (d, 3H, CH₃, ⁱPr, ³J_{H-H} = 6.8 Hz), 1.41 (m, 1H, CH, ⁱPr), 3.37 (pt, 1H, CH-O, J_{H-H} = 8.4 Hz), 3.5 (m, 2H), 3.6-3.71 (m, 2H), 6.82 (m, 2H, CH=), 6.90 (m, 2H, CH=), 7.00-7.15 (m, 3H, CH=), 7.34 (m, 3H, CH=), 7.68 (d, 1H, CH=, ³J_{H-H} = 7.6 Hz), 7.72 (d, 1H, CH=, ³J_{H-H} = 8.0 Hz), 8.07 (s, 1H, CH=), 8.19 (s, 1H, CH=). ¹³C{¹H} (100.6 MHz, C₆D₆): $\delta = 0.21$ (d, CH₃, SiMe₃, J_{C-P} = 3.8 Hz), 0.7 (CH₃, SiMe₃), 19.0 (CH₃, ⁱPr), 19.4 (CH₃, ⁱPr), 29.2 (CH₂), 33.5 (CH, ⁱPr), 70.4 (CH₂-O), 73.1 (CH-N), 121.4-153.1 (aromatic carbons), 164.9 (C=N). MS HR-ESI [found 700.2437, C₃₉H₄₄NO₄PSi₂ (M-Na)⁺ requires 700.2439].

L6d. Yield: 261.5 mg (40%); ³¹P NMR (161.9 MHz, C₆D₆): $\delta = 134.4$ ppm (s). ¹H NMR (400 MHz, C₆D₆): $\delta = 0.75$ (d, 3H, CH₃, ⁱPr, ³J_{H-H} = 6.4 Hz), 0.96 (d, 3H, CH₃,

ⁱPr, ³J_{H-H} = 6.4 Hz), 1.44 (s, 9H, CH₃, ^tBu), 1.60 (m, 1H, CH, ⁱPr), 1.70 (s, 9H, CH₃, ^tBu), 1.31-1.8 (m, 10H, CH₂), 2.27 (m, 2H, CH₂), 2.56 (m, 4H, CH₂), 2.78 (m, 2H, CH₂), 3.58 (m, 1H, CH-O), 3.75 (m, 3H, CH-O, CH₂), 3.81 (m, 1H, CH-N), 6.9 (m, 1H, CH=), 7.1 (m, 3H, CH=), 7.17 (m, 1H, CH=), 7.43 (m, 1H, CH=). ¹³C{¹H} (100.6 MHz, C₆D₆): δ = 18.4 (CH₃, ⁱPr), 18.7 (CH₃, ⁱPr), 22.8 (CH₂), 23.0 (CH₂), 23.1 (CH₂), 23.2 (CH₂), 27.4 (CH₂), 27.7 (CH₂), 28.6 (CH₂), 28.6 (CH₂), 29.6 (CH₂), 30.0 (d, CH₃, ^tBu, J_{C-P} = 4.7 Hz), 31.5 (CH₃, ^tBu), 33.0 (CH, ⁱPr), 34.5 (C, ^tBu), 34.8 (C, ^tBu), 69.9 (CH₂-O), 72.6 (CH-N), 120.9-150.1 (aromatic carbons), 164.5 (C=N). MS HR-ESI [found 676.3524, C₄₁H₅₂NO₄P (M-Na)⁺ requires 676.3526].

L6e. Yield: 409.2 mg (68%); ³¹P NMR (161.9 MHz, C₆D₆): δ = 133.9 ppm (s). ¹H NMR (400 MHz, C₆D₆): δ = 0.66 (d, 3H, CH₃, ⁱPr, ³J_{H-H} = 6.4 Hz), 0.86 (d, 3H, CH₃, ⁱPr, ³J_{H-H} = 7.2 Hz), 1.39 (s, 9H, CH₃, ^tBu), 1.43 (m, 1H, CH, ⁱPr), 1.54 (s, 9H, CH₃, ^tBu), 1.69 (CH₃), 1.74 (CH₃), 2.01 (CH₃), 2.08 (CH₃), 3.48 (m, 1H, CH-O), 3.60 (m, 2H, CH-, CH-O), 3.70 (m, 2H, CH-, CH-N), 6.8-6.9 (m, 1H, CH=), 6.98 (m, 2H, CH=), 7.09 (m, 2H, CH=), 7.35 (m, 1H, CH=). ¹³C{¹H} (100.6 MHz, C₆D₆): δ = 16.2 (CH₃), 16.5 (CH₃), 18.3 (CH₃, ⁱPr), 18.6 (CH₃, ⁱPr), 20.0 (CH₃), 20.1 (CH₃), 28.4 (CH₂), 31.6 (d, CH₃, ^tBu, J_{C-P} = 4.6 Hz), 31.5 (CH₃, ^tBu), 32.9 (CH, ⁱPr), 34.5 (C, ^tBu), 34.8 (C, ^tBu), 69.8 (CH₂-O), 72.4 (CH-N), 120.7-150.0 (aromatic carbons), 164.4 (C=N). MS HR-ESI [found 624.3209, C₃₇H₄₈NO₄P (M-Na)⁺ requires 624.3213].

L7a. Yield: 470.3 mg (70%); ³¹P NMR (161.9 MHz, C₆D₆): δ = 139.2 ppm (s). ¹H NMR (400 MHz, C₆D₆): δ = 0.79 (s, 9H, CH₃, ^tBu), 1.28 (s, 18H, CH₃, ^tBu), 1.52 (s, 9H, CH₃, ^tBu), 1.53 (s, 9H, CH₃, ^tBu), 3.63-3.75 (m, 5H, CH₂, CH₂-O, CH-N), 6.82-6.91 (m, 2H, CH=), 7.0-7.15 (m, 1H, CH=), 7.36 (m, 2H, CH=), 7.39 (m, 1H, CH=), 7.59 (m, 2H, CH=). ¹³C{¹H} (100.6 MHz, C₆D₆): δ = 19.0 (CH₃, ⁱPr), 19.4 (CH₃, ⁱPr), 28.7 (CH₂), 31.6 (CH₃, ^tBu), 31.7 (CH₃, ^tBu), 31.9 (CH₃, ^tBu), 33.9 (C, ^tBu), 35.0 (C, ^tBu), 36.0 (C, ^tBu), 68.8 (CH₂-O), 76.6 (CH-N), 121.5-150.8 (aromatic carbons), 165.1 (C=N). MS HR-ESI [found 694.3992, C₄₂H₅₈NO₄P (M-Na)⁺ requires 694.3996].

L7b. Yield: 498.2 mg (72%); ³¹P NMR (161.9 MHz, C₆D₆): δ = 144.1 ppm (s). ¹H NMR (400 MHz, C₆D₆): δ = 0.33 (s, 9H, CH₃, SiMe₃), 0.55 (s, 9H, CH₃, SiMe₃), 0.73 (s, 9H, CH₃, ^tBu), 3.45-3.65 (m, 5H, CH₂, CH₂-O, CH-N), 6.82 (m, 2H, CH=), 6.87 (m, 2H, CH=), 7.00-7.15 (m, 4H, CH=), 7.35 (m, 2H, CH=), 7.68 (d, 1H, CH=, ³J_{H-H} = 8.4 Hz), 7.73 (d, 1H, CH=, ³J_{H-H} = 8.4 Hz), 8.07 (s, 1H, CH=), 8.18 (s, 1H, CH=). ¹³C{¹H} (100.6 MHz, C₆D₆): δ = 0.2 (d, CH₃, SiMe₃, J_{C-P} = 4.6 Hz), 0.7 (CH₃, SiMe₃), 26.3 (CH₃, ^tBu), 29.1 (CH₂), 33.4 (C, ^tBu), 68.6 (CH₂-O), 76.5 (CH-N), 121.1-153.1

(aromatic carbons), 164.9 (C=N). MS HR-ESI [found 714.2591, C₄₀H₄₆NO₄PSi₂ (M-Na)⁺ requires 714.2595].

L7c. Yield: 512.0 mg (74%); ³¹P NMR (161.9 MHz, C₆D₆): δ = 143.1 ppm (s). ¹H NMR (400 MHz, C₆D₆): δ = 0.33 (s, 9H, CH₃, SiMe₃), 0.56 (s, 9H, CH₃, SiMe₃), 0.74 (CH₃, ^tBu), 3.50-3.71 (m, 5H, CH₂, CH₂-O, CH-N), 6.81 (m, 2H, CH=), 6.89 (m, 2H, CH=), 7.00-7.16 (m, 3H, CH=), 7.34 (d, 2H, CH=, ⁴J_{H-H} = 2.2 Hz), 7.39 (m, 1H, CH=), 7.68 (d, 1H, CH=, ⁴J_{H-H} = 2.0 Hz), 7.72 (d, 1H, CH=, ⁴J_{H-H} = 2.1 Hz), 8.07 (s, 1H, CH=), 8.19 (s, 1H, CH=). ¹³C{¹H} (100.6 MHz, C₆D₆): δ = -0.5 (d, CH₃, SiMe₃, J_{C-P} = 4.62 Hz), 0.0 (CH₃, SiMe₃), 25.6 (CH₃, ^tBu), 28.3 (CH₂), 33.1 (C, ^tBu), 67.9 (CH₂-O), 75.7 (CH-N), 120.4-152.3 (aromatic carbons), 164.1 (C=N). MS HR-ESI [found 714.2592, C₄₀H₄₆NO₄PSi₂ (M-Na)⁺ requires 714.2595].

L8a: Yield: 261.5 mg (40%); ³¹P NMR (161.9 MHz, C₆D₆): δ = 137.0 ppm (s). ¹H NMR (400 MHz, C₆D₆): δ = 1.22 (s, 9H, CH₃, ^tBu), 1.24 (s, 9H, CH₃, ^tBu), 1.42 (s, 9H, CH₃, ^tBu), 1.45 (s, 9H, CH₃, ^tBu), 1.78 (s, 3H, CH₃), 1.80 (s, 3H, CH₃), 3.71 (m, 1H, CH₂-O), 3.98 (dd, 1H, CH₂-O, ²J_{H-H} = 10.0 Hz, ³J_{H-H} = 7.6 Hz), 4.92 (dd, 1H, CH-N, ³J_{H-H} = 9.6 Hz, ³J_{H-H} = 7.6 Hz), 6.83 (m, 1H, CH=), 6.90 (m, 1H, CH=), 7.01 (m, 2H, CH=), 7.09 (m, 3H, CH=), 7.21 (s, 1H, CH=), 7.23 (s, 1H, CH=), 7.03 (d, 1H, ³J_{H-H} = 2.0 Hz), 7.35 (d, 1H, ³J_{H-H} = 2.4 Hz), 7.54 (m, 2H, CH=). ¹³C{¹H} (100.6 MHz, C₆D₆): δ = 27.0 (CH₃), 27.9 (CH₃), 30.9 (CH₃, ^tBu), 31.2 (CH₃, ^tBu), 34.3 (C, ^tBu), 35.3 (C, ^tBu), 35.4 (C, ^tBu), 39.7 (C, CMe₂), 69.6 (CH-N), 74.5 (CH₂-O), 120.6-150.3 (aromatic carbons), 173.1 (C=N). MS HR-ESI [found 719.4098, C₄₆H₅₈NO₄P (M-H)⁺ requires 720.4103].

L8b. Yield: 261.5 mg (40%); ³¹P NMR (161.9 MHz, C₆D₆): δ = 142.1 ppm (s). ¹H NMR (400 MHz, C₆D₆): δ = 0.37 (s, 9H, CH₃-Si), 0.41 (s, 9H, CH₃-Si), 1.61 (s, 3H, CH₃), 1.67 (s, 3H, CH₃), 3.51 (t, 1H, CH₂-O, ³J_{H-H} = ²J_{H-H} = 10.0 Hz), 3.86 (dd, 1H, CH₂-O, ²J_{H-H} = 10.0 Hz, ³J_{H-H} = 8.0 Hz), 4.60 (dd, 1H, CH-N, ³J_{H-H} = 10.0 Hz, ³J_{H-H} = 8.0 Hz), 6.79 (m, 4H, CH=), 6.96 (m, 2H, CH=), 7.07 (m, 4H, CH=), 7.24 (m, 4H, CH=), 7.65 (m, 3H, CH=), 8.07 (s, 1H, CH=), 8.14 (s, 1H, CH=). ¹³C{¹H} (100.6 MHz, C₆D₆): δ = -0.2 (d, CH₃-Si, J_{C-P} = 4.5 Hz), 0.0 (CH₃-Si), 27.0 (CH₃), 27.9 (CH₃), 40.0 (C, CMe₂), 69.0 (CH-N), 74.1 (CH₂-O), 119.6-152.4 (aromatic carbons), 172.8 (C=N). MS HR-ESI [found 739.2698, C₄₄H₅₆NO₄PSi₂ (M+H)⁺ requires 739.2703].

L8c. Yield: 261.5 mg (40%); ³¹P NMR (161.9 MHz, C₆D₆): δ = 142.3 ppm (s). ¹H NMR (400 MHz, C₆D₆): δ = 0.38 (s, 9H, CH₃-Si), 0.40 (s, 9H, CH₃-Si), 1.62 (s, 3H, CH₃), 1.76 (s, 3H, CH₃), 3.48 (m, 1H, CH₂-O), 3.68 (dd, 1H, CH₂-O, ²J_{H-H} = 10.4 Hz, ³J_{H-H} = 8.0 Hz), 4.25 (dd, 1H, CH-N, ³J_{H-H} = 10.0 Hz, ³J_{H-H} = 8.0 Hz), 6.80 (m, 5H,

CH=), 6.88 (m, 1H, CH=), 6.9-7.1 (m, 5H, CH=), 7.23 (m, 4H, CH=), 7.63 (m, 1H, CH=), 7.66 (m, 1H, CH=), 8.08 (s, 1H, CH=), 8.09 (s, 1H, CH=). $^{13}\text{C}\{^1\text{H}\}$ (100.6 MHz, C_6D_6): $\delta = -0.2$ (d, $\text{CH}_3\text{-Si}$, $J_{\text{C-P}} = 4.5$ Hz), 0.0 ($\text{CH}_3\text{-Si}$), 26.8 (CH_3), 28.4 (CH_3), 39.7 (C, CMe_2), 69.0 (CH-N), 74.4 ($\text{CH}_2\text{-O}$), 119.9-152.3 (aromatic carbons), 172.5 (C=N). MS HR-ESI [found 739.2699, $\text{C}_{44}\text{H}_{56}\text{NO}_4\text{PSi}_2$ ($\text{M}+\text{H}$) $^+$ requires 739.2703].

L9a. Yield: 432.1 mg (62%); ^{31}P NMR (161.9 MHz, C_6D_6): $\delta = 139.1$ ppm (s). ^1H NMR (400 MHz, C_6D_6): $\delta = 1.27$ (s, 9H, CH_3 , ^tBu), 1.28 (s, 9H, CH_3 , ^tBu), 1.51 (s, 9H, CH_3 , ^tBu), 1.52 (s, 9H, CH_3 , ^tBu), 3.6 (pt, 1H, CH-O, $J_{\text{H-H}} = 8.4$ Hz), 3.8 (s, 2H, CH_2), 4.73 (dd, 1H, CH-O, $^2J_{\text{H-H}} = 10.0$ Hz, $^3J_{\text{H-H}} = 8.0$ Hz), 4.9 (m, 1H, CH-N), 6.8-7.15 (m, 7H, CH=), 7.39 (m, 4H, CH=), 7.59 (m, 2H, CH=). $^{13}\text{C}\{^1\text{H}\}$ (100.6 MHz, C_6D_6): $\delta = 28.7$ (CH_2), 30.9 (CH_3 , ^tBu), 31.2 (CH_3 , ^tBu), 34.3 (C, ^tBu), 35.3 (C, ^tBu), 69.6 (CH-N), 74.1 ($\text{CH}_2\text{-O}$), 120.8-150.2 (aromatic carbons), 166.0 (C=N). MS HR-ESI [found 714.3677, $\text{C}_{44}\text{H}_{54}\text{NO}_4\text{P}$ (M-Na) $^+$ requires 714.3683].

7.1.5.3. Synthesis of (*S*)-2-(2-(4-phenyl-4,5-dihydrooxazol-2-yl)propan-2-yl)phenol (161)

MeOH (7.21 ml, 0.29 mmol) was added to a solution of NaH (60% in mineral oil, 244.16 mg, 6.10 mmol) in THF (5.1 ml) at 0 °C under argon and string for 1 h. The solution of 3,3-dimethylbenzofuran-2(3*H*)-one **160** (700 mg, 5.55 mmol) in THF (5.1 ml) was added at 0 °C. The resultant mixture was warmed to room temperature during 1 h. A solution of (*S*)-(+)-2-phenylglycinol (837.34 mg, 6.10 mmol) in THF (5.1 ml) was added dropwise. The mixture was stirred for 2 h. The mixture was suspended in CH_2Cl_2 (30 mL) and washed with NaOH solution (2 × 50 mL), then with 2 M HCl solution to reach to pH = 2. After drying over MgSO_4 , solvent was evaporated to obtain intermediate (*S*)-*N*-(2-hydroxy-1-phenylethyl)-2-(2-hydroxyphenyl)-2-methylpropanamide as a white solid. Yield: 1.17 g (75%). ^1H NMR (400 MHz, C_6D_6): $\delta = 1.59$ (s, 3H, CH_3), 1.63 (s, 3H, CH_3), 3.72 (dd, 1H, $\text{CH}_2\text{-O}$, $^2J_{\text{H-H}} = 11.4$ Hz, $^3J_{\text{H-H}} = 7.2$ Hz), 3.90 (dd, 1H, $\text{CH}_2\text{-O}$, $^2J_{\text{H-H}} = 11.4$ Hz, $^3J_{\text{H-H}} = 4.0$ Hz), 5.11 (m, 1H, CH), 6.12 (d, 1H, NH, $^3J_{\text{H-H}} = 7.6$ Hz), 6.92 (m, 2H, CH=), 7.18 (m, 3H, CH=), 7.29 (m, 4H, CH=). $^{13}\text{C}\{^1\text{H}\}$ (100.6 MHz, C_6D_6): $\delta = 25.2$ (CH_3), 25.9 (CH_3), 45.3 (C, CMe_2), 55.6 (CH-N), 66.05 ($\text{CH}_2\text{-O}$), 117-155 (aromatic carbons).

To a cold (0 °C) solution of (*S*)-*N*-(2-hydroxy-1-phenylethyl)-2-(2-hydroxyphenyl)-2-methylpropanamide (1.25 g, 4.18 mmol) in CH_2Cl_2 (10 mL) was sequentially added triethylamine (2.91 mL, 20.88 mmol), DMAP (76 mg, 0.63 mmol) and methanesulfonyl

chloride (0.36 mL, 4.59 mmol). The resultant mixture was warmed to room temperature and stirred overnight. The excess methanesulfonyl chloride was hydrolyzed by adding water (10 mL) and heating to reflux for 30 min. Another portion of water (25 mL) was added, and the mixture was extracted with CH₂Cl₂ (3 × 25 mL). The combined organic phases were washed with saturated NaCl solution and dried over Na₂SO₄. After filtration and removal of the solvent under vacuum, the product was purified by flash chromatography, 5 % methanol in dichloromethane. Yield: 705 mg (60%). ¹H NMR (400 MHz, C₆D₆): δ = 1.69 (b, 6H, CH₃), 4.08 (b, 1H, CH₂), 4.63 (b, 1H, CH), 4.5.17 (b, 1H, CH₂), 6.8-7.4 (m, 9H, CH=). MS HR-ESI [found 281.1416, C₁₈H₁₉NO₂ requires 281.1417].

7.1.5.4. Synthesis of [PdPhI(L6a)]

A solution of [PhPdI(TMEDA)] (25 mg, 0.058 mmol) and the ligand **L6a** (38 mg, 0.058 mmol) in dry degassed benzene (3 ml) was stirred under Ar atmosphere at r.t. for 48 h. The reaction was monitored by ³¹P{¹H} NMR during this time. The organic solvent was removed under reduced pressure. Purification by column chromatography (neutral Al₂O₃; toluene/CH₂Cl₂ gradient 1:0 to 0:1) yielded the desired product as pale-yellow solid (37 mg, 66 %). ³¹P NMR (162 MHz, C₆D₆): δ = 139.23. ¹H NMR (400 MHz, C₆D₆): δ = 7.56 (d, 2H, *J* = 2.3 Hz, CH=), 7.46 (d, 1H, *J* = 2.3 Hz, CH=), 7.13 (d, 1H, ³*J*_{H-H} = 7.5 Hz, CH=), 7.02 (d, 1H, ³*J*_{H-H} = 6.9 Hz, CH=), 6.85-6.80 (m, 4H, CH=), 6.77 – 6.68 (m, 2H, CH=), 6.63 – 6.54 (m, 2H, CH=), 5.94 (d, 1H, ³*J*_{H-H} = 7.3 Hz, CH-N), 4.67 (d, 1H, ²*J*_{H-H} = 14.5 Hz, CH₂), 3.72 – 3.60 (m, 2H, CH-O), 3.10 (d, 1H, ²*J*_{H-H} = 14.6 Hz, CH₂), 2.94 (m, 1H, CH, ⁱPr), 1.58 (s, 18 H, CH₃, ^tBu), 1.19 (s, 9 H, CH₃, ^tBu), 1.13 (s, 9 H, CH₃, ^tBu), 0.97 (d, 3H, ³*J*_{H-H} = 6.8 Hz, CH₃, ⁱPr), 0.87 (d, 3H, ³*J*_{H-H} = 6.9 Hz, CH₃, ⁱPr). ¹³C{¹H} NMR (100 MHz, C₆D₆): δ = 166.3 (C=N), 138.7-124.7 (aromatic carbones), 121.3 (CH-N), 72.3 (CH-O), 34.6 (CH₂), 31.7 (CH₃, ^tBu), 31.5 (CH₃, ^tBu), 31.4 (CH₃, ^tBu), 31.3 (CH₃, ^tBu), 31.0 (C, ⁱPr), 19.3 (CH₃, ⁱPr), 16.2 (CH₃, ⁱPr). MS HR-ESI [found 840.3369, C₄₇H₆₁NO₄PPd (M-I)⁺ requires 840.3373].

7.1.5.5. Synthesis of [PdPhOTf(L6a)]

Silver triflate (16 mg, 0.062 mmol) was added to a vigorously stirred solution of the complex [PdPhI(L6a)] (30 mg, 0.031 mmol) in dry degassed THF (4 ml) under Ar atmosphere at room temperature. Stirring was continued for 1h, during which period a pale grey precipitate was formed. The reaction mixture then filtered over celite, and all

volatiles were removed under reduced pressure to yield the final product as a pale brown solid (55 mg, 90 %). ^{31}P NMR (162 MHz, CD_2Cl_2): $\delta = 96.99$. ^1H NMR (401 MHz, CD_2Cl_2): $\delta = 7.59$ (d, 1H, $^3J_{\text{H-H}} = 2.3$ Hz, CH=), 7.47 (d, 1H, $^3J_{\text{H-H}} = 2.1$ Hz, CH=), 7.34 – 7.27 (m, 3H, CH=), 7.09 (t, 1H, $^3J_{\text{H-H}} = 7.5$ Hz, CH=), 7.01 (dd, 1H, $^3J_{\text{H-H}} = 7.9$, 1.3 Hz, CH=), 6.99 – 6.88 (m, 6H, CH=), 5.84 (d, 1H, $^3J_{\text{H-H}} = 8.1$ Hz, CH-N), 4.57 (d, 1H, $^2J_{\text{H-H}} = 14.6$ Hz, CH_2), 4.48 (d, 1H, $^3J_{\text{H-H}} = 8.3$ Hz, CH-O), 4.32 – 4.27 (m, 1H, CH-O), 3.71 (d, 1H, $^2J_{\text{H-H}} = 14.5$ Hz, CH_2), 2.52 (m, 1H, CH, ^iPr), 1.60 (s, 9H, CH_3 , ^tBu), 1.54 (s, 9H, CH_3 , ^iPr), 1.34 (s, 9H, CH_3 , ^tBu), 1.30 (s, 9H, CH_3 , ^iPr), 1.07 (d, 3H, ^iPr , $^3J_{\text{H-H}} = 6.9$ Hz), 1.03 (d, 3H, ^iPr , $^3J_{\text{H-H}} = 6.7$ Hz). $^{13}\text{C}\{^1\text{H}\}$ NMR (101 MHz, CD_2Cl_2): $\delta = 169.2$ (C=N), 151.7–121.9 (aromatic carbones), 121.3 (CH-N), 70.9 (CH-O), 34.5 (CH_2), 31.9 (CH_3 , ^tBu), 31.6 (CH_3 , ^iPr), 31.4 (CH_3 , ^tBu), 31.0 (CH_3 , ^iPr), 30.0 (C, ^iPr), 19.1 (CH_3 , ^iPr), 16.4 (CH_3 , ^iPr). ^{19}F NMR (377 MHz, CD_2Cl_2): $\delta = -78.01$. MS HR-ESI [found 840.3376, $\text{C}_{47}\text{H}_{61}\text{NO}_4\text{PPd}$ (M-OTf) $^+$ requires 840.3373].

7.1.5.6. General procedure for Pd-catalyzed enantioselective Heck reactions with several triflates

A mixture of $[\text{Pd}_2(\text{dba})_3]\cdot\text{C}_6\text{H}_6$ (12 mg, 1.25×10^{-2} mmol) and the corresponding chiral ligand (2.3 equiv) in dry degassed solvent (3.0 mL) was stirred at room temperature for 20 min. The corresponding olefin (2.0 mmol), triflate (0.50 mmol) and *N*-diisopropylethylamine (1.0 mmol) were added to the catalyst solution. The vial was sealed and brought out and the solution was vigorously stirred at the desired temperature. After the desired reaction time, the reaction mixture was cooled to ambient temperature and internal standard (undecane, 0.5 mmol) was added. The mixture was diluted with additional diethyl ether and after agitation, the mixture was filtered through a short silica gel plug and analyzed by ^1H -NMR or GC to determine the conversion and regioselectivity. The crude was subjected to flash chromatography (pentane/ Et_2O) to give the purified product. Enantioselectivities were determined using chiral HPLC or GC (see supporting information for details).

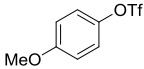
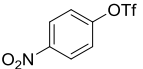
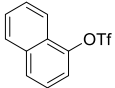
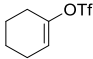
7.1.5.7. Pd-catalyzed enantioselective Heck reactions of 2,3-dihydrofuran with aryl halides

$[\text{Pd}(\text{dba})_2]\cdot\text{C}_6\text{H}_6$ (8.5 mg, 0.013 mmol) and ligand (0.015 mmol) in degassed ethylene glycol (1.0 mL) were stirred at room temperature for 20 min. Aryl halide (0.50

mmol), *N*-diisopropylethylamine (255 μ L, 1.5 mmol, 3 equiv), silver triflate (192.7 mg, 0.75 mmol, 1.5 equiv) and 2,3-dihydrofuran (75 μ L, 1.0 mmol, 2 equiv) were added to the catalyst solution. The vial was sealed and brought out and the mixture was vigorously stirred in an oil bath at 80 °C, for 24h. The reaction mixture was cooled to ambient temperature and internal standard (undecane, 0.5 mmol) was added. The mixture was diluted with additional diethyl ether and after agitation, the mixture was filtered through a short silica gel plug and analyzed by ¹H-NMR or GC to determine the conversion and regioselectivity. The crude was subjected to flash chromatography (pentane/Et₂O) to give the purified product. Enantioselectivities were determined using chiral HPLC or GC (see supporting information for details).

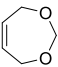
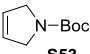

7.1.6. Supporting information

7.1.6.1. Table SI.1. Asymmetric Pd-catalyzed Heck reaction of several triflate sources to **S51**^a

L								
	%Conv (% 84) ^b	% <i>ee</i> ^c	%Conv (% 84) ^b	% <i>ee</i> ^c	%Conv (% 84) ^b	% <i>ee</i> ^c	%Conv (% 84) ^b	% <i>ee</i> ^c
L5a	100 (97)	65 (<i>R</i>)	83 (98)	67 (<i>R</i>)	89 (99)	71 (<i>R</i>)	100 (95)	68 (<i>R</i>)
L6a	100 (97)	89 (<i>R</i>)	88 (99)	94 (<i>R</i>)	92 (98)	97 (<i>R</i>)	100 (95)	94 (<i>R</i>)
L6b	57 (61)	49 (<i>S</i>)	39 (61)	38 (<i>S</i>)	40 (63)	51 (<i>S</i>)	67 (72)	37 (<i>S</i>)
L6c	99 (96)	79 (<i>R</i>)	85 (98)	84 (<i>R</i>)	91 (98)	91 (<i>R</i>)	100 (96)	82 (<i>R</i>)
L6d	94 (97)	91 (<i>R</i>)	89 (99)	97 (<i>R</i>)	89 (99)	98 (<i>R</i>)	100 (96)	95 (<i>R</i>)
L7a	34 (41)	85 (<i>R</i>)	16 (43)	79 (<i>R</i>)	31 (44)	76 (<i>R</i>)	49 (53)	76 (<i>R</i>)

^(a) [Pd₂(dba)₃], benzene (1.25×10⁻² mmol), **S51** (2.0 mmol), phenyl triflate (0.5 mmol), ligand (2.8×10⁻² mmol), THF (3 ml), ^tPr₂NEt (1 mmol), T = 50 °C, t = 24 h. ^(b) Conversion percentages determined by ¹H-NMR or GC. ^(c) Enantiomeric excesses measured by GC or HPLC.

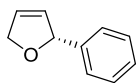
7.1.6.2. Table SI.2. Asymmetric Pd-catalyzed Heck reaction of substrates S52-S54 with PhOTf.

L	 S52		 S53		 S54	
	%Conv 162a	% <i>ee</i>	%Conv (% 163a)	% <i>ee</i>	%Conv (% 165a)	% <i>ee</i>
L5a	87	72 (<i>R</i>)	94 (97)	76 (<i>R</i>)	99 (95)	74 (<i>R</i>)
L6a	90	91 (<i>R</i>)	91 ⁽⁹⁶⁾	91 (<i>R</i>)	97 (95)	89 (<i>R</i>)
L6b	56	38 (<i>S</i>)	42 (94)	42 (<i>S</i>)	51 (93)	38 (<i>S</i>)
L6c	93	86 (<i>R</i>)	86 (97)	84 (<i>R</i>)	99 (95)	90 (<i>R</i>)
L6d	91	93 (<i>R</i>)	92 (98)	94 (<i>R</i>)	97 (96)	91 (<i>R</i>)
L7a	28	79 (<i>R</i>)	31 (64)	73 (<i>R</i>)	56 (61)	81 (<i>R</i>)

^(a) [Pd₂(dba)₃].benzene (1.25×10⁻² mmol), substrate (2.0 mmol), phenyl triflate (0.5 mmol), ligand (2.8×10⁻² mmol), THF (3 ml), ⁱPr₂NEt (1 mmol), T = 65 °C (for **S52** and **S53**) or 50 °C (for **S54**), t = 72 h (for **S52** and **S53**) or 48 h (for **S54**). ^(b) Conversion percentages determined by ¹H-NMR or GC. ^(c) Enantiomeric excesses measured by GC or HPLC.

7.1.6.3. Characterization details and methods for *ee* determination of Heck products

2-Phenyl-2,5-dihydrofuran (1a). Enantiomeric excess determined by GC using

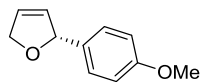


Chiralsil-Dex CB column (105 kPa H₂, 90 °C for 30 min, 10 °C/min, to 180 °C). t_R 17.4 min (*S*); t_R 18.3 min (*R*). ¹H NMR (CDCl₃): δ = 4.76

(m, 1H), 4.87 (m, 1H), 5.79 (m, 1H), 5.88 (m, 1H), 6.03 (m, 1H), 7.2-

7.4 (m, 5H).

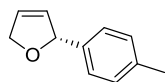
2-(4-Methoxyphenyl)-2,5-dihydrofuran (1b). Enantiomeric excess determined by



HPLC using Chiracel OD-H column (hexane/2-propanol=98/2, 0.5 mL/min, 254 nm). t_R 18.5 min (*S*); t_R 20.8 min (*R*). ¹H NMR (CDCl₃): δ = 3.80 (s, 3H), 4.69 (m, 1H), 4.84 (m, 1H), 5.75 (m,

1H): 5.87 (m, 1H), 6.04 (m, 1H), 6.88 (m, 2H), 7.23 (m, 2H).

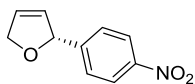
2-(4-Tolyl)-2,5-dihydrofuran (1c).²⁵ Enantiomeric excess determined by HPLC using



Chiracel IC-H column (hexane/2-propanol=98/2, 0.5 mL/min, 254 nm). t_R 21.1 min (*S*); t_R 22.2 min (*R*). ¹H NMR (CDCl₃): δ = 2.33 (s, 3H), 4.76 (m, 1H), 4.86 (m, 1H), 5.76 (m, 1H), 5.87 (m, 1H), 6.03

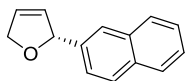
(m, 1H), 7.15 (d, 2H, *J* = 8 Hz), 7.19 (d, 2H, *J* = 8 Hz).

2-(4-Nitrophenyl)-2,5-dihydrofuran (1d). Enantiomeric excess determined by HPLC



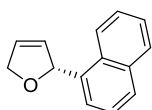
using Chiracel OJ-H column (hexane/2-propanol=87/13, 0.7 mL/min, 220 nm). t_R 11.4 min (*R*); t_R 12.6 min (*S*). $^1\text{H NMR}$ (CDCl_3): δ = 4.74 (m, 1H), 4.82 (m, 1H), 5.46 (m, 2H), 5.61 (m, 1H), 7.59 (d, 2H, J = 7.2 Hz), 7.79 (d, 2H, J = 7.2 Hz).

2-(Naphthalen-2-yl)-2,5-dihydrofuran (1e). Enantiomeric excess determined by



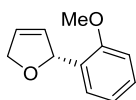
HPLC using Chiracel OD-H column (hexane/2-propanol=98/2, 0.5 mL/min, 210 nm). t_R 20.4 min (*S*); t_R 24.3 min (*R*). $^1\text{H NMR}$ (CDCl_3): δ = 4.83 (m, 1H), 4.96 (m, 1H), 5.94 (m, 2H), 6.07 (m, 1H), 7.41 (d, 1H, J = 8.4 Hz), 7.46 (m, 2H), 7.76 (s, 1H), 7.82 (m, 3H).

2-(Naphthalen-1-yl)-2,5-dihydrofuran (1f). Enantiomeric excess determined by



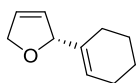
HPLC using Chiracel OD-H column (hexane/2-propanol=98/2, 0.5 mL/min, 210 nm). t_R 29.4 min (*R*); t_R 34.9 min (*S*). $^1\text{H NMR}$ (CDCl_3): δ = 4.87 (m, 2H), 6.05 (m, 1H), 6.55 (m, 1H), 7.46 (m, 4H), 7.76 (d, 1H, J = 8.0 Hz), 7.84 (m, 1H), 8.11 (d, 1H, J = 8.0 Hz).

2-(2-Methoxyphenyl)-2,5-dihydrofuran (1g). Enantiomeric excess determined by



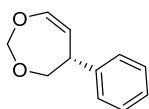
HPLC using Chiracel OJ-H column (hexane/2-propanol=98/2, 0.5 mL/min, 254 nm). t_R 16.8 min (*S*); t_R 18.5 min (*R*). $^1\text{H NMR}$ (CDCl_3): δ = 3.85 (s, 3H), 4.77 (m, 1H), 4.87 (m, 1H), 5.96 (m, 2H), 6.13 (m, 1H), 6.87 (d, 1H, J = 8.0 Hz), 6.95 (t, 1H, J = 7.6 Hz), 7.23 (m, 1H), 7.34 (d, 1H, J = 7.6 Hz).

2-(Cyclohex-1-en-1-yl)-2,5-dihydrofuran (1h). Enantiomeric excess determined by



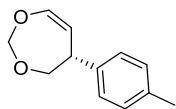
GC using Chiralsil-Dex CB column (115 kPa H_2 , 80 °C for 40 min, 10 °C/min, to 180 °C). t_R 27.5 min (*R*); t_R 29.6 min (*S*). $^1\text{H NMR}$ (CDCl_3): δ = 1.4-1.7 (m, 4H), 1.8-2.1 (m, 4H), 4.63 (m, 1H), 4.69 (m, 1H), 5.12 (m, 1H), 5.69 (m, 2H), 5.94 (m, 1H).

5-Phenyl-4,5-dihydro-1,3-dioxepine (16a). Enantiomeric excess determined by HPLC



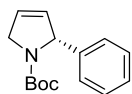
using Chiracel OD-H column (hexane/2-propanol=99/1, 0.5 mL/min, 210 nm). t_R 12.1 min (*R*); t_R 14.4 min (*S*). $^1\text{H NMR}$ (CDCl_3): δ = 3.46 (dd, 1H, J = 11.2 Hz, J = 8.4 Hz), 3.81 (m, 1H), 3.98 (dd, 1H, J = 12.0 Hz, J = 4.4 Hz), 4.85 (d, 1H, J = 7.2 Hz), 4.95 (m, 1H), 5.20 (d, 1H, J = 6.8 Hz), 6.48 (dd, 1H, J = 7.2 Hz, J = 2.0 Hz), 7.2-7.4 (m, 5H).

5-(4-Tolyl)-4,5-dihydro-1,3-dioxepine (16b). Enantiomeric excess determined by



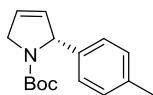
HPLC using Chiracel OD-H column (hexane/2-propanol=98/2, 0.5 mL/min, 210 nm). t_R 10.2 min (*R*); t_R 13.5 min (*S*). $^1\text{H NMR}$ (CDCl_3): δ = 2.33 (s, 3H), 3.42 (dd, 1H, J = 11.6 Hz, J =8.8 Hz), 3.77 (m, 1H), 3.96 (dd, 1H, J = 11.6 Hz, J = 4.4 Hz), 4.83 (m, 1H), 4.91 (dd, 1H, J = 7.4 Hz, J = 3.6 Hz), 5.20 (d, 1H, J = 7.2 Hz), 6.46 (dd, 1H, J = 7.4 Hz, J = 2.4 Hz), 7.1-7.2 (m, 4H)

***tert*-Butyl 2-phenyl-2,5-dihydro-1H-pyrrole-1-carboxylate (17a).** Enantiomeric



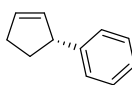
excess determined by HPLC using Chiracel IC column (hexane/2-propanol=95/5, 0.5 mL/min, 210 nm). t_R 18.3 min (*R*); t_R 19.9 min (*S*). $^1\text{H NMR}$ (CDCl_3): δ = 1.21 (s, 9H), 4.33 (s, 2H), 5.37 (s, 1H), 5.73 (s, 1H), 5.84 (s, 1H), 7.1-7.3 (m, 5H).

***tert*-Butyl 2-(4-tolyl)-2,5-dihydro-1H-pyrrole-1-carboxylate (17b).** Enantiomeric



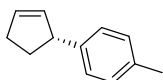
excess determined by HPLC using Chiracel OJ-H column (hexane/2-propanol=99/1, 0.5 mL/min, 210 nm). t_R 13.3 min (*S*); t_R 16.4 min (*R*). $^1\text{H NMR}$ (CDCl_3): δ = 1.32 (s, 9H), 2.32 (s, 3H), 4.28 (m, 2H), 5.41 (s, 1H), 5.71 (m, 1H), 5.85 (m, 1H), 7.0-7.2 (m, 4H).

Cyclopent-2-en-1-ylbenzene (19a). Enantiomeric excess determined by HPLC using



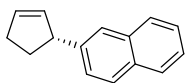
Chiracel OJ-H column (hexane/2-propanol=98/2, 0.5 mL/min, 210 nm). t_R 9.4 min (*S*); t_R 9.8 min (*R*). $^1\text{H NMR}$ (CDCl_3): δ = 1.73 (m, 1H), 2.3-2.6 (m, 3H), 3.99 (m, 1H), 5.78 (m, 1H), 5.94 (m, 1H), 7.18 (m, 3H), 7.28 (m, 2H).

1-(Cyclopent-2-en-1-yl)-4-methylbenzene (19b). Enantiomeric excess determined by



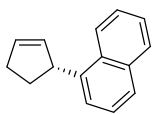
HPLC using Chiracel OJ-H column (hexane/2-propanol=98/2, 0.5 mL/min, 210 nm). t_R 10.2 min (*S*); t_R 11.1 min (*R*). $^1\text{H NMR}$ (CDCl_3): δ = 1.70 (m, 1H), 2.31 (s, 3H), 2.39 (m, 2H), 3.85 (m, 1H), 5.76 (m, 1H), 5.91 (m, 1H), 7.0-7.2 (m, 4H).

2-(Cyclopent-2-en-1-yl)naphthalene (19c). Enantiomeric excess determined by HPLC



using Chiracel OJ-H column (hexane/2-propanol=98/2, 0.5 mL/min, 210 nm). t_R 15.0 min (*R*); t_R 16.6 min (*S*). $^1\text{H NMR}$ (CDCl_3): δ = 1.80 (m, 1H), 2.4-2.6 (m, 3H), 4.05 (m, 1H), 5.84 (m, 1H), 5.99 (m, 1H), 7.31 (d, 1H, J = 8.4 Hz), 7.39 (m, 2H), 7.59 (s, 1H), 7.77 (m, 3H).

1-(Cyclopent-2-en-1-yl)naphthalene (19d). Enantiomeric excess determined by



HPLC using Chiracel OJ-H column (hexane/2-propanol=98/2, 0.5 mL/min, 210 nm). t_R 11.7 min (*S*); t_R 12.6 min (*R*). $^1\text{H NMR}$ (CDCl_3): δ = 1.78 (m, 1H), 2.49 (m, 2H), 2.62 (m, 1H), 4.65 (m, 1H), 5.95 (m, 1H), 6.04 (m, 1H), 7.30 (d, 1H, $J=7.2$ Hz), 7.39 (m, 1H), 7.49 (m, 2H), 7.69 (d, 1H, $J=8.0$ Hz), 7.85 (m, 1H), 8.16 (d, 1H, $J=8.4$ Hz).

7.1.7. References

1. For recent reviews, see: (a) Oestreich, M. *Angew. Chem., Int. Ed.* **2014**, *53*, 2282. (b) Diéguez, M.; Pàmies, O. *Carbohydrates-tools for estereoselective synthesis*. Ed. Boysen, M. M. K. Wiley-VCH Verlag GmbH & Co. KGaA, 2013, Chapter 11, 245. (c) Mc Cartney, D.; Guiry, P. J. *Chem. Soc. Rev.* **2011**, *40*, 5122. (d) V. Coeffard, P. J. Guiry, *Current Organic Chemistry* 2010, *14*, 212. (e) Oestreich, M. *Mizoroki-Heck Reaction*, Wiley-VCH, Weinheim, 2009. (f) Tietze, L. T.; Ila, H.; Bell, H. P. *Chem Rev.* **2004**, *104*, 3453. (g) Dai, L. X.; Tu, T.; You, S. L.; Deng, W. P.; Hou, X. L. *Acc. Chem. Res.* **2003**, *36*, 659. (h) Bolm, C.; Hildebrand, J. P.; Muñiz, K.; Hermanns, N. *Angew. Chem., Int. Ed.* **2001**, *44*, 3284. (i) Shibasaki, M.; Vogl E. M. in *Comprehensive Asymmetric Catalysis* (Eds. Jacobsen, E. N.; Pfaltz, A.; Yamamoto, H.), Springer, Heidelberg, 1999. (j) Loiseleur, O.; Hayashi, M.; Keenan, M.; Schemees, N.; Pfaltz, A. *J. Organomet. Chem.* **1999**, *576*, 16. (k) Beller, M.; Riermeier, T. H.; Stark G. in *Transition Metals for Organic Synthesis* (Eds. Beller, M.; Bolm, C.), Wiley-VCH, Weinheim, 1998. (l) Diederich, F.; Stang, P. J. *Metal-Catalyzed Cross-Coupling Reactions*, Wiley-VCH, Weinheim, 1998. (m) Magano, J.; Dunetz, J. *Chem. Rev.* **2011**, *111*, 2177. (n) Diéguez, M.; Pàmies, O. *Isr. J. Chem.* **2012**, *52*, 572.
2. Ozawa, F.; Kubo, A.; Hayashi, T. *J. Am. Chem. Soc.* **1991**, *113*, 1417.
3. a) O. Loiseleur, P. Meier, A.; Pfaltz, *Angew. Chem. Int. Ed. Engl.* **1996**, *35*, 200. b) O. Loiseleur, M. Hayashi, N. Schmees, A. Pfaltz, *Synthesis* **1997**, 1338.
4. For representative examples, see: (a) Hennessy, A. J.; Malone, Y. M.; Guiry, P. J. *Tetrahedron Lett.* **1999**, *40*, 9163. (b) Hennessy, A. J.; Connolly, D. J.; Malone, Y. M.; Guiry, P. J. *Tetrahedron Lett.* **2000**, *41*, 7757. (c) Hashimoto, Y.; Horie, Y.; Hayashi, M.; Saigo, K. *Tetrahedron: Asymmetry* **2000**, *11*, 2205. (d) Ogasawara, M.; Yoshida, K.; Hayashi, T. *Heterocycles* **2000**, *52*, 195. (e) Deng, W.-P.; Hou, X.-L.; Dai, L.-X.; Dong, X.-W. *Chem. Commun.* **2000**, 1483. (f) Gilbertson, S. R.; Genov, D. G.; Rheingold A.

L., *Org. Lett.* **2000**, 2, 2885. (g) Gilbertson, S. R.; Xie, D.; Fu, Z. *J. Org. Chem.* **2001**, 66, 7240. h) Gilbertson, S. R.; Fu, Z. *Org. Lett.* **2001**, 3, 161. (i) Tu, T.; Deng, W. P.; Hou, X. L.; Dai, ; Dong, X. C. *Chem. Eur. J.* **2003**, 9, 3073. (j) Tu, T.; Hou, X.-L.; Dai, L. X. *Org. Lett.* **2003**, 5, 3651. (k) Kilroy, T. G.; Cozzi, G. P.; End, N.; Guiry, P. J. *Synlett* **2004**, 106. l) Hou, X. L.; Dong, D. X.; Yuan, K. *Tetrahedron: Asymmetry* **2004**, 15, 2189. (m) Kilroy, T. G.; Cozzi, P. G.; End, N.; Guiry, P. J. *Synthesis* **2004**, 1879. (n) Rubina, M.; Sherrill, W. M.; Rubin, M. *Organometallics* **2008**, 27, 6393. (o) Wu, W.-Q.; Peng, Q.; Dong, D.-X.; Hou, X.-L.; Wu, Y.-D. *J. Am. Chem. Soc.* **2008**, 130, 9717. (p) Liu, D.; Dai, Q.; Zhang, X. *Tetrahedron* **2005**, 61, 6460. (q) Bélanger, E.; Pouliot, M.-F.; Paquin, J.-F. *Org. Lett.* **2009**, 11, 2201. (r) Fitzpatrick, M. O.; Müller-Bunz, H.; Guiry, P. J. *Eur. J. Org. Chem.* **2009**, 1889. (s) Belanger, É; Pouliot, M-F.; Courtemanche, M-A.; Paquin, J-F. *J. Org. Chem.* **2012**, 77, 317. (t) McCartney, D.; Nottingham, Ch.; Müller-Bunz, H.; Guiry, P. J. *J. Org. Chem.* **2015**, 80, 10151. (u) Rubina, M.; Sherrill, W.M. Barkov, A.Y.; Rubin, M. *Beilstein J. Org. Chem.* **2014**, 10, 1536.

5. To a lesser extension phosphinite-oxazoline, phosphine-N (N=pyridine, amine, phenylbenzoxazine, thiazole, imidazole have also been applied. See for example: (a) Yonehara, K.; Mori, K.; Hashizume, T.; Chung, K. G.; Ohe, K.; Uemura, S. *J. Organomet. Chem.* **2000**, 603, 40. (b) Malkov, A. V.; Bella, M.; Stará, I. G.; Kocóvsky, P. *Tetrahedron Lett.* **2001**, 42, 3045. (c) Bernardinelli, G. H.; Kündig, E. P.; Meier, P.; Pfaltz, A. Radkowski, K.; Zimmermann, N.; Neuburger-Zehnder, M. *Helv. Chim. Acta* **2001**, 84, 3233. (d) Kilroy, T. G.; Hennessy, A. J.; Connolly, D. J.; Malone, Y. M.; Farrell, A.; Guiry, P. J. *J. Mol. Cat. A: Chem.* **2003**, 196, 65. (e) Drury III, W. J.; Zimmermann, N.; Keenan, M.; Hayashi, M.; Kaiser, S.; Goddard, R.; Pfaltz, A. *Angew. Chem. Int. Ed.* **2004**, 116, 72. (f) Kaukoranta, P.; Källström, K.; Andersson, P. G. *Adv. Synth. Catal.* **2007**, 349, 2595. (g) Henriksen, S. T.; Norrby, P. O.; Kaukoranta, P.; Andersson, P. G. *J. Am. Chem. Soc.* **2008**, 130, 10414. (h) Werner, E. W.; Mei, T.-S.; Burckle, A. J.; Sigman, M. S. *Science* **2012**, 338, 1455. (i) Borrajo-Calleja, G. M.; Bizet, V.; Bürgi, T.; Mazet, C. *Chem. Sci.* **2015**, 6, 4807.

6. Nilsson, P.; Gold, H.; Larhed, M.; Hallberg, A. *Synthesis* **2002**, 1611.

7. (a) Wöste, T. H.; Oestrich, M. *Chem. Eur. J.* **2011**, 17, 11914. (b) Liu, J.; Zhou, J. *Chem. Commun.* **2013**, 49, 11758. (c) Hu, J.; Hu, Y.; Li, Y.; Zhou, J. *Chem. Commun.* **2013**, 49, 9425. (d) Wu, C.; Zhou, J. *J. Am. Chem. Soc.* **2014**, 136, 650. (e) Recently

Hou's and Ding's groups reported the use of phosphine-phosphine oxides for the construction of quaternary carbon centers, see. Zhang, Q.-S.; Wan, S.-L.; Chen, D.; Ding, C.-H.; Hou, X.-L. *Chem. Comm.* **2015**, *51*, 12235.

8. van Leeuwen, P. W. N. M.; Kamer, P. C. J.; Claver, C.; Pàmies, O.; Diéguez, M. *Chem. Rev.* **2011**, *111*, 2077.

9. (a) Diéguez, M.; Pàmies, O. *Acc. Chem. Res.* **2010**, *43*, 312. (b) Pàmies, O.; Andersson, P. G.; Diéguez, M. *Chem. Eur. J.* **2010**, *16*, 14232. (c) Magre, M.; Pàmies, O.; Diéguez, M. *Chem. Rec.* **2016**, *16*, 1578. (d) Pàmies, Diéguez, M. *Chem. Rec.* **2016**, *16*, 2460.

10. (a) Mata, Y.; Diéguez, M.; Pàmies, O.; Claver, C. *Org. Lett.* **2005**, *7*, 5597. (b) Mata, Y.; Pàmies, O.; Diéguez, M.; *Chem. Eur. J.* **2007**, *13*, 3296. (c) Mazuela, J.; Pàmies, O.; Diéguez, M. *Chem. Eur. J.* **2010**, *16*, 3434.

11. See for instance: (a) Van Strijdonck, G. F. P.; Boele, M. D. K.; Kamer, P. C. J.; de Vries, J. G.; van Leeuwen, P. W. N. M. *Eur. J. Inorg. Chem.* **1999**, 1073. (b) Rosner, T.; Le Bars, J.; Pfaltz, A.; Blackmond, D. G. *J. Am. Chem. Soc.* **2001**, *123*, 1848. (c) Rosner, T.; Pfaltz, A.; Blackmond, D. G. *J. Am. Chem. Soc.* **2001**, *123*, 4621. (d) Rothenberg, G.; Cruz, S. C.; van Strijdonck, G. P. F.; Hoefsloot, H. C. J. *Adv. Synth. Catal.* **2004**, *346*, 467. (e) Dodds, D. L.; Boele, M. D. K.; van Strijdonck, G. P. F.; de Vries, J. G.; van Leeuwen, P. W. N. M.; Kamer, P. C. J. *Eur. J. Inorg. Chem.* **2012**, 1660. (f) Mathew, J. S.; Klusmann, M.; Iwamura, H.; Valera, F.; Futran, A.; Emanuelsson, E. A. C.; Blackmond D. G. *J. Org. Chem.* **2006**, *71*, 4711.

12. Hii, K. K.; Claridge, T. D. W.; Brown, J. M. *Angew. Chem. Int. Ed.* **1997**, *36*, 984.

13. Yang, D.; Wang, L.; Han, F.; Li, D.; Zhao, D.; Wang, R. *Angew. Chem. Int. Ed.* **2015**, *54*, 2185.

14. Harrowven, D. C.; Lucasa, M. C.; Howes, P. D. *Tetrahedron* **2001**, *57*, 791.

15. The use of commercially available [Pd₂(dba)₃]-dba led to some reproducibility problems between batches due to the presence of different amounts of free dba. For these reason we removed the free dba by recrystallization in benzene. Zalesskiy, S. S.; Ananikov, V. A. *Organometallics* **2012**, *31*, 2302.

16. Takano, S.; Dsmizu, K.; Ogasawara, K. *Synlett* **1993**, 393.

17. To our knowledge only three reports deals with the coupling of substrate **S52**. (a) Pfaltz et al., in ref 3b, reported the phenylation of **S52** with Pd/**93c** system with 92% *ee* and 70% conv in 7 days using higher temperature (70 °C). (b) Gilberston et al., in ref.

4g, reported the phenylation of **S52** with Pd/**99b** system with 96% *ee* and 50% conversion in 2 days using higher temperature (70 °C). (c) Zhou et al., in ref 7b, reported the coupling of **S52** with 1-Napf-OTf using 3 mol% of biphosphine oxides ligands with 92% *ee* in 2 days at higher temperature, 70 °C.

18. For representative examples, see: (a) Antonow, D.; Thurston, D. E. *Chem. Rev.* **2011**, *111*, 2815. (b) Smith III, A. B.; Charnley, A. K.; Hirschmann, R. *Acc. Chem. Res.* **2011**, *44*, 180. (c) Rahman, K. M.; James, C. H.; Bui, T. T. T.; Drake, A. F.; Thurston, D. E. *J. Am. Chem. Soc.* **2011**, *133*, 19376. (d) Antonow, D.; Kaliszczak, M.; Kang, G. D.; Coffils, M.; Tiberghien, A. C.; Cooper, N.; Barata, T.; Heidelberger, S.; James, C. H.; Zloh, M.; Jenkins, T. C.; Reszka, A. P.; Neidle, S.; Guichard, S. M.; Jodrell, D. I.; Hartley, J. A.; Howard, P. W.; Thurston, D. E. *J. Med. Chem.* **2010**, *53*, 2927. (e) Lloyd, J.; Finlay, H. J.; Vacarro, W.; Hyunh, T.; Kover, A.; Bhandaru, R.; Yan, L.; Atwal, K.; Conder, M. L.; Jenkins-West, T.; Shi, H.; Huang, C.; Li, D.; Sun, H.; Levesque, P. *Bioorg. Med. Chem. Lett.* **2010**, *20*, 1436. (f) Rahman, K. M.; Vassoler, H.; James, C. H.; Thurston, D. E. *ACS Med. Chem. Lett.* **2010**, *1*, 427.

19. Mei, T.-S.; Werner, E. W.; Burckle, A. J.; Sigman, M. S. *J. Am. Chem. Soc.* **2013**, *135*, 6830.

20. Yang, Z.; Zhou, J. *J. Am. Chem. Soc.* **2012**, *134*, 11833.

21. Tschoerner, M.; Pregosin, P. S.; Albinati, A. *Organometallics* **1999**, *18*, 670.

22. This compound has been prepared following the procedure described in Holder, J. C.; Zou, L.; Marziale, A. N.; Liu, P.; Lan, Y.; Gatti, M.; Kikushima, K.; Houk, K. N.; Stoltz, B. M. *J. Am. Chem. Soc.*, **2013**, *135*, 14996.

23. Hansch, C.; Leo, A.; Taft, R. W. *Chem. Rev.* **1991**, *91*, 165.

24. Buisman, G. J. H.; Kamer, P. C. J.; van Leeuwen, P. W. N. M. *Tetrahedron: Asymmetry* **1993**, *4*, 1625.

25. Wu, C.; Zhou, J. *J. Am. Chem. Soc.* **2014**, *136*, 650.

Chapter 8.

Conclusions

Conclusions

1. *Progres in perfluoroalkylation of aromatic compounds.* The conclusions of this chapter can be summarized as follows:

- For the first time, the successful production of CuCF_3 reagent in continuous flow process in four different set up configurations have been carried out. Based on the reagent sensitivity and important parameters which should be taken in account for preparation of the reagent several modifications were done in order to reach to the high yield comparable to the nonindustrial batch setting. The reagent efficiency was also examined in the trifluoromethylation of different aromatic halides. The results therefore demonstrated the high efficiency of the CuCF_3 reagent in continuous flow regime.

- We have successfully trifluoromethylated and pentafluoroethylated a broad range of vinylic bromides and iodides (44 examples with different electron donating and withdrawing groups) with R_fH -derived CuCF_3 and CuC_2F_5 to give the corresponding fluoroalkylated olefins. These reactions proceed with high yields and excellent chemo- and stereoselectivity under mild reaction conditions. Twelve examples of trifluoromethylated and pentafluoroethylated products were isolated in 1-10 mmol scale. The X-ray structure of two perfluoroalkylated compounds are also presented to confirm the structure and stereochemistry in the solid state.

2. *Ru- and Ir-catalyzed transfer hydrogenation and dehydrogenation reactions.* The conclusions of this chapter can be summarized as follows:

- A series of O-functionalised 1,2,3-triazolyldiene iridium(III) and ruthenium(II) complexes were successfully synthesized and applied in transfer hydrogenation of benzophenone. Ether- and hydroxy-substituted 1,2,3-triazolyldiene iridium(III) complexes were isolated with the ligand both in mono- and bidentate coordination mode. Also, monodentated and C,O-bidentated, hydroxy-functionalised 1,2,3-triazolyldiene ruthenium complexes are described. The monodentated complexes were converted to the chelating species by chloride abstraction and vice versa, the chelates were transformed into monodentate ligands in the presence of excess of halide. Transfer hydrogenation studies revealed that pendant hydroxy-donors substantially enhance the catalytic activity of the triazolyldiene iridium(III) catalyst while analogous hydroxy-

functionalised triazolylidene ruthenium(II) complexes did not outperform analogous unfunctionalised complexes. Generally, activity was much higher for the ruthenium(II) complexes than the iridium(III) homologues, which hints towards diverging activation mechanisms.

- For the first time mixed benzoxazole/thiazole-MIC ligands were synthesized by efficient click reactions. For comparison purposes we also synthesized the ether-functionalized 1,2,3-triazolylidene analogous. We used these ligands to generate the corresponding Ir(I) and Ir(III) benzoxazole/thiazole/ether-appended MIC complexes. The coordination was successfully achieved by a transmetalation protocol and the corresponding complexes were fully characterized by ^1H and ^{13}C NMR spectroscopy, high resolution mass spectrometry, elementary analysis and X-ray diffraction. We also successfully applied these complexes in transfer hydrogenation of a broad range of ketones, including the most challenging heteroaromatic ones, aldehydes and imines in high activities (TOF's up to $2090 \text{ mol x (mol x h)}^{-1}$). The best results were obtained with the Ir(I) containing an ether-appended MIC catalyst precursor. Although there are some metal-carbene species, mainly Ru-NHC complexes, able to promote these transformations more efficiently, our results compete favorably with known Ir-MIC catalytic systems. We also obtain high activity in the reduction of a broad range of olefins. The catalytic performance is relatively insensitive to the olefins substitution pattern and to the geometry of the double bond. Similar high activities were therefore achieved for a range of linear mono-, 1,2-di- and 1,1-disubstituted olefins as well as for cyclic olefins (TOF's up to $260 \text{ mol x (mol x h)}^{-1}$). Ir(I) ether-triazolylidene catalyst precursor is also one of the rare examples of catalyst able to efficiently reduce a broad range of olefins. Finally, high activities could also be obtained in the reduction of α,β -unsaturated ketones and allylic alcohols. Mechanistic investigations indicated that the transfer hydrogenation of ketones proceeds via an iridium-monohydride species, being the rate determining step the C=O insertion on the M-H bond.

- We also successfully applied these iridium complexes to the base-free Ir-catalyzed dehydrogenation reactions with 12 different primary and secondary alcohols. In this case and in contrast to the TH, Ir(III) complexes specially complexes showed better results rather than Ir(I) counterparts. The mechanistic studies by KIE and Hammet plots seems to indicate that the substrate coordination to the metal center is the rate determining step.

3. Iridium molecular catalysts for catalytic water oxidation. The conclusions of this chapter can be summarized as follows:

- Benzoxazole/thiazole-triazolylidene iridium (III) complexes synthesized in previous chapter were successfully applied in the water oxidation reactions using CAN and NaIO₄ as oxidants. Using CAN as oxidant at low pH, the catalyst precursors provided similar activities (TOF's ca 0.06 s⁻¹) and lower than those achieved using parent pyridine complex. However, excellent activities (much better than related pyridine analogues; TOF's up to 0.58 s⁻¹) were achieved when using more appealing almost neutral conditions (pH = 5.6) and NaIO₄ as oxidant.

- In this chapter we have also disclosed the electrochemical properties of the complexes in a non-protic solvent as well as in aqueous solution at different pHs. We have also studied the Cl⁻/H₂O ligand exchange propensity of the complexes in water solution. The results indicated that the chloro anion can be exchanged by water. In this respect both dicationic mono- and diaquo complexes have been synthesized.

4. Pd-catalyzed asymmetric intermolecular Heck reaction. The conclusions of this chapter can be summarized as follows:

- A reduced but structurally valuable library of phosphite-oxazoline ligands have been successfully synthesized and applied in the enantioselective Pd-catalyzed intermolecular Heck reaction. These ligands, which are prepared in a few steps from commercially available materials, include the benefits of the high robustness of the phosphite moiety and the additional control provided by the flexibility of the chiral pocket through a modular ligand scaffold. Other advantages of these ligands are that they are solid, stable to air and other oxidizing agents and are, therefore, easy to handle and can be manipulated and stored in air. In a simple two or four step-procedure several ligand parameters could easily be tuned to maximize the catalyst performance. We have therefore investigated the effect of systematically changing the oxazoline substituents and its configuration, the substituents in the benzylic position and the substituents and configurations of the biaryl phosphite moiety. By carefully selecting the ligand parameters we could obtain high activities, regio- and enantioselectivities in both enantiomers of the Heck products using several cyclic substrates and a broad range of triflates. The results are comparable to the best one reported in the literature. Another advantage with these ligands and in contrast to the vast majority of P-N ligands, in

our case the ligands that provided the best enantioselectivities contained the ⁱPr substituent in the oxazoline moiety instead of the pricy ^tBu substituent.

- In this paper we have also carried out mechanistic investigations by combining kinetics studies and Hammet plots. The results suggest that the alkene insertion is the rate determining step. The mechanistic results also indicate that although dibenzylideneacetone (dba) doesn't play any role in the catalysis it is necessary to prevent the catalyst deactivation to form the Pd-black.

Chapter 9.

Summary

Summary

It is widely accepted that sustainable industrial production and the generation of clean energy must be two of the pillars of our society. Huge amounts of resources for research and technological development in this direction have been dedicated. Catalysis is one of the driving force of these advances. Catalyzed chemical processes allow to increase production, reduce the number of reaction steps, work under more favorable energy conditions and generate less byproducts than the uncatalyzed processes. The improvement of the catalyst stability and selectivity is a fundamental and strategic research for achieving sustainable industrial production and clean energy generation. In this respect, this thesis focused on improving the current state-of-the-art by the design, synthesis and screening of new molecular catalysts very active and selective for catalytic reactions of industrial interest and for water oxidation. The main innovations can be divided in two parts:

The first part of the thesis (done in the ICIQ, 2012-15) is about perfluoroalkylation of aromatic substrates. Perfluoroalkylated organic compounds have an outstanding place in pharmaceuticals and agrochemicals. There are some famous drugs containing CF_3 and C_2F_5 groups and also compounds including C_2F_5 group are more biologically active. Therefore, the development of new suitable protocols for their synthesis are an important field of research. After the introduction (Chapter 2), Chapter 3 is focused in perfluoroalkylation of organic compounds. This part is divided in two sections. Section 3.1 presents the first continuous flow process for the synthesis of a superior trifluoromethylating reagent, "ligandless" CuCF_3 , from fluoroform, by far the best CF_3 source in terms of availability, cost and atom economy. In section 3.2, the target was the trifluoromethylation and pentafluoroethylation of a variety of vinylic bromides and iodides (44 examples with several electron donating and withdrawing groups) with R_fH -derived CuR_f ($\text{R}_f = \text{CF}_3, \text{C}_2\text{F}_5$) to give the corresponding fluoroalkylated olefins. These reactions proceed with high yields and excellent chemo- and stereoselectivity under mild reaction conditions.

The second part of the thesis (done in the URV, 2015-17) is about the preparation of tailor-made catalysts for C-X forming (transfer hydrogenation, dehydrogenation, and intermolecular Heck reactions) and water oxidation reactions. This part of the thesis is divided in four parts. The first part is a general introduction (Chapter 4) about the

importance of the design and preparation of ligands in the synthesis of organic compounds and then a detailed review of the four reactions studied are contemplated. Chapter 5 contains two sections on the development of new Ru- and Ir-complexes with mesionic carbene-based ligands. The first section 5.1 includes the synthesis and characterization of iridium(III) and ruthenium(II) complexes bearing pendant hydroxy- and ester-wingtip substituents. Both monodentate and C,O-bidentate binding modes were observed for these O-functionalised triazolylidene complexes. The catalytic activity of the complexes was compared in transfer hydrogenation, revealing that pendant hydroxyfunctionalities are beneficial for enhancing the performance of triazolylidene iridium(III) catalysts, while they have no effect in ruthenium-catalyzed transfer hydrogenation. The second section 5.2 reports the first examples of mixed benzoxazole/thiazole-MIC ligands. We used these ligands to generate the corresponding Ir(I) and Ir(III) benzoxazole/thiazole/ether-appended MIC complexes. The coordination was achieved by a transmetalation protocol and the corresponding complexes were fully characterized. Apart from synthetic and structural aspects, we also present the successful application of these complexes in transfer hydrogenation of a broad range of substrates (ketones, aldehydes, imines, etc.) and also the more challenging mono-, di- and trisubstituted olefins and in the base-free dehydrogenation reactions of alcohols. We also discuss some mechanistic insights for both transformations.

Then, Chapter 6 focuses on the application of previous benzoxazole/thiazole-triazolylidene iridium complexes on water oxidation using CAN and NaIO₄ as oxidants. Using CAN as oxidant at low pH, the catalyst precursors provided similar activities (TOF's ca 0.06 s⁻¹) and lower than those achieved using parent pyridine complex. However, excellent activities (much better than related pyridine analogues; TOF's up to 0.58 s⁻¹) were achieved when using more appealing almost neutral conditions (pH = 5.6) and NaIO₄ as oxidant. In this chapter we have also disclosed the electrochemical properties of the complexes in a non-protic solvent as well as in aqueous solution at different pHs. We have also studied the Cl⁻/H₂O ligand exchange propensity of the complexes in water solution.

Finally, Chapter 7 includes the synthesis of a reduced but structurally valuable library of phosphite-oxazoline ligands for the enantioselective Pd-catalyzed Heck reaction of several cyclic substrates and triflates. These ligands, which are prepared in a few steps from commercially available materials include the benefits of the high robustness of the phosphite moiety and the additional control provided by the flexibility of the chiral

pocket through a modular ligand scaffold. Other advantages of these ligands are that they are solid, stable to air and other oxidizing agents and are, therefore, easy to handle and can be manipulated and stored in air. In a simple two or four step-procedure, several ligand parameters have been easily tuned to maximize the catalyst performance. In this paper we also carried out mechanistic investigations by combining in situ NMR studies of key intermediates and kinetics studies.

Chapter 10.

Appendix

Appendix

10.1. List of publications

1. Synthesis, Hemilability, and Catalytic Transfer Hydrogenation Activity of Iridium(III) and Ruthenium(II) Complexes Containing Oxygen-functionalised Triazolylidene Ligands. René Pretorius, Zahra Mazloomi, Martin Albrecht. *J. Organomet. Chem.* **2017**, <http://dx.doi.org/10.1016/j.jorganchem.2017.05.014>.
2. Trifluoromethylation and Pentafluoroethylation of Vinylic Halides with Low-Cost R_fH-Derived CuR_f (R_f = CF₃, C₂F₅). Anton Lishchynskyi, Zahra Mazloomi, Vladimir V. Grushin. *Synlett* **2015**, 26, 45. (Cluster)
3. Continuous Process for Production of CuCF₃ via Direct Cupration of Fluoroform. Zahra Mazloomi, Atul Bansode, Pedro Benavente, Anton Lishchynskyi, Atsushi Urakawa, and Vladimir V. Grushin. *Org. Process Res. Dev.* **2014**, 18, 1020. (Special Issue: Fluorine chemistry 14, 10th most read articles in June 2014)
4. Organoplatinum(II) Complexes Containing Chelating or Bridging Bis(N-Heterocyclic Carbene) Ligands: Formation of a Platinum(II) Carbonate Complex by Aerial CO₂ Fixation. Jamali, Sirous; Milic, Dalibor; Kia, Reza; Mazloomi, Zahra; Abdolahi, Halimeh, *Dalton Trans.* **2011**, 40, 9362. (Selected for front cover of the Journal)
5. Cyclometalated Cluster complex with a Butterfly-Shaped Pt₂Ag₂ Core. Sirous Jamali, Zahra Mazloomi, S. Masoud Nabavizadeh, Dalibor Milic, Reza Kia and Mehdi Rashidi. *Inorg. Chem.* **2010**, 49, 2721.

10.2. Meeting contributions

1. 5th CARISMA Meeting - Catalytic routines for small molecule activation, 6-8th March 2017, Lisbon, Portugal. (Oral presentation)
2. 5th CARISMA Meeting - Catalytic routines for small molecule activation, 6-8th March 2017, Lisbon, Portugal. (Plenary STSM flash presentation)

3. 1st Trans Pyrenean meeting in catalysis, 12-14th October 2016, Toulouse, France. (Oral presentation)
4. 6th EuCHEMS chemistry congress 11-15th September 2016, Seville, Spain. (Poster)
5. 40th “A. Corbella” international summer school on organic synthesis isos 2015. 14-18th June 2015, Gargnano, Italy. (Poster)
6. 3th CARISMA Meeting - Catalytic routines for small molecule activation, 18-20th March 2015, Tarragona, Spain. (Member of organizing committee)
7. ICIQ's 10th Anniversary scientific Symposium 16-18th July 2014, Tarragona, Spain. (Poster)
8. 7th European symposium on Metal-mediated efficient organic synthesis and ICIQ summer school, 22-27th July 2012, Tarragona, Spain. (Participant)
9. Nobel campus “Chemistry for life” 1-4th July 2012, Tarragona, Spain. (Participant)
10. 24th International conference on organometallic chemistry 18-23th July 2010, Taiwan. (Poster)
11. 11th Iranian inorganic chemistry conference 13-14th May 2009, Esfahan, Iran. (Poster)

10.3 Stays in other research groups

1. From 13.02.2017 until 24.02.2017 as a short visiting stay in order to familiar with water oxidation equipments in the group of Dr Xavier Sala in the UAB University, Barcelona, Spain.
2. From 01.02.2016 until 30.04.2016 as a three months visiting abroad in the group of Prof. Martin Albrecht in the Bern University, Bern, Switzerland.



UNIVERSITAT
ROVIRA i VIRGILI



Institut Català
d'Investigació Química